Identification of essential, dispensable and modulatory domains in the core herpesvirus membrane fusion components gB and gH

Inauguraldissertation

zur

Erlangung des akademischen Grades eines

Doktors der Naturwissenschaften
(Dr. rer. nat.)

der

Mathematisch-Naturwissenschaftlichen Fakultät

der

Universität Greifswald

vorgelegt von
Melina Vallbracht
geboren am 19.09.1989
in Hagen, NRW

Greifswald, Juni 2018

Dekan:	Prof. Dr. Werner Weitschies
1. Gutachter:	Prof. Dr. Dr. h.c. Thomas C. Mettenleiter
2. Gutachter:	Prof. Dr. Christian Sinzger
3. Gutachter:	Prof. Dr. Kay Grünewald
Tag der Promotion:	29.11.2018

To my parents

Table of Contents

List of abbreviations

aa	amino acid
A	alanine
Å	Ångström
BAC	bacterial artificial chromosome
BiFC	bimolecular fluorescence complementation
BoHV-1	*Bovine alphaherpesvirus* 1
C	cysteine
CD	cytoplasmic domain
CH	cholesterol
C-terminus	carboxy-terminus
D	aspartic acid
DNA	deoxyribonucleic acid
ds	double-stranded
E	glutamic acid
EBV	Epstein-Barr virus
e.g.	*exempli gratia* (for example)
EGFP	enhanced green fluorescent protein
EHV-1	*Equid alphaherpesvirus* 1
EM	electron microscopy
ER	endoplasmic reticulum
et al.	*et altera*
F	phenylalanine
FACS	fluorescence-activated cell sorter
FL	fusion loop
FP	fusion peptide
g	glycoprotein
G	glycine
gpi	glycosylphosphatidylinositol
gH^C	gH-core fragment
H	histidine
HA	hemagglutinin
HCMV	human cytomegalovirus

HIV	human immunodeficiency virus
HSV	Herpes simplex virus
HVEM	herpesvirus entry mediator
i.a.	*inter alia*
i.e.	*id est*
IF	immunofluorescence
kbp	kilobase pairs
kDa	kilo Dalton
L	leucine
MPR	membrane proximal region
N	asparagine
nm	nanometer
N-terminus	amino-terminus
P	proline
PFD	pro-fusion domain
PH	pleckstrin homology
PrV	Pseudorabies virus
Q	glutamine
R	arginine
S	serine
SLB	syntaxin-like bundle
T	triangulation number
TMD	transmembrane domain
TNF	tumor necrosis factor
V	valine
X-ray	Röntgen radiation
Y	tyrosine
α	alpha
Δ	delta
%	percent

1 Introduction

1.1 Principle of membrane fusion

Membrane fusion is the process by which two initially separated lipid membranes merge into a single continuous bilayer. It is one of the most fundamental processes in life. In fact, without it, life would cease to exist (Blumenthal, Clague *et al.* 2003; Jahn, Lang *et al.* 2003; Leabu 2006).

Diverse biological processes are dependent on membrane fusion events and at least three major types can be distinguished: [1] *Cell-cell fusion*, a crucial biological event essential for fertilization during sexual reproduction and for tissue formation during development. [2] *Intracellular vesicle fusion*, required for assembly and maintenance of organelles, protein trafficking and exocytosis. [3] *Fusion of pathogens with their host cells*, representing a key step in cell invasion by enveloped viruses such as herpesviruses, influenza virus or human immunodeficiency virus (HIV) (Jahn, Lang *et al.* 2003; Stein, Primakoff *et al.* 2004; Martens and McMahon 2008; Sapir, Avinoam *et al.* 2008).

Despite the diversity of physiological conditions involving membrane fusion, an ordered sequence of basic steps appears common in all types of membrane fusion events (Fig. 1) (Jahn, Lang *et al.* 2003). First, close contact between lipid bilayers must be established. This is a high energy-demanding process since repulsive hydration forces, which occur between lipid bilayers at short separation distances (20 Å/2 nm), need to be overcome (Shemer and Podbilewicz 2003; Martens and McMahon 2008; Aeffner, Reusch *et al.* 2012). Thus, the hydration (water) layer, that is associated with the polar lipid head groups, must be removed to allow direct interaction between the two lipid bilayers (Rand and Parsegian 1984; Leikin, Parsegian *et al.* 1993). Numerous studies on membrane fusion, including biochemical and structural analyses of isolated membranes (Leikina and Chernomordik 2000; Aeffner, Reusch *et al.* 2012) as well as live cell imaging (Zhao, Hamid *et al.* 2016) have demonstrated that the energy required for this process is minimized by the formation of a point-like membrane protrusion (Fig. 1A), which transforms into a hemifused, stalk-like intermediate (Fig. 1B). During the hemifusion state, which is defined as lipid mixing without content mixing, the outer membrane leaflets of the opposed bilayers have merged whereas the inner leaflets remain separate (Chernomordik and Kozlov 2005; Chernomordik and Kozlov 2008). According to the widely accepted “stalk-pore hypothesis”, the formed stalk expands radially and brings the inner leaflets of the two bilayers together. The resulting structure is referred to as hemifusion diaphragm (Fig. 1C) (Chernomordik, Kozlov *et al.* 1995; Kozlovsky, Chernomordik *et al.* 2002). Lateral tension

emerging in the extending hemifusion diaphragm is assumed to promote rupture of the bilayer and fusion pore formation. Fusion pore opening and mixing of inner aqueous contents complete the fusion process (Fig. 1D) (Kozlovsky, Chernomordik *et al.* 2002; Mondal Roy and Sarkar 2011).

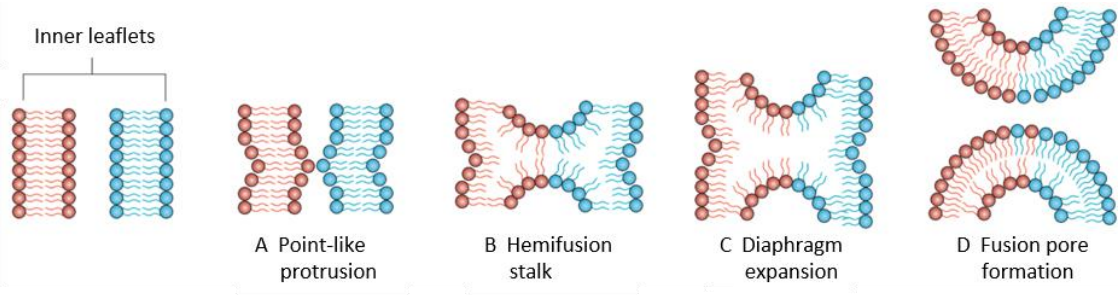

Figure 1: Schematic representation of the membrane fusion process following the stalk-pore model. (A) Fusion starts from a point-like membrane protrusion minimizing the repulsive forces between the lipid bilayers. (B) The inner leaflets fuse to form a stalk-like structure. Expansion of the hemifusion stalk leads to formation of a diaphragm. (C) Extension of the diaphragm promotes fusion of the inner leaflets and (D) formation of a fusion pore. Adapted from (Ogle, Cascalho *et al.* 2005).

Altogether, although fusion of two separate bilayers is thermodynamically favored, several energy barriers such as the hydration and electrostatic repulsions between the equally charged membrane surfaces, as well as the lateral tension of the lipid bilayer interface, need to be overcome for fusion to occur (Chernomordik, Melikyan *et al.* 1987; Leikin, Parsegian *et al.* 1993; Kozlovsky, Chernomordik *et al.* 2002; Chernomordik and Kozlov 2003; Chernomordik and Kozlov 2008; Kielian 2014). Specialized proteins, termed fusion proteins, provide the energy required for the membrane fusion process at the appropriate time and place (Chernomordik and Kozlov 2008; Harrison 2015; Han, Pluhackova *et al.* 2017). Research on viral fusion protein mediated membrane fusion has pioneered the current knowledge on the membrane fusion process in general (Hernandez, Hoffman *et al.* 1996; Harrison 2015).

1.2 Structure and mechanism of viral fusion proteins

The nucleocapsids of enveloped viruses are enclosed by host-derived lipid bilayers (Buchmann and Holmes 2015). In order to enter the host cell and initiate an infection, the virion envelope must fuse with cellular membranes, leading to release of the viral contents into the cytosol. This central fusion event can occur either at the cell surface or, following virus internalization, within cellular endocytic compartments (Yamauchi and Helenius 2013; Kielian 2014; Boulant, Stanifer *et al.* 2015). To mediate this process, enveloped viruses have evolved specialized surface proteins, which are anchored in the viral envelope and termed fusion proteins, or fusogens. These proteins are activated once the virus arrives at the surface of the host cell or the appropriate intracellular compartment, such as an endosome (Harrison 2015).

Crystallographic studies of fusion proteins from several viruses have revealed a variety of molecular architectures (Bullough, Hughson *et al.* 1994; Weissenhorn, Dessen *et al.* 1997;

Modis, Ogata *et al.* 2004; Heldwein, Lou *et al.* 2006; Roche, Bressanelli *et al.* 2006; DuBois, Vaney *et al.* 2013; Burke and Heldwein 2015). Despite their vast structural and genetic divergence, these proteins seem to catalyze fusion by a common overall mechanism of action (Schibli and Weissenhorn 2004; Kielian and Rey 2006; Kadlec, Loureiro *et al.* 2008; Baquero, Albertini *et al.* 2013; Li and Modis 2014; Rey and Lok 2018). Fusion proteins are thought to provide the energy to overcome the kinetic barrier to fusion by refolding from a metastable, high-energy prefusion form to an energetically more stable postfusion conformation (Kielian and Rey 2006; White, Delos *et al.* 2008; Harrison 2015). Remarkably, to date, all postfusion structures of viral proteins reveal a trimeric hairpin conformation (Kielian and Rey 2006; Harrison 2015).

In general terms, the entry process is thought to require three steps: receptor-binding, activation and membrane fusion (Sathiyamoorthy, Chen *et al.* 2017). Binding of the virus to an appropriate cell surface receptor or other host cell factors initiates the membrane fusion process. Receptor binding and membrane fusion can be mediated by a single viral protein (*e.g.*, Env in retroviruses or HA in orthomyxoviruses) or distributed among multiple proteins (*e.g.*, in herpesviruses and paramyxoviruses) (Harrison 2015). For some viruses, the initial interaction with the host cell is sufficient to trigger the fusion reaction (Hunter 1997). However, the specific fusion trigger depends on the virus. The currently described mechanisms by which viral fusion proteins can be triggered are diverse and at least five types of fusion triggers can be distinguished: exposure to low pH (Marsh and Helenius 1989; White and Whittaker 2016), receptor binding or a combination of receptor binding followed by low pH or other (unknown) triggers (Matsuyama, Delos *et al.* 2004; Moller-Tank and Maury 2015), sequential interaction with a receptor and a co-receptor (Wilen, Tilton *et al.* 2012; Ozorowski, Pallesen *et al.* 2017), as well as receptor binding to a separate attachment protein (Smith, Popa *et al.* 2009).

Prior to the fusion triggering signal the viral fusion proteins reside in a metastable high-energy prefusion state on the viral membrane (Fig. 2A). Upon triggering, they undergo a series of conformational rearrangements (Harrison 2015). Previously masked hydrophobic segments, termed fusion peptides [FPs] or fusion loops [FLs], are exposed and extended for interactions with the opposing target membrane (White, Delos *et al.* 2008). This results in simultaneous anchorage of the extended intermediate in the viral and cellular membrane (Fig. 2B). The formation of a trimeric extended intermediate termed “prehairpin” is postulated for all viral fusion proteins (Kim, Donald *et al.* 2011; Kielian 2014; Li and Modis 2014). The prehairpin intermediate is unstable and rapidly folds back into an energetically more favorable postfusion hairpin conformation (Fig. 2C-D). In this state, the FPs or FLs are positioned at the same end of the protein as the transmembrane domain (TMD) (Fig. 2D) (Kielian and Rey 2006). The insertion of the fusion segments and the subsequent fold-back process of the extended intermediates

drive distortion of the two membranes, resulting in formation of a lipid stalk or hemifusion intermediate (Chernomordik and Kozlov 2003; Kozlov, McMahon *et al.* 2010) (see section 1.1). Finally, fusion pore opening, allowing delivery of the viral contents and subsequent infection, is thought to require the concerted action of more than one fusion protein trimer. However, the number of involved trimers and the nature of interactions between them may vary between different viruses and, yet, remains largely elusive for most viruses (Kielian and Rey 2006; Plonsky, Kingsley *et al.* 2008; Harrison 2015).

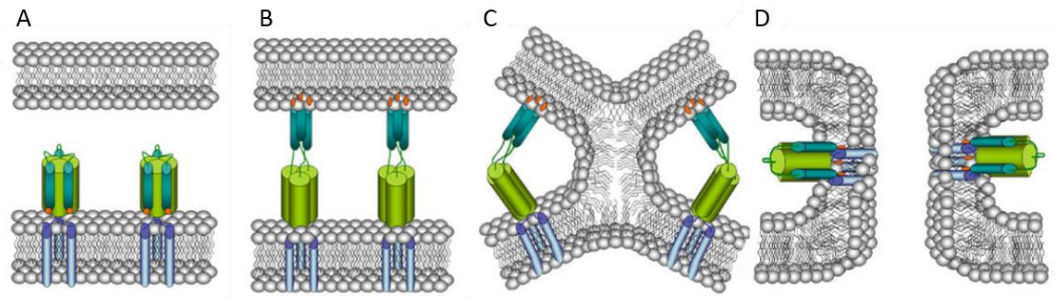

Figure 2: Conformational changes in influenza virus hemagglutinin (HA) during membrane fusion. (A) The prefusion form. HA resides in a prefusion state on the viral membrane. (B) Extended intermediate. After binding to the receptor (not shown) fusion is triggered by low pH. An extended intermediate conformation is generated in which the hydrophobic fusion peptides (orange) are extended towards the target membrane. (C) After anchoring into the membrane the intermediate folds back into a trimeric hairpin, positioning the transmembrane domains and fusion peptides in close proximity. (D) The post-fusion conformation. A fusion pore forms when the fusion peptides and the transmembrane domains are positioned adjacent to each other in the same membrane. Adapted from (Wessels and Weninger 2009).

On the basis of common pre- and postfusion structural features, viral fusion proteins have been classified into three distinct classes (Kielian and Rey 2006; White, Delos *et al.* 2008). In 1981, the structure of influenza virus hemagglutinin (HA), the founding member and prototype of class I viral fusion proteins, was determined (Wilson, Skehel *et al.* 1981). Class I fusion proteins, which encompass those of retroviruses, orthomyxoviruses, several members of the paramyxoviruses, filoviruses, arenaviruses, and coronaviruses are predominantly composed of α-helical structures and contain N-terminally located hydrophobic FPs (Lamb and Jardetzky 2007; Kielian 2014). Both, in the pre- and postfusion state, class I fusion proteins are trimeric and contain a central α-helical coiled-coil structure (Schibli and Weissenhorn 2004; Weissenhorn, Hinz *et al.* 2007). Fusogens of class I must be activated (or "primed") by proteolytic cleavage before they can be triggered to induce fusion. Proteolytic cleavage separates the fusion protein into a receptor binding and a fusion subunit, whereby the latter contains both the FP and the TMD (White and Whittaker 2016). The primed fusion protein can then be triggered by acidification within an endosomal compartment, as in the case of influenza HA (Skehel and Wiley 2000), or by receptor interactions of an attachment protein, leading to exposure of the FPs (Harrison 2015).

14 years after the elucidation of the influenza HA structure, the structure of the tick borne encephalitis virus fusion protein E was solved, leading to the identification of a novel class II of fusion proteins (Rey, Heinz *et al.* 1995; Kielian 2006). Members of this class are found in alphaviruses and flaviviruses, phleboviruses and rubella virus (Kielian 2006; Dessau and Modis 2013; DuBois, Vaney *et al.* 2013; Kielian 2014; Halldorsson, Li *et al.* 2018). In contrast to class I fusion proteins, members of the second class are three-domain proteins mainly composed of beta-sheets, which contain a fusion peptide located in an internal loop (Modis 2014). Unlike class I fusion proteins, their oligomeric state during the fusion process changes from prefusion dimers to postfusion trimers (Kielian 2006). Class II fusion proteins are primed for fusion by cleavage of a second viral surface protein, which acts as a chaperone, preventing premature triggering of the fusogen by low pH (Lobigs and Garoff 1990; Guirakhoo, Heinz *et al.* 1991; Stiasny, Allison *et al.* 2001).

Glycoprotein (g)B of herpesviruses (Heldwein, Lou *et al.* 2006; Backovic, Longnecker *et al.* 2009; Burke and Heldwein 2015; Li, Yang *et al.* 2017; Vallbracht, Brun *et al.* 2017), the G protein of rhabdoviruses (Roche, Bressanelli *et al.* 2006; Roche, Rey *et al.* 2007), glycoprotein 64 (gp64) of baculoviruses (Kadlec, Loureiro *et al.* 2008) and thogotovirus Gp (Peng, Zhang *et al.* 2017) possess structural features from both, class I and class II fusion proteins and were therefore postulated to define a novel, third class of viral fusion proteins (Steven and Spear 2006; Backovic and Jardetzky 2009). The determined three-dimensional structures of the ectodomains of all these proteins are proposed to represent postfusion conformations. The Vesicular Stomatitis virus (VSV) G protein is the only class III fusion protein for which high-resolution structures of both the pre- and postfusion conformation are available (Roche, Bressanelli *et al.* 2006; Roche, Rey *et al.* 2007; Abou-Hamdan, Belot *et al.* 2018). The postfusion structures of class III fusion proteins reveal trimeric, rod-like molecules. Each of the three protomers is composed of five domains, of which three are predominantly made of beta-sheets. The fusion peptides are located in an internal loop, characteristic of class II proteins (Backovic and Jardetzky 2009). As a hallmark of class I fusion proteins, the postfusion structures of class III proteins contain a central trimeric coiled-coil (Steven and Spear 2006). VSV G or baculovirus gp64 are “generalists”, which are able to mediate all steps of the fusion reaction on their own. In contrast, herpesvirus gB is not able to function alone but requires activation by additional viral surface glycoproteins (Cooper and Heldwein 2015). The molecular mechanism of herpesvirus induced membrane fusion is remarkably complex and as yet only poorly understood. The components of the herpesvirus fusion machinery and the nature of their interplay were intensively studied in this thesis and are therefore introduced in the following section.

1.3 Herpesvirus induced membrane fusion

1.3.1 The herpesvirus family

The order *Herpesvirales* contains enveloped animal viruses with large linear double-stranded (ds) deoxyribonucleic acid (DNA) genomes of 125 - 295 kilobase pairs (kbp), encoding between 70 and 223 proteins (Davison, Eberle *et al.* 2009; Davison 2010). Ancestors of all herpesviruses emerged approximately 180 to 220 million years ago and today more than 100 individual species have been discovered, known to infect a wide range of animals "from molluscs to men" (McGeoch, Cook *et al.* 1995; Mettenleiter, Klupp *et al.* 2009; Davison 2010). Sequence-based phylogeny classifies the order *Herpesvirales* into three families. The best studied family *Herpesviridae* contains viruses infecting mammals, birds and reptiles (Davison 2010). This family is further divided into the three subfamilies *Alpha-*, *Beta-*, and *Gammaherpesvirinae*. Members of the three families differ, inter alia, in their host range and properties of the life cycle. The present thesis focusses on the fusion mechanism of alphaherpesviruses, which, compared to beta-, and gammaherpesviruses, have the broadest host range. They are characterized by a rapid lytic replication, a pronounced neurotropism and the propensity to establish lifelong latency in sensory ganglia (Davison 2010). Alphaherpesviruses include important human pathogens such as Herpes simplex virus 1 and 2 (HSV-1/2, *Human alphaherpesvirus 1/2*) and Varicella-zoster virus (VZV, *Human alphaherpesvirus* 3). Moreover, this subfamily contains economically important animal viruses such as *Bovine alphaherpesvirus 1* (BoHV-1), *Equid alphaherpesvirus 1* (EHV-1) and Pseudorabies virus (PRV, *Suid alphaherpesvirus 1*). Beyond its significance as an economically important pathogen, PrV has served as a model for the study of alphaherpesvirus biology in natural hosts and in tissue culture (Mettenleiter 1996; Pomeranz, Reynolds *et al.* 2005; Mettenleiter 2008; Mettenleiter, Klupp *et al.* 2009). Thus, in the present thesis PrV was used as a tool to study the molecular mechanism of herpesvirus mediated membrane fusion.

Morphologically, herpes virions are unique and comprise four structurally distinct elements, the core, capsid, tegument and envelope (Mettenleiter 2002; Davison, Eberle *et al.* 2009). The core contains the linear dsDNA genome enclosed by an icosahedral (T=16) capsid (Booy, Newcomb *et al.* 1991). Together they form the nucleocapsid, which is embedded in a proteinaceous layer, termed tegument (Zhou, Chen *et al.* 1999). The tegument with the nucleocapsid is surrounded by a host cell derived lipid-bilayer, the envelope, containing multiple copies of different virus-encoded, and mostly glycosylated proteins (Granzow, Weiland *et al.* 1997; Davison, Eberle *et al.* 2009; Mettenleiter, Klupp *et al.* 2009). PrV (Mettenleiter 1994; Mettenleiter 2008) and HSV (Campadelli-Fiume and Menotti 2007) encode at least 11 different

envelope glycoproteins. A specific set of these envelope glycoproteins plays an essential role in virus entry.

1.3.2 The alphaherpesvirus fusion machinery

The entry mechanism utilized by herpesviruses is more complex than the mechanism employed by most other enveloped viruses. Whereas the majority of enveloped viruses depend on only one or two envelope glycoproteins for entry, herpesviruses require the coordinated action of at least three viral envelope glycoproteins. The homotrimeric gB and the heterodimeric complex of transmembrane glycoprotein H and anchorless glycoprotein L (gH/gL), constitute the "core fusion machinery", which is conserved throughout the entire *Herpesviridae* (Eisenberg, Atanasiu *et al.* 2012). This fusion machinery in PrV and most other alphaherpesviruses is proposed to be activated by binding of the essential attachment glycoprotein D (gD) to specific host cell receptors (Connolly, Whitbeck *et al.* 2001; Krummenacher, Carfi *et al.* 2013). These four components are thought to orchestrate membrane fusion through a sequential activation process (Atanasiu, Saw *et al.* 2010; Eisenberg, Atanasiu *et al.* 2012). However, although crystal structures are available for all four components, the molecular details of this cascade of events, ultimately leading to membrane fusion, remain enigmatic.

1.3.2.1 Receptor-mediated activation of entry by gD

An initial and reversible interaction of extracellular alphaherpes virions with the target cell is established by binding of attachment glycoprotein C (gC) to heparan sulfate moieties of cell surface proteoglycans. Although gC mediated attachment is beneficial for productive virus infection, it is not essential for the entry process (Mettenleiter 1989; Mettenleiter, Zsak *et al.* 1990; Shieh, WuDunn *et al.* 1992; Karger and Mettenleiter 1993; Laquerre, Argnani *et al.* 1998). In the absence of gC, attachment of HSV-1 to cell surface heparan sulfate can also be mediated by gB, which does not apply for BoHV-1 gB (Herold, Visalli *et al.* 1994; Klupp, Karger *et al.* 1997). The initial interaction by gC or gB is not sufficient for viral entry, but stable binding of gD to an appropriate cellular receptor is required (Karger and Mettenleiter 1993; McClain and Fuller 1994; Spear, Manoj *et al.* 2006). Alphaherpesviruses have the capacity to bind multiple cell surface molecules via gD, partially explaining their broad host range (Spear, Eisenberg *et al.* 2000; Li, Lu *et al.* 2017). The currently described gD receptors include the tumor necrosis factor (TNF) receptor-related protein herpesvirus entry mediator (HVEM) (Montgomery, Warner *et al.* 1996; Warner, Geraghty *et al.* 1998; Carfi, Willis *et al.* 2001), 3-O-sulfonated-heparan sulfate (Shukla, Liu *et al.* 1999) and three members of the immunoglobulin superfamily, namely, the poliovirus receptor related protein (HveD; CD155) (Mendelsohn, Wimmer *et al.* 1989; Geraghty,

Krummenacher *et al.* 1998), nectin-2 (HveB) (Warner, Geraghty *et al.* 1998) and nectin-1 (HveC) (Geraghty, Krummenacher *et al.* 1998; Di Giovine, Settembre *et al.* 2011; Li, Lu *et al.* 2017). Nectin-1 is the most broadly used gD receptor mediating entry of PrV, HSV-1, HSV-2 as well as BoHV-1 (Spear, Eisenberg *et al.* 2000; Li, Lu *et al.* 2017).

Binding of gD to one of its cellular receptors plays a key role in triggering the membrane fusion cascade (Krummenacher, Carfi *et al.* 2013). The crystal structures of both, the ectodomain of unliganded PrV and HSV gD, as well as HSV gD in complex with nectin-1 have been determined at high resolution (Carfi, Willis *et al.* 2001; Krummenacher, Supekar *et al.* 2005; Di Giovine, Settembre *et al.* 2011; Zhang, Yan *et al.* 2011; Lu, Zhang *et al.* 2014; Li, Lu *et al.* 2017). Structural and functional studies support a model in which receptor binding of gD would displace the carboxy (C)-terminus of the gD ectodomain, including the so called pro-fusion domain (PFD), leading to exposure of the fusion-activating interface of gD. This conformational change in gD has been suggested to enable it to interact with gH/gL and trigger gB mediated membrane fusion (Connolly, Whitbeck *et al.* 2001; Fusco, Forghieri *et al.* 2005; Gallagher, Saw *et al.* 2013; Fan, Longnecker *et al.* 2014). However, how receptor-activated gD transmits the fusion triggering signal to the other glycoproteins remains largely unknown. Functional studies on HSV-1 provide indirect evidence for physical and functional interaction between gD and gH/gL ectodomains, involving residues located within the gD PFD and the two amino (N)-terminal domains of gH (Atanasiu, Whitbeck *et al.* 2007; Avitabile, Forghieri *et al.* 2007; Fan, Longnecker *et al.* 2014; Fan, Longnecker *et al.* 2015).

During infection within the host, herpesviruses can disseminate by direct spread from an infected cell to a non-infected neighboring cell (cell-to-cell spread) (see section 1.4). While the requirements for gD receptor interaction in entry of free virions are the same as during cell-to-cell spread in HSV (Pertel, Fridberg *et al.* 2001), direct cell-to-cell spread of PrV, including transsynaptic spread in animals, can occur independently of gD (Rauh and Mettenleiter 1991; Peeters, de Wind *et al.* 1992; Mulder, Pol *et al.* 1996). This phenomenon has been exploited for reversion analyses of gD-negative PrV mutants in cell culture (Schmidt, Klupp *et al.* 1997; Schmidt, Gerdts *et al.* 2001). After passage of cells infected with gD-deleted PrV mutants, gH and gB acquired compensatory mutations, which supported efficient gD-independent entry (Schmidt, Gerdts *et al.* 2001). Moreover, mutations in gH and/or gB have also been shown to compensate for absence of gD receptors during HSV-1 or BoHV-1 entry and cell-cell fusion in *in vitro* cell fusion assays (Schröder, Linde *et al.* 1997; Atanasiu, Cairns *et al.* 2013; Uchida, Chan *et al.* 2013; Gatta, Petrovic *et al.* 2015; Atanasiu, Saw *et al.* 2016; Petrovic, Gianni *et al.* 2017). These studies demonstrated that essential functions encoded in gD can be compensated for and, thus, implies that gD is not central to the fusion process. Other alphaherpesviruses such as VZV

lack a gD homolog (Davison and Scott 1986). In VZV, the receptor binding function is mediated by glycoprotein E (Li, Krogmann *et al.* 2007).

According to the current model, the proposed direct interaction between gD and gH/gL ectodomains leads to conformational changes in the heterodimer, enabling it to activate the *bona fide* fusion protein gB (see Fig. 3) (Atanasiu, Saw *et al.* 2010; Chowdary, Cairns *et al.* 2010; Eisenberg, Atanasiu *et al.* 2012; Stampfer and Heldwein 2013; Atanasiu, Saw *et al.* 2016). Although gB has been identified as a class III fusion protein (see section 1.2), it depends on the gH/gL complex for fusion. However, the detailed function of the heterodimer is only incompletely understood.

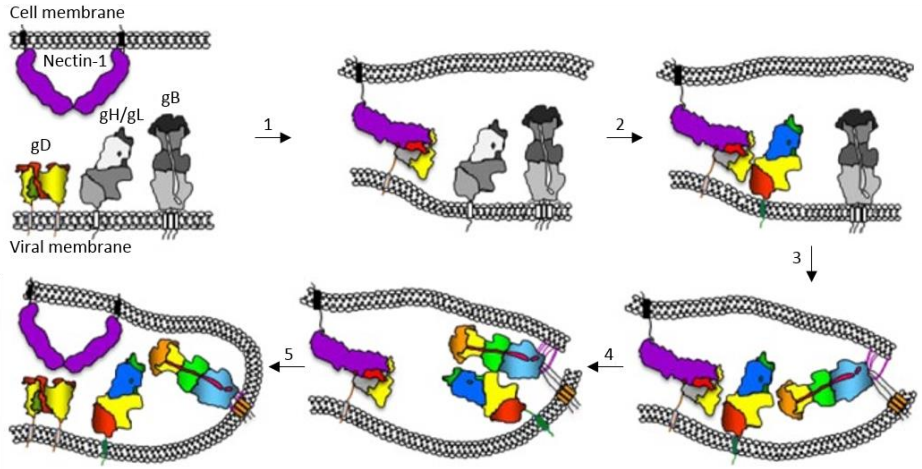

Figure 3: Schematic diagram of the proposed sequential events leading to alphaherpesvirus entry. (1) Binding of gD to specific cellular receptors (nectin-1 is shown) initiates the entry process. (2) Receptor binding triggers a conformational change in gD enabling it to interact with gH/gL. (3) This interaction leads to a conformational change in gH/gL which then interacts with gB to upregulate it into a fusogenic state. This process may involve interaction of gB with a cell surface protein, insertion of the gB fusion loops into the opposing lipid membrane and (4) interaction between the ectodomains of gH/gL and gB. (5) This converts gB from a pre- to a postfusion form, resulting in fusion of the viral envelope with cellular membranes and delivery of the nucleocapsid into the cell. The proteins were drawn based on published structures with the corresponding domains. Where prefusion structures were not available, the proteins are shown in gray. Adapted from (Eisenberg, Atanasiu et al. 2012).

1.3.2.2 Structure and role of the gH/gL complex

gH is a type I transmembrane protein consisting of a signal peptide, a large N-terminal ectodomain and a short cytoplasmic domain (CD). In contrast, gL lacks a membrane anchor and is noncovalently associated with the gH ectodomain, forming the heterodimeric gH/gL complex (Klupp, Visser *et al.* 1992; Klupp, Baumeister *et al.* 1994; Chowdary, Cairns *et al.* 2010; Matsuura, Kirschner *et al.* 2010; Eisenberg, Atanasiu *et al.* 2012; Xing, Oliver *et al.* 2015). Due to its lack of a membrane anchor gL is dependent on association with gH for virion incorporation (Hutchinson, Browne *et al.* 1992; Kaye, Gompels *et al.* 1992; Liu, Gompels *et al.* 1993; Klupp, Baumeister *et al.* 1994). However, while gL is required for correct folding and transport of gH in most herpesviruses, including HSV-1, Epstein-Barr virus (EBV, *Human gammaherpesvirus 4*), and VZV (Roop, Hutchinson *et al.* 1993; Yaswen, Stephens *et al.* 1993; Duus and Grose 1996;

Chowdary, Cairns *et al.* 2010), it is not essential for gH virion incorporation in PrV, BoHV-4, *Murid gammaherpesvirus* 4, and HSV-2 (Klupp, Fuchs *et al.* 1997; Cairns, Friedman *et al.* 2007; Gillet, May *et al.* 2007; Lete, Machiels *et al.* 2012). Nevertheless, presence of gL is required for herpesvirus entry (Klupp, Fuchs *et al.* 1997; Cairns, Friedman *et al.* 2007), but its function during this process remains largely elusive. HSV-1 gH/gL has been shown to use αvβ6- and αvβ8-integrins as receptors, regulating the route and timing of infection (Gianni, Salvioli *et al.* 2013; Cooper and Heldwein 2015). In the presence of receptor-bound gD and gB, binding of HSV-1 gH/gL to integrins has been shown to promote gL dissociation from gH (Gianni, Massaro *et al.* 2015). Therefore, gL was hypothesized to act as a regulator of gH preventing its premature activation (Gianni, Massaro *et al.* 2015). Dissociated HSV-1 gL has been recently suggested to regulate restoration of the membrane asymmetry after viral entry through binding to phospholipid scramblase-1 (Cheshenko, Pierce *et al.* 2018).

Although gL is required for entry, gL-deleted PrV is capable of limited cell-to-cell spread, which has been used for reversion analysis by repeated passages in cell culture (Klupp and Mettenleiter 1999). After several passages a phenotypic revertant, designated PrV-ΔgLPass, was isolated, which had regained wild-type like replication properties. Interestingly, instead of wild-type gH, PrV-ΔgLPass was found to express a gDgH hybrid protein, which lacked the predicted gL-interaction domain of gH, and consisted of the N-terminal 271 amino acids (aa) of gD, including the receptor binding domain, fused to the C-terminal 590 aa of gH. The gDgH chimera was able to substitute for gL, gH and gD in virus entry and cell-cell fusion assays (Klupp and Mettenleiter 1999; Klupp, Nixdorf *et al.* 2000). In contrast to PrV, no gL-negative infectious virus mutants have been reported in the *Simplexviruses* (Cairns, Milne *et al.* 2003). To understand the gH/gL function in more detail, a second PrV mutant, replicating productively without gL, was characterized in the present thesis (section 5.2, **paper II**).

The gH/gL heterodimer is proposed to play a role in regulation of gB fusogenicity (Roche, Bressanelli *et al.* 2006; Backovic, Longnecker *et al.* 2009; Backovic, DuBois *et al.* 2010; Chowdary, Cairns *et al.* 2010; Matsuura, Kirschner *et al.* 2010; Atanasiu, Cairns *et al.* 2013; Xing, Oliver *et al.* 2015; Atanasiu, Saw *et al.* 2016). Physical interactions between HSV gH/gL and gB have been suggested using coflotation liposome binding assays (Cairns, Whitbeck *et al.* 2011) and bimolecular fluorescence complementation (BiFC) (Atanasiu, Whitbeck *et al.* 2007; Avitabile, Forghieri *et al.* 2007; Avitabile, Forghieri *et al.* 2009). The BiFC studies indicated that HSV-1 gB and gH/gL, fused to fragments of fluorescent proteins, interact in transfected cells. However, receptor binding of gD was shown to be necessary for the interaction (Atanasiu, Whitbeck *et al.* 2007; Avitabile, Forghieri *et al.* 2007; Avitabile, Forghieri *et al.* 2009). For membrane fusion, a

direct interaction between the ectodomains of gH/gL and gB has been proposed (Atanasiu, Saw *et al.* 2010).

Despite low gH sequence conservation even within the alphaherpesvirus subfamily, the crystal structures of the gH/gL ectodomains of HSV-2 (Chowdary, Cairns *et al.* 2010), EBV (Matsuura, Kirschner *et al.* 2010), VZV (Xing, Oliver *et al.* 2015), and of a core fragment of PrV gH (Backovic, DuBois *et al.* 2010) reveal a strikingly similar four-domain organization (Fig. 4) (Backovic, DuBois *et al.* 2010). Although experimental evidence indicate that gH/gL may act as a fusion protein (Galdiero, Falanga *et al.* 2005; Galdiero, Falanga *et al.* 2007), the structures do not resemble any known viral fusion protein.

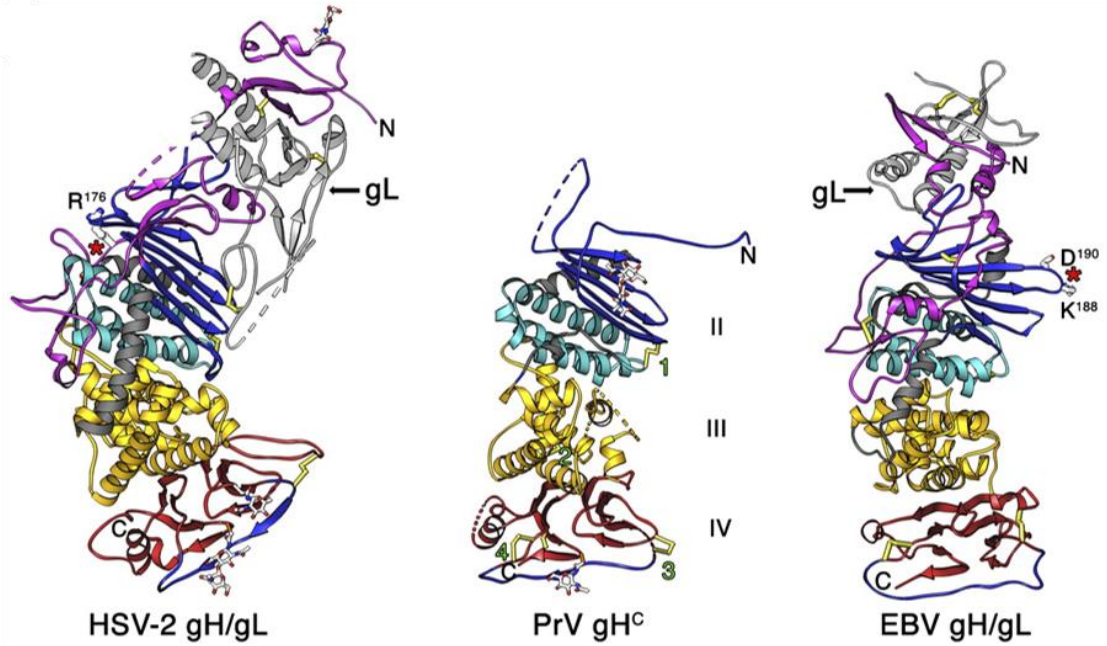

Figure 4: Domain organization of the PrV gH-core fragment (gH^C) and comparison to HSV-2 and EBV homologs. The molecules were structurally aligned on the SLB (cyan) and are displayed in the same orientation. N- and C-termini are labeled. The gH N domain is shown in magenta and gL in pale gray, which together constitute domain I, which is missing in PrV gH^C. In domain II, the conserved structural elements, fence and SLB, are highlighted in blue and cyan, respectively, with the remainder in gray. Domain III is colored in yellow and domain IV in red with the flap highlighted in blue. Green numbers mark the four disulfide bonds in PrV gH. The glycans are displayed as sticks. Regions which do not have a superposable counterpart in the different structures are colored in dark gray. The integrin binding sites in HSV-2 and EBV gH are indicated with red stars. Adapted from (Backovic, DuBois *et al.* 2010).

The least conserved N-terminal gH domain I (Fig. 4, purple), which was not included in the PrV gH-core fragment, has been shown to form tight contacts with gL for HSV-2 and EBV (Chowdary, Cairns *et al.* 2010; Matsuura, Kirschner *et al.* 2010). The functional importance for gL binding and membrane fusion of this structurally uncharacterized domain in PrV gH was investigated in this thesis (section 5.3, **paper III**).

gH domain II contains two structurally conserved elements. A sheet of five antiparallel beta-chains termed “fence” (Fig. 4, blue) is connected to a bundle of three α-helices. Due to its structural similarities to the N-terminal domain of the eukaryotic fusion proteins syntaxin 1A and 6, this 3-helix structure has been designated as syntaxin-like bundle (SLB; Fig. 4, cyan)

(Backovic, DuBois *et al.* 2010). Although this parallel with intracellular vesicle fusion is intriguing, there is no evidence for a large conformational change in gH, which would lead to exposure of this motif for oligomerization or interaction with membranes (Backovic, DuBois *et al.* 2010). However, the integrity and flexibility of the SLB are relevant for the function of PrV gH in membrane fusion (Böhm, Eckroth *et al.* 2015). gH domains I and II have been proposed to functionally interact with gD in HSV-1 (Fan, Longnecker *et al.* 2015). However, the interaction has been suggested to be transient or weak (Atanasiu, Whitbeck *et al.* 2007; Avitabile, Forghieri *et al.* 2007; Fan, Longnecker *et al.* 2015).

Domain III (Fig. 4, yellow) is composed of eight consecutive α-helices comprising a highly conserved amino acid stretch (^{437}serine-proline-cysteine^{439}). Cysteine (C) in this stretch is involved in the formation of a strictly conserved disulfide bond (in PrV between C439 and C404), which has been shown to be important for regulation of membrane fusion (Backovic, DuBois *et al.* 2010; Schröter, Klupp *et al.* 2014; Möhl, Schröter *et al.* 2015). Moreover, the gB-binding site on gH has been suggested to be located in domain III, since the epitope of neutralizing antibody LP11, which blocks interaction of gB with gH/gL and thereby prevents fusion, maps in this region (Chowdary, Cairns *et al.* 2010). However, the exact binding site has not been determined.

The most conserved region of gH is the membrane proximal domain IV (Fig. 4, red), which consists of a beta-sandwich comprising two opposed four-stranded beta-sheets, which are connected via a long crossover segment, termed “flap” (Fig. 4, blue) (Backovic, DuBois *et al.* 2010). The flap, supported by an asparagine (N)-linked glycan at position 627 in PrV gH, whose functional relevance was investigated in this thesis (section 5.5, **paper V**), covers a conserved patch of hydrophobic amino acids. Movement of the flap during a receptor-triggered conformational change of gH has been proposed to enable interaction of the underlying hydrophobic surface with the viral envelope to promote membrane fusion (Backovic, DuBois *et al.* 2010; Fuchs, Backovic *et al.* 2012). In line, mutagenesis studies have revealed functional relevance (Fuchs, Backovic *et al.* 2012) but also functional conservation (Böhm, Backovic *et al.* 2016) of domain IV between PrV and HSV-1.

Important roles have also been ascribed to the structurally uncharacterized TMD and the short CD of gH (19 aa in PrV; 14 aa in HSV-1). Mutations in the HSV-1 gH TMD, substitution by analogous domains from other glycoproteins, or replacement by a lipid-anchor resulted in non-functional proteins (Harman, Browne *et al.* 2002; Jones and Geraghty 2004). The CDs of HSV-1, VZV and EBV gH have been implicated in regulation of gB fusogenicity (Browne, Bruun *et al.* 1996; Harman, Browne *et al.* 2002; Pasieka, Maresova *et al.* 2003; Suenaga, Satoh *et al.* 2010; Yang, Arvin *et al.* 2014; Rogalin and Heldwein 2015; Chen, Jardetzky *et al.* 2016). Functional studies on HSV support a model in which the gH CD would directly interact with the gB CD by

acting as a “wedge” to release the fusion restricting gB CD “clamp” (see section 1.3.2.3), allowing gB to execute membrane fusion (Rogalin and Heldwein 2015). The gH CD of VZV, however, was hypothesized to act as a “gate keeper”, controlling access to functional domains of neighboring proteins, thereby *e.g.*, allowing or preventing phosphorylation of the gB CD (Yang, Arvin *et al.* 2014). However, despite functional significance of the TMD and CD of gH, a soluble form of HSV-1 gH, lacking both domains, was able to induce low levels of fusion in a cell-based fusion assay (Atanasiu, Saw *et al.* 2010), whereas this was not observed for EBV (Kirschner, Omerovic *et al.* 2006; Rowe, Connolly *et al.* 2013). The functional relevance of the PrV gH TMD and CD for membrane fusion was analyzed in this thesis (section 5.4, **paper IV**).

1.3.2.3 gB and its role in herpesvirus entry

Despite the apparent variation in the initial fusion trigger, herpesvirus fusion mechanisms converge at the point of gB activation by the gH/gL complex (Cooper and Heldwein 2015). gB is the most highly conserved herpesvirus glycoprotein and has been suggested to be the *bona fide* fusion protein due to structural similarities with the otherwise unrelated VSV G (Roche, Bressanelli *et al.* 2006). Together with VSV G (Roche, Bressanelli *et al.* 2006) and baculovirus gp64 (Kadlec, Loureiro *et al.* 2008) gB has been classified as class III fusion protein (Heldwein, Lou *et al.* 2006; Backovic, Longnecker *et al.* 2009; Burke and Heldwein 2015; Chandramouli, Ciferri *et al.* 2015; Li, Yang *et al.* 2017). By comparison with other class III fusion proteins, gB appears to contain all features necessary to effect fusion (Cooper and Heldwein 2015), raising the legitimate question as to why it is reliant on gH/gL for fusion.

Herpesvirus gB is a type I transmembrane protein, composed of a large ectodomain, a hydrophobic membrane proximal region (MPR), a single-span TMD, and a CD. The crystal structures of the postfusion ectodomains of gB of HSV-1 (Heldwein, Lou *et al.* 2006), EBV (Backovic, Longnecker *et al.* 2009), HCMV (Burke and Heldwein 2015; Chandramouli, Ciferri *et al.* 2015) and PrV (section 5.6, **paper VI**) (Li, Yang *et al.* 2017), reveal a spike-like trimer, in which each of the three protomers is arranged into a hairpin structure (Fig. 5B). This hairpin architecture is common to the postfusion structures of viral fusion proteins from all classes (Kielian and Rey 2006).

The gB postfusion trimer is stabilized by multiple inter-subunit contacts, which are established by domains I-V (Fig. 5, blue to red) of each of the three protomers, which twist around the equivalent regions of their counterparts (Heldwein, Lou *et al.* 2006; Backovic and Jardetzky 2009; Backovic, Longnecker *et al.* 2009; Burke and Heldwein 2015; Chandramouli, Ciferri *et al.* 2015; Cooper and Heldwein 2015; Li, Yang *et al.* 2017; Vallbracht, Brun *et al.* 2017).

Fusion activated gB is thought to undergo large conformational rearrangements unmasking the initially buried hydrophobic segments termed fusion loops, for interactions with the target membrane. The gB ectodomain contains two putative FLs, which are located in domain I (Fig. 5, blue) and exposed at the base of the molecule adjacent to the C-terminus of the ectodomain (Fig. 5, black asterisks) (Heldwein, Lou *et al.* 2006; Backovic, Longnecker *et al.* 2009; Burke and Heldwein 2015; Chandramouli, Ciferri *et al.* 2015; Li, Yang *et al.* 2017; Vallbracht, Brun *et al.* 2017). Since the amino acid sequences of herpesvirus gB FLs are poorly conserved compared to FLs in other class III fusion proteins, their identification was difficult until structural data became available. Based on structural homology with the well-defined FLs of the VSV G protein (Sun, Belouzard *et al.* 2008; Baquero, Albertini *et al.* 2015), the two loops exposed at the tips of the crystallized HSV-1 gB ectodomain (Heldwein, Lou *et al.* 2006) were suggested to form the FLs. This hypothesis was confirmed by extensive mutagenesis studies demonstrating the importance of several hydrophobic residues within the two loops, as well as polar and charged residues at the sides of FL2 for membrane binding and fusion (Hannah, Heldwein *et al.* 2007; Lin and Spear 2007; Hannah, Cairns *et al.* 2009; Maurer, Zeev-Ben-Mordehai *et al.* 2013). Exposure of the FLs in HSV-1 gB has been proposed to be regulated by the MPR (Shelly, Cairns *et al.* 2012). The structure of PrV gB and the molecular details of how its FLs insert into the lipid bilayer were investigated in this thesis (section 5.4, **paper VI**).

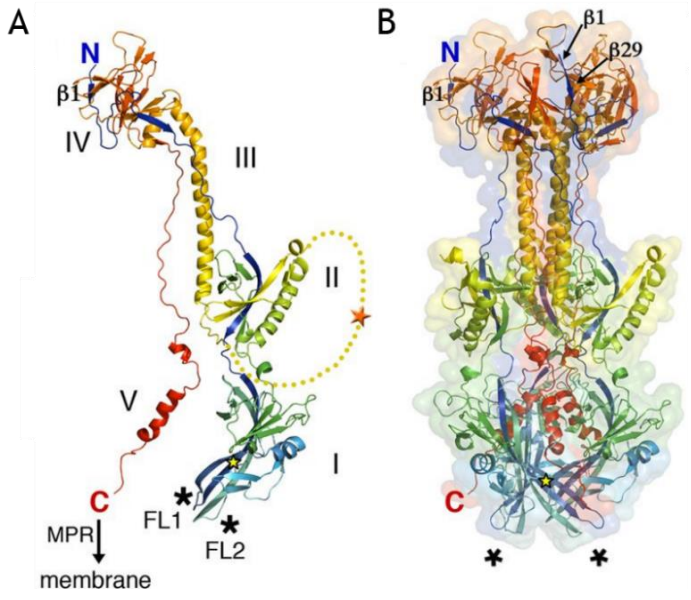

Figure 5: PrV gB ectodomain structure. Structure of the PrV gB monomer (A) and trimer (B). Ribbon and molecular-surface representations are shown. gB ectodomains I-V are colored from blue (N-terminus) to red (C-terminus). N- and C-termini are labeled and domains are numbered (I to V). Fusion loops (FL) are marked by black asterisks. The orange star indicates the putative location of the furin cleavage site. MPR: membrane proximal region. Adapted from (Vallbracht, Brun *et al.* 2017).

Domain II (Fig. 5, green) adopts a fold reminiscent of the pleckstrin homology (PH) domain. This is suggestive of interactions with lipids or proteins (Heldwein, Lou *et al.* 2006; Eisenberg, Atanasiu *et al.* 2012) since these domains, present in a variety of cellular proteins, allow phosphoinositide and peptide binding (Blomberg, Baraldi *et al.* 1999; Lemmon 2007). This region in gB has been suggested to be involved in interaction with gH/gL, since certain monoclonal

antibodies which bind to this domain (Cairns, Fontana *et al.* 2014), prevented association with gH/gL (Atanasiu, Whitbeck *et al.* 2010; Eisenberg, Atanasiu *et al.* 2012).

In contrast to HSV gB, processing of PrV gB involves proteolytic cleavage by cellular furin, whose cleavage site is located in a flexible linker connecting domains II and III (Li, Yang *et al.* 2017; Vallbracht, Brun *et al.* 2017) (Fig. 5A, orange star). However, cleavage of gB by furin is dispensable for gB function (Kopp, Blewett *et al.* 1994; Strive, Borst *et al.* 2002; Okazaki 2007).

Domain III contains the prominent, centrally located α-helix, which together with the α-helices from two other protomers form the trimeric α-helical coiled-coil core, characteristic for class III fusion proteins (Backovic and Jardetzky 2009). The central α-helix extends to the top or "crown" domain of the molecule, which is formed by domain IV (Fig. 5, orange) (Heldwein, Lou *et al.* 2006; Backovic, Longnecker *et al.* 2009; Burke and Heldwein 2015; Chandramouli, Ciferri *et al.* 2015; Li, Yang *et al.* 2017; Vallbracht, Brun *et al.* 2017).

Domain V extends from one end of the molecule to the other and packs tightly into the groove formed by the other two protomers, resulting in an extensive trimerization interface (Fig 5, red) (Heldwein, Lou *et al.* 2006; Backovic and Jardetzky 2009; Vallbracht, Brun *et al.* 2017). The long C-terminal arm of this domain has been shown to pack against the coiled-coil core in an antiparallel fashion, forming the so called "coil-arm complex". This complex is reminiscent of the six-helix bundle, which provides the energy for fusion mediated by class I fusion proteins (White, Delos *et al.* 2008). Therefore, the complex has been proposed to perform a similar function in HSV gB (Heldwein, Lou *et al.* 2006; Connolly and Longnecker 2012; Fan, Kopp *et al.* 2017). Mutations within the C-terminal arm of domain V reduced fusion activity without affecting protein expression and, therefore, were suggested to destabilize the postfusion conformation or stabilize the prefusion conformation of gB (Fan, Kopp *et al.* 2017).

In contrast to the well characterized postfusion conformation of the gB ectodomain, a high-resolution structure of the prefusion state has not been obtained yet. Despite extensive effort made to destabilize the postfusion trimer (Vitu, Sharma *et al.* 2013), or to stabilize prefusion gB (Silverman, Sharma *et al.* 2010), soluble forms of the gB ectodomain never adopted a putative prefusion conformation (Baquero, Albertini *et al.* 2015). Therefore, it was hypothesized that other regions of gB, such as the MPR, the TMD, and/or the CD, are necessary to establish and maintain the metastable prefusion conformation (Vitu, Sharma *et al.* 2013). Recently, the full-length HSV-1 gB has been characterized in cell-derived vesicles using electron cryotomography, revealing, in addition to the known trimeric postfusion form, a shorter and more condensed conformation of gB, possibly representing a putative prefusion conformation (Zeev-Ben-Mordehai, Vasishtan *et al.* 2016). In this conformation, the gB FLs have been reported to be apart and pointing away from the viral membrane (Zeev-Ben-Mordehai, Vasishtan *et al.* 2016).

In contrast, a second, similarly condensed form of gB has been reported, in which the FLs were found to point towards the anchoring membrane (Fontana, Atanasiu *et al.* 2017). However, whether these forms represent gB in an intermediate, or prefusion conformation and whether gH/gL is required to maintain gB in its metastable form, remains unclear (Zeev-Ben-Mordehai, Vasishtan *et al.* 2016; Fontana, Atanasiu *et al.* 2017).

While the fusogenic function of gB appears to reside in its ectodomain, the adjoining MPR, TMD and CD play key roles in the regulation of gB fusogenicity. The TMD and MPR have both been shown to be essential for correct folding, transport, and function of HSV-1 gB (Cai, Person *et al.* 1988; Rasile, Ghosh *et al.* 1993; Gilbert, Ghosh *et al.* 1994; Zheng, Maidji *et al.* 1996; Lin and Spear 2007; Silverman, Greene *et al.* 2012). Moreover, the HSV gB TMD has been proposed to play an essential role in the later stages of fusion, since replacement by a lipid-anchor resulted in fusion arrest at the hemifusion stage (Jones and Geraghty 2004).

The individually expressed CD of HSV-1 gB forms trimers, which associate stably with lipid membranes (Chowdary and Heldwein 2010). Moreover, the presence of a membrane has been demonstrated to be required for the trimeric CD to adopt its fully folded conformation (Silverman, Greene *et al.* 2012). Therefore, the ability to stably bind to lipid membranes has been proposed to be a key feature of the CD essential for its structural organization and function to regulate gB fusogenicity (Chowdary and Heldwein 2010; Silverman, Greene *et al.* 2012). Only recently, the crystal structure of full length HSV-1 gB was determined, demonstrating that the MPR, TMD and CD form a trimeric pedestal underneath the ectodomain (Cooper, Georgieva *et al.* 2018). The gB CD was shown to form an intertwined trimer (Cooper, Georgieva *et al.* 2018), which appears to negatively regulate fusion, since both naturally occurring and engineered point mutations, truncations, or insertions, were found to enhance the fusion activity of gB of different herpesviruses including PrV (Klupp, Nixdorf *et al.* 2000; Nixdorf, Klupp *et al.* 2000), HSV (Gage, Levine *et al.* 1993; Foster, Melancon *et al.* 2001; Diakidi-Kosta, Michailidou *et al.* 2003; Ruel, Zago *et al.* 2006), VZV (Heineman and Hall 2002), and EBV (Haan, Lee *et al.* 2001; Garcia, Chen *et al.* 2013; Chen, Jardetzky *et al.* 2016). Mutations in the gB CD, found to increase gB fusogenicity, have been proposed to either act by disrupting the interaction of the CD with the membrane or the inter-protomer contacts preventing the CD from adopting its fully folded conformation (Chowdary and Heldwein 2010; Cooper, Georgieva *et al.* 2018). Thus, it was hypothesized that the HSV-1 gB CD acts a clamp, which braces against the viral membrane, and thereby stabilizes the gB prefusion form (Vitu, Sharma *et al.* 2013; Cooper and Heldwein 2015; Rogalin and Heldwein 2015; Cooper, Georgieva *et al.* 2018). Overall, fusion mediated by alphaherpesviruses is a precisely regulated process in which the CD of gB is apparently of critical importance.

1.4 Direct viral cell-to-cell spread and *in vitro* fusion assays

PrV and other herpesviruses, such as HSV, can infect cells via two distinct routes, either through attachment and subsequent entry of extracellular virions (cell-free spread) or through spread via direct cell-cell contact while remaining cell associated. The latter mode is referred to as “direct cell-to-cell spread”, which is mechanistically only poorly understood (Cocchi, Menotti *et al.* 2000; Sattentau 2008; Mothes, Sherer *et al.* 2010; Miranda-Saksena, Denes *et al.* 2018). Early evidence for direct cell-to-cell spread was the fact that viruses were able to spread in the presence of neutralizing antibodies, which completely block the spread of cell-free virus (Mothes, Sherer *et al.* 2010). Thus, by spreading directly from infected to uninfected cells, herpesviruses have been proposed to be able to evade immunological, but also biophysical and kinetic barriers (Sattentau 2008).

Several studies using glycoprotein deficient PrV and HSV mutants revealed that the mechanisms for entry of free virions and direct cell-to-cell spread are similar, but not identical. In PrV the two processes can be clearly separated by the requirements for gD. As noted above (section 1.3.2.1), gD deficient virus mutants are not infectious as extracellular particles but capable of spreading by cell-cell contact *in vitro* (Rauh and Mettenleiter 1991; Peeters, de Wind *et al.* 1992). A similar situation has been shown to occur *in vivo*. Whereas gD is essential for entry of PrV, cell-cell spread and also transsynaptic spread of PrV in mice and pigs occurs independent of gD (Babic, Mettenleiter *et al.* 1993; Mulder, Pol *et al.* 1996). Conversely, PrV and HSV mutants lacking the gE/gI complex efficiently enter cells, but are unable to efficiently disseminate by direct cell-to-cell spread *in vivo* (Dingwell, Brunetti *et al.* 1994; Enquist, Dubin *et al.* 1994; Kritas, Pensaert *et al.* 1994; Dingwell, Doering *et al.* 1995; Mulder, Pol *et al.* 1996; Farnsworth and Johnson 2006). The gE/gI complex localizes to cell-cell junctions, favoring the spread of virions across these junctions *in vitro* (Dingwell and Johnson 1998) and *in vivo* (Dingwell, Brunetti *et al.* 1994). It has been hypothesized that gE/gI promotes cell-to-cell spread by binding to unknown receptors, which are specific to tight junctions (Johnson, Webb *et al.* 2001; Polcicova, Goldsmith *et al.* 2005; Farnsworth and Johnson 2006). Like HSV-1 gE, HSV-1 gD accumulates at junctions between epithelial cells, where it interacts with nectin-1 (Krummenacher, Baribaud *et al.* 2003). In contrast to PrV, direct cell-to-cell spread of HSV requires gD and a gD receptor (Pertel, Fridberg *et al.* 2001).

Herpesviruses have evolved at least two mechanisms to spread directly from cell-to-cell. As noted above, they can either utilize already existing cell-cell contacts, such as neurological synapses or establish a new contact by inducing fusion of two adjacent cells. The latter mode could result in formation of multinucleated cells, termed syncytia, or might be restricted to localized “microfusion” events, which would allow the maintenance of structural independence

of the cells (Sattentau 2008; Zhong, Agosto *et al.* 2013; Mateo, Generous *et al.* 2015). The existence of small fusion pores between PrV infected neurons has been demonstrated by transfer of a low molecular weight dye (McCarthy, Tank *et al.* 2009). Whereas induction of large syncytia is a hallmark of infections with *e.g.*, the extremely cell-associated VZV (Esiri and Tomlinson 1972; Litwin, Jackson *et al.* 1992; Harson and Grose 1995; Pasieka, Maresova *et al.* 2004), HSV infection usually does not result in syncytia formation *in vivo* (Read, Person *et al.* 1980). However, some clinical HSV isolates with mutations in several glycoproteins (*i.a*. gB) have been found to form syncytia (Cai, Gu *et al.* 1988; Baghian, Huang *et al.* 1993; Engel, Boyer *et al.* 1993; Gage, Levine *et al.* 1993; Diakidi-Kosta, Michailidou *et al.* 2003).

Induction of syncytia formation can also be achieved by transiently expressing the relevant proteins in susceptible cells *in vitro* in the absence of infection. Coexpression of the core fusion machinery components gB and gH/gL and receptor binding gD of PrV and HSV-1 and 2 has been shown to be necessary and sufficient to induce membrane fusion (Turner, Bruun *et al.* 1998; Klupp, Nixdorf *et al.* 2000; Muggeridge 2000; Fan, Grantham *et al.* 2002; McShane and Longnecker 2005). In contrast to HSV, induction of PrV membrane fusion has been shown to occur in the absence of gD (Klupp, Nixdorf *et al.* 2000). Thus, PrV gD is essential for entry, whereas direct cell-to-cell spread occurs efficiently in the absence of gD *in vitro* and *in vivo* (Rauh and Mettenleiter 1991; Peeters, de Wind *et al.* 1992; Mulder, Pol *et al.* 1996). In this regard, the transient transfection fusion system more closely resembles cell-to-cell spread than fusion during viral entry (Klupp, Nixdorf *et al.* 2000). In general, transient fusion assays are a useful tool to quantitate membrane fusion and to study the herpesvirus induced fusion process in the absence of infection. Different fusion assay systems have been developed, in which the evaluation or quantitation of fusion activity is often based on counting the number of nuclei within a syncytium (Turner, Bruun *et al.* 1998; Klupp, Nixdorf *et al.* 2000; Muggeridge 2000; Fan, Grantham *et al.* 2002; McShane and Longnecker 2005). In the present thesis, a transient transfection-based fusion assay protocol was established, facilitating evaluation (section 5.1, **paper I**).

2 Objectives

Herpesviruses are ubiquitous pathogens, which establish lifelong infections and cause a substantial disease burden (Davison, Eberle *et al.* 2009). They have been infecting their hosts for hundreds of millions of years and still prevention or treatment of herpesvirus infections pose a challenge in the 21st century (Field and Vere Hodge 2013). Herpesviruses must traverse the host-cell plasma membrane to succeed in infection. To meet this challenge, they have evolved specialized surface glycoproteins which mediate fusion of the virion envelope with the cellular membrane. The fusion process is mediated by the core fusion machinery, composed of the *bona fide* fusion glycoprotein gB, the presumably gB activating gH/gL heterodimer, and other species-specific receptor binding proteins like alphaherpesvirus gD (Eisenberg, Atanasiu *et al.* 2012). However, the molecular details of how this complex machinery accomplishes membrane fusion, remain enigmatic. Yet, a detailed mechanistic knowledge of this process would be important for the development of efficient countermeasures against a variety of diseases.

The aim of this thesis was three-fold: Firstly, a robust infection-free, transfection-based cell-fusion assay should be established, which can serve as useful surrogate for viral-cell and cell-cell fusion. With the aid of this assay, the requirements and capabilities of the alphaherpesvirus PrV fusion machinery components gB, gH/gL and gD to induce fusion should be investigated.

Despite its identification as a class III fusion protein, herpesvirus gB it not able to mediate membrane fusion autonomously but depends on the presence of the gH/gL heterodimer, whose detailed function remains largely unknown. Thus, secondly, the function of the essential gH/gL complex should be investigated in more detail by using two different approaches, reversion analysis and site-directed mutagenesis, to identify regions in gH important for membrane fusion. PrV provides the unique opportunity to investigate gH/gL function by reversion analysis of gL-negative, entry-deficient virus mutants by serial cell-culture passages. A first passaging experiment already resulted in isolation of an infectious gL-negative PrV mutant, in which the function of gL was compensated by generation of a gDgH hybrid protein (Klupp and Mettenleiter 1999). Here, a second gL-independently replicating virus mutant designated PrV-ΔgLPassB4.1 should be characterized to understand the requirements for gL-independent infectivity, and ultimately to shed more light on gL function, and on the actual role of gH during membrane fusion. Interestingly, gH expressed by gL-independently replicating mutants specifies compensatory mutations in the predicted gL-binding domain. This structurally uncharacterized part of gH should be investigated with respect to its function in membrane fusion. Moreover, it should be elucidated which other regions in gH are necessary to induce membrane fusion and whether gH needs to be firmly anchored in the membrane to fulfil its role. Thus, the functional

roles of the cytoplasmic domain, the transmembrane domain but also the importance of N-glycans in PrV gH were investigated.

Thirdly, the structure and function of the *bona fide* fusion gB of PrV should be investigated aiming at understanding the molecular mechanism of how the initial interaction between gB and the host cell membrane is established. In detail, it should be determined which amino acids in the gB fusion loops are important and, particularly, which properties of these key residues are needed to establish gB membrane anchorage and realize membrane fusion.

3 Publications

I

(I) Transient Transfection-based Fusion Assay for Viral Proteins

Melina Vallbracht, Christina Schröter, Barbara G. Klupp and Thomas C. Mettenleiter

Bio-Protocol

Volume 7, Issue 5

March 2017

doi: 10.21769/BioProtoc.2162

bio-protocol www.bio-protocol.org/e2162 Vol 7, Iss 05, Mar 05, 2017
DOI:10.21769/BioProtoc.2162

Transient Transfection-based Fusion Assay for Viral Proteins

Melina Vallbracht, Christina Schröter, Barbara G. Klupp and Thomas C. Mettenleiter*

Institute of Molecular Virology and Cell Biology, Friedrich-Loeffler-Institut, 17493 Greifswald-Insel Riems, Germany
*For correspondence: thomas.mettenleiter@fli.de

[Abstract] Membrane fusion is vital for entry of enveloped viruses into host cells as well as for direct viral cell-to-cell spread. To understand the fusion mechanism in more detail, we use an infection free system whereby fusion can be induced by a minimal set of the alphaherpesvirus pseudorabies virus (PrV) glycoproteins gB, gH and gL. Here, we describe an optimized protocol of a transient transfection based fusion assay to quantify cell-cell fusion induced by the PrV glycoproteins.

Keywords: Herpesvirus, Pseudorabies virus, Membrane fusion, Virus entry, Glycoproteins gB, gH/gL, Transfection

[Background] Membrane fusion is essential for entry and spread of enveloped viruses. Many enveloped viruses require only one or two viral proteins to mediate attachment to host cells and membrane fusion, and the molecular mechanisms are well understood (Harrison, 2015). In contrast, herpesviruses use a more complex mechanism requiring a receptor-binding protein and the core fusion machinery composed of gB and the heterodimeric gH/gL complex for infectious entry. The mechanism leading to fusion of herpesvirus envelopes with cellular membranes is only incompletely understood. Detailed knowledge of the molecular basis of herpesvirus entry and spread is important for efficient countermeasures against a variety of diseases. A better understanding is aided by studying the cell fusion activity of cells transiently expressing the relevant proteins. Different model systems, whereby fusion is induced with a minimal set of the core fusion machinery represented by glycoproteins gB and gH/gL and receptor-binding gD, in the absence of infection, have been developed, for example, for herpes simplex viruses type 1 and 2 (HSV-1 and 2 [Turner *et al.*, 1998; Muggeridge, 2000; McShane and Longnecker, 2005]). Unlike HSV-1 and 2, PrV does not require signaling of gD for membrane fusion during direct cell-to-cell spread, reducing the number of relevant proteins to three (Schmidt *et al.*, 1997). These systems are also used to quantify membrane fusion. However, the evaluation or quantitation of fusion activity, which is often based on counting the number of nuclei of a formed syncytium, is very time consuming. Our incentive to develop the present protocol was to improve the current protocol to facilitate and accelerate evaluation, and make results more robust and comparable by combining important factors like size and number of formed syncytia. Here, we describe an optimized protocol for an *in vitro* transient transfection based cell-cell fusion assay to quantify membrane fusion induced by the PrV glycoproteins gB and gH/gL (Schröter *et al.*, 2015). However, we know that this assay also is functional with other fusion-active glycoproteins, not just those of pseudorabies virus.

bio-protocol www.bio-protocol.org/e2162 Vol 7, Iss 05, Mar 05, 2017
DOI:10.21769/BioProtoc.2162

Materials and Reagents

1. 1.5 ml tubes (*e.g.*, Fisher Scientific, catalog number: S348903)
2. 24-well cell culture plate (*e.g.,* Corning, Costar®, catalog number: 3527)
3. Pipette tips 10 µl (TipOne) (STARLAB INTERNATIONAL, catalog number: S1110-3000)
4. Pipette tips 1 ml (Greiner Bio One International, catalog number: 740290)
5. Pipette tips 100 µl (Greiner Bio One International, catalog number: 739290)
6. *pcDNA3* (Thermo Fisher Scientific, Invitrogen)
   Note: pcDNA3 from Invitrogen is no longer available. Alternatively, pcDNA3.1(+) (Thermo Fisher Scientific, catalog number: V79020) can be used.
7. Rabbit kidney (RK13) cells (Collection of Cell Lines in Veterinary Medicine-RIE 109)
8. MEM Eagle (Hank's salts and L-glutamine) (Sigma-Aldrich, catalog number: M4642)
9. MEM (Earle's salts) (Thermo Fisher Scientific, catalog number: 61100061)
10. Sodium bicarbonate ($NaHCO_3$) (Carl Roth, catalog number: 6885.1)
11. NEA (nonessential amino acids) (Biochrom, catalog number: K 0293)
12. Na-pyruvate (EMD Millipore, catalog number: 106619)
13. Tris-HCl (pH 8.5)
14. Fetal bovine serum (FBS) (Biowest, catalog number: S181G)
15. Lipofectamine® 2000 reagent (Thermo Fisher Scientific, catalog number: 11668027)
16. Opti-MEM® reduced serum medium (Thermo Fisher Scientific, catalog number: 31985062)
17. Sodium chloride (NaCl) (Carl Roth, catalog number: 9265.1)
18. Potassium chloride (KCl) (Carl Roth, catalog number: 5346.1)
19. Dextrose (Sigma-Aldrich, catalog number: D9434)
20. Trypsin (1:250) powder (Thermo Fisher Scientific, catalog number: 27250018)
21. Ethylenediaminetetraacetic acid (EDTA) (SERVA Electrophoresis, catalog number: 11280.01)
22. Paraformaldehyde (Carl Roth, catalog number: 0335.1)
23. 10% growth media (see Recipes)
24. 3% paraformaldehyde (see Recipes)
25. 10 mM Tris HCl (pH 8.5) (see Recipes)
26. Alsever's-Trypsin Versen (ATV-) solution (see Recipes)

Note: Solutions and media #6, 11, 14, 15, 16, 21, 22, 23, 24 and 26 should be kept at 4 °C.

Equipment

1. T75 flask (*e.g.,* Corning, catalog number: 430725U)
2. Incubator (*e.g.*, Panasonic, Sanyo, model: MCO-19AIC or Fisher Scientific, catalog number: 12826756)
3. Fluorescence microscope (*e.g.,* Nikon Instruments, model: Eclipse Ti-S)
4. Super high pressure mercury lamp power supply (*e.g.,* Nikon Instruments, model: C-SCH1)

bio-protocol www.bio-protocol.org/e2162 Vol 7, Iss 05, Mar 05, 2017
DOI:10.21769/BioProtoc.2162

5. Light source (*e.g.,* Nikon Instruments, model: LH-M100C-1)
6. Vortexer (*e.g.*, Fisher Scientific, catalog number: S96461A)
7. Laminar flow hood (Thermo Fisher Scientific, Thermo Scientific™, model: Safe 2020 Class II, catalog number: 51026637)
8. Centrifuges for 1.5 ml tubes (*e.g.*, Eppendorf, model: 5415 D)
9. Pipette controller (*e.g.,* pipetboy acu 2, VWR, catalog number: 37001-856)
10. Nanophotometer (*e.g.,* VWR, IMPLEN, model: P330, catalog number: CA11027-294)

Software

1. Computer running software NIS-Elements V 4.00.01 (Nikon, Düsseldorf, Germany)

Procedure

A. Preparation of plasmids
   1. Dilute the plasmids expressing the putative fusion proteins to 200 ng/µl with Tris-HCl pH 8.5 (see Recipes). Include a plasmid expressing an autofluorescent protein (*e.g.*, GFP or mCherry) as a marker to facilitate evaluation of the assay. Here, a concentration of 100 ng/µl is sufficient.
      Note: The expression plasmids we use for our experiments are based on pcDNA3, a mammalian expression vector with constitutive transgene expression under control of the human cytomegalovirus immediate-early 1 promoter/enhancer complex and a neomycin-resistance pEGFP-N1 as marker to facilitate evaluation of the assay (Schröter et al., 2015).

B. Preparation of cells
   1. Grow rabbit kidney (RK13) cells in Eagle's minimum essential medium supplemented with 10% FBS. Trypsinize cells with ATV (Recipe 3) and seed ~1.8 x 10^5 cells per well onto 24-well cell culture dishes.
   2. On the following day, use cells for transfection. Cells should have a confluency of 80-90%.
      Note: Cell confluency for optimal transfection efficiency varies depending on the cell type. For RK13 and Vero cells 80-90% confluency is suggested.

C. Transfection
   1. Prepare DNA-mixture and Lipofectamine-mixture in separate tubes.
      a. DNA-mixture:
         Use 200 ng of each of the expression plasmids and dilute the DNA-mixture in 50 µl Opti-MEM.
      b. Lipofectamine-mixture:

bio-protocol www.bio-protocol.org/e2162 Vol 7, Iss 05, Mar 05, 2017
DOI:10.21769/BioProtoc.2162

Use 1 µl Lipofectamine 2000™ in 50 µl Opti-MEM per well. Add Lipofectamine drop-wise to 50 µl Opti-MEM and mix gently. Incubate Lipofectamine-mixture for 5 min at room temperature.

Note: The optimal amount of Lipofectamine varies depending on the cell type. For RK13 and Vero cells 1 µl per 24-well is suggested.

2. Add Lipofectamine-mixture drop-wise into DNA-mixture, gently tap the solution and incubate for 20 min at room temperature (RT) (Video 1).

   Note: It is important to mix gently but thoroughly to allow formation of the DNA-lipidcomplex.

Video 1. Tutorial: How to add Lipofectamine-mixture drop-wise to DNA-mixture

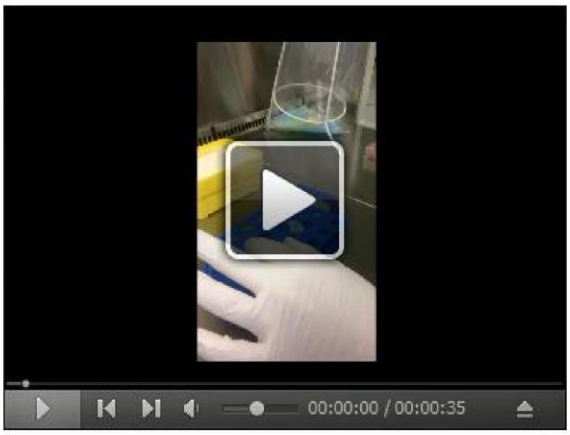

3. Remove media from the cells and add the transfection-solution drop-wise directly to the cell-monolayer (Video 2).

   Note: To allow equal distribution of the transfection-solution add it circularly drop-by-drop onto the monolayer (Video 2).

Video 2. Tutorial: How to add transfection solution to the cell-monolayer

bio-protocol www.bio-protocol.org/e2162 Vol 7, Iss 05, Mar 05, 2017
DOI:10.21769/BioProtoc.2162

4. Add an additional 200 µl Opti-MEM to the cells to prevent drying of cells.
5. Incubate cells at 37 °C and 5% CO_2 for 3 h.
6. After 3 h, remove the transfection-solution from the cells and add fresh MEM supplemented with 2% FBS to the cells and incubate them 18-24 h at 37 °C and 5% CO_2. For an overview of the whole procedure see Figure 1.

   Note: To achieve comparable results, use exactly the same incubation time in each experiment before fixing the cells.

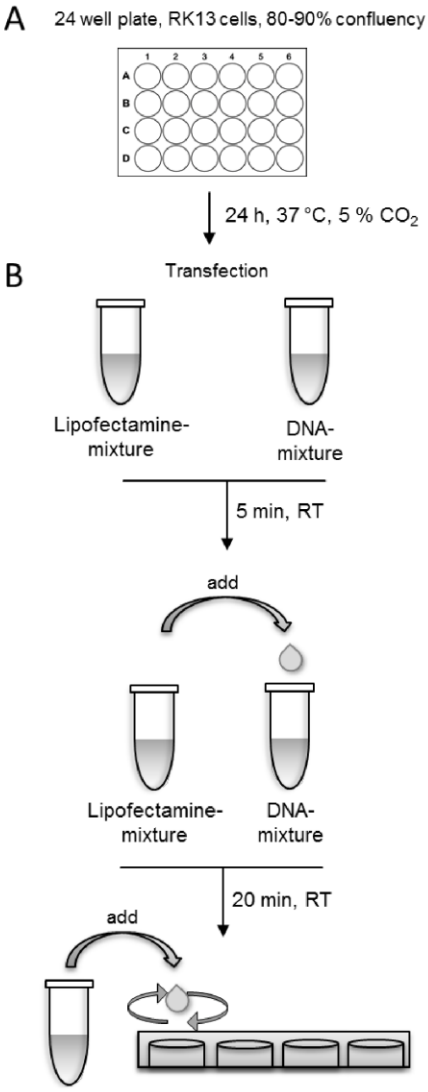

Figure 1. Schematic presentation of the transfection procedure

D. Fixation

1. Prepare 3% PFA (see Recipes).
2. Remove media and wash cell monolayer for 2 min with ~1 ml PBS per well using a rocker at RT.

bio-protocol www.bio-protocol.org/e2162 Vol 7, Iss 05, Mar 05, 2017
DOI:10.21769/BioProtoc.2162

3. Remove PBS and fix cells with 200 µl 3% PFA per well. Fix cells for 20 min at RT.
4. Wash cells 2 x with 1 ml PBS per well.
5. Add 1 ml PBS per well and store cells at 4 °C.

E. Determination of fusion activity

Note: To quantify fusion activity the number and the area of green-fluorescing syncytia with three or more nuclei is measured using a Nikon Eclipse Ti-S fluorescence microscope and Nikon NIS-Elements imaging software.

1. Use fixed cells for determination of fusion activity by fluorescence microscopy.
2. Open NIS-Elements imaging software (Nikon) and select corresponding type of fluorescence and objective (*e.g.,* FITC, 10x) (see Figure 2 red boxes).
3. Select Measure → Manual Measurement → Area (Figure 2A, Video 3).

   Note: NIS-Elements supports units including: pixels, nanometers, micrometers, millimeters, centimeters, decimeters, meters, inches, and mils. For our measurements we use micrometers.

bio-protocol www.bio-protocol.org/e2162 Vol 7, Iss 05, Mar 05, 2017
DOI:10.21769/BioProtoc.2162

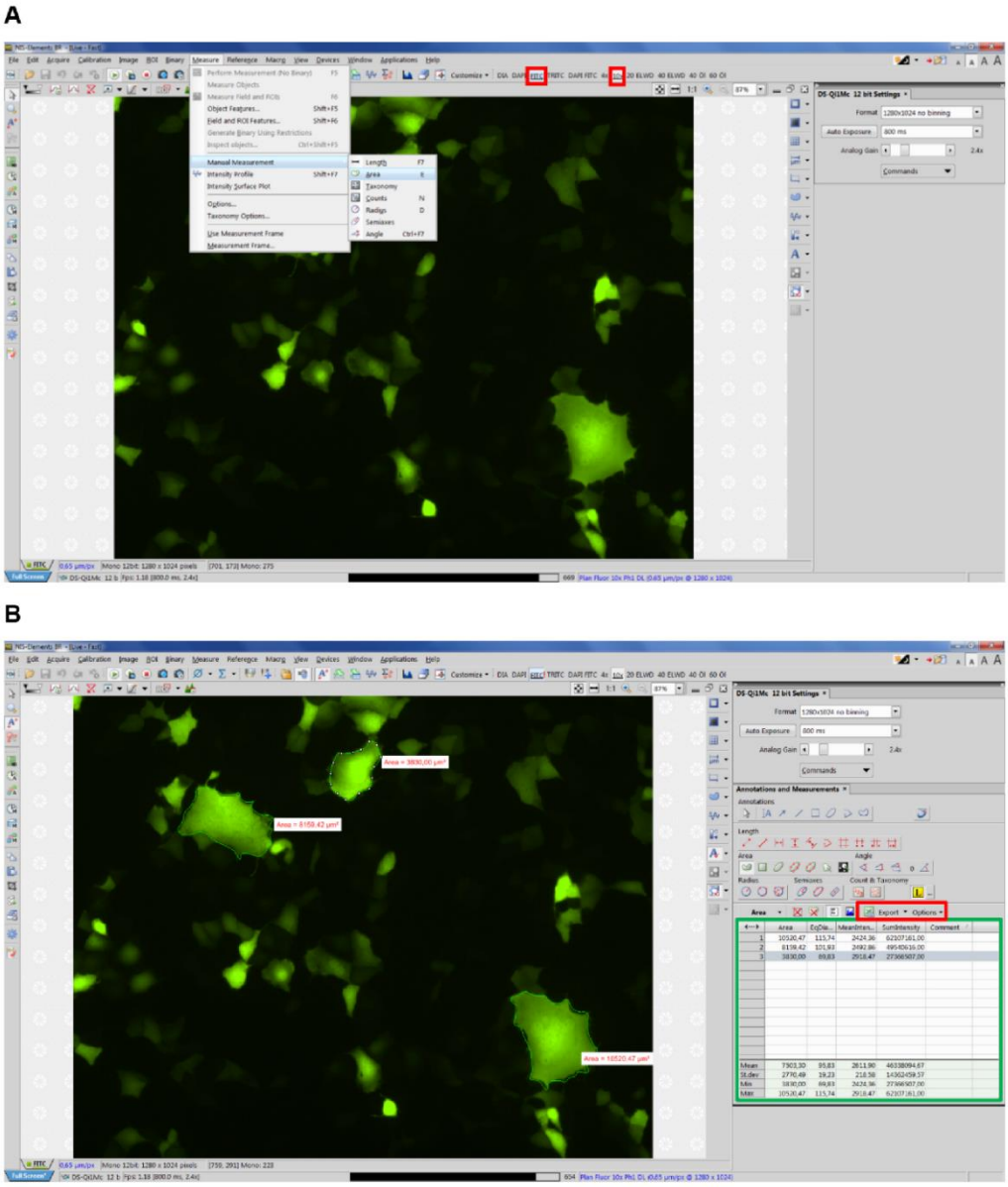

Figure 2. Example view of NIS Elements software. A. Selecting manual measurement; B. Exporting data.

Note: First, measure the area of syncytia on the right-hand corner of the screen, since each syncytium will be marked with a white icon on its right site, which can hinder the view over syncytia to the right of it (see Figure 2B).

4. Measure all apparent syncytia in 10 fields of view (~5.5 mm^2 each), each time starting in the top right-hand corner of the corresponding image. The data, including number of each syncytium as well as mean syncytia area will appear in a table on the lower right-hand corner (see Figure 2B green box, Video 3).

bio-protocol www.bio-protocol.org/e2162 Vol 7, Iss 05, Mar 05, 2017
DOI:10.21769/BioProtoc.2162

Video 3. Tutorial: How to measure syncytia with NIS Elements software

5. Export the data directly to an Excel file or a text file by clicking the export options button (see Figure 3 red box). (Select whether to export the data to an Excel file or a text file.) You can modify the name and path of the file via the browse button.
6. Repeat the entire experiment at least three times on three different days to calculate the relative fusion activity and corresponding standard deviations (SD).

Data analysis

1. To calculate the total fusion activity for each sample, corresponding to a given well, multiply the number of syncytia with the mean syncytia area of the 10 fields of view.
   E.g., you counted 107 syncytia and the mean syncytia area was 7,048 μm^2, the fusion activity would be 107 x 7,048.6 = 754,200.2.
2. Calculate the standard deviation (SD) of the total fusion activity of each sample by comparing the fusion activities estimated for each of the three independent experiments.
3. The relative fusion activity of the different samples is determined by comparing their total fusion activity to the positive control (*e.g.,* wild-type gB, gH and gL), which should be set as 100%.
   E.g., if the total fusion activity of the positive control is 754,200.2 and the fusion activity of the test sample was 431,708.6, the relative fusion activity of the test sample would be (100/754,200.2) x 431,708.6 = 57% (Figure 3).
   Note: Use Excel/Prism or comparable tools to facilitate calculations and create graphs.
4. Representative data

bio-protocol www.bio-protocol.org/e2162 Vol 7, Iss 05, Mar 05, 2017
DOI:10.21769/BioProtoc.2162

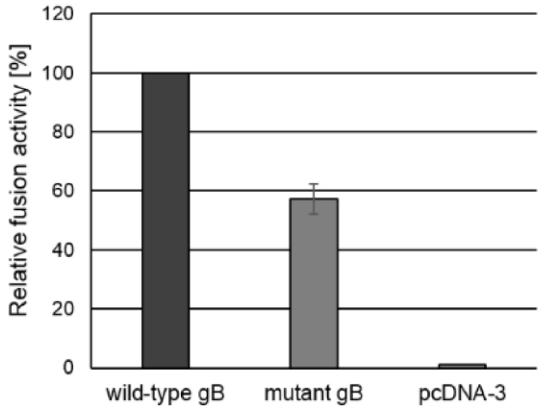

Figure 3. Fusion activity. To test for fusion activity RK13 cells were cotransfected with expression plasmids encoding wild-type gB or mutated gB, and gH, gL and gD as well as EGFP to facilitate evaluation of the assay by fluorescence microscopy. Assays conducted with a plasmid encoding wild-type gB in combination with wild-type gH, gL and gD were set as 100%. Assays with the empty expression vector pcDNA3 served as negative control. One day after transfection, the areas of cells containing three or more nuclei were measured and multiplied by the number of syncytia to determine the fusion activity. Corresponding standard deviations for three independent assays were calculated.

Recipes

1. 10% growth media (1 L), pH 7.2
   The following reagents should be dissolved in double distilled water to a final volume of 1 L:
   5.32 g MEM Eagle (Hank's salt)
   4.76 g MEM (Earle's salt)
   1.25 g $NaHCO_3$
   10 ml NEA
   120 mg Na-pyruvate
2. 10 mM Tris-HCl, pH 8.5
   Prepare 2 M stock solution (500 ml):
   121.14 g Tris HCl
   Adjust pH to 8.5 with ~50 ml fuming HCl
   Dilute stock solution 1:20 with ddH_2O
3. Alsever's-Trypsin Versen (ATV-)solution, pH 7.2
   8.5 g NaCl
   0.4 g KCl
   1.0 g dextrose
   0.58 g $NaHCO_3$
   0.5 g trypsin 1:250

bio-protocol www.bio-protocol.org/e2162 Vol 7, Iss 05, Mar 05, 2017
DOI:10.21769/BioProtoc.2162

0.2 g EDTA
Ad 1 L ddH_2O

4. 3% PFA (100 ml)
   3 g paraformaldehyde
   100 ml PBS
   Let PFA dissolve at 65 °C

Acknowledgments

This protocol was adapted and modified from a previous study (Schroter *et al.*, 2015). This work was supported by grants from DFG (ME 854/11).

References

1. Harrison, S. C. (2015). Viral membrane fusion. *Virology* 479-480: 498-507.
2. Turner, A., Bruun, B., Minson, T. and Browne, H. (1998). Glycoproteins gB, gD, and gHgL of herpes simplex virus type 1 are necessary and sufficient to mediate membrane fusion in a Cos cell transfection system. *J Virol* 72(1): 873-875.
3. Muggeridge, M. I. (2000). Characterization of cell-cell fusion mediated by herpes simplex virus 2 glycoproteins gB, gD, gH and gL in transfected cells. *J Gen Virol* 81(Pt 8): 2017-2027.
4. McShane, M. P. and Longnecker, R. (2005). Analysis of fusion using a virus-free cell fusion assay. *Methods Mol Biol* 292: 187-196.
5. Schmidt, J., Klupp, B. G., Karger, A. and Mettenleiter, T. C. (1997). Adaptability in herpesviruses: glycoprotein D-independent infectivity of pseudorabies virus. *J Virol* 71(1): 17-24.
6. Schröter, C., Vallbracht, M., Altenschmidt, J., Kargoll, S., Fuchs, W., Klupp, B. G. and Mettenleiter, T. C. (2015). Mutations in pseudorabies virus glycoproteins gB, gD, and gH functionally compensate for the absence of gL. *J Virol* 90(5): 2264-2272.

II

(II) Mutations in Pseudorabies Virus Glycoproteins gB, gD, and gH Functionally Compensate for the Absence of gL

Christina Schröter, Melina Vallbracht, Jan Altenschmidt, Sabrina Kargoll, Walter Fuchs, Barbara G. Klupp, Thomas C. Mettenleiter

Journal of Virology

Volume 90, Number 5

March 2016

doi: 10.1128/JVI.02739-15

AMERICAN SOCIETY FOR MICROBIOLOGY | Journal of Virology

Mutations in Pseudorabies Virus Glycoproteins gB, gD, and gH Functionally Compensate for the Absence of gL

Christina Schröter, Melina Vallbracht, Jan Altenschmidt,* Sabrina Kargoll,* Walter Fuchs, Barbara G. Klupp, Thomas C. Mettenleiter

Institute of Molecular Virology and Cell Biology, Friedrich-Loeffler-Institut, Greifswald-Insel Riems, Germany

ABSTRACT

Entry of herpesviruses depends on the combined action of viral glycoprotein B (gB) and the heterodimeric gH/gL complex, which are activated by binding of the virion to specific cellular receptors. While gB carries signatures of a bona fide fusion protein, efficient membrane fusion requires gH/gL. However, although gB and gH/gL are essential for entry, the alphaherpesvirus pseudorabies virus (PrV) is capable of limited cell-to-cell spread in the absence of gL. To understand gH/gL function in more detail, the limited spread of PrV-ΔgL was used for reversion analyses by serial cell culture passages. In a first experiment, an infectious gL-negative mutant in which gL function was replaced by generation of a gD-gH hybrid protein was isolated (B. G. Klupp and T. C. Mettenleiter, J Virol 73:3014–3022, 1999). In a second, independent experiment PrV-ΔgLPassB4.1, which also replicated productively without gL, was isolated. Sequence analysis revealed mutations in gH but also in gB and gD. In a transfection-based fusion assay, two amino acid substitutions in the N-terminal part of $gH^{B4.1}$ ($L^{70}P$ and $W^{103}R$) were found to be sufficient to compensate for lack of gL, while mutations present in $gB^{B4.1}$ enhanced fusogenicity. Coexpression of $gB^{B4.1}$ with the homologous $gH^{B4.1}$ resulted in strongly increased syncytium formation, which was further augmented by truncation of the $gB^{B4.1}$ C-terminal 29 amino acids. Nevertheless, gH was still required for membrane fusion. Surprisingly, coexpression of $gD^{B4.1}$ blocked syncytium formation in the fusion assays, which could be attributed to a $V^{106}A$ substitution within the ectodomain of $gD^{B4.1}$.

IMPORTANCE

In contrast to many other enveloped viruses, herpesviruses rely on the concerted action of four viral glycoproteins for membrane fusion during infectious entry. Although the highly conserved gB shows signatures of a fusion protein, for fusion induction it requires the gH/gL complex, whose role is still elusive. Here we demonstrated fusion activation by gH in the absence of gL after reversion analysis of gL-deleted pseudorabies virus. This gL-independent fusion activity depended on single amino acid exchanges affecting the gL-binding domain in gH, increasing fusogenicity in gB and allowing negative fusion regulation by gD. Thus, our results provide novel information on the interplay in the fusion machinery of herpesviruses.

Infection of susceptible cells by herpesviruses occurs by fusion of the viral envelope with the host cell plasma membrane or, after endocytic uptake, with the membrane of the endosome. For both processes a cascade of events has to be initiated, whose molecular details are still not completely understood. The conserved viral glycoprotein B (gB) and the heterodimeric gH/gL complex form the core fusion machinery and are required for fusion during virus entry and direct virus transmission to neighboring cells (reviewed in references 1 and 2).

In the alphaherpesviruses herpes simplex virus 1 (HSV-1) and pseudorabies virus (PrV), the cascade ultimately leading to membrane fusion is initiated by interaction of the essential viral attachment glycoprotein gD to specific host cell receptors. As shown for HSV-1, this results in a conformational rearrangement in gD. The C-terminal 50 amino acids (aa) of the ectodomain, which are tightly folded around the N-terminal part in the unbound state, are displaced by receptor binding, thereby opening the structure (3, 4). This conformational switch is believed to signal, in a yet-unknown manner, to the gH/gL complex, which in turn triggers membrane fusion catalyzed by gB (reviewed in references 1 and 2).

The crystal structures of HSV-1 gB and Epstein-Barr virus (EBV) gB are surprisingly similar to structures of the fusion proteins vesicular stomatitis virus (VSV) G and baculovirus gp64 (5–8). All three fusion proteins are characterized by an alpha-helical coiled-coil domain, similar to that in class I fusion proteins, and extended hairpins with fusion peptides, similar to class II fusion proteins, which led to the allocation of a new class of fusion proteins, designated class III (reviewed in references 1 and 2). In spite of the close structural similarity, in contrast to VSV G and baculovirus gp64, herpesvirus gB alone is not sufficient to induce efficient membrane fusion but depends on the presence of the gH/gL complex.

The role of the gH/gL complex, and in particular of gL, during membrane fusion is still unclear. Although gH has been proposed to act as a fusion protein (9–11), the deduced crystal structures revealed no features of viral fusion proteins, and amino acid

Received 29 October 2015 **Accepted** 3 December 2015

Accepted manuscript posted online 9 December 2015

Citation Schröter C, Vallbracht M, Altenschmidt J, Kargoll S, Fuchs W, Klupp BG, Mettenleiter TC. 2016. Mutations in pseudorabies virus glycoproteins gB, gD, and gH functionally compensate for the absence of gL. J Virol 90:2264–2272. doi:10.1128/JVI.02739-15.

Editor: R. M. Longnecker

Address correspondence to Thomas C. Mettenleiter, thomas.mettenleiter@fli.bund.de.

* Present address: Jan Altenschmidt, Dianova GmbH, Hamburg, Germany; Sabrina Kargoll, Institute of Biochemistry, University of Greifswald, Greifswald, Germany.

stretches which had been suspected as potential fusion peptides are deeply buried within the molecule, arguing against a direct role in merging of lipid membranes (12). gL depends on interaction with gH for membrane association and virion incorporation due to the lack of a membrane anchor (13–16). It was long considered a chaperone for gH since it is required for correct folding, transport, and virion incorporation of gH in HSV-1 and EBV (13, 17). However, in PrV, bovine herpesvirus 4, and murid herpesvirus 4, gH is incorporated into virions also in the absence of gL. Nevertheless, gL is required for entry (18–20), pointing to a role beyond chaperoning.

While PrV gL is essential for membrane fusion during entry, direct transmission of infectivity to neighboring noninfected cells, a process which is also mediated by the core fusion machinery, occurs to a limited extent also in the absence of gL (19). The capability for restricted cell-to-cell-spread of PrV-ΔgL was used for reversion analysis by repeated passages in cell culture. This led to the isolation of a revertant virus which replicated like the wild type, demonstrating that gL function can be compensated by mutations elsewhere in the virus genome (21). The compensatory mutation in PrV-ΔgLPass could be attributed to the formation of a hybrid protein consisting of the N-terminal 271 amino acids of gD fused to the C-terminal 590 amino acids of gH, thereby deleting the gL-interaction domain (21). This gDH hybrid protein is sufficient to complement not only the absence of gL but also lack of wild-type gH and gD, singly or in different combinations, and to induce extensive syncytia after coexpression with only gB (22), indicating that gL is not directly involved in activating the fusion process.

The recently solved crystal structures of EBV gH/gL (23), HSV-2 gH/gL (24), and a core fragment of PrV gH (12), in combination with mutational analyses, shed further light on the function of the gH/gL complex. Despite low conservation of the primary amino acid sequences (25), the gH structures were surprisingly similar, and the gH ectodomains could be divided into three (24) or four (12, 23) distinct regions. Domain I, comprising the N terminus of gH, is tightly associated with gL, and its secondary structure depends on presence of both proteins (23, 24). In the PrV gH structure, which was derived from the gH core fragment present in the gDH hybrid protein (12, 21), this domain is missing. Nevertheless, PrV gH domains II to IV can be easily correlated to the gH/gL structures of EBV and HSV-2 (12). Domain II consists of a sheet of antiparallel beta-chains designated "fence" and a syntaxin-like bundle (SLB) consisting of three alpha-helices with structural similarities to cellular syntaxins (12). Integrity of the SLB and flexibility between domains II and III are important for PrV gH maturation, transport, and function (26). Domain III contains eight alpha-helices and harbors a highly conserved amino acid stretch (serine-proline-cysteine) which plays an important role in fusion (27). Domain IV, the best conserved region of gH, is composed of two four-stranded beta-sheets with connection to a region designated the "flap," which covers a stretch of hydrophobic amino acids (12). Recent studies indicated that movement of the flap and the subsequent exposure of the hydrophobic patch are important for PrV gH function during membrane fusion (28).

We wondered whether formation of a gD-gH hybrid protein would be the only way to overcome absence of gL function. Thus, we repeated the passaging experiment with gL-deleted PrV and isolated additional infectious revertants which apparently did not produce the hybrid protein. Characterization of one of them, designated PrV-ΔgLPassB4.1, revealed compensatory mutations not only in gH but also in gB and gD, pointing to a tight regulatory balance between gD, gH(/gL), and gB.

MATERIALS AND METHODS

Cells and viruses. Rabbit kidney (RK13) and RK13-gH/gL cells (29) were grown in Dulbecco's modified Eagle's minimum essential medium (MEM) supplemented with 10% fetal calf serum at 37°C. All viruses used in this study were derived from PrV strain Kaplan (PrV-Ka) (30). PrV mutants lacking gL have been described previously (19, 29).

Passaging of PrV-ΔgL. Passaging of PrV-ΔgL was done as described before (21). Briefly, RK13 cells were incubated with PrV-ΔgL at a low multiplicity of infection (MOI), trypsinized when the cell monolayer was confluent, and reseeded until infectivity in the supernatant was stably detectable. Subsequently, the precleared supernatant was used to infect fresh RK13 cells. One single-plaque isolate derived from the supernatant of the 100th passage and designated PrV-ΔgLPassB4.1 was further characterized.

***In vitro* growth kinetics.** For analysis of growth kinetics, RK13 cells were infected with PrV-Ka, PrV-ΔgL, or PrV-ΔgLPassB4.1 at an MOI of 0.5 for 2 h at 4°C. The inoculum was removed, prewarmed medium was added, and cells were incubated for 2 h at 37°C. Thereafter, virus that had not penetrated was inactivated by low-pH treatment (31). Cells and supernatant were harvested at different times after inactivation and titrated on RK13 and RK13-gH/gL cells. For plaque size measurement, cells were infected with the same set of viruses under plaque assay conditions for 2 days. Cells were fixed and analyzed by indirect immunofluorescence using an anti-pUL19 serum (32). Images were taken using a Nikon Eclipse Ti-S fluorescence microscope, and plaque areas were measured using the Nikon NIS-Elements imaging software (Nikon, Düsseldorf, Germany).

Expression plasmids. Generation of expression plasmids for PrV-Ka gB, gD, gH, and gL has been described previously (22). pcDNA-gB008 expresses a truncated gB lacking the C-terminal 29 amino acids (aa), including predicted endocytosis motifs (33). It possesses a higher fusogenic potential than full-length gB (22). The open reading frames of PrV-ΔgLPassB4.1 gB and gH were amplified by PCR and cloned as described previously (22, 33). The $gD^{B4.1}$ open reading frame was PCR amplified from PrV-ΔgLPassB4.1 genomic DNA using primers gDfw and gDrv (Table 1), and truncated $gB^{B4.1}$ ($gB^{B4.1}$008) was obtained with primers gB ASS FW (33) and gBmutΔK^{883}/008R (Table 1). The numbering of amino acids in gB is derived from GenBank accession number JF797218.1 (34), while the other proteins were deduced from accession number JQ809328.1 (35). PCR products were cloned into pcDNA3 (Invitrogen) via restriction sites which had been introduced by the primers. Expression plasmids for gB^{Ka} E^{290}G, gB^{Ka} G^{672}R, and gB^{Ka} E^{290}G/G^{672}R as well as for mutants $gD^{B4.1}$ V^{25}A, $gD^{B4.1}$ V^{106}A, $gD^{B4.1}$ FS^{379} (frameshifted), gD^{Ka} A^{25}V, gD^{Ka} A^{106}V, and gD^{Ka} A^{25}V/A^{106}V were generated using the QuikChange II XL site-directed mutagenesis kit (Agilent) as described recently (27) and primers shown in Table 1. Expression plasmids for gB^{Ka} ΔK^{883}, gB E^{290}G/ΔK^{883}, and gB^{Ka} G^{672}R/ΔK^{883} were created by ligation of BamHI/FseI cleavage products derived from pcDNA-gB or the respective mutated plasmids and pcDNA-$gB^{B4.1}$. Correct mutagenesis and cloning were verified by sequencing. Protein expression was controlled by indirect immunofluorescence and Western blotting after transfection into RK13 cells (data not shown).

Fusion assays. Fusion activity of the different glycoprotein mutants was tested after transfection of RK13 cells as described recently (27). Approximately 1.8×10^5 RK13 cells per well were seeded into 24-well culture dishes. On the following day, cells were transfected with 125 ng each of the expression plasmids in different combinations and with pEGFP-N1 (Clontech) as a marker in 50 μl serum-free MEM using 1 μl polyethylenimine (PEI). Empty vector (pcDNA3) served as negative control. The mixture was incubated for 15 min at room temperature and then added to the cells. After 24 h at 37°C, cells were washed with phosphate-buffered

TABLE 1 Primers used in this study

Primer	Sequence (5′→3′)[a]	Restriction site	Location[b]
gDfw	CAC **AGA ATT C**AC CTG CCA GCG CCA TGC	EcoRI	121132–121148
gDrv	CAC **AGA ATT C**CA TCG ACG CCG GTA CTG C	EcoRI	122370–121353
gBmutΔK^{883}/008R	CC**G AAT TC**C TAC CCG CTG TTC TTG CGC GC	EcoRI	16138–16157
gBmutE^{290}G F	CGT CGA GGA GGT GGG GGC GCG CTC CG		17943–17918
gBmutE^{290}G R	CG GAG CGC GCC CCC ACC TCC TCG ACG		17918–17943
gBmutG^{672}R F	CGC TAC TTT AAG CTG AGG AGC GGG TAC G		16799–16772
gBmutG^{672}R R	C GTA CCC GCT CCT CAG CTT AAA GTA GCG		16772–16799
gDmut V25A-fwd	G GAC GCC GTG CCC GCG CCG ACC TTC CCC C		121164–121173
gDmut V25A-rev	G GGG GAA GGT CGG CGC GGG CAC GGC GTC C		121173–121164
gDmut A25V-fwd	G GAC GCC GTG CCC GTG CCG ACC TTC CCC C		121164–121173
gDmut A25V-rev	G GGG GAA GGT CGG CAC GGG CAC GGC GTC C		121173–121164
gDmut V106A-fwd	GCG GAC GGG TGC GCG CAC CTG CTG TAC		121247–121255
gDmut V106A-rev	GTA CAG CAG GTG CGC GCA CCC GTC CGC		121255–121247
gDmut A106V-fwd	GCG GAC GGG TGC GTG CAC CTG CTG TAC		121247–121255
gDmut A106V-rev	GTA CAG CAG GTG CAC GCA CCC GTC CGC		121255–121247

[a] Nucleotide substitutions are underlined, and added restriction sites are in bold.
[b] Primer sequence locations in the PrV-Ka genome corresponding to accession number JF797218.1 (34) for gB primers or JQ809328.1 (35) for gD and gH primers.

saline (PBS), fixed with 3% paraformaldehyde (PFA) for 20 min, and washed two times with PBS. Syncytium formation was analyzed using a Nikon Eclipse Ti-S fluorescence microscope and the Nikon NIS-Elements imaging software (Nikon, Düsseldorf, Germany). The area of cells with three or more nuclei within 10 fields of view was measured, and the mean value was multiplied by the number of syncytia to give the total fusion activity. The experiment was repeated three times, and average percent values with respect to control transfections, as well as standard deviations, were calculated.

RESULTS

Isolation of PrV-ΔgLPassB4.1. In the first passaging experiment, a PrV-ΔgL revertant which efficiently entered cells in the absence of gL after formation of a hybrid gene expressing a gDH hybrid protein was isolated (21). Since the formation of this hybrid gene was unexpected, we tested whether it would be repeated in an independent passaging experiment or whether other compensatory mutations inducing membrane fusion in the absence of gL could be unraveled. From the supernatant of an independent passage experiment with RK13 cells, one isolate, designated PrV-ΔgLPassB4.1, was further investigated.

Characterization of PrV-ΔgLPassB4.1 in cell culture showed, in contrast to PrV-ΔgL, productive virus replication in non-complementing cells, with plaque areas reaching approximately 80% and 20- to 80-fold-lower titers than PrV-Ka (Fig. 1). Virus propagation on gL-expressing cells had no influence on the *in vitro* replication properties (data not shown), corroborating the gL-independent phenotype.

Sequencing of genes encoding glycoproteins involved in fusion in PrV-ΔgLPassB4.1. To test whether changes in the components of the herpesvirus fusion machinery account for the gL-independent entry and membrane fusion mechanism, the complete open reading frames encoding gH, gB, and gD were amplified from genomic PrV-ΔgLPassB4.1 DNA and cloned into the eukaryotic expression vector pcDNA3 (Invitrogen). Sequencing of the gH$^{B4.1}$ open reading frame revealed two amino acid changes, L^{70}P and W^{103}R, which are both located in the predicted gL-binding domain. PrV-ΔgLPassB4.1 gB contains two amino acid changes in the ectodomain (E^{290}G and G^{672}R) and a deletion of a lysine residue at position 883 (ΔK^{883}) in the cytoplasmic domain, while gD specifies two point mutations in the ectodomain (A^{25}V and A^{106}V) and a frameshift mutation after codon 378 leading to an altered and truncated cytoplasmic tail (Fig. 2).

Mutations in the predicted gL-binding domain of gH$^{B4.1}$ substitute for gL in transient cell-cell fusion assays. As shown before, cotransfection of expression plasmids encoding PrV glycoproteins gB, gH, and gL results in the formation of multiple syncytia (22). In contrast to a similar assay reported for HSV-1 (36), addition of the plasmid encoding PrV gD only moderately enhances fusion, while omission of gL significantly reduces fusion (22). In both systems, however, in the absence of gB or gH expression, syncytium formation was reduced to background levels.

To analyze the effects of the mutations in the predicted gL-binding domain of gH$^{B4.1}$, RK13 cells were transfected with plasmids coding for gB^{Ka} and gH^{Ka} or gH$^{B4.1}$ in the presence or absence of gL expression. At 1 day posttransfection, the area of cells containing more than two nuclei was measured and multiplied by the total number of syncytia. Mean values from three independent assays with corresponding standard deviations are shown in Fig. 3. Results from assays with gB^{Ka}, gH^{Ka}, and gL were set as 100%. Substitution of gH^{Ka} by gH$^{B4.1}$ resulted in an only slightly reduced total fusion activity, but in contrast to assays with gH^{Ka}, expression of gL had no enhancing effect, demonstrating gL-independent function.

Mutations present in gB$^{B4.1}$ enhance cell-cell fusion. To test for the influence of the mutations in gB$^{B4.1}$, it was coexpressed with gH^{Ka}. Coexpression increased fusion activity by approximately 2.5-fold compared to that in assays with gB^{Ka}, gH^{Ka}, and gL. Syncytium formation was further augmented by coexpression of gB$^{B4.1}$ with the homologous gH$^{B4.1}$, which resulted in approximately 6.5-fold-higher values (Fig. 4). Additional expression of gL had no effect (results not shown).

To elucidate which of the three amino acid changes in gB$^{B4.1}$ account for the higher fusion activity, the mutations were introduced into gB^{Ka} singly or in combinations. Fusion activity was tested by coexpression of gH^{Ka} and the different gB mutants, and fusion activity observed with gB$^{B4.1}$ and gH^{Ka} was set as 100%. The single-amino-acid substitution G^{672}R and the deletion of lysine at position 883 (ΔK^{883}) increased fusion activity compared to that of gB^{Ka} (Fig. 5), while pronounced syncytium formation similar to that of gB$^{B4.1}$ was achieved by the combination of both mutations.

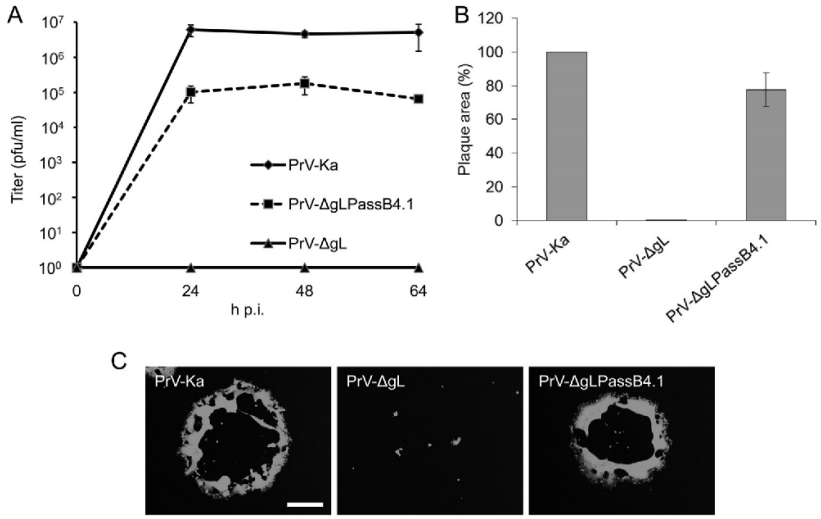

FIG 1 *In vitro* growth properties of PrV-ΔgLPassB4.1. (A) For growth kinetics, RK13 cells were infected with PrV-Ka, PrV-ΔgL, or PrV-ΔgLPassB4.1 at an MOI of 0.5. Total cell lysates were harvested after 24, 48, and 64 h and titrated on RK13 cells. Given are mean values from three independent experiments with the corresponding standard deviations. (B) Cells were infected with PrV-Ka, PrV-ΔgL, or PrV-ΔgLPassB4.1 under plaque assay conditions and fixed at 2 days postinfection. Infected cells were visualized by indirect immunofluorescence with a monospecific anti-pUL19 serum, and plaque areas were measured. Plaque areas formed by PrV-Ka were set as 100%, and values for PrV-ΔgL and PrV-ΔgLPassB4.1 were calculated accordingly. Shown are the mean values and standard deviations from three independent experiments. (C) Representative images. Bar, 400 μm.

The replacement of glutamate with glycine at position 290 had no significant effect on fusion (Fig. 5).

Deletion of the C-terminal 29 amino acids in PrV-ΔgLPassB4.1 gB results in excessive cell-cell fusion. Deletion of 29 amino acids from the C terminus of gB^{Ka}, including predicted dileucine- and tyrosine-based sorting signals, resulted in the accumulation of gB at the cell surface and significantly enhanced fusion activity (22, 33). To analyze whether the same C-terminal truncation further increases fusion activity of $gB^{B4.1}$ and whether this might be suffi-

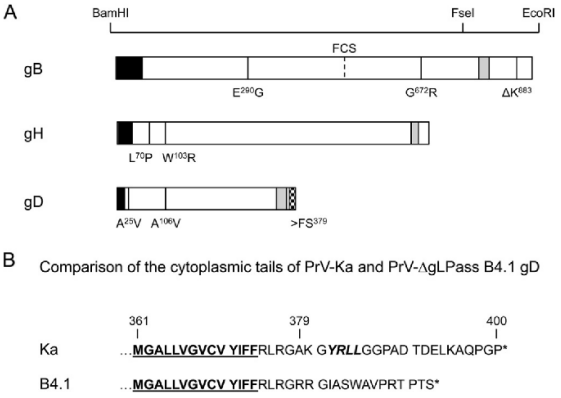

FIG 2 Mutations in PrV-ΔgLPassB4.1. (A) Amino acid changes found in PrV-ΔgLPassB4.1 gB, gH, and gD compared to PrV-Ka are indicated at the corresponding positions in one-letter code. Restriction enzyme recognition sites used for cloning of gB mutants are indicated above the diagram. The predicted signal sequences are shown in black and the transmembrane domains in gray. The location of the furin cleavage site (FCS) in gB is given. The frameshift mutation (>FS^{379}) in $gD^{B4.1}$, which results in an altered cytoplasmic tail, is indicated by a checkered box. (B) Amino acid sequences of the gD^{Ka} and $gD^{B4.1}$ C termini. Residues predicted to reside within the membrane are underlined, and the C-terminal ends are marked by asterisks. Indicated by italics is the predicted endocytosis motif in gD^{Ka} which is lost in $gD^{B4.1}$ (58).

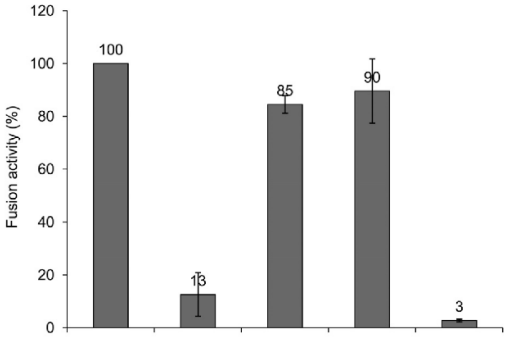

gB	Ka	Ka	Ka	Ka	Ka
gH	Ka	Ka	B4.1	B4.1	-
gL	+	-	+	-	-

FIG 3 Mutations in gH substitute for gL function in transient-transfection fusion assays. To test whether the mutations present in $gH^{B4.1}$ are sufficient to compensate for lack of gL, RK13 cells were cotransfected with expression plasmids for gB^{Ka} and gH^{Ka} or $gH^{B4.1}$ in the presence or absence of gL expression as indicated. Results from assays with gB^{Ka}, gH^{Ka}, and gL were set as 100%. As a negative control, an assay with the gB^{Ka} expression plasmid only (the DNA amount was adjusted by addition of empty vector) was used. The relative fusion activity (number of syncytia × syncytium area) with corresponding standard deviation from three independent experiments is depicted.

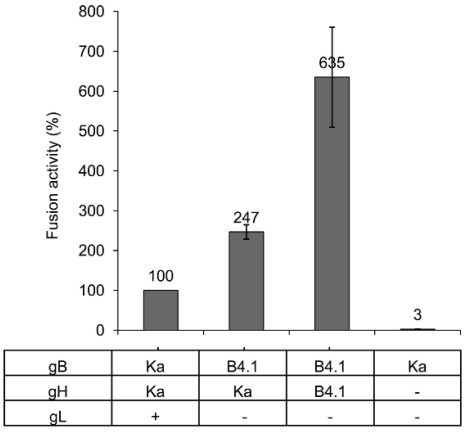

FIG 4 $gB^{B4.1}$ contains fusion-enhancing mutations. To test for fusion activity of $gB^{B4.1}$, RK13 cells were cotransfected with combinations of plasmids expressing the different glycoproteins as indicated. Results from assays with gB^{Ka}, gH^{Ka}, and gL were set as 100%, and those with the gB^{Ka} expression plasmid only (together with empty vector) served as negative control. Shown are the mean values and corresponding standard deviations from three independent experiments (these data, originating from a larger data set testing multiple variables, are also included in Fig. 7).

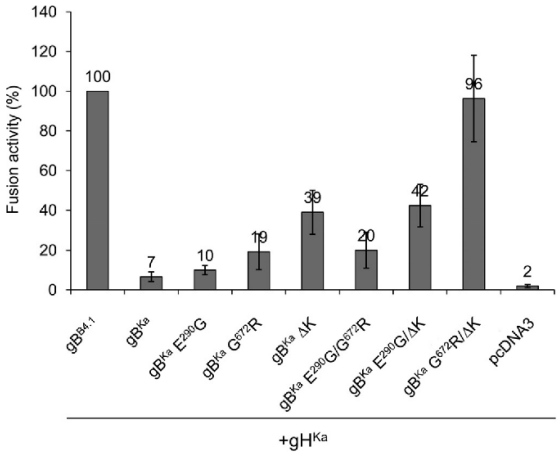

FIG 5 The $G^{672}R$ mutation and the deletion of K^{883} in the cytoplasmic tail of $gB^{B4.1}$ account for enhanced fusion activity. To test which changes in $gB^{B4.1}$ are responsible for the higher fusion activity, mutations were introduced singly or in combinations into gB^{Ka}. Fusion activity in combination with gH^{Ka} was measured in cotransfected RK13 cells, and results from assays with $gB^{B4.1}$ and gH^{Ka} were set as 100%. Given are mean values from three independent experiments with corresponding standard deviations.

cient for gB-only-mediated membrane fusion, gH^{Ka} was coexpressed with either full-length gB^{Ka}, C-terminally truncated gB^{Ka}008, $gB^{B4.1}$, or C-terminally truncated $gB^{B4.1}$008 (Fig. 6). Mean values from three independent experiments, with results from gB^{Ka}008 coexpressed with gH^{Ka} set as 100%, and corresponding standard deviations are shown in Fig. 6A. Full-length $gB^{B4.1}$ already showed levels of syncytium formation comparable to those of the highly fusogenic gB^{Ka}008. However, coexpression of $gB^{B4.1}$008 with gH^{Ka} resulted in excessive syncytium formation, with 3.5-fold-higher values. However, despite this extreme fusion activity with gH^{Ka}, $gB^{B4.1}$008 alone was not sufficient to induce cell-cell fusion above background levels. Representative images are shown in Fig. 6B.

PrV-ΔgLPassB4.1 gD inhibits cell-cell fusion. Although PrV-ΔgLPassB4.1 showed a syncytial phenotype in cell culture (Fig. 1), hyperfusion as observed after coexpression of $gB^{B4.1}$ and $gH^{B4.1}$ in transient assays was not obvious. To investigate the influence on fusion of $gD^{B4.1}$, which carries two amino acid substitutions ($A^{25}V$ and $A^{106}V$) in the ectodomain and a frameshift mutation affecting the cytoplasmic tail (Fig. 2), fusion assays were repeated in the presence of either gD^{Ka} or $gD^{B4.1}$. As shown in Fig. 7, coexpression of gD^{Ka} slightly enhanced the number and size of syncytia not only with the wild-type glycoproteins but, even more significantly, also with $gB^{B4.1}$ and $gH^{B4.1}$. In striking contrast, coexpression of $gD^{B4.1}$ completely blocked syncytium formation in assays with the homologous PrV-ΔgLPassB4.1-derived proteins and also with the wild-type proteins (Fig. 7).

The $A^{106}V$ mutation is responsible for the fusion inhibition of $gD^{B4.1}$. To test whether the amino acid substitutions in the ectodomain ($A^{25}V$ and $A^{106}V$) or the frameshift mutation (FS^{379}) affecting the C terminus is responsible for the inhibitory effect of $gD^{B4.1}$, the different mutations were introduced into gD^{Ka} or repaired in $gD^{B4.1}$ separately or in combinations. While the mutation $A^{25}V$ or the nucleotide insertion after codon 378 in gD^{Ka} affected syncytium formation only slightly, the $A^{106}V$ substitution resulted in a complete abrogation of cell-cell fusion. Consistently, restoration of alanine at position 106 in $gD^{B4.1}$ rescued fusion activity (Fig. 8). The other mutations, either repaired in $gD^{B4.1}$ or introduced into gD^{Ka}, affected syncytium formation only marginally.

DISCUSSION

Most enveloped viruses use only one or two viral proteins for receptor binding and membrane fusion, and the molecular details are well understood for several of them (reviewed in reference 37). In contrast, the molecular basis for membrane fusion induced by herpesviruses, which engage four or more different proteins, is still largely enigmatic. We demonstrate here that the absence of a herpesvirus protein, gL, which normally forms a heterodimeric complex with gH and is essential for entry, can be compensated by mutations (i) within the gL-binding domain of gH resulting in loss of gL interaction, (ii) within gB enhancing its fusogenicity, and (iii) within gD to allow negative regulation of excess fusion.

Elucidation of the crystal structures of the key players in fusion from different herpesviruses has sparked studies on membrane fusion using targeted mutagenesis (26, 28, 38–41). Here, we used a different approach, designated reversion analysis, to select for spontaneous mutations which compensate for defects induced by the absence of a crucial component of the fusion-inducing machinery. Repeated passaging of respective deletion mutants in cultured cells resulted in the isolation of revertants which were able to productively infect cells in the absence of either gD, gL, or C-terminally truncated gB (21, 42, 43). The absence of gL was compensated by the formation of a hybrid gene encoding the N-terminal 271 amino acids of gD fused to the 590 C-terminal amino acids of gH, thereby lacking the first 96 gH codons, which encompass the

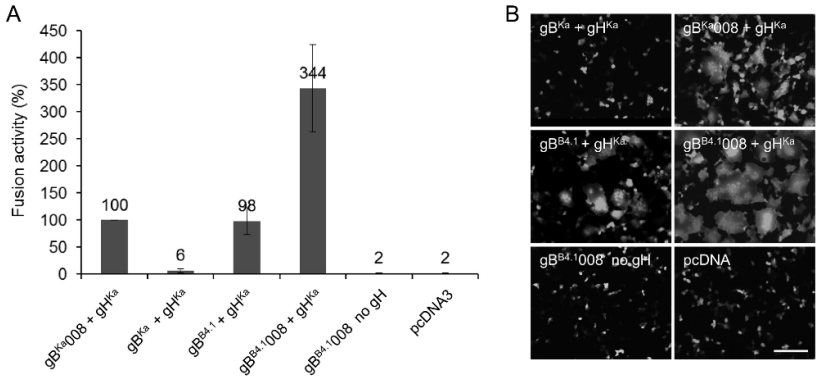

FIG 6 Deletion of the C-terminal 29 amino acids from $gB^{B4.1}$ leads to excessive cell-cell fusion. (A) To analyze the influence of the deletion of the 29 C-terminal amino acids in $gB^{B4.1}$, RK13 cells were cotransfected with the corresponding gB expression plasmids and pcDNA-gH^{Ka}. Results from assays with gB^{Ka}008 and gH^{Ka} were set as 100%. Transfection fusion assays were repeated three times, and mean values and corresponding standard deviations were calculated. (B) Representative images. Bar, 100 μm.

predicted gL interaction domain (21). This gDH hybrid protein was able to complement viruses lacking gD, gH, or gL singly or in combination (29) and was sufficient to induce efficient cell-cell fusion in transient-transfection fusion assays in combination with only gB (22), reducing the number of proteins required for herpesvirus-induced membrane fusion to two.

From an independent passage experiment with gL-deleted PrV, we isolated another revertant, designated PrV-ΔgLPassB4.1. In this revertant, no genetic rearrangement comprising the gH or gD gene region was observed, but sequence analyses revealed two amino acid changes in the N-terminal gL-binding domain of gH ($L^{70}P$ and $W^{103}R$). To test the impact of these mutations on membrane fusion, we used our transfection-based cell-cell fusion assay (27). This assay partially reflects fusion during entry but more closely resembles fusion during direct cell-to-cell spread, for which gD is not required in PrV (44, 45). Coexpression of PrV gB^{Ka}, gH^{Ka}, and gL^{Ka} is sufficient to induce multiple syncytia in rabbit kidney cells without the need for activation of the core fusion machinery by binding of gD to cellular receptors (22). This contrasts the situation found in HSV-1 (36). Here, we show that PrV $gH^{B4.1}$ in combination with gB^{Ka} induced cell-cell fusion in the absence of gD and gL to an extent comparable to that observed after coexpression of all four wild-type proteins. This indicates that the two mutations in the N-terminal part of $gH^{B4.1}$ are sufficient to compensate for the absence of gL and its function in membrane fusion. As a consequence, addition of the gL expression

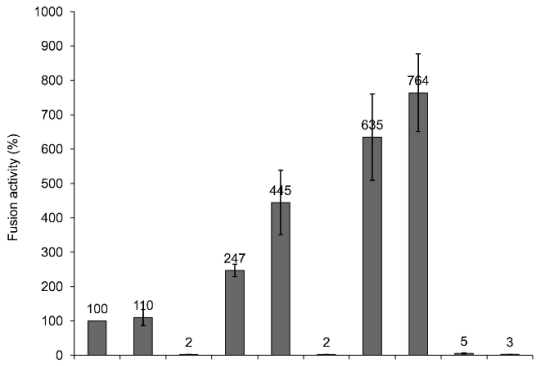

gB	Ka	Ka	Ka	B4.1	B4.1	B4.1	B4.1	B4.1	B4.1	Ka
gH	Ka	Ka	Ka	Ka	Ka	Ka	B4.1	B4.1	B4.1	-
gD	-	Ka	B4.1	-	Ka	B4.1	-	Ka	B4.1	-
gL	+	+	+	-	-	-	-	-	-	-

FIG 7 PrV-ΔgLPassB4.1 gD inhibits cell fusion. RK13 cells were cotransfected with the indicated expression plasmids. Fusion activity in assays including gB^{Ka}, gH^{Ka}, and gL but without gD was set at 100%. Shown are mean relative values from three independent experiments with standard deviations.

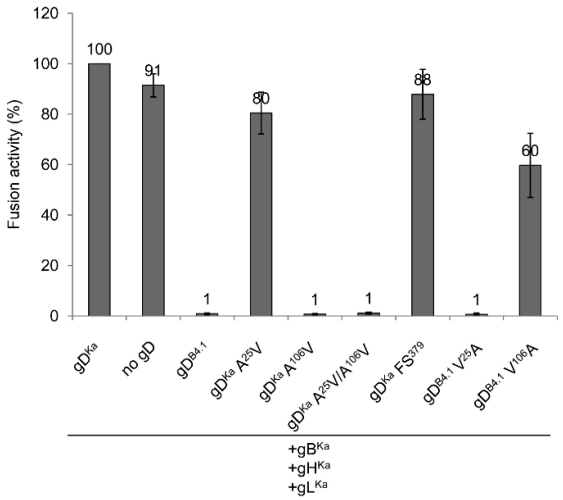

FIG 8 The amino acid substitution $A^{106}V$ is responsible for fusion inhibition by $gD^{B4.1}$. Mutations found in $gD^{B4.1}$ were introduced into gD^{Ka} or repaired in $gD^{B4.1}$ and tested in transfection fusion assays with gB^{Ka}, gH^{Ka}, and gL^{Ka}. Shown are mean values and standard deviations from three independent experiments, with results from cotransfections with gB^{Ka}, gD^{Ka}, gH^{Ka}, and gL^{Ka} set as 100%.

plasmid had no fusion promoting effect (Fig. 3), and coprecipitation studies demonstrated that $gH^{B4.1}$ is unable to interact with gL (data not shown). Unfortunately, gH domain I comprising the two amino acid substitutions was not present in the recently solved crystal structure of PrV gH (12) and is the least conserved region within herpesvirus gH proteins, so the impact of the amino acid substitutions on gH structure cannot be predicted. However, elucidation of the crystal structure of $gH^{B4.1}$ might shed light on the conformation of a gH primed for fusion activation without gL.

Cell lines stably expressing $gH^{B4.1}$ complemented plaque formation by mutants lacking gL, gH, or both proteins simultaneously to approximately 80% of wild-type virus diameters, but titers derived from these cells reached only approximately 10^4 PFU/ml (data not shown). This indicates that the two amino acid substitutions in $gH^{B4.1}$ compensate for gL function during direct cell-cell spread but are not sufficient to compensate for all gL functions during the viral replication cycle. Since, therefore, additional mutations must have occurred, we focused on the other components of the fusion machinery as the most auspicious candidates. In contrast to the first PrV-ΔgLPass revertant (21), analysis of PrV-ΔgLPassB4.1 disclosed additional mutations in gB and gD.

$gB^{B4.1}$ specifies two amino acid substitutions in the ectodomain and a deletion of one of two consecutive lysine residues present at positions 883 and 884 in the cytoplasmic tail (ΔK^{883}). Fusion assays showed that $gB^{B4.1}$ in combination with gH^{Ka} resulted in fusion activity 2- to 3-fold-higher than that of PrV-Ka gB and gH/gL (Fig. 4). Coexpression of $gB^{B4.1}$ with the homologous $gH^{B4.1}$ further increased fusion by 6.5-fold (Fig. 4), indicating that mutations present in both proteins act cooperatively on membrane fusion. To test which mutation(s) is/are relevant for the enhanced fusogenicity of $gB^{B4.1}$, they were introduced singly and in combinations into gB^{Ka}. Simultaneous replacement of glycine 672 by arginine ($G^{672}R$) and deletion of lysine at position 883 (ΔK^{883}) resulted in $gB^{B4.1}$-like fusion activity, while the substitution $E^{290}G$ had no significant influence (Fig. 5). Glycine 672 in PrV gB corresponds to the well-conserved G^{644} in HSV-1 gB, which is located in domain IV (5). This domain of HSV-1 gB is postulated to undergo extensive conformational rearrangements during the conversion of the pre- to the postfusion form (5, 46). It is conceivable that the replacement of the small and neutral glycine by the bulky and charged arginine decreases the necessary energy for this conformational change.

The cytoplasmic domain of gB plays an important role in fusion regulation (33, 47–53). Cell-cell fusion in transfection-based assays could be significantly enhanced by deleting the most C-terminal amino acids, including the predicted endocytosis motifs (33, 52–56). Although it was originally speculated that enhanced presence of gB at the plasma membrane increases cell-cell fusion, recent data showed that the degree of surface localization is not necessarily causally related to increased fusion (52).

For EBV and HSV-1 gB, it could be shown that the cytoplasmic tail interacts with lipid membranes (48, 49, 57). Recent data indicate that predicted alpha-helical domains in the cytoplasmic tail of HSV-1 gB, designated h3 and h2b, function as clamps for stabilization of the prefusion form (53). For PrV gB, two helical regions are predicted in the cytoplasmic tail (33). The absence of helical domain II in PrV gB008 resulted in significantly enhanced fusion (22). Lysine residues at position 883/884 are located at the C-terminal end of helical domain I. Deletion of one of the basic amino acids may weaken this interaction with the membrane, thereby reducing the constraint on fusion. Whether electrostatic interactions with the membrane indeed play a role in fusion regulation has yet to be verified.

Coexpression of full-length $gB^{B4.1}$ with gH^{Ka} and gL already resulted in fusion activity similar to that with gB^{Ka}008 lacking the C-terminal 29 amino acids (Fig. 6). An identical C-terminal deletion increased fusion activity of $gB^{B4.1}$ further, by approximately 3-fold compared to that of gB^{Ka}008 and $gB^{B4.1}$. Restoration of lysine 883 of $gB^{B4.1}$008 did not affect syncytium formation (data not shown), supporting the hypothesis that the gB cytoplasmic tail modulates fusion and that both changes, deletion of several amino acids from the C terminus and deletion of a single basic residue, affect the fusion process similarly by altering gB membrane interactions.

Considering the hyperfusogenic activity of $gB^{B4.1}$ with $gH^{B4.1}$ in transient-transfection fusion assays, it is surprising that PrV-ΔgLPassB4.1 is competent to replicate at all and does not exhibit an excessive syncytial phenotype (Fig. 1). This could be due to the mutations present in the putative receptor-binding domain in $gD^{B4.1}$ and/or the frameshift in the cytoplasmic tail, which shortens the protein and deletes a functional endocytosis motif (YRLL) (Fig. 2) (58). Coexpression of $gD^{B4.1}$ in fusion assays completely inhibited syncytium formation (Fig. 7), demonstrating a dominant negative effect on membrane fusion, which was also observed in the simultaneous presence of gD^{Ka} (data not shown). The $A^{106}V$ mutation seems to play the major role, since its introduction into gD^{Ka} (gD^{Ka} $A^{106}V$) inhibited fusion completely. However, introduction of $A^{25}V$ into gD^{Ka} also moderately reduced fusion to 80%, and repair of $V^{106}A$ in $gD^{B4.1}$ resulted in only approximately 60% of wild-type fusion activity (Fig. 8). Further studies including insertion of the mutated and wild-type versions of gD into the wild-type and passaged virus backgrounds are needed to investigate the molecular basis for the fusion-inhibiting function of $gD^{B4.1}$.

In summary, our results show that absence of PrV gL can be functionally compensated not only by formation of a gDH hybrid protein but also by a combination of point mutations in gH, gB, and gD. The mutations present in $gH^{B4.1}$ are located in the gL-binding domain and might mimic the gD-activated gH/gL complex. Mutations present in the ectodomain and in the cytoplasmic tail of $gB^{B4.1}$ could facilitate the conformational change from the pre- to the postfusion form and resulted in a hyperfusogenic phenotype. Excessive fusogenicity, however, seems to be counteracted by mutations in $gD^{B4.1}$ which inhibit fusion in transient-transfection assays to restrict it to a level compatible with productive virus replication.

ACKNOWLEDGMENTS

We thank Cindy Meinke for expert technical assistance and Britta Möhl, Northwestern University, Chicago, IL, for help in the interpretation of the influence of mutations on the structure.

FUNDING INFORMATION

Deutsche Forschungsgemeinschaft (DFG) provided funding to Thomas C. Mettenleiter under grant number DFG Me 854/11-1.

REFERENCES

1. **Atanasiu D, Saw WT, Cohen GH, Eisenberg RJ.** 2010. Cascade of events governing cell-cell fusion induced by herpes simplex virus glycoproteins gD, gH/gL, and gB. J Virol **84:**12292–12299. http://dx.doi.org/10.1128/JVI.01700-10.

2. **Eisenberg RJ, Atanasiu D, Cairns TM, Gallagher JR, Krummenacher C, Cohen GH.** 2012. Herpes virus fusion and entry: a story with many characters. Viruses **4:**800–832. http://dx.doi.org/10.3390/v4050800.
3. **Fusco D, Forghieri C, Campadelli-Fiume G.** 2005. The pro-fusion domain of herpes simplex virus glycoprotein D (gD) interacts with the gD N terminus and is displaced by soluble forms of viral receptors. Proc Natl Acad Sci U S A **102:**9323–9328. http://dx.doi.org/10.1073/pnas.0503907102.
4. **Krummenacher C, Supekar VM, Whitbeck JC, Lazear E, Connolly SA, Eisenberg RJ, Cohen GH, Wiley DC, Carfi A.** 2005. Structure of unliganded HSV gD reveals a mechanism for receptor-mediated activation of virus entry. EMBO J **24:**4144–4153. http://dx.doi.org/10.1038/sj.emboj.7600875.
5. **Heldwein EE, Lou H, Bender FC, Cohen GH, Eisenberg RJ, Harrison SC.** 2006. Crystal structure of glycoprotein B from herpes simplex virus 1. Science **313:**217–220. http://dx.doi.org/10.1126/science.1126548.
6. **Backovic M, Longnecker R, Jardetzky TS.** 2009. Structure of a trimeric variant of the Epstein-Barr virus glycoprotein B. Proc Natl Acad Sci U S A **106:**2880–2885. http://dx.doi.org/10.1073/pnas.0810530106.
7. **Roche S, Bressanelli S, Rey FA, Gaudin Y.** 2006. Crystal structure of the low-pH form of the vesicular stomatitis virus glycoprotein G. Science **313:**187–191. http://dx.doi.org/10.1126/science.1127683.
8. **Kadlec J, Loureiro S, Abrescia NG, Stuart DI, Jones IM.** 2008. The postfusion structure of baculovirus gp64 supports a unified view of viral fusion machines. Nat Struct Mol Biol **15:**1024–1030. http://dx.doi.org/10.1038/nsmb.1484.
9. **Duus KM, Hatfield C, Grose C.** 1995. Cell surface expression and fusion by the varicella-zoster virus gH:gL glycoprotein complex: analysis by laser scanning confocal microscopy. Virology **210:**429–440. http://dx.doi.org/10.1006/viro.1995.1359.
10. **Galdiero S, Falanga A, Vitiello M, Browne H, Pedone C, Galdiero M.** 2005. Fusogenic domains in herpes simplex virus type 1 glycoprotein H. J Biol Chem **280:**28632–28643. http://dx.doi.org/10.1074/jbc.M505196200.
11. **Galdiero S, Falanga A, Vitiello M, D'Isanto M, Collins C, Orrei V, Browne H, Pedone C, Galdiero M.** 2007. Evidence for a role of the membrane-proximal region of herpes simplex virus type 1 glycoprotein H in membrane fusion and virus inhibition. Chembiochem **8:**885–895. http://dx.doi.org/10.1002/cbic.200700044.
12. **Backovic M, DuBois RM, Cockburn JJ, Sharff AJ, Vaney MC, Granzow H, Klupp BG, Bricogne G, Mettenleiter TC, Rey FA.** 2010. Structure of a core fragment of glycoprotein H from pseudorabies virus in complex with antibody. Proc Natl Acad Sci U S A **107:**22635–22640. http://dx.doi.org/10.1073/pnas.1011507107.
13. **Hutchinson L, Browne H, Wargent V, Davis-Poynter N, Primorac S, Goldsmith K, Minson AC, Johnson DC.** 1992. A novel herpes simplex virus glycoprotein, gL, forms a complex with glycoprotein H (gH) and affects normal folding and surface expression of gH. J Virol **66:**2240–2250.
14. **Kaye JF, Gompels UA, Minson AC.** 1992. Glycoprotein H of human cytomegalovirus (HCMV) forms a stable complex with the HCMV UL115 gene product. J Gen Virol **73:**2693–2698. http://dx.doi.org/10.1099/0022-1317-73-10-2693.
15. **Klupp BG, Baumeister J, Karger A, Visser N, Mettenleiter TC.** 1994. Identification and characterization of a novel structural glycoprotein in pseudorabies virus, gL. J Virol **68:**3868–3878.
16. **Liu DX, Gompels UA, Nicholas J, Lelliott C.** 1993. Identification and expression of the human herpesvirus 6 glycoprotein H and interaction with an accessory 40K glycoprotein. J Gen Virol **74:**1847–1857. http://dx.doi.org/10.1099/0022-1317-74-9-1847.
17. **Roop C, Hutchinson L, Johnson DC.** 1993. A mutant herpes simplex virus type 1 unable to express glycoprotein L cannot enter cells, and its particles lack glycoprotein H. J Virol **67:**2285–2297.
18. **Gillet L, May JS, Colaco S, Stevenson PG.** 2007. Glycoprotein L disruption reveals two functional forms of the murine gammaherpesvirus 68 glycoprotein H. J Virol **81:**280–291. http://dx.doi.org/10.1128/JVI.01616-06.
19. **Klupp BG, Fuchs W, Weiland E, Mettenleiter TC.** 1997. Pseudorabies virus glycoprotein L is necessary for virus infectivity but dispensable for virion localization of glycoprotein H. J Virol **71:**7687–7695.
20. **Lete C, Machiels B, Stevenson PG, Vanderplasschen A, Gillet L.** 2012. Bovine herpesvirus type 4 glycoprotein L is nonessential for infectivity but triggers virion endocytosis during entry. J Virol **86:**2653–2664. http://dx.doi.org/10.1128/JVI.06238-11.
21. **Klupp BG, Mettenleiter TC.** 1999. Glycoprotein gL-independent infectivity of pseudorabies virus is mediated by a gD-gH fusion protein. J Virol **73:**3014–3022.
22. **Klupp BG, Nixdorf R, Mettenleiter TC.** 2000. Pseudorabies virus glycoprotein M inhibits membrane fusion. J Virol **74:**6760–6768. http://dx.doi.org/10.1128/JVI.74.15.6760-6768.2000.
23. **Matsuura H, Kirschner AN, Longnecker R, Jardetzky TS.** 2010. Crystal structure of the Epstein-Barr virus (EBV) glycoprotein H/glycoprotein L (gH/gL) complex. Proc Natl Acad Sci U S A **107:**22641–22646. http://dx.doi.org/10.1073/pnas.1011806108.
24. **Chowdary TK, Cairns TM, Atanasiu D, Cohen GH, Eisenberg RJ, Heldwein EE.** 2010. Crystal structure of the conserved herpesvirus fusion regulator complex gH-gL. Nat Struct Mol Biol **17:**882–888. http://dx.doi.org/10.1038/nsmb.1837.
25. **Klupp BG, Mettenleiter TC.** 1991. Sequence and expression of the glycoprotein gH gene of pseudorabies virus. Virology **182:**732–741. http://dx.doi.org/10.1016/0042-6822(91)90614-H.
26. **Böhm SW, Eckroth E, Backovic M, Klupp BG, Rey FA, Mettenleiter TC, Fuchs W.** 2015. Structure-based functional analyses of domains II and III of pseudorabies virus glycoprotein H. J Virol **89:**1364–1376. http://dx.doi.org/10.1128/JVI.02765-14.
27. **Schröter C, Klupp BG, Fuchs W, Gerhard M, Backovic M, Rey FA, Mettenleiter TC.** 2014. The highly conserved proline at position 438 in pseudorabies virus gH is important for regulation of membrane fusion. J Virol **88:**13064–13072. http://dx.doi.org/10.1128/JVI.01204-14.
28. **Fuchs W, Backovic M, Klupp BG, Rey FA, Mettenleiter TC.** 2012. Structure-based mutational analysis of the highly conserved domain IV of glycoprotein H of pseudorabies virus. J Virol **86:**8002–8013. http://dx.doi.org/10.1128/JVI.00690-12.
29. **Klupp B, Altenschmidt J, Granzow H, Fuchs W, Mettenleiter TC.** 2008. Glycoproteins required for entry are not necessary for egress of pseudorabies virus. J Virol **82:**6299–6309. http://dx.doi.org/10.1128/JVI.00386-08.
30. **Kaplan AS, Vatter AE.** 1959. A comparison of herpes simplex and pseudorabies viruses. Virology **7:**394–407. http://dx.doi.org/10.1016/0042-6822(59)90068-6.
31. **Mettenleiter TC.** 1989. Glycoprotein gIII deletion mutants of pseudorabies virus are impaired in virus entry. Virology **171:**623–625. http://dx.doi.org/10.1016/0042-6822(89)90635-1.
32. **Klupp BG, Granzow H, Mettenleiter TC.** 2000. Primary envelopment of pseudorabies virus at the nuclear membrane requires the UL34 gene product. J Virol **74:**10063–10073. http://dx.doi.org/10.1128/JVI.74.21.10063-10073.2000.
33. **Nixdorf R, Klupp BG, Karger A, Mettenleiter TC.** 2000. Effects of truncation of the carboxy terminus of pseudorabies virus glycoprotein B on infectivity. J Virol **74:**7137–7145. http://dx.doi.org/10.1128/JVI.74.15.7137-7145.2000.
34. **Szpara ML, Tafuri YR, Parsons L, Shamim SR, Verstrepen KJ, Legendre M, Enquist LW.** 2011. A wide extent of inter-strain diversity in virulent and vaccine strains of alphaherpesviruses. PLoS Pathog **7:**e1002282. http://dx.doi.org/10.1371/journal.ppat.1002282.
35. **Grimm KS, Klupp BG, Granzow H, Müller FM, Fuchs W, Mettenleiter TC.** 2012. Analysis of viral and cellular factors influencing herpesvirus-induced nuclear envelope breakdown. J Virol **86:**6512–6521. http://dx.doi.org/10.1128/JVI.00068-12.
36. **Turner A, Bruun B, Minson T, Browne H.** 1998. Glycoproteins gB, gD, and gHgL of herpes simplex virus type 1 are necessary and sufficient to mediate membrane fusion in a Cos cell transfection system. J Virol **72:**873–875.
37. **Harrison SC.** 2015. Viral membrane fusion. Virology **479–480:**498–507. http://dx.doi.org/10.1016/j.virol.2015.03.043.
38. **Atanasiu D, Saw WT, Gallagher JR, Hannah BP, Matsuda Z, Whitbeck JC, Cohen GH, Eisenberg RJ.** 2013. Dual split protein-based fusion assay reveals that mutations to herpes simplex virus (HSV) glycoprotein gB alter the kinetics of cell-cell fusion induced by HSV entry glycoproteins. J Virol **87:**11332–11345. http://dx.doi.org/10.1128/JVI.01700-13.
39. **Chen J, Jardetzky TS, Longnecker R.** 2013. The large groove found in the gH/gL structure is an important functional domain for Epstein-Barr virus fusion. J Virol **87:**3620–3627. http://dx.doi.org/10.1128/JVI.03245-12.
40. **Möhl BS, Sathiyamoorthy K, Jardetzky TS, Longnecker R.** 2014. The conserved disulfide bond within domain II of Epstein-Barr virus gH has divergent roles in membrane fusion with epithelial cells and B cells. J Virol **88:**13570–13579. http://dx.doi.org/10.1128/JVI.02272-14.
41. **Vleck SE, Oliver SL, Brady JJ, Blau HM, Rajamani J, Sommer MH, Arvin AM.** 2011. Structure-function analysis of varicella-zoster virus gly-

coprotein H identifies domain-specific roles for fusion and skin tropism. Proc Natl Acad Sci U S A **108:**18412–18417. http://dx.doi.org/10.1073/pnas.1111333108.

42. **Schmidt J, Klupp BG, Karger A, Mettenleiter TC.** 1997. Adaptability in herpesviruses: glycoprotein D-independent infectivity of pseudorabies virus. J Virol **71:**17–24.
43. **Nixdorf R, Klupp BG, Mettenleiter TC.** 2001. Role of the cytoplasmic tails of pseudorabies virus glycoproteins B, E and M in intracellular localization and virion incorporation. J Gen Virol **82:**215–226. http://dx.doi.org/10.1099/0022-1317-82-1-215.
44. **Rauh I, Mettenleiter TC.** 1991. Pseudorabies virus glycoproteins gII and gp50 are essential for virus penetration. J Virol **65:**5348–5356.
45. **Peeters B, de Wind N, Hooisma M, Wagenaar F, Gielkens A, Moormann R.** 1992. Pseudorabies virus envelope glycoproteins gp50 and gII are essential for virus penetration, but only gII is involved in membrane fusion. J Virol **66:**894–905.
46. **Connolly SA, Jackson JO, Jardetzky TS, Longnecker R.** 2011. Fusing structure and function: a structural view of the herpesvirus entry machinery. Nat Rev Microbiol **9:**369–381. http://dx.doi.org/10.1038/nrmicro2548.
47. **Ruel N, Zago A, Spear PG.** 2006. Alanine substitution of conserved residues in the cytoplasmic tail of herpes simplex virus gB can enhance or abolish cell fusion activity and viral entry. Virology **346:**229–237. http://dx.doi.org/10.1016/j.virol.2005.11.002.
48. **Silverman JL, Greene NG, King DS, Heldwein EE.** 2012. Membrane requirement for folding of the herpes simplex virus 1 gB cytodomain suggests a unique mechanism of fusion regulation. J Virol **86:**8171–8184. http://dx.doi.org/10.1128/JVI.00932-12.
49. **Garcia NJ, Chen J, Longnecker R.** 2013. Modulation of Epstein-Barr virus glycoprotein B (gB) fusion activity by the gB cytoplasmic tail domain. mBio **4:**e00571–12. http://dx.doi.org/10.1128/mBio.00571-12.
50. **Bold S, Ohlin M, Garten W, Radsak K.** 1996. Structural domains involved in human cytomegalovirus glycoprotein B-mediated cell-cell fusion. J Gen Virol **77:**2297–2302. http://dx.doi.org/10.1099/0022-1317-77-9-2297.
51. **Gage PJ, Levine M, Glorioso JC.** 1993. Syncytium-inducing mutations localize to two discrete regions within the cytoplasmic domain of herpes simplex virus type 1 glycoprotein B. J Virol **67:**2191–2201.
52. **Fan Z, Grantham ML, Smith MS, Anderson ES, Cardelli JA, Muggeridge MI.** 2002. Truncation of herpes simplex virus type 2 glycoprotein B increases its cell surface expression and activity in cell-cell fusion, but these properties are unrelated. J Virol **76:**9271–9283. http://dx.doi.org/10.1128/JVI.76.18.9271-9283.2002.
53. **Rogalin HB, Heldwein EE.** 23 September 2015. The interplay between the HSV-1 gB cytodomains and the gH cytotail during cell-cell fusion. J Virol http://dx.doi.org/10.1128/JVI.02391-15.
54. **Baghian A, Huang L, Newman S, Jayachandra S, Kousoulas KG.** 1993. Truncation of the carboxy-terminal 28 amino acids of glycoprotein B specified by herpes simplex virus type 1 mutant amb1511-7 causes extensive cell fusion. J Virol **67:**2396–2401.
55. **Chowdary TK, Heldwein EE.** 2010. Syncytial phenotype of C-terminally truncated herpes simplex virus type 1 gB is associated with diminished membrane interactions. J Virol **84:**4923–4935. http://dx.doi.org/10.1128/JVI.00206-10.
56. **Chen J, Zhang X, Jardetzky TS, Longnecker R.** 2014. The Epstein-Barr virus (EBV) glycoprotein B cytoplasmic C-terminal tail domain regulates the energy requirement for EBV-induced membrane fusion. J Virol **88:**11686–11695. http://dx.doi.org/10.1128/JVI.01349-14.
57. **Park SJ, Seo MD, Lee SK, Lee BJ.** 2008. Membrane binding properties of EBV gp110 C-terminal domain; evidences for structural transition in the membrane environment. Virology **379:**181–190. http://dx.doi.org/10.1016/j.virol.2008.06.031.
58. **Ficinska J, Van Minnebruggen G, Nauwynck HJ, Bienkowska-Szewczyk K, Favoreel HW.** 2005. Pseudorabies virus glycoprotein gD contains a functional endocytosis motif that acts in concert with an endocytosis motif in gB to drive internalization of antibody-antigen complexes from the surface of infected monocytes. J Virol **79:**7248–7254. http://dx.doi.org/10.1128/JVI.79.11.7248-7254.2005.

(III) Functional Relevance of the N-Terminal Domain of Pseudorabies Virus Envelope Glycoprotein H and Its Interaction with Glycoprotein L

III

Melina Vallbracht, Sascha Rehwald, Barbara G. Klupp, Thomas C. Mettenleiter, Walter Fuchs

Journal of Virology

Volume 91, Issue 9

May 2017

doi: 10.1128/JVI.00061-17

AMERICAN SOCIETY FOR MICROBIOLOGY | Journal of Virology®

VIRUS-CELL INTERACTIONS

Functional Relevance of the N-Terminal Domain of Pseudorabies Virus Envelope Glycoprotein H and Its Interaction with Glycoprotein L

Melina Vallbracht, Sascha Rehwaldt, Barbara G. Klupp, Thomas C. Mettenleiter, Walter Fuchs

Institute of Molecular Virology and Cell Biology, Friedrich-Loeffler-Institut, Greifswald-Insel Riems, Germany

ABSTRACT Several envelope glycoproteins are involved in herpesvirus entry into cells, direct cell-to-cell spread, and induction of cell fusion. The membrane fusion protein glycoprotein B (gB) and the presumably gB-activating heterodimer gH/gL are essential for these processes and conserved throughout the *Herpesviridae*. However, after extended cell culture passage of gL-negative mutants of the alphaherpesvirus pseudorabies virus (PrV), phenotypic revertants could be isolated which had acquired spontaneous mutations affecting the gL-interacting N-terminal part of the gH ectodomain (gDH and $gH^{B4.1}$) (B. G. Klupp and T. C. Mettenleiter, J Virol 73:3014–3022, 1999; C. Schröter, M. Vallbracht, J. Altenschmidt, S. Kargoll, W. Fuchs, B. G. Klupp, and T. C. Mettenleiter, J Virol 90:2264–2272, 2016). To investigate the functional relevance of this part of gH in more detail, we introduced an in-frame deletion of 66 codons at the 5′ end of the plasmid-cloned gH gene ($gH^{32/98}$). The N-terminal signal peptide was retained, and the deletion did not affect expression or processing of gH but abrogated its function in *in vitro* fusion assays. Insertion of the engineered gH gene into the PrV genome resulted in a defective mutant (pPrV-$gH^{32/98}$K), which was incapable of entry and spread. Interestingly, *in vitro* activity of mutated $gH^{32/98}$ was restored when it was coexpressed with hyperfusogenic $gB^{B4.1}$, obtained from a passaged gL deletion mutant of PrV. Moreover, the entry and spread defects of pPrV-$gH^{32/98}$K were compensated by the mutations in $gB^{B4.1}$ in *cis*, as well as in *trans*, independent of gL. Thus, PrV gL and the gL-interacting domain of gH are not strictly required for function.

IMPORTANCE Membrane fusion is crucial for infectious entry and spread of enveloped viruses. While many enveloped viruses require only one or two proteins for receptor binding and membrane fusion, herpesvirus infection depends on several envelope glycoproteins. Besides subfamily-specific receptor binding proteins, the core fusion machinery consists of the conserved fusion protein gB and the gH/gL complex. The role of the latter is unclear, but it is hypothesized to interact with gB for fusion activation. Using isogenic virus recombinants, we demonstrate here that gL and the gL-binding domain of PrV gH are not strictly required for membrane fusion during virus entry and spread when concomitantly mutations in gB are present which increase its fusogenicity. Thus, our results strongly support the notion of a functional gB-gH interaction during the fusion process.

KEYWORDS herpesvirus, pseudorabies virus, glycoproteins gH/gL, membrane fusion, virus entry, glycoprotein B

Received 11 January 2017 **Accepted** 15 February 2017

Accepted manuscript posted online 22 February 2017

Citation Vallbracht M, Rehwaldt S, Klupp BG, Mettenleiter TC, Fuchs W. 2017. Functional relevance of the N-terminal domain of pseudorabies virus envelope glycoprotein H and its interaction with glycoprotein L. J Virol 91:e00061-17. https://doi.org/10.1128/JVI.00061-17.

Editor Richard M. Longnecker, Northwestern University

Address correspondence to Thomas C. Mettenleiter, thomas.mettenleiter@fli.de.

Entry of enveloped viruses into host cells proceeds through fusion of the envelope with the host cell plasma membrane or with endosomal membranes. Whereas many viruses require only one or two receptor binding and/or fusion protein(s),

herpesviruses are dependent on at least four viral envelope glycoproteins for this process. Subfamily-specific proteins like the alphaherpesvirus glycoprotein D (gD) mediate receptor binding, while the core fusion machinery conserved in all members of the *Herpesviridae*, comprising mammalian, avian, and reptilian herpesviruses, is composed of the homotrimeric glycoprotein B (gB) and a heterodimeric complex of the integral membrane glycoprotein H and the anchorless glycoprotein L (gH/gL) (reviewed in references 1 and 2).

Activation of the fusion machinery of pseudorabies virus ([PrV] *Suid alphaherpesvirus 1*) and of herpes simplex viruses 1 and 2 ([HSV-1/2] *Human alphaherpesvirus 1* and *2*) is initiated by binding of gD to specific cellular receptors like nectin-1 or herpesvirus entry mediator (HVEM) (3). Receptor binding leads to conformational changes in the C-terminal region of the HSV-1 gD ectodomain (4, 5). According to the current model, this conformational rearrangement of gD induces interaction with the gH/gL complex, which in turn is thought to activate the bona fide fusion protein gB to execute membrane fusion (6–9). While gD signaling is generally required for triggering membrane fusion in HSV, PrV gD is dispensable for direct cell-to-cell spread and *in vitro* cell fusion (10–12). Moreover, gD deletion mutants of PrV and bovine alphaherpesvirus 1 (BoHV-1) could be isolated, which were replication competent in cell culture in the presence of compensatory mutations in gB and gH (13–15), indicating that gD is not central to the fusion process.

Homologs of gB are found in all members of the *Herpesviridae*. The crystal structure of the ectodomain resembles that of a class III fusion protein, including a trimeric fold, a central alpha-helical coiled coil, and internal bipartite fusion loops (16). Several gB postfusion forms and a more condensed conformation of full-length HSV-1 gB, which is proposed to represent a prefusion or intermediate state, have been determined (17). Although gBs of HSV-1 (16) and of Epstein-Barr virus ([EBV] *Human gammaherpesvirus 4*) (18) share no sequence similarities with other class III fusion proteins, such as vesicular stomatitis virus (VSV) glycoprotein G (19) or baculovirus gp64 (20), their crystal structures are highly similar. However, unlike the latter proteins, gB is not able to merge membranes on its own but requires activation by the gH/gL complex (8, 21).

gH is a type I transmembrane protein with a short cytoplasmic tail and a large N-terminal ectodomain. It is associated with gL, which lacks a membrane anchor (2, 8, 22, 23). Although much work has gone into understanding the function of the gH/gL complex during membrane fusion, its role remains enigmatic. Despite experimental evidence that gH/gL may act as a fusion protein itself (24, 25), the recently determined crystal structures of soluble EBV gH/gL (22), HSV-2 gH/gL (8), varicella-zoster virus ([VZV] *Human alphaherpesvirus 3*) gH/gL (23), and of a core fragment of PrV gH (26) revealed no structural features resembling any known viral fusion protein. Furthermore, the structural analyses indicate that previously identified putative fusogenic and membrane-interacting peptides of HSV-1 gH are not exposed at the surface of gH and are unlikely to become available for interaction with membranes upon a conformational change (26). Interestingly, the structural analyses showed that the domain organization of the four gH homologs is strikingly similar although their amino acid sequences are only poorly conserved.

The most highly conserved region of gH is the membrane-proximal domain IV (designated H3 in HSV-2), which consists of a beta-sandwich comprising two opposed four-stranded beta-sheets, which are connected via a long crossover segment of the polypeptide chain, designated flap. Since the flap covers a conserved patch of hydrophobic amino acid residues, its movement during a receptor-triggered conformational change of gH is thought to enable interaction of the underlying hydrophobic surface with the viral envelope to promote the fusion process (26, 27). Functional conservation of this domain in PrV and HSV-1 could be demonstrated by analysis of chimeric gH consisting of PrV domains I to III and HSV-1 domain IV. This chimeric protein was not only capable of inducing membrane fusion when expressed together with HSV-1 or PrV gB and with PrV gD and gL but also supported replication of gH-deleted PrV (28). The less conserved domain III (H2) is composed of eight alpha-helices and contains a highly

conserved amino acid stretch (serine-proline-cysteine) important for regulation of membrane fusion (29). Domain II (H1B) contains the "fence," a sheet of antiparallel beta-chains, and a highly conserved bundle of three alpha-helices, designated syntaxin-like bundle (SLB) because of its structural similarities to a specific domain of cellular syntaxins. Recent studies indicate that the integrity and flexibility of the SLB are relevant for the function of PrV gH in membrane fusion (30). The N-terminal domain I of gH forms tight contacts with gL, and the presence of both proteins is critical for the secondary structure and the hydrophobic core of this domain in HSV and EBV (8, 22).

Due to a lack of a membrane anchor, gL is dependent on association with gH for virion incorporation (31–34). However, while gL is required for correct folding and transport of gH in most herpesviruses, it is not essential for gH virion incorporation in PrV, bovine gammaherpesvirus 4, and murid gammaherpesvirus 4 (35–37). More importantly, gL-deleted PrV mutants (PrV-ΔgL) are capable of limited cell-to-cell spread although they are defective in entry into target cells. However, after reversion analyses by serial cell culture passages, these gL-deleted PrV mutants regained wild-type-like replication properties by acquiring compensatory mutations in the gH, gB, and gD genes (38, 39).

Two independent reversion analyses resulted in two different revertants, but both contained compensatory mutations involving the predicted gL interaction domain of gH, which is located within the amino-terminal part of the gH ectodomain. The first passaging experiment selected for a chimeric gDH hybrid protein, which lacked the predicted gL interaction domain and consisted of the N-terminal 217 amino acids of gD, including the receptor binding domain, fused to the C-terminal 590 amino acids of gH (38). This hybrid protein was able to substitute not only for the lack of gL but also for the absence of wild-type gH and gD in complementation and in *in vitro* fusion assays (12). Recently, another infectious revertant, designated PrV-ΔgLPassB4.1, was isolated and characterized. As in gDH, compensatory mutations occurred in the gH gene of PrV-ΔgLPassB4.1 ($gH^{B4.1}$) also located in the predicted gL-binding domain (39). Two point mutations in $gH^{B4.1}$ (L70P and W103R) were found to be sufficient to compensate for the lack of gL in transfection-based fusion assays. However, mutations were also detected in gB ($gB^{B4.1}$), which resulted in enhanced fusogenicity and gL-independent *in vitro* fusion also in the presence of wild-type gH, although further enhanced syncytium formation was observed after coexpression of $gB^{B4.1}$ with the homologous $gH^{B4.1}$ (39).

To investigate the functional relevance of the N-terminal part of the gH ectodomain in more detail and, in particular, in virus-infected cells, we deleted the predicted gL-binding domain (66 codons at the 5′ end, yielding $gH^{32/98}$) in the plasmid-cloned PrV gH gene and tested the mutated gH in a virus-free transfection-based cell fusion assay. Furthermore, the mutated gH gene was inserted into the cloned PrV genome (27) in the presence or absence of gL and wild-type or mutated gB. Protein expression, as well as *in vitro* replication properties, including penetration, growth kinetics, and plaque formation of the obtained virus mutants, was investigated.

RESULTS

Deletion of the gL-binding domain of PrV gH does not affect protein expression and virion incorporation. To investigate the functional relevance of the predicted gL-binding domain in PrV gH, we deleted codons 32 to 97 in the plasmid-cloned gH gene ($gH^{32/98}$). The deletion excludes the signal peptide of gH, which is predicted to be cleaved behind amino acid 30 (Fig. 1B). To compare transient expression and processing of $gH^{32/98}$ with those of the wild-type gH of PrV strain Kaplan (gH^{Ka}), RK13 cells were transfected with expression plasmids pcDNA-$gH^{32/98}$KDE or pcDNA-gHKDE. (30) After 48 h cell lysates were analyzed by Western blotting. Targeted deletion of the predicted gL-binding domain led to expression of a truncated $gH^{32/98}$ protein with a molecular mass of approximately 80 kDa, whereas the apparent mass of mature wild-type gH was approximately 90 kDa (Fig. 2). Smaller proteins representing immature gH precursors or degradation products were significantly less abundant, indicating

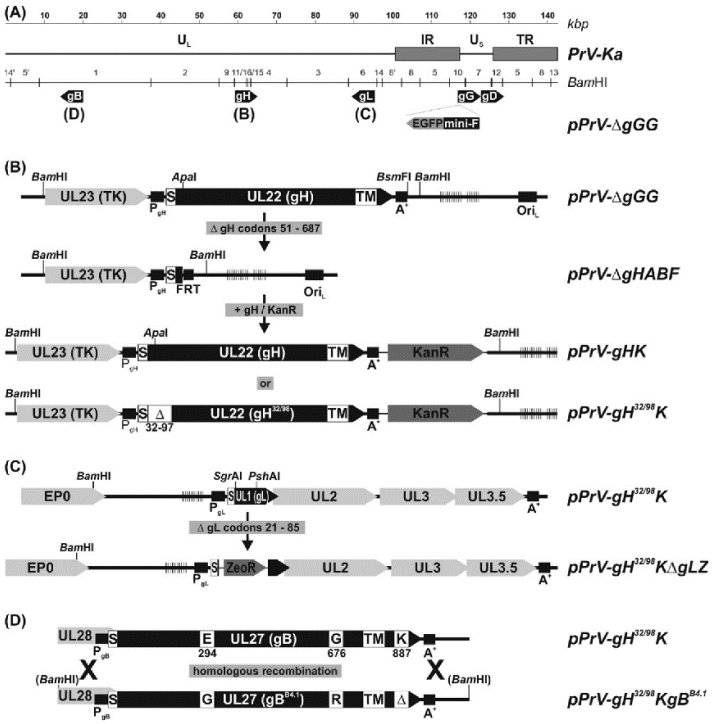

FIG 1 Construction of virus mutants. (A) The wild-type PrV-Ka genome consists of unique long and short regions (U_L and U_S, respectively), and inverted repeat sequences (IR, internal repeat; TR, terminal repeat). The positions of the relevant glycoprotein genes (gB, gD, gG, gH, and gL) are indicated. An EGFP expression cassette and a mini-F vector for BAC replication were inserted at the nonessential gG locus. (B) After deletion of the wild-type gH gene, modified forms were reinserted together with a kanamycin resistance gene (Kan^r) by mutagenesis in *E. coli*. (C) In a similar manner, the gL gene was replaced by a zeocin resistance gene (Zeo^r). (D) Replacement of wild-type gB by mutated gB$^{B4.1}$ was achieved by homologous recombination in BAC- and transfer plasmid-cotransfected RK13 cells and subsequent plaque purification of viable progeny viruses. Designations of virus recombinants, relevant restriction sites, regulatory sequences like promoters (P_{gX}), polyadenylation signals (A^+), an origin of DNA replication (ORI_L), an Flp recombinase target site (FRT), and open reading frames (pointed rectangles) are indicated. The locations of signal peptides (S), transmembrane domains (TM), deletions (Δ), and amino acid substitutions in the deduced glycoproteins are highlighted. Vertical lines indicate tandem repeat sequences. TK, thymidine kinase. EP0, early protein 0.

that processing or stability of gH$^{32/98}$ was not affected. Indirect immunofluorescence analyses of cells transfected with the expression plasmids for gH^{Ka} or gH$^{32/98}$ demonstrated that the introduced in-frame deletion of the gL-binding domain had no apparent effect on expression level, cytoplasmic distribution, or surface localization of the protein (data not shown).

After insertion of gH$^{32/98}$ into the PrV genome, Western blot analyses of RK13 cells infected with phenotypically complemented virions of the resulting mutants pPrV-gH$^{32/98}$K and pPrV-gH$^{32/98}$KΔgLZ or with wild-type gH-containing mutants pPrV-gHK and pPrV-gHKΔgLZ (Fig. 1B and C) again revealed similar expression levels of truncated gH$^{32/98}$ and of gH^{Ka} (Fig. 3A, top panel). Presence or absence of gL had no detectable effect on expression or processing of gH. However, only small amounts of immature 16- to 18-kDa forms of gL were detectable in cells infected with pPrVgH$^{32/98}$K, in contrast to an abundant 20-kDa gL in pPrV-gHK-infected cells (Fig. 3A, second panel). This indicates that gH$^{32/98}$ is unable to bind gL, which leads either to impaired gL processing and/or to rapid secretion of mature gL. Replacement of wild-type gB^{Ka} by the hyperfusogenic mutant gB$^{B4.1}$ (39) in pPrVgH$^{32/98}$KgB$^{B4.1}$ and pPrVgH$^{32/98}$KΔgLZgB$^{B4.1}$

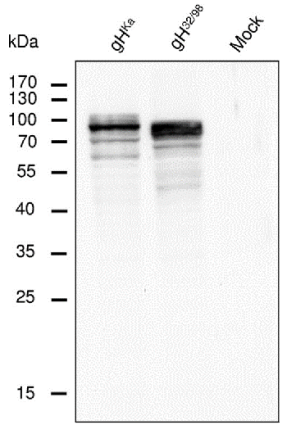

FIG 2 Western blot analyses of transfected RK13 cells. Lysates prepared 48 h after transfection with expression plasmids for wild-type gH^{Ka}, modified $gH^{32/98}$, or the empty vector (Mock) were separated by SDS-PAGE. The blot was incubated with a PrV gH-specific rabbit antiserum. Molecular masses (kDa) of marker proteins are indicated.

(Fig. 1D) did not alter the apparent molecular masses of the gB gene products nor the efficiency of furin cleavage of the precursor protein (Fig. 3A, third panel). Analysis of sucrose gradient-purified virions showed that $gH^{32/98}$ is efficiently incorporated into virus particles irrespective of gL and of the presence of either gB^{Ka} or $gB^{B4.1}$ (Fig. 3B, top panel). As expected, gL was only detectable in virions of pPrV-gHK which contained gH^{Ka} (Fig. 3B, second panel). Purity of the virion preparations was confirmed by the absence of pUL31, which is present only in infected cells and in primary enveloped particles in the perinuclear space (Fig. 3, bottom panels) (40).

Targeted deletion of the gL-binding domain leads to significantly reduced *in vitro* fusion activity of gH, which can be restored by compensatory mutations in gB. Cell-cell fusion can be induced by coexpression of PrV or HSV glycoproteins gB, gD, and gH/gL in plasmid-transfected cells *in vitro* (12, 41). While the expression of all four HSV glycoproteins is necessary to induce membrane fusion, PrV gB and gH/gL are

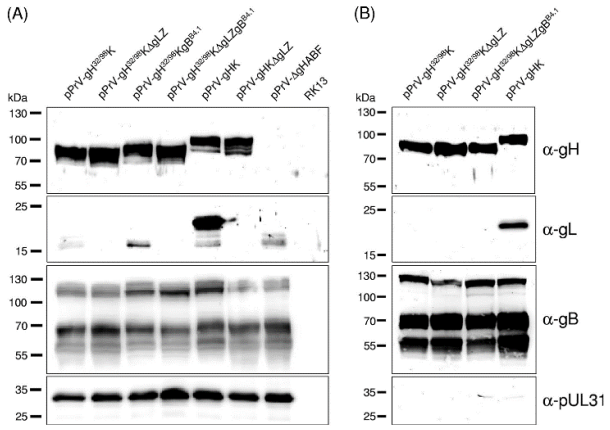

FIG 3 Western blot analyses of PrV-infected cells and purified virions. Lysates of RK13 cells prepared 20 h after infection (MOI of 5) with the indicated virus recombinants (A), and purified virion proteins were separated by SDS-PAGE (B). Blots were incubated with monospecific rabbit antiserum against PrV glycoproteins gH, gL, and gB and the nonstructural UL31 protein. Molecular masses of marker proteins are indicated.

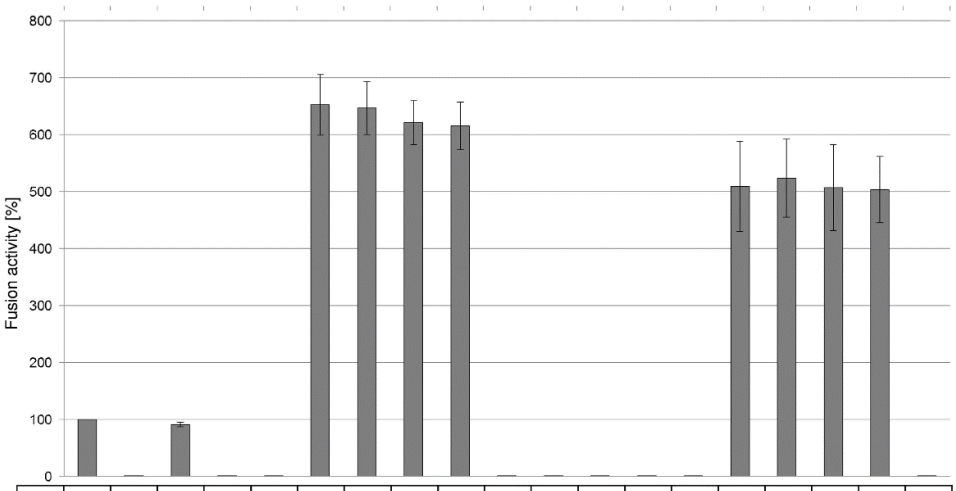

gL	Ka	/	Ka	/	/	Ka	/	Ka	/	/	Ka	/	Ka	/	Ka	/	Ka	/	/
gD	Ka	Ka	/	/	/	Ka	Ka	/	/	/	Ka	Ka	/	/	Ka	Ka	/	/	/
gH	Ka	Ka	Ka	Ka	/	Ka	Ka	Ka	Ka	/	32/98	32/98	32/98	32/98	32/98	32/98	32/98	32/98	/
gB	Ka	Ka	Ka	Ka	Ka	B4.1	B4.1	B4.1	B4.1	B4.1	Ka	Ka	Ka	Ka	B4.1	B4.1	B4.1	B4.1	/

FIG 4 *In vitro* fusion assays. RK13 cells were cotransfected with expression plasmids for EGFP, wild-type gB (gB^{Ka}), or mutated $gB^{B4.1}$ and, optionally, gH^{Ka} or $gH^{32/98}$, gD^{Ka}, and gL^{Ka}. One day posttransfection the areas of green fluorescing syncytia were measured, and total fusion activity was determined by multiplication of the mean syncytium area with the number of syncytia in 10 randomly selected fields. Fusion activities obtained with the four wild-type glycoproteins were set as 100%. Shown are the mean relative values and standard deviations of three independent experiments.

sufficient for this process, and the additional expression of PrV gD enhances *in vitro* fusion activity only moderately (12). However, omission of either gB or gH results in total abrogation of membrane fusion in either system.

To analyze the influence of the deletion of the predicted gL-binding domain of gH ($gH^{32/98}$) on *in vitro* fusion activity, RK13 cells were cotransfected with expression plasmids encoding the mutated PrV $gH^{32/98}$, wild-type gB^{Ka}, and optionally gL and gD. In addition, enhanced green fluorescent protein (EGFP) was coexpressed to facilitate evaluation of the assays by fluorescence microscopy. Assays with plasmids encoding wild-type gH^{Ka}, gB^{Ka}, gL, and gD served as positive controls, and results were set as 100%. Assays with the empty expression vector pcDNA3 served as negative controls. One day after transfection, the areas of cells containing three or more nuclei were measured and multiplied by the number of syncytia to quantify fusion activity. As expected, after cotransfection of wild-type gH^{Ka}, gB^{Ka}, and gL, formation of multiple syncytia was observed. However, fusion activity was completely abolished when either gL was omitted or $gH^{32/98}$ was expressed instead of wild-type gH^{Ka} (Fig. 4). This suggested that the gL-binding domain of gH and/or the presence of gL in the fusion complex is essential for its function. As reported earlier, omission of gD had only minor effects on fusion induced by wild-type gB^{Ka}, gH^{Ka}, and gL (Fig. 4).

In recent studies, we identified an infectious gL-deleted PrV mutant, which carries compensatory mutations in the gH, gB, and gD ($gH^{B4.1}$, $gB^{B4.1}$, and $gD^{B4.1}$) genes. While the mutations in $gH^{B4.1}$ were found to be sufficient to compensate for the lack of gL in transient assays, the mutations present in $gB^{B4.1}$ enhanced fusion activity (39). Therefore, it was investigated whether $gH^{32/98}$ is able to trigger fusogenicity of the presumably more fusion prone $gB^{B4.1}$ independent of gL. Interestingly, the fusion activity achieved with $gH^{32/98}$ and $gB^{B4.1}$ was much higher (approximately 550%) than that observed with the four wild-type proteins (Fig. 4). Moreover, fusion

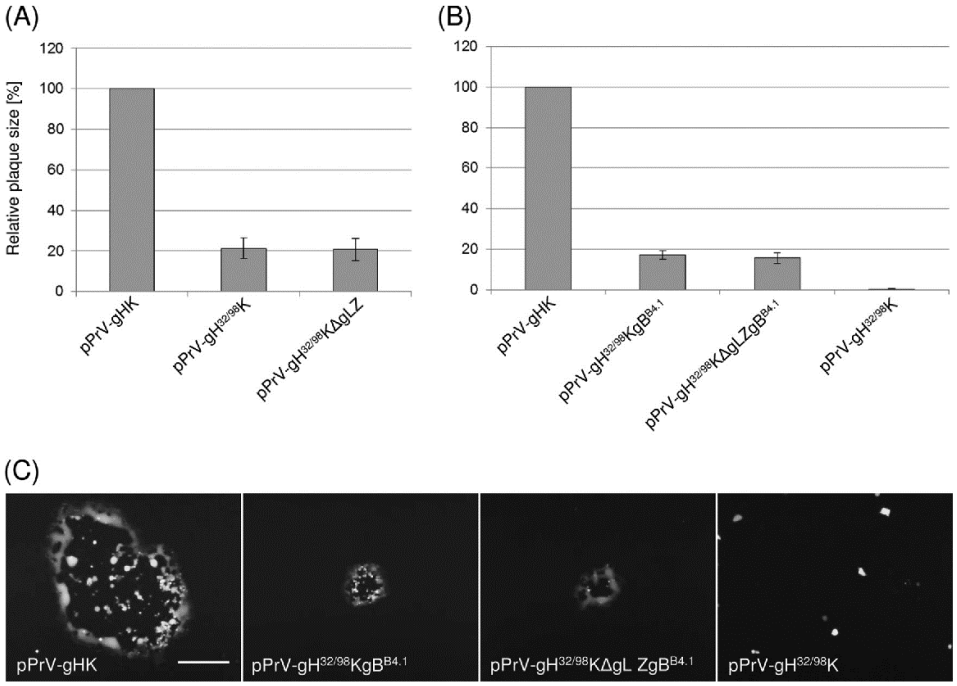

FIG 5 Plaque assays on RK13-gB$^{B4.1}$ (A) or RK13 cells (B). Cells were infected with the indicated PrV recombinants and incubated for 48 h under plaque assay conditions. Areas of 30 plaques per virus were measured, and percentages of wild-type (pPrV-gHK) sizes were calculated. Mean values and standard deviations of four independent experiments are shown. (C) Representative images of infected RK13 cells. Bar, 500 μm.

activity obtained with gH$^{32/98}$ in combination with gB$^{B4.1}$ reached approximately 80% of that obtained with wild-type gH in combination with gB$^{B4.1}$, and in both cases this was independent of gL (Fig. 4). However, gB$^{B4.1}$ alone was not sufficient to induce cell-cell fusion (39) (Fig. 4).

In summary, the wild-type-like *in vitro* syncytium formation mediated by gH$^{32/98}$ together with gB$^{B4.1}$ demonstrates that gL and the gL-binding domain of gH are dispensable for PrV glycoprotein-mediated membrane fusion if gB is modified by adaptive or compensatory mutations increasing its fusogenicity. This clearly differs from the situation in the gDH hybrid protein, which compensates the absence of gL without the requirement for modification in gB.

Deletion of the gL-binding domain in gH$^{32/98}$ abrogates virus replication and spread. After insertion of the mutated gH$^{32/98}$ gene into the PrV genome by bacterial artificial chromosome (BAC) mutagenesis in *Escherichia coli*, no infectious virus of the resulting GFP-expressing recombinants pPrV-gH$^{32/98}$K and pPrV-gH$^{32/98}$KΔgLZ (Fig. 1) could be reconstituted in transfected RK13 cells, whereas an otherwise identical recombinant containing wild-type gH (pPrV-gHK) replicated efficiently. On *trans*-complementing RK13-gH/gL cells (42), the gH$^{32/98}$-containing PrV mutants could, however, be isolated and propagated, indicating that they had no defects elsewhere in their genomes. After infection of RK13 cells with phenotypically complemented pPrV-gH$^{32/98}$K (Fig. 5) or pPrV-gH$^{32/98}$KΔgLZ (data not shown), only single GFP-expressing cells were observed, as described for gH-negative PrV mutants (11, 43). In growth kinetics studies performed on RK13 cells, no infectious progeny virus of pPrV-gH$^{32/98}$K could be detected at any time (Fig. 6), even if titrations were performed on RK13-gH/gL cells (data not shown). Thus, gH$^{32/98}$, although expressed and incorporated into virions, appeared to be nonfunctional in the viral context.

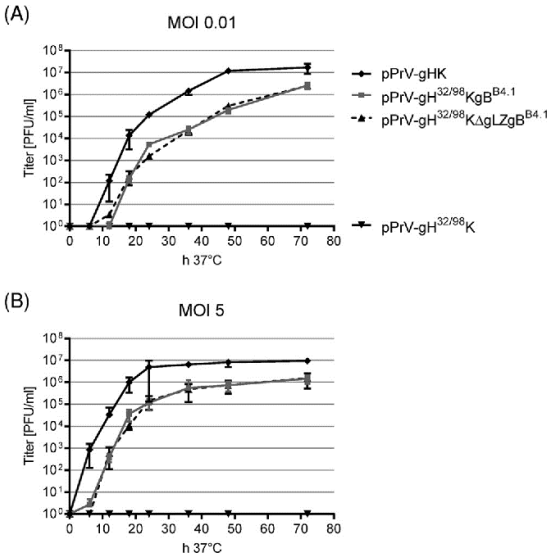

FIG 6 *In vitro* growth kinetics of PrV mutants. RK13 cells were infected with pPrV-gHK, pPrV-gH$^{32/98}$K, pPrV-gH$^{32/98}$KgB$^{B4.1}$, or pPrV-gH$^{32/98}$KΔgLZgB$^{B4.1}$ at an MOI of 0.01 (A) or 5 (B). Cells were harvested together with the supernatants after 0, 6, 12, 18, 24, 36, 48, and 72 h at 37°C and lysed by freeze-thawing, and progeny virus titers were determined on RK13 cells. Shown are mean results of four independent experiments with corresponding standard deviations.

Replication competence of pPrV-gH$^{32/98}$K can be restored by compensatory mutations in gB. Since transient *in vitro* fusion assays revealed that gH$^{32/98}$ regained almost wild-type activity when coexpressed with the mutated gB of PrV-ΔgLPassB4.1 (see above), we assessed whether gB$^{B4.1}$ is able to rescue the function of gH$^{32/98}$ also in the viral context. A recombinant RK13 cell line which constitutively expressed gB$^{B4.1}$ was used for replication studies. On RK13-gB$^{B4.1}$ cells pPrV-gH$^{32/98}$K and pPrV-gH$^{32/98}$KΔgLZ spread to plaque areas of nearly 20% of the wild-type (pPrV-gHK) sizes (Fig. 5A). However, infectious titers remained 1,000-fold lower than the wild-type titer (results not shown). To exclude effects of inadequate gB expression or competition between gB$^{B4.1}$ provided by the cells and the viral wild-type protein, the gB gene of the gH$^{32/98}$-expressing PrV mutants was exchanged by homologous recombination after cotransfection of normal RK13 cells with BAC DNA of pPrV-gH$^{32/98}$K or pPrV-gH$^{32/98}$KΔgLZ and a transfer plasmid containing the PCR-amplified gB gene region of PrV-ΔgLPassB4.1 (Fig. 1D). This led to PrV mutants which could be efficiently propagated in noncomplementing cells. Sequence analyses of the gB genes of several plaque isolates revealed that all of them exhibited the two described point mutations leading to amino acid substitutions in the ectodomain of gB$^{B4.1}$, E^{294}G and G^{676}R (Fig. 1D) (39). In contrast, two other described mutations of the gB$^{B4.1}$ gene, leading to deletion of a lysine residue in the cytoplasmic tail (ΔK^{887}) and of a duplicated stretch of 4 amino acids (AVRA) from positions 115 to 118 of wild-type gB^{Ka}, were not always introduced, indicating an inferior functional relevance. pPrV-gH$^{32/98}$KgB$^{B4.1}$ and pPrV-gH$^{32/98}$KΔgLZgB$^{B4.1}$, used for further characterization, exhibited the C-terminal deletion, but not the N-terminal mutation (Fig. 1D). In addition to the three mutations in gB and the desired deletions in gH/gL, no unwanted alterations were found in the gB, gD, gH, or gL genes of the investigated PrV mutants.

Whereas pPrV-gH$^{32/98}$K and pPrV-gH$^{32/98}$KΔgLZ were incapable of spread in RK13 cells, pPrV-gH$^{32/98}$KgB$^{B4.1}$ and pPrV-gH$^{32/98}$KΔgLZgB$^{B4.1}$ were able to form plaques although these were approximately 80% smaller than those formed by pPrV-gHK (Fig. 5B and C). Presence or absence of gL had no effect on plaque sizes of the gB$^{B4.1}$-rescued gH$^{32/98}$ mutants, and the size reduction compared to that of wild-type plaques was similar to that on gB$^{B4.1}$-expressing cells (Fig. 5A).

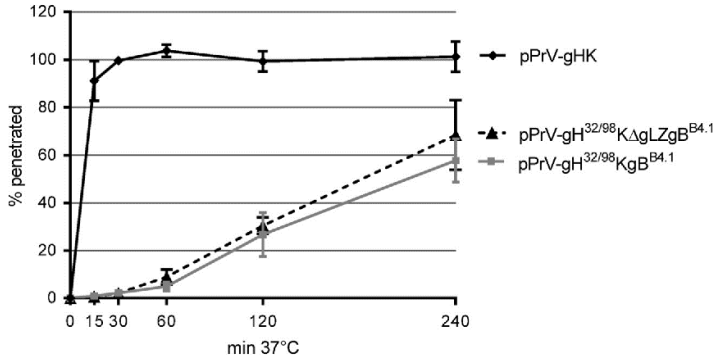

FIG 7 Penetration kinetics of PrV mutants. RK13 cells were infected with approximately 250 PFU of pPrV-gHK, pPrV-gH$^{32/98}$KgB$^{B4.1}$, or pPrV-gH$^{32/98}$KΔgLZgB$^{B4.1}$. After adsorption at 4°C, the cells were incubated for 0, 15, 30, 60, 120, and 240 min at 37°C prior to acid inactivation of nonpenetrated virus. Numbers of plaques formed after 48 h were compared to those obtained without inactivation. Mean percentages of three independent experiments and standard deviations are shown.

To investigate the influence of the targeted deletion of the gL binding domain of gH in combination with the hyperfusogenic gB$^{B4.1}$ on formation of infectious virus particles, RK13 cells were infected at multiplicities of infection (MOIs) of 0.01 (Fig. 6A) or 5 (Fig. 6B), and total progeny virus titers were determined 0, 6, 12, 18, 24, 36, 48, and 72 h postinfection (p.i.) on complementing RK13-gH/gL and noncomplementing RK13 cells. Since titers on both cell lines were almost identical, only those from RK13 cells are shown. Whereas no infectious pPrV-gH$^{32/98}$K particles were formed in RK13 cells, pPrV-gH$^{32/98}$KgB$^{B4.1}$ and pPrV-gH$^{32/98}$KΔgLZgB$^{B4.1}$ grew to final titers of $>10^6$ PFU/ml, approximately 1 $\log_{10}$ unit lower than those of pPrV-gHK (Fig. 6). Thus, with respect to productive replication, *cis*-complementation of the gH$^{32/98}$ mutants by virus-expressed gB$^{B4.1}$ was much more efficient than *trans*-complementation on gB$^{B4.1}$-expressing cells (see above). Plaque sizes, growth kinetics, and maximum titers of the gB$^{B4.1}$-rescued viruses, pPrV-gH$^{32/98}$KgB$^{B4.1}$ and pPrV-gH$^{32/98}$KΔgLZgB$^{B4.1}$, were almost indistinguishable, indicating that in the absence of the gL-binding domain of gH, gL itself is no longer relevant for entry and viral spread. However, mutations in gB$^{B4.1}$ were obviously essential for function of gH$^{32/98}$.

Penetration of pPrV-gH$^{32/98}$KgB$^{B4.1}$ and pPrV-gH$^{32/98}$KΔgLZgB$^{B4.1}$ recombinants is significantly delayed. Replication kinetics of pPrV-gH$^{32/98}$KgB$^{B4.1}$ and pPrV-gH$^{32/98}$KΔgLZgB$^{B4.1}$ after infection at both low and high MOIs revealed a markedly delayed titer increase compared to the titer of wild-type gH-expressing pPrV-gHK (Fig. 6). To investigate whether this effect was due to impaired virus entry, penetration studies were carried out. Whereas entry of pPrV-gHK into RK13 cells occurred very fast, with approximately 90% of infectious input virus protected from inactivation by low-pH treatment after 15 min at 37°C (Fig. 7), penetration of pPrV-gH$^{32/98}$KgB$^{B4.1}$ and pPrV-gH$^{32/98}$KΔgLZgB$^{B4.1}$ was significantly delayed. Even after 4 h, only 60 to 70% of the infectious particles of pPrV-gH$^{32/98}$KgB$^{B4.1}$ and pPrV-gH$^{32/98}$KΔgLZgB$^{B4.1}$ were internalized, and again no difference was observed between the gL-expressing and the gL-deleted mutants (Fig. 7). Penetration kinetics of pPrV-gH$^{32/98}$K and PrV-gH$^{32/98}$KΔgLZ could not be investigated since these mutants become infectious only after phenotypic complementation with wild-type gH. Nevertheless, our studies confirm that gL and the gL-binding domain of PrV gH are not strictly required for membrane fusion during virus entry and spread. However, in the viral context the minimum functional fusion complex consisting of N-terminally truncated gH$^{32/98}$ and point-mutated gB$^{B4.1}$ of PrV is less efficient with respect to speed or rate of fusion events than wild-type glycoproteins gB, gD, gH, and gL.

DISCUSSION

Herpesviruses infect cells by fusion of the viral envelope with cellular membranes. While many other enveloped viruses use a single protein for attachment and fusion, herpesviruses require at least two conserved core fusion machinery components, gB and the heterodimeric gH/gL complex, and additional nonconserved subfamily-specific receptor binding proteins like gD (reviewed in references 2, 6, and 9).

In our previous work, we analyzed the relevance of the gH/gL complex by reversion analyses of gL-deleted PrV mutants (38, 39) and site-directed mutagenesis of PrV gH domains II, III, and IV (27, 30). In the present study, these approaches were extended to the structurally uncharacterized N-terminal gH domain I, which in HSV-2 and EBV was shown to tightly interact with gL (8, 22). In the previously described gL-independently replicating PrV mutants, this domain was either affected by point mutations (39) or replaced by the N-terminal part of gD, resulting in a gDH hybrid protein (38). Since chimeric gDH lacks gH amino acids 1 to 96, we artificially introduced a similar in-frame deletion of gH codons 32 to 97 ($gH^{32/98}$) to investigate gD-independent function of truncated gH. The retained gH amino acids 1 to 30 are predicted to represent a cleaved N-terminal signal peptide required for translocation into the endoplasmic reticulum. Thus, the resulting N terminus of mature $gH^{32/98}$ was similar to that of the gH core fragment (amino acids 107 to 639), whose crystal structure has been recently solved (26).

Deletion of the predicted gL-binding domain in $gH^{32/98}$ did not impair expression and processing of gH in plasmid-transfected cells (Fig. 2) and showed no apparent differences from wild-type gH with respect to intracellular localization or cell surface expression. Furthermore, $gH^{32/98}$ was efficiently incorporated into virions independent of gL (Fig. 3). This is in line with the previously described gL-independent virion incorporation of wild-type PrV gH (35), whereas in other herpesviruses like HSV-1 or VZV, gL is required for maturation and transport of gH to the future budding sites (31, 44–46). Several N-terminally truncated HSV-2 gH variants have been reported, which are transported without gL but still require gL for function (47). By amino acid substitutions in the corresponding part of HSV-2 gH, potential key residues were identified and hypothesized to form an endoplasmic reticulum (ER) retention signal, which is hidden in the presence of gL and then allows transport of the gH/gL complex to the future budding sites (47). However, these key residues are not conserved in PrV, VZV, or EBV. Furthermore, HSV-2 gL is considered to represent a scaffolding protein for gH (8) and was shown to be required for proper folding and function of the gH/gL complex (47). Although the N-terminal domain is not required for correct processing or virion targeting of PrV gH, its complex partner gL was incompletely processed in or secreted from cells infected with virus mutants expressing $gH^{32/98}$ and was undetectable in extracellular virus particles. This demonstrates that $gH^{32/98}$ is unable to bind and to target gL, which lacks a transmembrane domain, into virions. Thus, as hypothesized, amino acids 32 to 97 of PrV gH contain a region essential for gL interaction.

To investigate the impact of the deletion of the gL-binding domain of PrV gH on membrane fusion, we used a transient-transfection-based fusion assay (39) (Fig. 4). Unlike the wild-type protein, $gH^{32/98}$ exhibited no detectable *in vitro* fusion activity when coexpressed with wild-type gB, gD, and gL. Omission of gD only slightly reduced activity of the wild-type glycoprotein set, whereas gL was indispensable (12, 39). Since PrV gD is obviously not required for *in vitro* fusion, the dysfunction of $gH^{32/98}$ in our fusion assays was unlikely due to an impaired interaction with gD. Whereas the N-terminally mutated $gH^{B4.1}$ and gDH of gL-independently replicating PrV mutants mediated considerable gL-independent *in vitro* fusion activity when they were coexpressed with wild-type gB (12, 38, 39), $gH^{32/98}$ was inactive independent of gL. Thus, our results suggest that the deletion in gH domain I leads to downstream structural alterations which affect interaction with gB so that $gH^{32/98}$ is not able to activate wild-type gB. In wild-type gH association with gL and in gDH, the gD part might induce or maintain a conformation of gH required for triggering gB-mediated fusion. In line

with this hypothesis, the domain I-domain II interface of gH/gL has been considered to be relevant for gB activation in EBV and VZV (23, 48). However, when $gH^{32/98}$ was used in combination with the mutated $gB^{B4.1}$ obtained from the passaged, phenotypically reverted gL deletion mutant PrV-ΔgLPassB4.1 (39), fusion activity was rescued to a 5-fold higher level than observed with the wild-type set of glycoproteins, and this activity was independent of gD and gL (Fig. 4). Also in combination with wild-type gH, fusogenicity of $gB^{B4.1}$ was gL independent and much higher than that of wild-type gB (39). This indicates that the conformational changes required for fusion might be facilitated by the mutations present in $gB^{B4.1}$ and could be triggered even in the absence of gL and by suboptimal gH variants. Nevertheless, the gH trigger remained indispensable also for $gB^{B4.1}$ (Fig. 4) (39).

In accordance with the missing *in vitro* fusion activity of wild-type gB together with $gH^{32/98}$, engineered PrV recombinants expressing this protein combination were incapable of cell-to-cell spread and produced no infectious virus particles (Fig. 5 and 6). Thus, unlike gDH (38), $gH^{32/98}$ is nonfunctional also in the viral context, confirming that the gD part of gDH is required for function of the hybrid protein in triggering fusion. However, on cells expressing $gB^{B4.1}$, plaque formation of pPrV-$gH^{32/98}$K and pPrV-$gH^{32/98}$KΔgLZ was restored. The same effect was observed after replacement of the wild-type gB gene by $gB^{B4.1}$, and the resulting mutants pPrV-$gH^{32/98}$K$gB^{B4.1}$ and pPrV-$gH^{32/98}$KΔgLZ$gB^{B4.1}$ could be efficiently propagated on cells providing neither gB nor gH in *trans* (Fig. 5 and 6). Interestingly, the plaques produced by the $gH^{32/98}$ mutants in the presence of $gB^{B4.1}$ were approximately 80% smaller, and their maximum titers were one order of magnitude lower than those of isogenic PrV recombinants expressing wild-type gB, gD, gH, and gL, whereas *in vitro* fusion activity of $gH^{32/98}$ and $gB^{B4.1}$ was much higher than that of the complete wild-type glycoprotein set. These quantitative differences support the assumption that the mechanisms of membrane fusion during syncytium formation, virus entry, and virus spread are similar but not identical. Possibly, premature fusion events between cells and intracellular membranes induced by the hyperfusogenic $gB^{B4.1}$ interfere with the efficiency of virion formation and spread. Furthermore, investigation of penetration kinetics revealed that entry of PrV mutants expressing truncated $gH^{32/98}$ and $gB^{B4.1}$ is considerably delayed compared to that in wild-type PrV (Fig. 7), which might contribute to the reduced plaque sizes and titers. Western blot analyses of purified virions of pPrV-$gH^{32/98}$K$gB^{B4.1}$ and pPrV-$gH^{32/98}$KΔgLZ$gB^{B4.1}$ (Fig. 3B) provided no evidence that delayed penetration could be a consequence of less efficient virion incorporation of the two mutated glycoproteins. Thus, more likely, interaction of truncated $gH^{32/98}$ with gD after receptor binding or with $gB^{B4.1}$ prior to fusion might be less efficient than in wild-type particles. On the other hand, it is also conceivable that the $gH^{32/98}$/$gB^{B4.1}$-expressing PrV recombinants use endocytic/phagocytic pathways instead of direct fusion with the plasma membrane to enter cells.

For HSV-1 and -2 it has been shown recently that gH/gL rather than gB governs the speed and rate of fusion, with gH being the main contributor (49). The observed delay in penetration mediated by $gH^{32/98}$ also emphasizes the importance of gH as a fusion regulator. In previous studies we detected similarly delayed penetration kinetics of PrV mutants which contained artificial disulfide bonds fixing the syntaxin-like bundle of alpha-helices in gH domain II, indicating that structural changes in gH are required to trigger fusion (30). Alterations in gH interaction with gD might play a role in this context since the N-terminal domain I, deleted in $gH^{32/98}$, and domain II, comprising the syntaxin-like bundle, are the proposed interaction sites with gD in HSV-1 (50). Although PrV gD, unlike its HSV-1 homolog, is not generally required for membrane fusion, it is essential for infectious entry of extracellular virus particles (10, 11). Since, according to the current model, gD is thought to interact with gH/gL upon binding to one of its cellular receptors (4, 5), which then leads to activation of gH/gL to trigger gB fusogenicity (8), it is conceivable that activation of $gH^{32/98}$ by gD is impaired due to the missing N-terminal domain. Conversion of gH/gL to an activated state by receptor-bound gD was recently suggested to be a key step in the fusion pathway. In a

corresponding study, HSV-2 gH/gL with a deletion of 28 residues at the gH N terminus (gHΔ48/gL) was shown to induce low-level *in vitro* fusion without gD, suggesting that gHΔ48/gL resembled activated gH/gL (51). In contrast, the N-terminal deletion of 66 residues in PrV $gH^{32/98}$ rendered the protein inactive in the presence of wild-type gB, irrespective of the presence or absence of gD and gL.

Remarkably, the gDH chimeric protein, which exhibits almost exactly the same deletion in the gH portion as $gH^{32/98}$, showed wild-type-like function in transient fusion assays and during viral infection (12, 38). This suggests that the physical linkage in gDH might enable direct activation of the gH moiety after binding of the gD domain to a receptor. Furthermore, it is conceivable that the gD part of gDH adopts a stabilizing or modulating influence on gH structure which is normally executed by gL. Interestingly, unlike the PrV gDH protein (38), similar HSV-1 gDgH chimeras were not able to functionally substitute for gD, gH, or gL in either virus-free fusion assays of transfected cells or in complementation studies (52). This might reflect a larger dependence of the HSV-1 membrane fusion complex on gL and native gD. Concordantly, unlike the situation in HSV-1, gD is dispensable for cell-to-cell spread of PrV, gL is dispensable for virion incorporation of PrV gH, and fully replication competent gL and gD deletion mutants of PrV could be isolated after extended cell culture passage (10, 13, 38, 39).

Unlike deletion in PrV gDH, deletion of the gL-binding domain in $gH^{32/98}$ results in a protein which is apparently unable to acquire the structure necessary for proper interaction with wild-type gB. This supports the idea that gH or gH/gL activates, rather than represses, gB fusion activity. In accordance with this it has been found that HSV-1 gH comes into close proximity to gB only after binding of gD to one of its receptors, suggesting that gB and gH/gL do not constitutively interact (9, 53). Furthermore, it is conceivable that activation of $gH^{32/98}$ by receptor-bound gD is impaired, thereby preventing subsequent activation of wild-type gB, whereas mutated $gB^{B4.1}$ can be activated by $gH^{32/98}$ in a gD-independent manner. This hypothesis, however, remains to be verified.

In any case our present study shows that deletion of the gL-binding domain from gH (amino acids 32 to 97) led to a complete loss of *in vitro* fusion activity and function in the viral context in the presence of wild-type gB and that these defects were rescued to a considerable extent by mutated $gB^{B4.1}$ isolated from the passaged gL deletion mutant, PrV-ΔgLPassB4.1 (39). $gB^{B4.1}$ exhibits a replacement of glutamic acid by glycine at position 294 in domain I, which also contains the fusion loops required for function (16, 17). Furthermore, it has been hypothesized that replacement of the well-conserved glycine 676 by arginine in domain IV of $gB^{B4.1}$ might decrease the energy required for the extensive conformational rearrangements of this protein part during the conversion of the pre- to the postfusion form (39).

In summary, our previous results from reversion analyses of gL-deleted PrV (38, 39) could now be confirmed and expanded by directed mutation of the gH gene in a cloned virus genome. Consistently, our findings reinforce the notion that gB and gH are the core players in herpesvirus-mediated membrane fusion. Although gL is usually also an essential component of the fusion machinery, its absence can be compensated by mutations in gH and/or gB. Our present study further demonstrates that the gL binding domain of PrV gH is dispensable for maturation and virion incorporation of gH, and, conditionally, also for membrane fusion in transient assays, as well as during viral entry and spread. However, compensatory mutations within gB are required to restore a functional fusion machinery. Thus, the core fragment of PrV gH analyzed by crystallography (26) indeed represents the core functional unit which can support membrane fusion without the need for gD and gL. Furthermore, this study emphasizes the importance of direct gH-gB interaction for the fusion process.

MATERIALS AND METHODS

Cells and viruses. Rabbit kidney (RK13) cells were grown in Dulbecco's modified Eagle's minimum essential medium (MEM) supplemented with 10% fetal calf serum (FCS) at 37°C. The viruses described in

TABLE 1 Oligonucleotide primers for mutagenesis, PCR, and sequence analyses

Primer name	Sequence (5′→ 3′)[a]	Nucleotide positions[a,b]
PGH32/98-F	CTCGCCCGCGGCGCG/CCGCCCGTCTCCGCG	60848–60862/61061–61075
PGH32/98-R	CGCGGAGACGGGCGG/CGCGCCGCGGGCGAG	60848–60862/61061–61075 (r)
UL1-For	**CACAAAGCTT**AGGATACACCAGCCGCGATG	95482–95501 (r)
UL1-Rev	**CACAGAATTC**GGTCTCTTACTCGGCGGGGG	95008–95027
PgBR-F	**ACAGGATCC**CTTCGCGCACGACACGC	19984–20000 (r)
PgBR-R	**ACAGGATCC**TCATCGTGGTCGCGGTC	16250–16266
gB-AssFW	**TAACGGATCC**ATGCCCGCTGGTGGCGG	19657–19673 (r)
gB-AssRV	**CAGAATTC**CTACAGGGCGTCGGGGTCC	16911–16929
gB-P3	GATCTCCTGCACGGGGACGGGCACG	19032–19056 (r)
gB-P7	CCATCTACCGGCGGCGCTACAACA	18329–18352 (r)
gD-For	**CACAGAAT**TCACCTGCCAGCGCCATGC	121129–121148
gD-Rev	**CACAGAATTC**CATCGACGCCGGTACTGC	122353–122370 (r)
PgH-PSF	TTCACGTCGGAGATGGGG	60611–60628
PgH-PSF2	GGAAGCCCTTCGACCAG	61875–61891
PgHK-PSR	CGCGAGCCCATTTATACCC	(Kan^r)
PgH-PSR2	GTCGAGCAGGCTGAAGG	62055–62071 (r)
PgH-WH3	TGCACGAGAGCGACGACTACC	61479–61499
PgH-E555AR	CAGGTGCTGGGAC**G**CGGGCATGCGATC	62420–62446 (r)

[a]Nucleotide positions in the PrV Ka genome refer to GenBank accession number JQ809328 (57). Nonmatching nucleotides are shown in boldface, and restriction sites for cloning of PCR products are underlined.

[b]Slashes in the first two primer sets denote the deletion of nucleotide positions 60863 through 61060. Reverse-strand PCR primers are indicated (r). PgHK-PSR binds to the inserted kanamycin resistance gene (Kan^r) of the PrV recombinants.

this study were derived from pPrV-ΔgHABF (30), which is a gH-deleted mutant of PrV strain Kaplan (PrV-Ka) cloned as a bacterial artificial chromosome (BAC) (27). Viruses were propagated in normal RK13 cells, the gH- and gL-expressing cell line RK13-gH/gL (42), or RK13-gB$^{B4.1}$ cells. The last cell line was obtained after stable transfection (X-tremeGENE HP reagent; Roche) of RK13 cells with pcDNA-gB$^{B4.1}$ (39). For plaque assays, the virus inoculum was removed 2 h after infection, and cells were overlaid with semisolid medium containing 6 g/liter methylcellulose.

Mutagenesis of the cloned gH gene and generation of gH$^{32/98}$-expressing PrV mutants. Expression plasmid pcDNA-gHKDE (30) containing the gH open reading frame ([ORF] UL22) of PrV-Ka was used for in-frame deletion of the predicted gL-binding domain (codons 32 to 97) by site-directed mutagenesis (QuikChange II XL kit; Agilent) with the complementary pair of oligonucleotide primers PGH32/98-F and PGH32/98-R (Table 1). The resulting expression plasmid pcDNA-gH$^{32/98}$KDE was digested with DrdI, and a 3.3-kbp fragment containing the modified gH gene together with a downstream kanamycin resistance (Kan^r) gene was purified from an agarose gel and used for red-mediated mutagenesis of pPrV-ΔgHABF as described previously (27, 30) (Fig. 1). LB agar plates supplemented with kanamycin (50 μg/ml) and chloramphenicol (30 μg/ml) were used for selection of the desired BAC recombinants. DNA of the BAC recombinant pPrV-gH$^{32/98}$K was obtained from overnight liquid cultures of single bacterial colonies by alkaline lysis, phenol-chloroform extraction, isopropanol precipitation, and RNase treatment. BAC DNA was used for transfection (FuGene HD transfection reagent; Promega) of RK13-gH/gL cells, and progeny virus isolated from single plaques was propagated and characterized.

Generation of gL-negative PrV mutants. The gL ORF (UL1) of PrV-Ka was amplified from genomic DNA by PCR with primers UL1-For and UL1-Rev (Table 1) and inserted into expression vector pcDNA3 (Thermo Fisher Scientific) via engineered HindIII and EcoRI restriction sites. From pcDNA-UL1 a 0.2-kbp PshAI/SgrAI fragment containing gL codons 21 to 85 was deleted and replaced by a 0.45-kbp Eco72I fragment extracted from pcDNA3.1ZEO (Thermo Fisher Scientific). After cleavage of the resulting pcDNA-ΔgLZ with HindIII and EcoRI, the 0.75-kbp insert containing the zeocin resistance gene flanked by UL1 sequences was isolated and used for BAC mutagenesis of pPrV-gH$^{32/98}$K and other mutants (Fig. 1C). The desired gL-negative BAC recombinants were selected on LB agar plates with zeocin (25 μg/ml) and chloramphenicol. Infectious virus of pPrV-gH$^{32/98}$KΔgLZ was isolated and propagated on RK13-gH/gL cells.

Replacement of wild-type gB by mutated gB$^{B4.1}$. A 3.75-kbp fragment containing the gB gene region of PrV-ΔgLPassB4.1 (39) was amplified by PCR with primers PgBR-F and PgBR-R (Table 1) and cloned into BamHI-digested pUC19 (New England BioLabs) via engineered restriction sites. The obtained transfer plasmid pUC-PgB$^{B4.1}$R, together with BAC DNA of pPrV-gH$^{32/98}$K or pPrV-gH$^{32/98}$KΔgLZ, was used for cotransfection of normal RK13 cells (Fig. 1D). Homologous recombination led to replication-competent progeny viruses, and two plaque isolates designated pPrV-gH$^{32/98}$KgB$^{B4.1}$ and pPrV-gH$^{32/98}$KΔgLZgB$^{B4.1}$ were further analyzed. All generated PrV mutants were characterized by restriction analysis and Southern blot hybridization of viral DNA (results not shown). Furthermore, the complete coding regions of gB, gD, gH, and gL were PCR amplified and sequenced using the primers indicated in Table 1, a BigDye Terminator, version 1.1, cycle sequencing kit, and a 3130 genetic analyzer (Applied Biosystems).

Western blot analyses. RK13 cells were harvested 48 h after transfection (X-tremeGENE HP reagent; Roche) with gH expression plasmids or 20 h after infection with PrV recombinants at an MOI of 5. Virions

were purified from culture supernatants by sucrose gradient centrifugation (35). Protein samples (5 μg of virion proteins or lysates of approximately 10^4 cells per lane) were separated by discontinuous sodium dodecyl sulfate-polyacrylamide gel electrophoresis (SDS-PAGE), transferred to nitrocellulose membranes, and incubated with antibodies as described previously (54). Monospecific rabbit antiserum against PrV gH (38), gB (55), gL (35), and pUL31 (40) were used at a dilution of 1:10,000 (gH), 1:50,000 (gB, pUL31), or 1:1,000 (gL).

***In vitro* fusion assays.** To analyze the fusogenic potential of $gH^{32/98}$, approximately 3×10^5 RK13 cells per well were seeded into 12-well cell culture plates. On the following day, cells were transfected with 400 ng each of expression plasmids for EGFP (pEGFP-N1; Clontech) and for PrV glycoprotein gB^{Ka}, $gB^{B4.1}$, gD^{Ka}, gH^{Ka} (12, 30, 39), or $gH^{32/98}$ (this study) in 100 μl of Opti-MEM using 2 μl of Lipofectamine 2000 (Thermo Fisher Scientific). Empty vector (pcDNA3) served as a negative control and was added to achieve a total DNA amount of 2 μg in all assays. The mixture was incubated for 20 min at room temperature and added to the cells. After 3 h cells were washed with phosphate-buffered saline (PBS) and incubated in MEM supplemented with 5% FCS for another 24 h at 37°C. Thereafter, cells were washed with PBS, fixed with 3% paraformaldehyde (PFA) for 20 min, and washed two times with PBS. Syncytium formation was analyzed using an Eclipse Ti-S fluorescence microscope and NIS-Elements imaging software (Nikon). Total fusion activity was determined by multiplication of the area of cells with three or more nuclei by the number of syncytia within 10 fields of view (5.5 mm^2 each). The experiment was repeated four times, and average percent values of positive-control transfections as well as standard deviations were calculated.

***In vitro* replication studies.** For determination of growth kinetics, confluent monolayers of RK13 cells in 96-well plates were infected with the phenotypically complemented mutant pPrV-$gH^{32/98}$K, pPrV-$gH^{32/98}$K$gB^{B4.1}$, pPrV-$gH^{32/98}$KΔgLZ$gB^{B4.1}$, or the wild-type gH revertant pPrV-gHK (30) at an MOI of 0.01 or 5 and consecutively incubated on ice for 1 h and at 37°C for 2 h. Subsequently, the inoculum was removed, nonpenetrated virus was inactivated by low-pH treatment (56), and fresh medium was added. Immediately thereafter and after 6, 12, 18, 24, 36, 48, and 72 h at 37°C, the cells were harvested together with the supernatants and lysed by freeze-thawing (−70°C and 37°C). Progeny virus titers were determined by plaque assays on RK13 cells and RK13-gH/gL cells. After 48 h at 37°C under semisolid medium, 30 plaques or areas of cells infected with either of the GFP-expressing viruses were measured microscopically, and percentages of wild-type (pPrV-gHK) sizes were calculated. Mean results of three independent growth kinetics studies and comparative plaque assays, as well as standard deviations, were determined.

***In vitro* penetration kinetics.** For analysis of penetration kinetics, RK13 cells grown in six-well plates were infected on ice with approximately 250 PFU of PrV-gHK, pPrV-$gH^{32/98}$K$gB^{B4.1}$, or pPrV-$gH^{32/98}$KΔgLZ$gB^{B4.1}$. After 1 h, the inoculum was replaced by prewarmed medium, and cells were incubated at 37°C. Before and 15, 30, 60, 120, and 240 min after the temperature shift, remaining extracellular virus particles were inactivated by low-pH treatment. Thereafter, cells were washed two times with PBS and overlaid with semisolid medium. For 100% penetration controls, infected cells were washed with PBS only and overlaid with semisolid medium. After 2 days at 37°C, plaques were counted, and the penetration rate was calculated by comparing the determined numbers with those in the corresponding controls. Mean values and standard deviations from three independent assays were determined.

ACKNOWLEDGMENTS

These studies were supported by the Deutsche Forschungsgemeinschaft (DFG grant Me 854/11-2).

We thank B. Wanner for providing plasmids for BAC mutagenesis and G. Strebelow for performing sequence analyses. The technical assistance of A. Landmesser, K. Günther, and K. Biebl is greatly appreciated.

REFERENCES

1. Harrison SC. 2015. Viral membrane fusion. Virology 479–480:498–507. https://doi.org/10.1016/j.virol.2015.03.043.
2. Eisenberg RJ, Atanasiu D, Cairns TM, Gallagher JR, Krummenacher C, Cohen GH. 2012. Herpes virus fusion and entry: a story with many characters. Viruses 4:800–832. https://doi.org/10.3390/v4050800.
3. Heldwein EE, Krummenacher C. 2008. Entry of herpesviruses into mammalian cells. Cell Mol Life Sci 65:1653–1668. https://doi.org/10.1007/s00018-008-7570-z.
4. Di Giovine P, Settembre EC, Bhargava AK, Luftig MA, Lou H, Cohen GH, Eisenberg RJ, Krummenacher C, Carfi A. 2011. Structure of herpes simplex virus glycoprotein D bound to the human receptor nectin-1. PLoS Pathog 7:e1002277. https://doi.org/10.1371/journal.ppat.1002277.
5. Lazear E, Whitbeck JC, Zuo Y, Carfi A, Cohen GH, Eisenberg RJ, Krummenacher C. 2014. Induction of conformational changes at the N terminus of herpes simplex virus glycoprotein D upon binding to HVEM and nectin-1. Virology 448:185–195. https://doi.org/10.1016/j.virol.2013.10.019.
6. Atanasiu D, Saw WT, Cohen GH, Eisenberg RJ. 2010. Cascade of events governing cell-cell fusion induced by herpes simplex virus glycoproteins gD, gH/gL, and gB. J Virol 84:12292–12299. https://doi.org/10.1128/JVI.01700-10.
7. Gianni T, Amasio M, Campadelli-Fiume G. 2009. Herpes simplex virus gD forms distinct complexes with fusion executors gB and gH/gL in part through the C-terminal profusion domain. J Biol Chem 284:17370–17382. https://doi.org/10.1074/jbc.M109.005728.
8. Chowdary TK, Cairns TM, Atanasiu D, Cohen GH, Eisenberg RJ, Heldwein EE. 2010. Crystal structure of the conserved herpesvirus fusion regulator complex gH-gL. Nat Struct Mol Biol 17:882–888. https://doi.org/10.1038/nsmb.1837.
9. Cooper RS, Heldwein EE. 2015. Herpesvirus gB: a finely tuned fusion machine. Viruses 7:6552–6569. https://doi.org/10.3390/v7122957.
10. Rauh I, Mettenleiter TC. 1991. Pseudorabies virus glycoproteins gII and gp50 are essential for virus penetration. J Virol 65:5348–5356.
11. Peeters B, de Wind N, Hooisma M, Wagenaar F, Gielkens A, Moormann R.

1992. Pseudorabies virus envelope glycoproteins gp50 and gII are essential for virus penetration, but only gII is involved in membrane fusion. J Virol 66:894–905.
12. Klupp BG, Nixdorf R, Mettenleiter TC. 2000. Pseudorabies virus glycoprotein M inhibits membrane fusion. J Virol 74:6760–6768. https://doi.org/10.1128/JVI.74.15.6760-6768.2000.
13. Schmidt J, Klupp BG, Karger A, Mettenleiter TC. 1997. Adaptability in herpesviruses: glycoprotein D-independent infectivity of pseudorabies virus. J Virol 71:17–24.
14. Schröder C, Linde G, Fehler F, Keil GM. 1997. From essential to beneficial: glycoprotein D loses importance for replication of bovine herpesvirus 1 in cell culture. J Virol 71:25–33.
15. Schmidt J, Gerdts V, Beyer J, Klupp BG, Mettenleiter TC. 2001. Glycoprotein D-independent infectivity of pseudorabies virus results in an alteration of in vivo host range and correlates with mutations in glycoproteins B and H. J Virol 75:10054–10064. https://doi.org/10.1128/JVI.75.21.10054-10064.2001.
16. Heldwein EE, Lou H, Bender FC, Cohen GH, Eisenberg RJ, Harrison SC. 2006. Crystal structure of glycoprotein B from herpes simplex virus 1. Science 313:217–220. https://doi.org/10.1126/science.1126548.
17. Zeev-Ben-Mordehai T, Vasishtan D, Hernandez Duran A, Vollmer B, White P, Prasad Pandurangan A, Siebert CA, Topf M, Grunewald K. 2016. Two distinct trimeric conformations of natively membrane-anchored full-length herpes simplex virus 1 glycoprotein B. Proc Natl Acad Sci U S A 113:4176–4181. https://doi.org/10.1073/pnas.1523234113.
18. Backovic M, Longnecker R, Jardetzky TS. 2009. Structure of a trimeric variant of the Epstein-Barr virus glycoprotein B. Proc Natl Acad Sci U S A 106:2880–2885. https://doi.org/10.1073/pnas.0810530106.
19. Roche S, Bressanelli S, Rey FA, Gaudin Y. 2006. Crystal structure of the low-pH form of the vesicular stomatitis virus glycoprotein G. Science 313:187–191. https://doi.org/10.1126/science.1127683.
20. Kadlec J, Loureiro S, Abrescia NG, Stuart DI, Jones IM. 2008. The post-fusion structure of baculovirus gp64 supports a unified view of viral fusion machines. Nat Struct Mol Biol 15:1024–1030. https://doi.org/10.1038/nsmb.1484.
21. Atanasiu D, Whitbeck JC, de Leon MP, Lou H, Hannah BP, Cohen GH, Eisenberg RJ. 2010. Bimolecular complementation defines functional regions of herpes simplex virus gB that are involved with gH/gL as a necessary step leading to cell fusion. J Virol 84:3825–3834. https://doi.org/10.1128/JVI.02687-09.
22. Matsuura H, Kirschner AN, Longnecker R, Jardetzky TS. 2010. Crystal structure of the Epstein-Barr virus (EBV) glycoprotein H/glycoprotein L (gH/gL) complex. Proc Natl Acad Sci U S A 107:22641–22646. https://doi.org/10.1073/pnas.1011806108.
23. Xing Y, Oliver SL, Nguyen T, Ciferri C, Nandi A, Hickman J, Giovani C, Yang E, Palladino G, Grose C, Uematsu Y, Lilja AE, Arvin AM, Carfi A. 2015. A site of varicella-zoster virus vulnerability identified by structural studies of neutralizing antibodies bound to the glycoprotein complex gHgL. Proc Natl Acad Sci U S A 112:6056–6061. https://doi.org/10.1073/pnas.1501176112.
24. Galdiero S, Falanga A, Vitiello M, Browne H, Pedone C, Galdiero M. 2005. Fusogenic domains in herpes simplex virus type 1 glycoprotein H. J Biol Chem 280:28632–28643. https://doi.org/10.1074/jbc.M505196200.
25. Galdiero S, Falanga A, Vitiello M, D'Isanto M, Collins C, Orrei V, Browne H, Pedone C, Galdiero M. 2007. Evidence for a role of the membrane-proximal region of herpes simplex virus type 1 glycoprotein H in membrane fusion and virus inhibition. Chembiochem 8:885–895. https://doi.org/10.1002/cbic.200700044.
26. Backovic M, DuBois RM, Cockburn JJ, Sharff AJ, Vaney MC, Granzow H, Klupp BG, Bricogne G, Mettenleiter TC, Rey FA. 2010. Structure of a core fragment of glycoprotein H from pseudorabies virus in complex with antibody. Proc Natl Acad Sci U S A 107:22635–22640. https://doi.org/10.1073/pnas.1011507107.
27. Fuchs W, Backovic M, Klupp BG, Rey FA, Mettenleiter TC. 2012. Structure-based mutational analysis of the highly conserved domain IV of glycoprotein H of pseudorabies virus. J Virol 86:8002–8013. https://doi.org/10.1128/JVI.00690-12.
28. Böhm SW, Backovic M, Klupp BG, Rey FA, Mettenleiter TC, Fuchs W. 2015. Functional characterization of glycoprotein H chimeras composed of conserved domains of the pseudorabies virus and herpes simplex virus 1 homologs. J Virol 90:421–432. https://doi.org/10.1128/JVI.01985-15.
29. Schröter C, Klupp BG, Fuchs W, Gerhard M, Backovic M, Rey FA, Mettenleiter TC. 2014. The highly conserved proline at position 438 in pseudorabies virus gH is important for regulation of membrane fusion. J Virol 88:13064–13072. https://doi.org/10.1128/JVI.01204-14.
30. Böhm SW, Eckroth E, Backovic M, Klupp BG, Rey FA, Mettenleiter TC, Fuchs W. 2015. Structure-based functional analyses of domains II and III of pseudorabies virus glycoprotein H. J Virol 89:1364–1376. https://doi.org/10.1128/JVI.02765-14.
31. Hutchinson L, Browne H, Wargent V, Davis-Poynter N, Primorac S, Goldsmith K, Minson AC, Johnson DC. 1992. A novel herpes simplex virus glycoprotein, gL, forms a complex with glycoprotein H (gH) and affects normal folding and surface expression of gH. J Virol 66:2240–2250.
32. Kaye JF, Gompels UA, Minson AC. 1992. Glycoprotein H of human cytomegalovirus (HCMV) forms a stable complex with the HCMV UL115 gene product. J Gen Virol 73:2693–2698. https://doi.org/10.1099/0022-1317-73-10-2693.
33. Klupp BG, Baumeister J, Karger A, Visser N, Mettenleiter TC. 1994. Identification and characterization of a novel structural glycoprotein in pseudorabies virus, gL. J Virol 68:3868–3878.
34. Liu DX, Gompels UA, Nicholas J, Lelliott C. 1993. Identification and expression of the human herpesvirus 6 glycoprotein H and interaction with an accessory 40K glycoprotein. J Gen Virol 74:1847–1857. https://doi.org/10.1099/0022-1317-74-9-1847.
35. Klupp BG, Fuchs W, Weiland E, Mettenleiter TC. 1997. Pseudorabies virus glycoprotein L is necessary for virus infectivity but dispensable for virion localization of glycoprotein H. J Virol 71:7687–7695.
36. Lete C, Machiels B, Stevenson PG, Vanderplasschen A, Gillet L. 2012. Bovine herpesvirus type 4 glycoprotein L is nonessential for infectivity but triggers virion endocytosis during entry. J Virol 86:2653–2664. https://doi.org/10.1128/JVI.06238-11.
37. Gillet L, May JS, Colaco S, Stevenson PG. 2007. Glycoprotein L disruption reveals two functional forms of the murine gammaherpesvirus 68 glycoprotein H. J Virol 81:280–291. https://doi.org/10.1128/JVI.01616-06.
38. Klupp BG, Mettenleiter TC. 1999. Glycoprotein gL-independent infectivity of pseudorabies virus is mediated by a gD-gH fusion protein. J Virol 73:3014–3022.
39. Schröter C, Vallbracht M, Altenschmidt J, Kargoll S, Fuchs W, Klupp BG, Mettenleiter TC. 2015. Mutations in pseudorabies virus glycoproteins gB, gD, and gH functionally compensate for the absence of gL. J Virol 90:2264–2272. https://doi.org/10.1128/JVI.02739-15.
40. Fuchs W, Klupp BG, Granzow H, Osterrieder N, Mettenleiter TC. 2002. The interacting UL31 and UL34 gene products of pseudorabies virus are involved in egress from the host-cell nucleus and represent components of primary enveloped but not mature virions. J Virol 76:364–378. https://doi.org/10.1128/JVI.76.1.364-378.2002.
41. Turner A, Bruun B, Minson T, Browne H. 1998. Glycoproteins gB, gD, and gHgL of herpes simplex virus type 1 are necessary and sufficient to mediate membrane fusion in a Cos cell transfection system. J Virol 72:873–875.
42. Klupp B, Altenschmidt J, Granzow H, Fuchs W, Mettenleiter TC. 2008. Glycoproteins required for entry are not necessary for egress of pseudorabies virus. J Virol 82:6299–6309. https://doi.org/10.1128/JVI.00386-08.
43. Babic N, Klupp BG, Makoschey B, Karger A, Flamand A, Mettenleiter TC. 1996. Glycoprotein gH of pseudorabies virus is essential for penetration and propagation in cell culture and in the nervous system of mice. J Gen Virol 77:2277–2285. https://doi.org/10.1099/0022-1317-77-9-2277.
44. Roop C, Hutchinson L, Johnson DC. 1993. A mutant herpes simplex virus type 1 unable to express glycoprotein L cannot enter cells, and its particles lack glycoprotein H. J Virol 67:2285–2297.
45. Klyachkin YM, Stoops KD, Geraghty RJ. 2006. Herpes simplex virus type 1 glycoprotein L mutants that fail to promote trafficking of glycoprotein H and fail to function in fusion can induce binding of glycoprotein L-dependent anti-glycoprotein H antibodies. J Gen Virol 87:759–767. https://doi.org/10.1099/vir.0.81563-0.
46. Duus KM, Grose C. 1996. Multiple regulatory effects of varicella-zoster virus (VZV) gL on trafficking patterns and fusogenic properties of VZV gH. J Virol 70:8961–8971.
47. Cairns TM, Friedman LS, Lou H, Whitbeck JC, Shaner MS, Cohen GH, Eisenberg RJ. 2007. N-terminal mutants of herpes simplex virus type 2 gH are transported without gL but require gL for function. J Virol 81:5102–5111. https://doi.org/10.1128/JVI.00097-07.
48. Möhl BS, Chen J, Sathiyamoorthy K, Jardetzky TS, Longnecker R. 2016. Structural and mechanistic insights into the tropism of Epstein-Barr Virus. Mol Cells 39:286–291. https://doi.org/10.14348/molcells.2016.0066.

49. Atanasiu D, Saw WT, Eisenberg RJ, Cohen GH. 2016. Regulation of herpes simplex virus glycoprotein-induced cascade of events governing cell-cell fusion. J Virol 90:10535–10544. https://doi.org/10.1128/JVI.01501-16.
50. Fan Q, Longnecker R, Connolly SA. 2015. A Functional Interaction between herpes simplex virus 1 glycoprotein gH/gL domains I and II and gD is defined by using alphaherpesvirus gH and gL chimeras. J Virol 89:7159–7169. https://doi.org/10.1128/JVI.00740-15.
51. Atanasiu D, Cairns TM, Whitbeck JC, Saw WT, Rao S, Eisenberg RJ, Cohen GH. 2013. Regulation of herpes simplex virus gB-induced cell-cell fusion by mutant forms of gH/gL in the absence of gD and cellular receptors. mBio 4:e00046-13. https://doi.org/10.1128/mBio.00046-13.
52. Cairns TM, Milne RS, Ponce-de-Leon M, Tobin DK, Cohen GH, Eisenberg RJ. 2003. Structure-function analysis of herpes simplex virus type 1 gD and gH-gL: clues from gDgH chimeras. J Virol 77:6731–6742. https://doi.org/10.1128/JVI.77.12.6731-6742.2003.
53. Atanasiu D, Whitbeck JC, Cairns TM, Reilly B, Cohen GH, Eisenberg RJ. 2007. Bimolecular complementation reveals that glycoproteins gB and gH/gL of herpes simplex virus interact with each other during cell fusion. Proc Natl Acad Sci U S A 104:18718–18723. https://doi.org/10.1073/pnas.0707452104.
54. Pavlova SP, Veits J, Keil GM, Mettenleiter TC, Fuchs W. 2009. Protection of chickens against H5N1 highly pathogenic avian influenza virus infection by live vaccination with infectious laryngotracheitis virus recombinants expressing H5 hemagglutinin and N1 neuraminidase. Vaccine 27:773–785. https://doi.org/10.1016/j.vaccine.2008.11.033.
55. Kopp M, Granzow H, Fuchs W, Klupp BG, Mundt E, Karger A, Mettenleiter TC. 2003. The pseudorabies virus UL11 protein is a virion component involved in secondary envelopment in the cytoplasm. J Virol 77:5339–5351. https://doi.org/10.1128/JVI.77.9.5339-5351.2003.
56. Mettenleiter TC. 1989. Glycoprotein gIII deletion mutants of pseudorabies virus are impaired in virus entry. Virology 171:623–625. https://doi.org/10.1016/0042-6822(89)90635-1.
57. Grimm KS, Klupp BG, Granzow H, Muller FM, Fuchs W, Mettenleiter TC. 2012. Analysis of viral and cellular factors influencing herpesvirus-induced nuclear envelope breakdown. J Virol 86:6512–6521. https://doi.org/10.1128/JVI.00068-12.

(IV) Functional Relevance of the Transmembrane Domain and Cytoplasmic Tail of the Pseudorabies Virus Glycoprotein H for Membrane Fusion

IV

Melina Vallbracht, Walter Fuchs, Barbara G. Klupp and Thomas C. Mettenleiter

Journal of Virology

Volume 92, Issue 12

June 2018

doi: 10.1128/JVI.00084-18

AMERICAN SOCIETY FOR MICROBIOLOGY | Journal of Virology®

VIRUS-CELL INTERACTIONS

Functional Relevance of the Transmembrane Domain and Cytoplasmic Tail of the Pseudorabies Virus Glycoprotein H for Membrane Fusion

Melina Vallbracht,[a] Walter Fuchs,[a] Barbara G. Klupp,[a] Thomas C. Mettenleiter[a]

[a]Institute of Molecular Virology and Cell Biology, Friedrich-Loeffler-Institut, Greifswald-Insel Riems, Germany

ABSTRACT Herpesvirus membrane fusion depends on the core fusion machinery, comprised of glycoproteins B (gB) and gH/gL. Although gB structurally resembles autonomous class III fusion proteins, it strictly depends on gH/gL to drive membrane fusion. Whether the gH/gL complex needs to be membrane anchored to fulfill its function and which role the gH cytoplasmic (CD) and transmembrane domains (TMD) play in fusion is unclear. While the gH CD and TMD play an important role during infection, soluble gH/gL of herpes simplex virus 1 (HSV-1) seems to be sufficient to mediate cell-cell fusion in transient assays, arguing against an essential contribution of the CD and TMD. To shed more light on this apparent discrepancy, we investigated the role of the CD and TMD of the related alphaherpesvirus pseudorabies virus (PrV) gH. For this purpose, we expressed C-terminally truncated and soluble gH and replaced the TMD with a glycosylphosphatidylinositol (gpi) anchor. We also generated chimeras containing the TMD and/or CD of PrV gD or HSV-1 gH. Proteins were characterized in cell-based fusion assays and during virus infection. Although truncation of the CD resulted in decreased membrane fusion activity, the mutant proteins still supported replication of gH-negative PrV, indicating that the PrV gH CD is dispensable for viral replication. In contrast, PrV gH lacking the TMD, membrane-anchored via a lipid linker, or comprising the PrV gD TMD were nonfunctional, highlighting the essential role of the gH TMD for function. Interestingly, despite low sequence identity, the HSV-1 gH TMD could substitute for the PrV gH TMD, pointing to functional conservation.

IMPORTANCE Enveloped viruses depend on membrane fusion for virus entry. While this process can be mediated by only one or two proteins, herpesviruses depend on the concerted action of at least three different glycoproteins. Although gB has features of bona fide fusion proteins, it depends on gH and its complex partner, gL, for fusion. Whether gH/gL prevents premature fusion or actively triggers gB-mediated fusion is unclear, and there are contradictory results on whether gH/gL function requires stable membrane anchorage or whether the ectodomains alone are sufficient. Our results show that in pseudorabies virus gH, the transmembrane anchor plays an essential role for gB-mediated fusion while the cytoplasmic tail is not strictly required.

KEYWORDS herpesvirus, pseudorabies virus, glycoproteins, gH/gL complex, gB, membrane fusion, virus entry

Infectious entry of enveloped viruses into cells requires fusion of the viral envelope with a host cell membrane. To meet this challenge, enveloped viruses have evolved specialized surface glycoproteins enabling them to bind to a cellular receptor and to catalyze membrane merging. Many well-studied enveloped viruses, e.g., influenza viruses or rhabdoviruses, require only a single viral protein to mediate both functions.

Received 5 March 2018 **Accepted** 29 March 2018

Accepted manuscript posted online 4 April 2018

Citation Vallbracht M, Fuchs W, Klupp BG, Mettenleiter TC. 2018. Functional relevance of the transmembrane domain and cytoplasmic tail of the pseudorabies virus glycoprotein H for membrane fusion. J Virol 92:e00376-18. https://doi.org/10.1128/JVI.00376-18.

Editor Richard M. Longnecker, Northwestern University

Address correspondence to Thomas C. Mettenleiter, thomas.mettenleiter@fli.de.

In contrast, herpesviruses use a more complex apparatus, which involves multiple viral glycoproteins. The core fusion machinery consists of glycoprotein B (gB) and the heterodimeric complex of gH and gL (gH/gL). This subset of glycoproteins is conserved across the *Herpesviridae*, while receptor binding is primarily mediated by nonconserved subfamily-specific glycoproteins (reviewed in references 1 and 2). The alphaherpesviruses pseudorabies virus (PrV; *Suid alphaherpesvirus 1*) and herpes simplex viruses 1 and 2 (HSV-1/2; *Human alphaherpesvirus 1/2*), for example, require gD and a gD-specific cellular receptor such as nectin-1 or herpesvirus entry mediator (HVEM) (3). Other herpesviruses lack a gD homolog, and receptor binding function is mediated by, e.g., varicella-zoster virus (VZV; human herpesvirus 3) glycoprotein E (gE) (4, 5) or gp42 of Epstein-Barr virus (EBV) (6–8).

The current model for herpesvirus membrane fusion assumes that the entry glycoproteins are activated in a cascade-like fashion to promote membrane fusion (9, 10). Activation of the *Simplexvirus* fusion machinery is initiated by binding of gD to one of its cellular receptors, which leads to a conformational change in the C-terminal region of the gD ectodomain, as shown for HSV-1 (11–14). This activated gD is thought to trigger gH/gL, which, in turn, is presumed to activate the bona fide fusion protein gB by direct interaction of their respective ectodomains (9, 15–18). A similar mechanism has been proposed for the *Varicellovirus* PrV (19). The related *Varicellovirus* VZV, on the other hand, has to initiate fusion via a fundamentally different mechanism, since it completely lacks a gD homolog (4, 5).

The crystal structures of the gB ectodomains resemble those of typical class III fusion proteins, including a trimeric fold, internal bipartite fusion loops, and a central alpha-helical coiled-coil (20–23). Despite its similarities to other class III fusion proteins, such as the G protein of vesicular stomatitis virus or baculovirus gp64 (24, 25), gB is not able to drive membrane fusion on its own but depends on the presence of the gH/gL complex (16, 18). However, the role of the gH/gL complex during fusion is still elusive.

Unlike gB, the crystal structures of EBV gH/gL (26), HSV-2 gH/gL (16), VZV gH/gL (27), and a core fragment of PrV gH (28) revealed no features typical for fusion proteins, and the experimental data point to a regulatory role (16, 21, 24, 26–28). While correct folding and transport of gH depends on the presence of gL in most herpesviruses (16, 29), it is not essential for gH virion incorporation in PrV (30). Moreover, infection of PrV can occur in the absence of gL, and/or the gL-binding domain in gH, when compensatory mutations in gD, gH, and/or gB are present (31–33), indicating that gL is not directly involved in the membrane fusion process, at least in PrV. In contrast, gL is required for fusion in HSV-1 and HSV-2, and no gL-negative infectious virus mutants have been reported in the simplexviruses.

For membrane fusion, a direct interaction between the ectodomains of gB and gH/gL has been proposed (9). Nevertheless, previous data demonstrated important functions for the transmembrane (TMD) and the cytoplasmic domains (CD) of gB and gH, for which structural information is currently lacking. However, the gB CD obviously restricts membrane fusion, since truncation of or point mutations within this region are reported to increase the fusogenic activity in several herpesviruses (17, 34–36). The 93-amino-acid (aa) CD of PrV gB contains two predicted alpha-helical domains. A C-terminally truncated PrV gB lacking one of these domains (gB008) (34), including an overlapping endocytosis motif, resulted in significantly enhanced cell surface expression as well as increased fusion activity in virus-free cell-cell fusion assays (32, 34, 37). PrV gB mutants lacking both alpha-helical domains (gB007), the complete CD (gB006), or the CD and the TMD (gB005) were unable to complement gB-negative PrV (34). Surprisingly, the defect in gB007, which still mediated direct cell-to-cell spread, was compensated for by two mutations in the gB ectodomain (38), showing a functional interplay between sequences in the CD and the ectodomain. In addition, the CDs of EBV and HSV-1 gB were reported to directly interact with lipid membranes (39, 40), indicating that the gB CD functions as a clamp, stabilizing the prefusion form of gB (41).

In contrast to gB, the gH CD is very short, with an only poorly conserved amino acid sequence even within the alphaherpesvirus subfamily (Fig. 1A). The CDs of HSV-1, VZV,

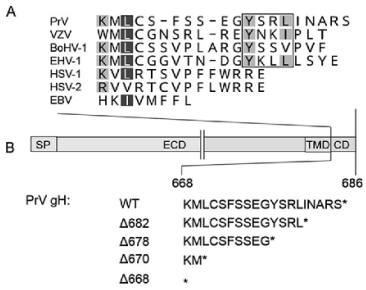

FIG 1 Sequence alignment of gH cytoplasmic domains of different herpesviruses and schematic representation of the generated gH mutants. (A) The alignment was generated using ClustalW (Geneious 10.3.2). Residues are colored according to their conservation (white letters on dark gray background, 80 to 100%; black letters on light gray, 60 to 80%). The YXXϕ endocytosis motif is boxed. Sequences of herpesvirus gH used for the alignment correspond to gH of pseudorabies virus (PrV; AAA47466), varicella-zoster virus (VZV; AH010537.2), bovine alphaherpesvirus 1 (BoHV-1; CAA41677), equid alphaherpesvirus 1 (EHV-1; AY464052), human alphaherpesvirus 1 (HSV-1; AJE60179), human alphaherpesvirus 2 (HSV-2; CAB06746), and Epstein-Barr virus (EBV; V01555.2). (B) The PrV gH open reading frame and the amino acid sequence of the cytoplasmic domains of the generated truncation mutants are shown. SP, signal peptide; ECD, ectodomain; TMD, transmembrane domain; CD, cytoplasmic domain.

and EBV gH had been linked to regulation of cell fusion (7, 42, 43), and a direct interaction between the CDs of EBV gH and gB was reported recently (7), pointing to an important role of the CDs in fusion. However, truncations of the cytoplasmic domains in HSV-1, VZV, and EBV gH had different consequences in terms of fusion activity. Stepwise truncations of the 14-aa HSV-1 gH CD resulted in a gradual reduction in fusion levels, whereas deletion of the complete HSV-1 gH CD completely abrogated cell-cell fusion activity, even in the presence of hyperfusogenic gB variants (41), as well as its ability to complement a gH-negative mutant (42). These studies indicate that the CD, or at least part of it, is essential for HSV-1 gH function. It had been hypothesized that it acts as a wedge to release the gB CD clamp, allowing gB to exert its fusion function (41). Surprisingly, a 5-aa insertion in the membrane-proximal part of the HSV-1 gH CD also prevented cell-cell fusion and complementation (44). Thus, either the length of the gH C tail is crucial or the membrane-proximal amino acids of the CDs, which are the most highly conserved, at least within the alphaherpesvirus gH homologs, comprising a basic amino acid (K or R, except in VZV gH) followed by a pair of neutral nonaromatic residues, execute specific functions.

In contrast to HSV-1, PrV, and EBV, full-length VZV gH is not functional in cell-cell fusion assays but requires truncation of the last 8 amino acids, comprising a predicted endocytosis motif, for function in these assays (43, 45, 46). In addition, it was shown that the length of the VZV gH CD is important for fusion regulation but not its amino acid composition. However, in these studies the membrane-proximal sequences were not altered, leaving their importance for fusion unclear (43). It was speculated that the gH CD acts as a gate keeper to control access to functional domains of neighboring proteins, e.g., allowing or preventing phosphorylation of the gB CD (43).

The EBV gH CD comprises only eight residues and was found to regulate fusion by altering gH binding to gp42 and epithelial cell attachment (7). Deletion of the last four amino acids had only marginal effects on cell-cell fusion. However, truncation to only two amino acids or complete deletion of the CD reduced fusion to background levels (7). Here, in contrast to VZV gH, the CD amino acid composition seems to be important, since replacement by foreign sequences resulted in significantly reduced fusion levels (7).

Besides the CD, the functional role of the gH TMD has also been discussed controversially. Mutations in the HSV-1 gH TMD, substitution of the gH TMD by analogous domains from other glycoproteins, or replacement by a glycosylphosphatidylinositol (gpi) anchor resulted in a nonfunctional protein (42, 47). These data indicate that HSV gH/gL needs to be anchored in the membrane by a specific TMD to fulfil its function. In

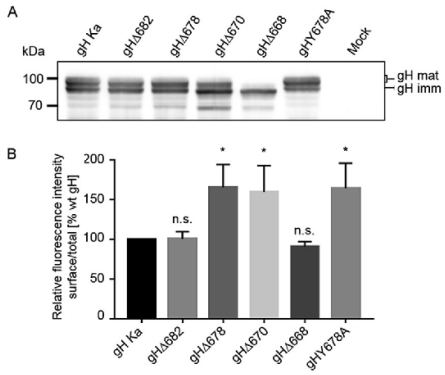

FIG 2 Expression and surface localization of gH truncation mutants. (A) Western blot analysis. Lysates prepared 48 h after transfection with expression plasmids for wild-type (gH Ka) or mutant gH in combination with gL or only the empty vector (mock) were separated by SDS-PAGE. Blots were probed for presence of mature (gH mat) and immature gH (gH imm). Molecular masses (kDa) of marker proteins are indicated on the left. (B) Flow cytometry. RK13 cells were transfected in parallel assays with expression plasmids for either wild-type or C-terminally truncated gH in combination with gL. After 24 h, cells were either permeabilized or not and then stained with a monoclonal antibody against gH and Alexa-Fluor 488-conjugated secondary antibodies, and fluorescence was measured. Bars represent the ratio between the mean fluorescence intensity (MFI) of cells expressing gH at the surface and MFI of total gH-positive cells. Results obtained for gH Ka were set as 100%. Mean values and standard deviations from three independent experiments are shown. Significance of differences from results obtained with wild-type gH is marked (*, $P < 0.05$). n.s., not significantly different from gH Ka.

contrast, recent studies suggested that soluble forms of HSV gH/gL are sufficient to induce gB-mediated fusion (9), while this was not observed for EBV (8, 48).

The poor sequence conservation of the gH CD and the divergent results in different herpesviruses highlight the need to study each gH homolog individually, especially in light of the different requirements to induce fusion. Thus, whereas in PrV gB and gH/gL are sufficient for the induction of syncytium formation by direct cell-cell fusion in transfection-based fusion assays (37), gD is required in HSV-1 (49). In VZV, which lacks a gD homolog, expression of gB and gH/gL is sufficient to induce membrane fusion in cell fusion assays, resembling the situation in PrV (5, 46). Moreover, EBV depends on the presence of receptor-binding gp42 for fusion of B cells (50, 51). Since the role of the CD and the TMD of PrV gH during membrane fusion had not been characterized, we investigated the functional relevance of the CD and the TMD of PrV gH by generating different C-terminal truncations and site-specific mutations, soluble gH, a gpi-anchored gH, as well as chimeras containing either only the TMD or TMD and CD of HSV-1 gH or PrV gD. These proteins were characterized for their ability to function in virus-free membrane fusion as well as virus infection.

RESULTS

Function of the PrV gH cytoplasmic domain. To investigate the functional relevance of the 19-amino-acid (aa) cytoplasmic domain (CD) of PrV gH, different truncated proteins were generated lacking either the C-terminal 5, 9, or 17 aa or the complete CD (gHΔ682, gHΔ678, gHΔ670, and gHΔ668, respectively) (Fig. 1B). Correct protein expression was analyzed by Western blotting of rabbit kidney cells (RK13) after cotransfection with expression plasmids encoding the different gH variants and gL. Expression of gH was detected using the monospecific anti-gH serum (31). In Western blots, immature gH (gH imm) as well as several processed forms (gH mat) were detected for all C-terminally truncated mutants retaining at least the two most membrane-proximal amino acids (Fig. 2A). After complete deletion of the CD (gHΔ668), predominantly immature gH was detected, indicating that the amino acids immediately following the transmembrane domain (TMD) are involved in efficient protein trafficking and/or

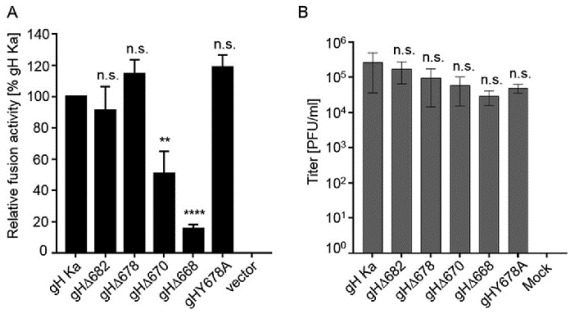

FIG 3 Cell-cell fusion activity of gH truncation mutants and transcomplementation of PrV-ΔgH. (A) RK13 cells were cotransfected with 200 ng of expression plasmids for EGFP in combination with full-length gB, gL, gH, or C-terminally truncated gH. Twenty-four hours posttransfection, the areas of green fluorescing syncytia were measured, and total fusion activity was determined by multiplication of the mean syncytium area with the number of syncytia in 10 fields of view. Fusion activities obtained with wild-type gH Ka, gB, and gL were set as 100%. Cells transfected with empty vector pcDNA3 served as a negative control (vector). Shown are mean relative values and standard deviations from four independent experiments with the corresponding standard deviations. Values significantly differing from those obtained with gH Ka are marked (**, $P < 0.01$; ****, $P < 0.0001$; all by unpaired *t* test with Welch correction). n.s., not significantly different from gH Ka. (B) gH Ka- or mutant gH-expressing RK13 cells were infected with PrV-ΔgH. Progeny virus titers were determined on wild-type PrV gH/gL-expressing cells and are given in PFU per ml. Cells transfected with the empty vector pcDNA3 served as a negative control. Shown are mean values for three independent assays with corresponding standard deviations. n.s., not significantly different from gH Ka.

maturation (Fig. 2A). In contrast to HSV gH, which depends on the presence of gL for correct maturation (52), gL is dispensable for maturation of PrV gH (30, 53). Thus, absence of gL did not influence processing of any of the gH proteins (data not shown).

Transport of the gH variants to the plasma membrane was investigated by flow cytometry of RK13 cells cotransfected with gH and gL expression plasmids. The analysis revealed that gHΔ682 and gHΔ668 were present on the surface at levels similar to those of wild-type (wt) gH (derived from PrV strain Kaplan [PrV-Ka]) (Fig. 2B), whereas deletion of the predicted tyrosine-based endocytosis motif YSRL, located at positions 679 to 682, as in gHΔ678 and gHΔ670 (Fig. 1), resulted in enhanced surface expression, indicating that the motif is functional (Fig. 2B). To further investigate this finding, tyrosine at position 678 was replaced by alanine (gHY678A). Flow cytometry of transfected cells revealed enhanced surface expression for gHY678A (Fig. 2B).

To analyze the role of PrV gH CD in membrane fusion, the different truncated mutants and gHY678A were tested in transient-transfection-based cell-cell fusion assays (Fig. 3A) (32, 54). Fusion activity was analyzed after cotransfection of RK13 cells with expression plasmids encoding either wild-type gH or the mutated PrV gH variants in combination with plasmids expressing wild-type gB and gL as well as enhanced green fluorescent protein (EGFP), which was used to facilitate evaluation by fluorescence microscopy (54). Assays with wild-type gH, gB, and gL served as positive controls, which were set as 100%, and assays with the gH expression plasmid replaced by the empty vector pcDNA3 served as negative controls (vector). Figure 3A shows that fusion activity obtained with gHΔ682, lacking the terminal 5 aa, was comparable to that of wild-type gH. gHΔ678, devoid of the last 9 aa, including the endocytosis motif, showed a slight increase in fusion activity, which was also evident in gHY678A-expressing cells, indicating that the enhanced cell surface localization promotes cell-cell fusion. However, despite efficient surface expression, expression of gHΔ670, with only two amino acids in the CD left, resulted in only approximately 50% fusion activity compared to that of the positive control. gHΔ668, lacking the complete CD, although showing impaired protein processing (Fig. 2A), was still able to mediate fusion to a limited extent, and fusion activity reached values of around 20%, while no fusion was observed in the absence of gH (Fig. 3A). These results indicate that the membrane-proximal part of the

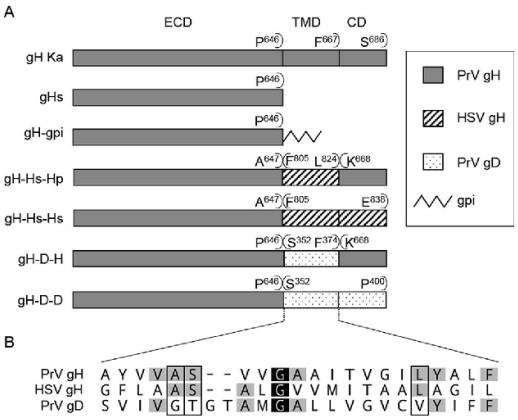

FIG 4 Schematic representation of the constructed gH mutants. (A) The PrV gH transmembrane domain (TMD) and/or cytoplasmic domain (CD) were deleted or replaced with a gpi anchor or the analogous region from HSV-1 or PrV gD. The constructs are illustrated, and each is named to indicate its composition with reference to the ectodomain (ECD), TMD, and CD. The first and last amino acids of the predicted (Geneious 10.3.2) components of the chimeric proteins are given above the respective bars. Amino acid positions refer to the sequences of PrV gH (GenBank accession number AAA47466), HSV-1 gH (GenBank accession number AJE60179), and PrV gD (GenBank accession number AFI70842.1). The proteins are not drawn to scale. (B) Sequence alignment of the predicted transmembrane domains of PrV and HSV-1 gH and PrV gD. The alignment was generated using ClustalW (Geneious 10.3.2). Residues are colored according to their conservation (white letters on black, 100%; black letters on light gray, 60 to 80%). Amino acids conserved in PrV and HSV gH but not in gD are boxed.

PrV gH CD contains sequences required for correct protein processing but is also involved in fusion regulation. However, the PrV gH CD was apparently not absolutely essential to mediate cell-cell fusion.

The ability of the gH mutants to function in virus entry was determined by transcomplementation of a gH-negative PrV mutant (Fig. 3B) (55). To this end, RK13 cells were transfected with expression plasmids encoding wild-type gH or the different gH mutants and subsequently infected with PrV-ΔgH at a multiplicity of infection (MOI) of 3. Progeny virus titers were determined on RK13-gH/gL cells (56). As shown in Fig. 3B, all gH mutants were able to complement gH-negative virus, but titers were gradually reduced with decreasing length of the CD. Titers derived from cells expressing gH completely lacking the CD (gHΔ668), however, showed only an approximately 10-fold reduction (Fig. 3B) despite compromised protein processing (Fig. 2A). No infectious virus could be detected after infection of vector-transfected (mock) cells. These results show that the PrV gH CD also is not essential for gH function during virus replication.

Expression of soluble, gpi-anchored, and chimeric gH constructs. To test for functional relevance of the transmembrane anchor, soluble gH (gHs) comprising only the PrV gH ectodomain (aa 1 to 646), as well as a glycosylphosphatidylinositol (gpi)-anchored version of gH (gH-gpi; gpi was added at position 646), were constructed (Fig. 4A). To investigate whether the gH TMD possesses specific features important for its function, gH chimeras were generated in which the TMD, or the TMD and CD of PrV gH, were replaced by the equivalent sequences from HSV-1 gH (gH-Hs-Hp and gH-Hs-Hs) or PrV gD (gH-D-H and gH-D-D) (Fig. 4A). Protein expression was analyzed by Western blotting and flow cytometry (Fig. 5). In contrast to wild-type gH, mature gHs was easily detectable in the supernatant of transfected cells, while immature forms of gHs were exclusively found in the cell lysate, demonstrating efficient secretion of anchorless gH (Fig. 5A). gH-gpi was also found in the supernatant after cleavage with phospholipase C (PLC), indicating correct processing (Fig. 5B). In Western blot experiments, expression patterns of all mutants were comparable to those of wild-type gH, indicating that the substitutions had no effect on protein processing and maturation (Fig. 5C).

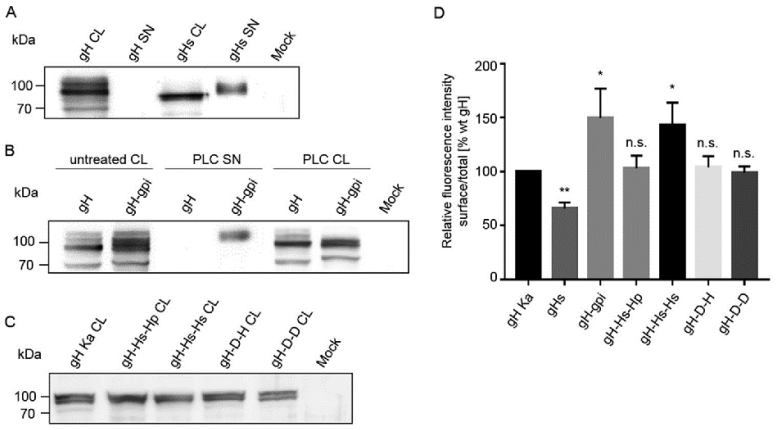

FIG 5 Expression and surface localization of gHs, gH-gpi, and gH chimeras. Cell lysates (CL) or supernatants (SN) harvested 48 h after transfection with expression plasmids for wild-type gH Ka, gHs (A), gH-gpi (B), the different gH chimeras (C), or the empty vector (mock) were separated by SDS-PAGE. To test whether the predicted gH-gpi is membrane associated via the gpi anchor, wild-type gH and gH-gpi-expressing cells were treated with PLC. Supernatants and lysates of PLC-treated cells were separated by SDS-PAGE. Blots were incubated with a PrV gH-specific rabbit polyclonal antiserum. Molecular masses (kDa) of marker proteins are indicated. (D) Total and cell surface expression of wild-type gH and the gH mutants was analyzed by flow cytometry. Bars represent the ratio between the mean fluorescence intensity (MFI) of cells expressing gH at the surface and MFI of total gH-positive cells. Results obtained for gH Ka were set as 100%. Mean values and standard deviations for three independent experiments are shown. Significance of differences from results obtained with gH Ka is marked (*, $P < 0.05$; **, $P < 0.01$). n.s., not significantly different from gH Ka.

Total expression and surface localization of the gH proteins were analyzed by flow cytometry of RK13 cells cotransfected with expression plasmids for gH and gL (Fig. 5D). These analyses revealed that gH-gpi was efficiently expressed at the cell surface, while only a significantly smaller proportion of gHs could be detected on the surface (Fig. 5D). Surface expression of gH-Hs-Hp, gH-D-H, and gH-D-D was comparable to that of gH Ka, whereas a significant increase in surface expression compared to that of wild-type gH was observed for gH-Hs-Hs (Fig. 5D).

Functional analysis of soluble, gpi-anchored, and chimeric gH constructs. The ability of the different gH mutants to function in cell-cell fusion and entry was investigated by fusion (Fig. 6A) and complementation assays (Fig. 6B). In contrast to the

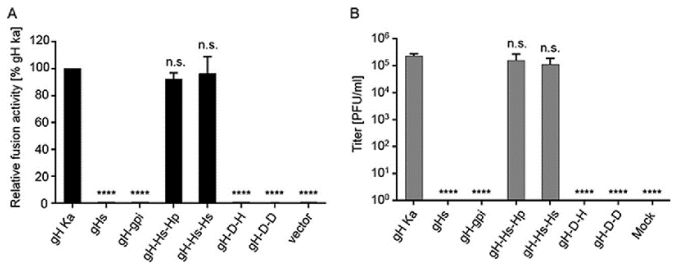

FIG 6 Cell-cell fusion activity of gHs, gH-gpi, and gH chimeras and transcomplementation of PrV-ΔgH. (A) Results of cell-cell fusion assays are expressed as percent fusion activity of wild-type gH in combination with gB and gL set as 100%. (B) Viral titers obtained in the transcomplementation assay are shown as gray bars and correspond to the number of PFU per ml. Shown are mean values and corresponding standard deviations for four independent experiments. Values significantly differing from those obtained with wild-type gH are marked (****, $P < 0.0001$ by unpaired *t* test with Welch correction). n.s., not significantly different from gH Ka.

closely related HSV-1, in which soluble forms of gH/gL were able to trigger fusion, although at only low levels (9), soluble PrV gH/gL was completely unable to induce fusion (Fig. 6A), even in the presence of hyperfusogenic gB variants (data not shown). Despite localization on the cell surface, no fusion activity could be observed for gH-gpi, gH-D-H, or gH-D-D. However, chimeras containing the HSV-1 gH TMD were able to efficiently mediate membrane fusion to levels comparable to that of wild-type gH.

In line with these results, gHs, gH-gpi, gH-D-H, and gH-D-D were not able to complement gH-negative PrV (Fig. 6B). However, chimeras containing the HSV-1 gH TMD efficiently complemented PrV-ΔgH, with only marginally reduced viral titers (Fig. 6B). Thus, our data demonstrate that membrane anchorage of PrV gH via a TMD is crucial for its function in fusion. This TMD has to fulfil specific requirements not provided by the PrV gD TMD but by the HSV-1 gH TMD. In summary, we show that the PrV gH TMD is important for its function during the fusion process.

DISCUSSION

Infectious entry of enveloped viruses requires fusion of the viral envelope with cellular membranes. In herpesviruses, this involves the conserved fusion machinery consisting of gB and the heterodimeric gH/gL complex. However, the molecular details of this process remain to be uncovered. Although it is accepted that gB is the actual fusion protein, the exact role of the gH/gL complex remains elusive. Despite its presence in all herpesviruses, the amino acid sequence of gH is only poorly conserved, even between members from the same subfamily (28). Not only the poor amino acid sequence conservation of gH but also the different requirements to induce fusion in different herpesviruses highlight the need to study each protein individually to elucidate common features and differences for a better understanding of the fusion process.

In contrast to that of HSV (49), PrV gL is not necessary for correct transport, processing, or virion incorporation of gH and, moreover, the gL-binding domain in PrV gH is dispensable for the fusion process in the presence of compensatory mutations in gH and/or gB (31, 33). Reports on HSV-1 indicated that soluble gH/gL, lacking the membrane anchor, is sufficient to mediate low levels of membrane fusion in transient assays (9). This was surprising in light of earlier data ascribing an important function to the transmembrane and cytoplasmic domains of HSV-1 gH (42, 47). However, a soluble form of EBV gH/gL was not sufficient to trigger membrane fusion (8, 48). These fundamental differences in the requirement for gH in different herpesviruses prompted us to investigate whether the requirements for fusion activation differ for members of different subfamilies or even between the closely related alphaherpesviruses HSV-1 and PrV.

For this purpose, we first generated C-terminally truncated gH variants. While deletion of the 5 C-terminal amino acids had no effect on cell-cell fusion or complementation of PrV-ΔgH, deletion or site-specific mutagenesis of the predicted endocytosis motif (^{678}YSRL^{681}) resulted in an enhanced cell surface expression (Fig. 2B) concomitant with higher levels of fusion activity (Fig. 3A). However, gHΔ670, which retained only the two membrane-proximal amino acids despite enhanced surface expression (Fig. 2B), showed a 50% reduction in fusion activity (Fig. 3A), pointing to a regulatory role of the gH CD, particularly the N-terminal half.

Congruent with our results, approximately half of the gH CD (10 of 19 aa, as in PrV gHΔ678) appears to be sufficient for full function, as was shown for EBV gH (4 of 8 aa) (7) and HSV-1 (8 of 14 aa) (41). Further deletion, however, resulted in a significant reduction of fusion activity, again pointing to a regulatory role for the membrane-proximal part of the gH CD (Fig. 3A). In contrast, despite its similarity to the PrV gH CD in length, the C-terminal half of the VZV gH CD (8 of 18 aa) obviously impairs cell-cell fusion and had to be removed for function in transfection-based cell-cell fusion assays (43, 46). This enhanced fusion activity resulted in increased syncytium formation in infected cells concomitant with a significant reduction in virus titers (43). VZV is characterized by its syncytial phenotype *in vivo*, is highly cell associated, and lacks a gD homolog (57–59). It can be speculated that the VZV gH CD partly fulfills the regulatory

role which is otherwise encoded in accessory proteins as, e.g., gD in HSV-1 or gp42 in EBV. PrV, which also belongs to the *Varicellovirus* genus, obviously exhibits an intermediate phenotype between HSV-1 and VZV regarding the importance of gD. Cell-cell fusion and direct cell-to-cell spread in PrV occur independently of gD (37, 60, 61) but without a significant syncytial phenotype *in vitro* or *in vivo*. Free virions even enter cells in the absence of gD when compensatory mutations in gB and gH are present (62). These data point to a well-balanced but virus-specific control of membrane fusion by a complex interplay between the receptor-binding factor and the components of the core fusion machinery which differ between the different herpesviruses.

The membrane-proximal gH CD residues of different alphaherpesviruses show a higher degree of conservation, comprised of a basic residue (K or R; the only exception is VZV) followed by two neutral nonaromatic residues (M, V, and L) (Fig. 1A). These residues, or at least the first two amino acids, appear to be important for efficient protein translocation, presumably by involvement in lipid interactions in the plasma membrane or the viral envelope (63). Correct trafficking is often influenced by the CD of type I transmembrane proteins. Since PrV gHΔ670 was efficiently processed and transported to the cell surface (Fig. 2B), the two remaining membrane-proximal residues seem to be sufficient for efficient transport through the secretory pathway. In contrast, gHΔ668, which completely lacks the CD, was mainly detected in its immature form (Fig. 2A). Nevertheless, surface expression of gHΔ668 was only slightly reduced compared to that of wt gH (Fig. 2B), and gHΔ668 still complemented PrV-ΔgH to only approximately 10-fold-reduced titers (Fig. 3B), indicating that the PrV gH CD, in contrast to the HSV-1 gH CD (41, 42), is not required for incorporation into the virus envelope to function during entry. In contrast to EBV gH (7), surface expression of HSV-1 gH lacking the CD seemed to be unaffected (41). However, the importance of the membrane-proximal residues might explain why a five-amino-acid insertion immediately after the TMD completely abrogated function (44, 64), as did complete deletion of the CD (41, 42).

The HSV-1 and VZV gH CDs were suggested to function as gatekeepers, utilizing their length to control access of functional domains within neighboring proteins (41, 43). Since PrV gH mutants gHΔ670 and gHΔ668 showed reduced fusion levels in combination with wild-type gB (Fig. 3A) or a more fusogenic variant (data not shown), it is possible that the PrV gH CD, although not essential, modulates fusion in a manner similar to that proposed for HSV. The HSV gH CD was suggested to act as a wedge to release the gB CD clamp, which enables activation of gB (41). Moreover, the conformation of the gH ectodomain may be altered by the truncations influencing interactions between the gB and gH ectodomains, although reactivity of truncated gH variants of HSV, VZV, and EBV with several conformation-dependent monoclonal antibodies was not affected. However, binding of the ectodomain of a truncated EBV gH to gp42 was shown to be altered (7, 41, 43). Because monoclonal antibodies for PrV gH recognizing conformational epitopes are lacking, a conformational alteration of the PrV gH ectodomain cannot be excluded.

Since the PrV gH CD was found to be dispensable for gH function during virus infection, we analyzed whether the membrane-spanning region is required. Thus, we expressed soluble gH (gHs; aa 1 to 646) lacking the CD and TMD (Fig. 4A). gHs was efficiently secreted into the supernatant of transiently transfected RK13 cells (Fig. 5A). However, no fusion activity or functional complementation was detectable (Fig. 6), even when gB variants with increased fusogenicity were coexpressed or when soluble forms of more fusogenic gH were used (data not shown). Thus, we conclude that membrane anchorage is essential for PrV gH function in fusion.

Replacement of the TMD (and CD) by a lipid anchor (gH-gpi), thereby anchoring the protein in only one leaflet of the lipid membrane, resulted in a nonfunctional protein (Fig. 6) despite efficient cell surface expression (Fig. 5D), again highlighting the importance of a membrane-spanning domain. This prompted us to investigate whether any transmembrane domain is sufficient for this purpose. To this end, we generated PrV gH chimeras in which the TMD (or TMD and CD) of PrV gH was replaced by the equivalent

sequence from PrV gD or HSV-1 gH (Fig. 4A). All chimeras were efficiently expressed and processed (Fig. 5C). While gH-D-H and gH-Hs-Hp, both containing the CD of PrV gH, as well as gH-D-D, were present at levels on the cell surface similar to those of the wt gH, gH-Hs-Hs revealed an increase in cell surface localization (Fig. 5D). The HSV CD does not show a typical endocytosis motif (Fig. 1A), which could explain the enhanced gH-Hs-Hs cell surface presentation. The PrV gD CD, however, contains a functional endocytosis motif (YRLL) (65), which is apparently also active in gH-D-D. Despite efficient processing and surface expression, neither gH-D-H nor gH-D-D was functional in cell-cell fusion and transcomplementation assays (Fig. 6). In line with our data, the HSV-1 gH TMD could not be replaced by the TMD of HSV-1 gD or other type I membrane proteins, such as CD8 and influenza HA, pointing to a gH-specific feature within the TMD of herpesvirus gH (42). In contrast, the HSV-gH TMD efficiently substituted for the TMD in PrV gH in both assays. This is consistent with previous results showing that the complete HSV-1 gH C-terminal part comprising the conserved domain IV, as well as TMD and CD, could functionally substitute for the corresponding part in PrV gH, pointing to functional conservation (53).

Sequence comparison between the PrV gD, PrV gH, and HSV-1 gH TMD reveals only one strictly conserved amino acid, a centrally located glycine (G) residue at amino acid position 655 in PrV and 812 in HSV gH (Fig. 4B). Although a crucial role for gH function was attributed to this particular glycine, its presence in the gD TMD (aa 362) apparently is not sufficient for functional complementation in gH (42). Three further amino acids are conserved between PrV and HSV gH TMD that are not present in the gD TMD (Fig. 4B). Interestingly, in HSV-1, mutation of two of them, namely, alanine (A) 808 and serine (S) 809, which correspond to A651 and S652 in PrV gH, resulted in severely compromised cell-cell fusion (42). With respect to the observed functional conservation of the TMD of HSV and PrV, a similar effect on fusion seems likely for PrV. The third conserved amino acid absent from gD is leucine (L) at amino acid position 663 in PrV. In HSV and PrV gH, L663, together with A651, S652, and G655, are located on one face of an alpha-helical wheel plot (42). This suggests that the gH TMD has an intrinsic property to interact with lipids or other molecules within the membrane, involving those four amino acids. However, the 21-aa TMD of HSV-1 gH is close to the lower limit for a transmembrane-spanning helix (42). The PrV gD TMD, in contrast, is comprised of 23 residues (38, 65). Thus, we cannot completely exclude that the difference in length and not the amino acid composition is responsible for the nonfunctional phenotype.

Our data highlight the importance of the PrV gH TMD, with its specific features (length and amino acid composition) for function in fusion, whereas, in contrast to HSV-1 (41, 42), the PrV gH CD is apparently not an essential component of the fusion machinery. Moreover, as observed for EBV (48) and unlike HSV (9), soluble forms of PrV gH/gL are unable to promote cell-cell fusion, even in the presence of gB proteins with increased fusogenic potential. Interestingly, the gD TMD is not able to substitute functionally for the gH TMD, although localization at the plasma membrane, indicative of proper membrane anchorage, was observed. We hypothesize that the PrV gH TMD specifically interacts with membrane components such as lipids or other molecules as a prerequisite for triggering membrane fusion. These specific interactions could also be mediated by the HSV gH TMD but not by the TMD of gD.

In summary, we demonstrate here the relevance of the PrV gH TMD and CD in membrane fusion. Whereas a specific gH TMD is essential for triggering fusion, the gH CD modulates fusion efficiency. Given the importance of the TMD with its specific requirements, fusion induction by soluble HSV-1 gH/gL or *in trans* with gB and gH/gL present in different membranes, as shown for HSV-1 (9) and human cytomegalovirus (66), is difficult to reconcile. Either fusion can be triggered differently by the homologous gH/gL proteins, which seems improbable, or the influence of the TMD is indeed more quantitative than qualitative, with a higher dependence of PrV gH for a boost in fusion activity by the TMD. In either case the presence of a correct TMD is of high relevance for PrV gH function.

TABLE 1 Oligonucleotide primers for mutagenesis, PCR and sequence analyses

Primer name[a]	Restriction site	Sequence[b] (5′–3′)	Nucleotide position[c]
Primers for construction of gH CD mutants			
DH-3	EcoRI	AGA ATT CAA AGT TTG CCG TGC CCG TC	60748–60766
gH_ECD R	XhoI	CACACTCGAG**CTA**CGGGGACACGGGCGC	62693–62707 (r)
gH Δ668-686	XhoI	CACACTCGAG**CTA**GAATAGGGCGTACAGGATCCC	62750–62770 (r)
gH Δ670-686	XhoI	CACACTCGAG**CTA**CATCTTGAATAGGGC	62762–62776 (r)
gH Δ678-686	XhoI	CACACTCGAG**CTA**GCCCTCGGAGGA	62780–62809 (r)
gH Δ682-686	XhoI	CACACTCGAG**TAA**CCGAGAATAGCC	62812–62798 (r)
Primers for construction of gH Y678A			
gH Y679A F		CCTCCGAGGGC**GC**TTCTCGGTTAATAAACG	62790–62819
gH Y679A R		CGTTTATTAACCGAGAA**GC**GCCCTCGGAGG	62790-62819 (r)
Primer for construction of gH-gpi			
gH Ka HindIII F	HindIII	CACAAGCTTAAAGTTTGCCGTGCCCGTC	60748–60766
gH ECD EcoRV R	EcoRV	CACAGATATCCGGGGACACGGGCGCGAGCCG	62687–62707 (r)
Primers for construction of gH chimeras			
P CD H TMD F		*TGGTTATGATTACCGCCGCCCTGGCTGGCATCCTA*/AAGATGCTCTGCAGC	H, 43828–43862; P, 62771–62785
P ECD H TMD R		*ATCATAACCACGCCCAGCGCAGAGGCGGCCAGAA*/AGGCCGGGGACACGGG	H, 43853–43886; P, 62696–62711 (r)
P ECD H TMD CD F		TCGCGCCCGTGTCCCCGGCC/*TTTCTGGCCGCCTCTGCG*	H, 43870–43887; P, 62691–62711
P ECD H TMD CD R		*GCCAGCCAGGGCGGCGGTAATCATAACCACGCCCAGCGCAGAGGCGGC CAGAA*/AGGCCGGGGACACGGGCGCGAGCC	H, 43834–42886; P, 62688–62711 (r)
H TMD P CD		*GCCGCCTCTGCGCTGGGCGTGGTTATGATTACCGCCGCCCTGGCTGGC ATCCTA*/ATGCTCTGCAGCTTCTCCTCCGAGG	H, 43828–43881; P, 62774–62798
gH Ka ECD gD TMD R		*CGTGCCGACGATCACCGA*/CGGGGACACGGGCGCGAGC	gD Ka, 122199–122215; gH Ka, 62689–62707 (r)
gH Ka ECD gD TMD F		GCTCGCGCCCGTGTCCCCG/*TCGGTGATCGTCGGCACG*	gH Ka, 62689–62707; gD Ka, 122198–122215
gD TM gH CD F		ACCGCGATGGGCGCGCTCCTGGTGGGCGTGTGCGTCTACATCTTCTTC/AA GATGCTCTGCAGCTTC	gH Ka, 62771–62788; gD Ka, 122219–122266
gD TM gH CD R		AGGAGCGCGCCCATCGCGGTGCCCGTGCCGACGATCACCGAC/GGG GACACGGGCGCGAG	gH Ka, 62707–62690; gD Ka, 122198–122238 (r)
HHV1gH-R	XhoI	*CACACTCGAG **TTA** TTCGCGTCTCC*	43783–43796 (r)
US6-rev	EcoRI	*CACAGAATTCC **ATC** GACGCCGGTACTGC*	121353–122370 (r)
DHrev1	XbaI	CATCTAGACACGCGCACGCAGAGAGT	62856–62874 (r)
Primer for sequencing			
T7		TAATACGACTCACTATAGGG	pcDNA3
SP6		CTCTAGCATTTAGGTGACACTATAG	pcDNA3 (r)
gH-WH3		TGCACGAGAGCGACGACTACC	61479–61499
gH-WH6		GGACATCGCCAACCCGCTCG	62356–62375

[a]Designations and components of the OE primers specify the virus. P, PrV; H, HSV-1; TMD, transmembrane domain; CD, cytoplasmic domain; ECD, ectodomain; F, forward; R, reverse. Nucleotide positions in the PrV Ka genome refer to GenBank accession no. JQ809328 and for HSV-1 strain F to GenBank accession no. GU734771.
[b]Nonmatching nucleotides are printed in boldface, and restriction sites for convenient cloning of PCR products are underlined. HSV-1 and PrV gD sequences are shown in italics.
[c]Reverse-strand PCR primers are indicated (r).

MATERIALS AND METHODS

Cells and viruses. Rabbit kidney (RK13) and RK13-gH/gL cells (56) were grown in Dulbecco's modified Eagle's minimum essential medium (MEM) supplemented with 10% fetal calf serum (FCS) at 37°C and 5% CO_2. The PrV mutant lacking gH (PrV-gHABF; here designated PrV-ΔgH) (55), which was derived from PrV strain Kaplan (PrV-Ka) (67), was propagated on RK13-gH/gL cells.

Expression plasmids. Construction of expression plasmids for PrV-Ka and HSV-1 F gB, gH, and gL has been described previously (37, 53). Expression plasmids for the truncated versions of gH and soluble gH were generated by PCR, using pcDNA-gH as the template, DH-3 as forward primer, and the corresponding reverse primers gH Δ668-686, gH Δ670-686, gH Δ678-686, gH Δ682-686, and gH ECD R (Table 1). PCR products were cloned after cleavage with EcoRI and XhoI into correspondingly digested pcDNA3

(Invitrogen). The expression plasmid for gHY678A was generated by site-directed mutagenesis (QuikChange II XL kit; Agilent) with the complementary pair of oligonucleotide primers (Table 1) and pcDNA-gH as the template. For generation of pcDNA-gH-gpi, the 5′-terminal part of the PrV gH open reading frame (ORF) was amplified from pcDNA-gH Ka using primers gH Ka HindIII F and gH ECD EcoRV (Table 1) and cleaved with HindIII and EcoRV. The 110-bp sequence comprising a gpi addition signal was purified from pspGPIsig (kind gift from G. Keil, Insel Riems, Germany) by cleavage with SmaI and EcoRI. The two fragments were ligated and subsequently cloned into pcDNA3 via HindIII and EcoRI restriction sites.

Expression plasmids for gH chimeras gH-Hs-Hs, gH-Hs-Hp, gH-D-D, and gH-D-H were generated by overlap extension PCR (OE-PCR) (68). The 5′-terminal parts of the PrV gH ORF were amplified from pcDNA-gH using primer DH-3 and the corresponding reverse OE primers (Table 1). For constructs with the TMD from HSV-1 gH but comprising the CD from PrV gH, the 3′-terminal part of the PrV gH ORF was amplified from pcDNA-gH using the desired forward OE primers in combination with the reverse primer DHrev1 (Table 1). The 3′-terminal parts of the HSV-1 gH or PrV gD ORF were amplified from pcDNA-H1FgH (53) or pcDNA-gD (32), respectively, with the appropriate forward OE primers and the reverse primer HHV1 gH-R or US6-rev, respectively (Table 1). The PCR products were purified, and 10 ng of each of the matching products, which overlapped by ≥15 bp, was mixed and amplified in a final PCR using only the primers for the termini. PCR products were cloned via restriction sites which had been introduced by the primers into correspondingly digested pcDNA3 (Table 1). Correct mutagenesis of all constructs was verified by sequencing (data not shown). Geneious software, version 10.2.3 (Biomatters), was used for analysis and comparison of DNA and protein sequences.

Western blot analyses. Protein expression was tested after transfection of the expression plasmids into RK13 cells. For this, approximately 1.8×10^5 RK13 cells per well were seeded onto 24-well cell culture plates. The following day, cells were transfected with 200 ng of the corresponding gH expression plasmid in 100 μl Opti-MEM using 1 μl Lipofectamine 2000 (Thermo Fisher Scientific). Empty vector (pcDNA3) served as a negative control. The mixture was incubated for 20 min at room temperature and subsequently added to the cells. After 3 h, cells were washed with phosphate-buffered saline (PBS) and incubated in MEM supplemented with 2% FCS at 37°C. Cells were lysed 48 h posttransfection, and samples were separated by discontinuous SDS-PAGE and transferred to nitrocellulose membranes. The membranes were incubated with the monospecific rabbit PrV gH antiserum (31), which was used at a dilution of 1:15,000. Binding of peroxidase-conjugated secondary antibodies (Jackson ImmunoResearch) was detected with Clarity Western ECL substrate (Bio-Rad) and recorded with a VersaDoc 4000 MP imager (Bio-Rad).

PLC treatment. Correct membrane attachment of gH by a gpi anchor was tested by treatment with phospholipase C (PLC). For this, transfected cells were incubated with PBS containing 0.2 U PLC (Boehringer) per ml. After 1 h on a shaker at room temperature, the supernatant was collected, centrifuged for 2 min at 13,000 rpm, and subsequently used for Western blot or immunofluorescence analysis.

Flow cytometry. RK13 cells were cotransfected with expression plasmids for gH and gL as described above and were detached after 24 h with 2 mM EDTA in PBS for 1 h at 4°C. Subsequently, cells were fixed with 4% paraformaldehyde (PFA) for 20 min at 4°C and washed with PBS supplemented with 2% bovine serum albumin (BSA) and 2 mM EDTA. Each sample was split into two fluorescence-activated cell sorting (FACS) tubes. While one aliquot was permeabilized with 0.5% saponin in PBS with 0.2% BSA for 30 min at 4°C to assay total gH expression, the second was incubated without saponin to test for plasma membrane localization of gH. After a washing step with 2 mM EDTA in PBS, cells were probed with a monoclonal gH antibody (31) at a dilution of 1:5 in PBS with 2% BSA for 1 h at 4°C. After another washing step with 2 mM EDTA in PBS, cells were incubated for 1 h at 4°C with a secondary antibody (Alexa Fluor 488, goat anti-mouse IgG; Invitrogen) at a dilution of 1:1,000 in PBS with 2% BSA. Samples were analyzed using a MACSQuant analyzer (Miltenyi Biotec). Surface expression of gH was quantified as the mean fluorescence intensity (MFI) of Alexa-488-positive, nonpermeabilized cells divided by the MFI of Alexa-488-positive, permeabilized cells. Results obtained for gH Ka were set as 100%. Mean values and standard deviations from three independent assays were determined.

Transient-transfection-based cell-cell fusion assays. Fusion activity of the different gH mutants was determined after transient transfection of RK13 cells as described recently (54). Briefly, cells were transfected with 200 ng each of the expression plasmids for EGFP (pEGFP-N1; Clontech) and for PrV glycoproteins gB, gL, and gH or mutant gH in 100 μl Opti-MEM using 1 μl Lipofectamine 2000 (32, 37). Empty vector (pcDNA3) served as the negative control. Cells were fixed 24 h posttransfection with 3% PFA. Syncytium formation was analyzed using an Eclipse Ti-S fluorescence microscope and NIS-Elements Imaging Software (Nikon). Total fusion activity was determined by multiplication of the area of cells with three or more nuclei by the number of syncytia within 10 fields of view (5.5 mm^2 each). Each experiment was repeated four times, and average percent values of positive-control transfections as well as standard deviations were calculated.

Transcomplementation assay. The ability of the gH mutants to function in virus entry was determined by transcomplementation of PrV-ΔgH (55). Cells were transfected with the gH expression plasmids as described above. Twenty-four hours posttransfection cells were infected with PrV-ΔgH at a multiplicity of infection (MOI) of 3 and consecutively incubated on ice for 1 h and at 37°C for 1 h. Subsequently, the inoculum was removed, nonpenetrated virus was inactivated by low-pH treatment (69), and 1 ml fresh medium was added. After 24 h at 37°C, the cells and supernatant were harvested and lysed by freeze-thawing (−80°C and 37°C). Progeny virus titers were determined on RK13-gH/gL cells (56).

Statistical analyses. The statistical significance of differences observed in flow cytometry, transient fusion assays, and transcomplementation assays was evaluated using unpaired *t* test with Welch correction provided by GraphPad Prism 7 software (GraphPad Software, Inc., San Diego, CA).

ACKNOWLEDGMENTS

These studies were supported by the Deutsche Forschungsgemeinschaft (DFG grant Me 854/11-2).

The technical assistance of Karla Günther is greatly appreciated. We thank Birke A. Tews, Michael Knittler, and Elke Rufer for their help with FACS analysis.

REFERENCES

1. Harrison SC. 2015. Viral membrane fusion. Virology 479-480:498–507.
2. Eisenberg RJ, Atanasiu D, Cairns TM, Gallagher JR, Krummenacher C, Cohen GH. 2012. Herpes virus fusion and entry: a story with many characters. Viruses 4:800–832. https://doi.org/10.3390/v4050800.
3. Heldwein EE, Krummenacher C. 2008. Entry of herpesviruses into mammalian cells. Cell Mol Life Sci 65:1653–1668. https://doi.org/10.1007/s00018-008-7570-z.
4. Li Q, Krogmann T, Ali MA, Tang WJ, Cohen JI. 2007. The amino terminus of varicella-zoster virus (VZV) glycoprotein E is required for binding to insulin-degrading enzyme, a VZV receptor. J Virol 81:8525–8532. https://doi.org/10.1128/JVI.00286-07.
5. Davison AJ, Scott JE. 1986. The complete DNA sequence of varicella-zoster virus. J Gen Virol 67(Part 9):1759–1816. https://doi.org/10.1099/0022-1317-67-9-1759.
6. Wang X, Kenyon WJ, Li Q, Mullberg J, Hutt-Fletcher LM. 1998. Epstein-Barr virus uses different complexes of glycoproteins gH and gL to infect B lymphocytes and epithelial cells. J Virol 72:5552–5558.
7. Chen J, Jardetzky TS, Longnecker R. 2016. The cytoplasmic tail domain of Epstein-Barr virus gH regulates membrane fusion activity through altering gH binding to gp42 and epithelial cell attachment. mBio 7:e01871-16. https://doi.org/10.1128/mBio.01871-16.
8. Rowe CL, Connolly SA, Chen J, Jardetzky TS, Longnecker R. 2013. A soluble form of Epstein-Barr virus gH/gL inhibits EBV-induced membrane fusion and does not function in fusion. Virology 436:118–126. https://doi.org/10.1016/j.virol.2012.10.039.
9. Atanasiu D, Saw WT, Cohen GH, Eisenberg RJ. 2010. Cascade of events governing cell-cell fusion induced by herpes simplex virus glycoproteins gD, gH/gL, and gB. J Virol 84:12292–12299. https://doi.org/10.1128/JVI.01700-10.
10. Atanasiu D, Whitbeck JC, Cairns TM, Reilly B, Cohen GH, Eisenberg RJ. 2007. Bimolecular complementation reveals that glycoproteins gB and gH/gL of herpes simplex virus interact with each other during cell fusion. Proc Natl Acad Sci U S A 104:18718–18723. https://doi.org/10.1073/pnas.0707452104.
11. Di Giovine P, Settembre EC, Bhargava AK, Luftig MA, Lou H, Cohen GH, Eisenberg RJ, Krummenacher C, Carfi A. 2011. Structure of herpes simplex virus glycoprotein D bound to the human receptor nectin-1. PLoS Pathog 7:e1002277. https://doi.org/10.1371/journal.ppat.1002277.
12. Lazear E, Whitbeck JC, Zuo Y, Carfi A, Cohen GH, Eisenberg RJ, Krummenacher C. 2014. Induction of conformational changes at the N-terminus of herpes simplex virus glycoprotein D upon binding to HVEM and nectin-1. Virology 448:185–195. https://doi.org/10.1016/j.virol.2013.10.019.
13. Krummenacher C, Supekar VM, Whitbeck JC, Lazear E, Connolly SA, Eisenberg RJ, Cohen GH, Wiley DC, Carfi A. 2005. Structure of unliganded HSV gD reveals a mechanism for receptor-mediated activation of virus entry. EMBO J 24:4144–4153. https://doi.org/10.1038/sj.emboj.7600875.
14. Connolly SA, Whitbeck JJ, Rux AH, Krummenacher C, van Drunen Littel-van den Hurk S, Cohen GH, Eisenberg RJ. 2001. Glycoprotein D homologs in herpes simplex virus type 1, pseudorabies virus, and bovine herpes virus type 1 bind directly to human HveC(nectin-1) with different affinities. Virology 280:7–18. https://doi.org/10.1006/viro.2000.0747.
15. Gianni T, Amasio M, Campadelli-Fiume G. 2009. Herpes simplex virus gD forms distinct complexes with fusion executors gB and gH/gL in part through the C-terminal profusion domain. J Biol Chem 284:17370–17382. https://doi.org/10.1074/jbc.M109.005728.
16. Chowdary TK, Cairns TM, Atanasiu D, Cohen GH, Eisenberg RJ, Heldwein EE. 2010. Crystal structure of the conserved herpesvirus fusion regulator complex gH-gL. Nat Struct Mol Biol 17:882–888. https://doi.org/10.1038/nsmb.1837.
17. Cooper RS, Heldwein EE. 2015. Herpesvirus gB: a finely tuned fusion machine. Viruses 7:6552–6569. https://doi.org/10.3390/v7122957.
18. Atanasiu D, Whitbeck JC, de Leon MP, Lou H, Hannah BP, Cohen GH, Eisenberg RJ. 2010. Bimolecular complementation defines functional regions of herpes simplex virus gB that are involved with gH/gL as a necessary step leading to cell fusion. J Virol 84:3825–3834. https://doi.org/10.1128/JVI.02687-09.
19. Li A, Lu G, Qi J, Wu L, Tian K, Luo T, Shi Y, Yan J, Gao GF. 2017. Structural basis of nectin-1 recognition by pseudorabies virus glycoprotein D. PLoS Pathog 13:e1006314. https://doi.org/10.1371/journal.ppat.1006314.
20. Heldwein EE, Lou H, Bender FC, Cohen GH, Eisenberg RJ, Harrison SC. 2006. Crystal structure of glycoprotein B from herpes simplex virus 1. Science 313:217–220. https://doi.org/10.1126/science.1126548.
21. Backovic M, Longnecker R, Jardetzky TS. 2009. Structure of a trimeric variant of the Epstein-Barr virus glycoprotein B. Proc Natl Acad Sci U S A 106:2880–2885. https://doi.org/10.1073/pnas.0810530106.
22. Burke HG, Heldwein EE. 2015. Crystal structure of the human cytomegalovirus glycoprotein B. PLoS Pathog 11:e1005227. https://doi.org/10.1371/journal.ppat.1005227.
23. Chandramouli S, Ciferri C, Nikitin PA, Calo S, Gerrein R, Balabanis K, Monroe J, Hebner C, Lilja AE, Settembre EC, Carfi A. 2015. Structure of HCMV glycoprotein B in the postfusion conformation bound to a neutralizing human antibody. Nat Commun 6:8176. https://doi.org/10.1038/ncomms9176.
24. Roche S, Bressanelli S, Rey FA, Gaudin Y. 2006. Crystal structure of the low-pH form of the vesicular stomatitis virus glycoprotein G. Science 313:187–191. https://doi.org/10.1126/science.1127683.
25. Kadlec J, Loureiro S, Abrescia NG, Stuart DI, Jones IM. 2008. The postfusion structure of baculovirus gp64 supports a unified view of viral fusion machines. Nat Struct Mol Biol 15:1024–1030. https://doi.org/10.1038/nsmb.1484.
26. Matsuura H, Kirschner AN, Longnecker R, Jardetzky TS. 2010. Crystal structure of the Epstein-Barr virus (EBV) glycoprotein H/glycoprotein L (gH/gL) complex. Proc Natl Acad Sci U S A 107:22641–22646. https://doi.org/10.1073/pnas.1011806108.
27. Xing Y, Oliver SL, Nguyen T, Ciferri C, Nandi A, Hickman J, Giovani C, Yang E, Palladino G, Grose C, Uematsu Y, Lilja AE, Arvin AM, Carfi A. 2015. A site of varicella-zoster virus vulnerability identified by structural studies of neutralizing antibodies bound to the glycoprotein complex gHgL. Proc Natl Acad Sci U S A 112:6056–6061. https://doi.org/10.1073/pnas.1501176112.
28. Backovic M, DuBois RM, Cockburn JJ, Sharff AJ, Vaney MC, Granzow H, Klupp BG, Bricogne G, Mettenleiter TC, Rey FA. 2010. Structure of a core fragment of glycoprotein H from pseudorabies virus in complex with antibody. Proc Natl Acad Sci U S A 107:22635–22640. https://doi.org/10.1073/pnas.1011507107.
29. Roop C, Hutchinson L, Johnson DC. 1993. A mutant herpes simplex virus type 1 unable to express glycoprotein L cannot enter cells, and its particles lack glycoprotein H. J Virol 67:2285–2297.
30. Klupp BG, Fuchs W, Weiland E, Mettenleiter TC. 1997. Pseudorabies virus glycoprotein L is necessary for virus infectivity but dispensable for virion localization of glycoprotein H. J Virol 71:7687–7695.
31. Klupp BG, Mettenleiter TC. 1999. Glycoprotein gL-independent infectivity of pseudorabies virus is mediated by a gD-gH fusion protein. J Virol 73:3014–3022.
32. Schröter C, Vallbracht M, Altenschmidt J, Kargoll S, Fuchs W, Klupp BG,

Mettenleiter TC. 2015. Mutations in pseudorabies virus glycoproteins gB, gD, and gH functionally compensate for the absence of gL. J Virol 90:2264–2272.
33. Vallbracht M, Rehwaldt S, Klupp BG, Mettenleiter TC, Fuchs W. 2017. Functional relevance of the N-terminal domain of pseudorabies virus envelope glycoprotein H and its interaction with glycoprotein L. J Virol 91:e00061-17. https://doi.org/10.1128/JVI.00061-17.
34. Nixdorf R, Klupp BG, Karger A, Mettenleiter TC. 2000. Effects of truncation of the carboxy terminus of pseudorabies virus glycoprotein B on infectivity. J Virol 74:7137–7145. https://doi.org/10.1128/JVI.74.15.7137-7145.2000.
35. Weise K, Kaerner HC, Glorioso J, Schroder CH. 1987. Replacement of glycoprotein B gene sequences in herpes simplex virus type 1 strain ANG by corresponding sequences of the strain KOS causes changes of plaque morphology and neuropathogenicity. J Gen Virol 68(Part 7): 1909–1919. https://doi.org/10.1099/0022-1317-68-7-1909.
36. Fan Z, Grantham ML, Smith MS, Anderson ES, Cardelli JA, Muggeridge MI. 2002. Truncation of herpes simplex virus type 2 glycoprotein B increases its cell surface expression and activity in cell-cell fusion, but these properties are unrelated. J Virol 76:9271–9283. https://doi.org/10.1128/JVI.76.18.9271-9283.2002.
37. Klupp BG, Nixdorf R, Mettenleiter TC. 2000. Pseudorabies virus glycoprotein M inhibits membrane fusion. J Virol 74:6760–6768. https://doi.org/10.1128/JVI.74.15.6760-6768.2000.
38. Nixdorf R, Klupp BG, Mettenleiter TC. 2001. Role of the cytoplasmic tails of pseudorabies virus glycoproteins B, E and M in intracellular localization and virion incorporation. J Gen Virol 82:215–226. https://doi.org/10.1099/0022-1317-82-1-215.
39. Silverman JL, Greene NG, King DS, Heldwein EE. 2012. Membrane requirement for folding of the herpes simplex virus 1 gB cytodomain suggests a unique mechanism of fusion regulation. J Virol 86: 8171–8184. https://doi.org/10.1128/JVI.00932-12.
40. Garcia NJ, Chen J, Longnecker R. 2013. Modulation of Epstein-Barr virus glycoprotein B (gB) fusion activity by the gB cytoplasmic tail domain. mBio 4:e00571-12. https://doi.org/10.1128/mBio.00571-12.
41. Rogalin HB, Heldwein EE. 2015. Interplay between the herpes simplex virus 1 gB cytodomain and the gH cytotail during cell-cell fusion. J Virol 89:12262–12272. https://doi.org/10.1128/JVI.02391-15.
42. Harman A, Browne H, Minson T. 2002. The transmembrane domain and cytoplasmic tail of herpes simplex virus type 1 glycoprotein H play a role in membrane fusion. J Virol 76:10708–10716. https://doi.org/10.1128/JVI.76.21.10708-10716.2002.
43. Yang E, Arvin AM, Oliver SL. 2014. The cytoplasmic domain of varicella-zoster virus glycoprotein H regulates syncytia formation and skin pathogenesis. PLoS Pathog 10:e1004173. https://doi.org/10.1371/journal.ppat.1004173.
44. Jackson JO, Longnecker R. 2010. Reevaluating herpes simplex virus hemifusion. J Virol 84:11814–11821. https://doi.org/10.1128/JVI.01615-10.
45. Pasieka TJ, Maresova L, Grose C. 2003. A functional YNKI motif in the short cytoplasmic tail of varicella-zoster virus glycoprotein gH mediates clathrin-dependent and antibody-independent endocytosis. J Virol 77: 4191–4204. https://doi.org/10.1128/JVI.77.7.4191-4204.2003.
46. Suenaga T, Satoh T, Somboonthum P, Kawaguchi Y, Mori Y, Arase H. 2010. Myelin-associated glycoprotein mediates membrane fusion and entry of neurotropic herpesviruses. Proc Natl Acad Sci U S A 107: 866–871. https://doi.org/10.1073/pnas.0913351107.
47. Jones NA, Geraghty RJ. 2004. Fusion activity of lipid-anchored envelope glycoproteins of herpes simplex virus type 1. Virology 324:213–228. https://doi.org/10.1016/j.virol.2004.03.024.
48. Kirschner AN, Omerovic J, Popov B, Longnecker R, Jardetzky TS. 2006. Soluble Epstein-Barr virus glycoproteins gH, gL, and gp42 form a 1:1:1 stable complex that acts like soluble gp42 in B-cell fusion but not in epithelial cell fusion. J Virol 80:9444–9454. https://doi.org/10.1128/JVI.00572-06.
49. Pertel PE, Fridberg A, Parish ML, Spear PG. 2001. Cell fusion induced by herpes simplex virus glycoproteins gB, gD, and gH-gL requires a gD receptor but not necessarily heparan sulfate. Virology 279:313–324. https://doi.org/10.1006/viro.2000.0713.
50. Mullen MM, Haan KM, Longnecker R, Jardetzky TS. 2002. Structure of the Epstein-Barr virus gp42 protein bound to the MHC class II receptor HLA-DR1. Mol Cell 9:375–385. https://doi.org/10.1016/S1097-2765(02)00465-3.
51. Rowe CL, Chen J, Jardetzky TS, Longnecker R. 2015. Membrane anchoring of Epstein-Barr virus gp42 inhibits fusion with B cells even with increased flexibility allowed by engineered spacers. mBio 6:e02285-14. https://doi.org/10.1128/mBio.02285-14.
52. Hutchinson L, Browne H, Wargent V, Davis-Poynter N, Primorac S, Goldsmith K, Minson AC, Johnson DC. 1992. A novel herpes simplex virus glycoprotein, gL, forms a complex with glycoprotein H (gH) and affects normal folding and surface expression of gH. J Virol 66: 2240–2250.
53. Böhm SW, Backovic M, Klupp BG, Rey FA, Mettenleiter TC, Fuchs W. 2016. Functional characterization of glycoprotein h chimeras composed of conserved domains of the pseudorabies virus and herpes simplex virus 1 homologs. J Virol 90:421–432. https://doi.org/10.1128/JVI.01985-15.
54. Vallbracht M, Schröter C, Klupp BG, Mettenleiter TC. 2017. Transient transfection-based fusion assay for viral proteins. Bio-Protocol 7:e2162. https://doi.org/10.21769/BioProtoc.2162.
55. Böhm SW, Eckroth E, Backovic M, Klupp BG, Rey FA, Mettenleiter TC, Fuchs W. 2015. Structure-based functional analyses of domains II and III of pseudorabies virus glycoprotein H. J Virol 89:1364–1376. https://doi.org/10.1128/JVI.02765-14.
56. Klupp B, Altenschmidt J, Granzow H, Fuchs W, Mettenleiter TC. 2008. Glycoproteins required for entry are not necessary for egress of pseudorabies virus. J Virol 82:6299–6309. https://doi.org/10.1128/JVI.00386-08.
57. Litwin V, Jackson W, Grose C. 1992. Receptor properties of two varicella-zoster virus glycoproteins, gpI and gpIV, homologous to herpes simplex virus gE and gI. J Virol 66:3643–3651.
58. Cheatham WJ, Dolan TF, Jr, Dower JC, Weller TH. 1956. Varicella: report of two fatal cases with necropsy, virus isolation, and serologic studies. Am J Pathol 32:1015–1035.
59. Esiri MM, Tomlinson AH. 1972. Herpes zoster. Demonstration of virus in trigeminal nerve and ganglion by immunofluorescence and electron microscopy. J Neurol Sci 15:35–48.
60. Rauh I, Mettenleiter TC. 1991. Pseudorabies virus glycoproteins gII and gp50 are essential for virus penetration. J Virol 65:5348–5356.
61. Peeters B, de Wind N, Broer R, Gielkens A, Moormann R. 1992. Glycoprotein H of pseudorabies virus is essential for entry and cell-to-cell spread of the virus. J Virol 66:3888–3892.
62. Schmidt J, Gerdts V, Beyer J, Klupp BG, Mettenleiter TC. 2001. Glycoprotein D-independent infectivity of pseudorabies virus results in an alteration of in vivo host range and correlates with mutations in glycoproteins B and H. J Virol 75:10054–10064. https://doi.org/10.1128/JVI.75.21.10054-10064.2001.
63. Wilson DW, Davis-Poynter N, Minson AC. 1994. Mutations in the cytoplasmic tail of herpes simplex virus glycoprotein H suppress cell fusion by a syncytial strain. J Virol 68:6985–6993.
64. Jackson JO, Lin E, Spear PG, Longnecker R. 2010. Insertion mutations in herpes simplex virus 1 glycoprotein H reduce cell surface expression, slow the rate of cell fusion, or abrogate functions in cell fusion and viral entry. J Virol 84:2038–2046. https://doi.org/10.1128/JVI.02215-09.
65. Ficinska J, Van Minnebruggen G, Nauwynck HJ, Bienkowska-Szewczyk K, Favoreel HW. 2005. Pseudorabies virus glycoprotein gD contains a functional endocytosis motif that acts in concert with an endocytosis motif in gB to drive internalization of antibody-antigen complexes from the surface of infected monocytes. J Virol 79:7248–7254. https://doi.org/10.1128/JVI.79.11.7248-7254.2005.
66. Wille PT, Wisner TW, Ryckman B, Johnson DC. 2013. Human cytomegalovirus (HCMV) glycoprotein gB promotes virus entry in trans acting as the viral fusion protein rather than as a receptor-binding protein. mBio 4:e00332-13. https://doi.org/10.1128/mBio.00332-13.
67. Kaplan AS, Vatter AE. 1959. A comparison of herpes simplex and pseudorabies viruses. Virology 7:394–407. https://doi.org/10.1016/0042-6822(59)90068-6.
68. Heckman KL, Pease LR. 2007. Gene splicing and mutagenesis by PCR-driven overlap extension. Nat Protoc 2:924–932. https://doi.org/10.1038/nprot.2007.132.
69. Mettenleiter TC. 1989. Glycoprotein gIII deletion mutants of pseudorabies virus are impaired in virus entry. Virology 171:623–625. https://doi.org/10.1016/0042-6822(89)90635-1.

(V) Functional Role of N-linked Glycosylation in Pseudorabies Virus Glycoprotein H

Melina Vallbracht, Barbara G. Klupp, Thomas C. Mettenleiter, Walter Fuchs

Journal of Virology

Volume 92, Issue 9

May 2018

doi: 10.1128/JVI.00084-18

V

AMERICAN SOCIETY FOR MICROBIOLOGY | Journal of Virology®

VIRUS-CELL INTERACTIONS

Functional Role of N-Linked Glycosylation in Pseudorabies Virus Glycoprotein gH

Melina Vallbracht,[a] Sascha Rehwaldt,[a] Barbara G. Klupp,[a] Thomas C. Mettenleiter,[a] Walter Fuchs[a]

[a]Institute of Molecular Virology and Cell Biology, Friedrich-Loeffler-Institut, Greifswald-Insel Riems, Germany

ABSTRACT Many viral envelope proteins are modified by asparagine (N)-linked glycosylation, which can influence their structure, physicochemical properties, intracellular transport, and function. Here, we systematically analyzed the functional relevance of N-linked glycans in the alphaherpesvirus pseudorabies virus (PrV) glycoprotein H (gH), which is an essential component of the conserved core herpesvirus fusion machinery. Upon gD-mediated receptor binding, the heterodimeric complex of gH and gL activates gB to mediate fusion of the viral envelope with the host cell membrane for viral entry. gH contains five potential N-linked glycosylation sites at positions 77, 162, 542, 604, and 627, which were inactivated by conservative mutations (asparagine to glutamine) singly or in combination. The mutated proteins were tested for correct expression and fusion activity. Additionally, the mutated gH genes were inserted into the PrV genome for analysis of function during virus infection. Our results demonstrate that all five sites are glycosylated. Inactivation of the PrV-specific N77 or the conserved N627 resulted in significantly reduced *in vitro* fusion activity, delayed penetration kinetics, and smaller virus plaques. Moreover, substitution of N627 greatly affected transport of gH in transfected cells, resulting in endoplasmic reticulum (ER) retention and reduced surface expression. In contrast, mutation of N604, which is conserved in the *Varicellovirus* genus, resulted in enhanced *in vitro* fusion activity and viral cell-to-cell spread. These results demonstrate a role of the N-glycans in proper localization and function of PrV gH. However, even simultaneous inactivation of all five N-glycosylation sites of gH did not severely inhibit formation of infectious virus particles.

IMPORTANCE Herpesvirus infection requires fusion of the viral envelope with cellular membranes, which involves the conserved fusion machinery consisting of gB and the heterodimeric gH/gL complex. The bona fide fusion protein gB depends on the presence of the gH/gL complex for activation. Viral envelope glycoproteins, such as gH, usually contain N-glycans, which can have a strong impact on their folding, transport, and functions. Here, we systematically analyzed the functional relevance of all five predicted N-linked glycosylation sites in the alphaherpesvirus pseudorabies virus (PrV) gH. Despite the fact that mutation of specific sites affected gH transport, *in vitro* fusion activity, and cell-to-cell spread and resulted in delayed penetration kinetics, even simultaneous inactivation of all five N-glycosylation sites of gH did not severely inhibit formation of infectious virus particles. Thus, our results demonstrate a modulatory but nonessential role of N-glycans for gH function.

KEYWORDS herpesvirus, pseudorabies virus, glycoprotein gH, membrane fusion, virus entry, N-linked glycosylation

Infectious entry of herpesviruses into cells depends on fusion of the viral envelope with host cell membranes. To accomplish this task, herpesviruses use specialized surface glycoproteins allowing them to bind to an appropriate cellular receptor and to execute membrane fusion. Whereas many enveloped viruses rely on a single protein for

Received 16 January 2018 **Accepted** 2 February 2018

Accepted manuscript posted online 7 February 2018

Citation Vallbracht M, Rehwaldt S, Klupp BG, Mettenleiter TC, Fuchs W. 2018. Functional role of N-linked glycosylation in pseudorabies virus glycoprotein gH. J Virol 92:e00084-18. https://doi.org/10.1128/JVI.00084-18.

Editor Richard M. Longnecker, Northwestern University

Address correspondence to Thomas C. Mettenleiter, thomas.mettenleiter@fli.de.

receptor binding and entry, multiple viral glycoproteins are involved in herpesvirus-mediated membrane fusion.

Glycoprotein B (gB) and the heterodimeric complex of membrane-bound glycoprotein H and anchorless glycoprotein L (gH/gL) constitute the core fusion machinery and are conserved across the *Herpesviridae*, a large family of enveloped double-stranded DNA viruses infecting mammals, birds, and reptiles (reviewed in references 1 and 2). Binding of nonconserved herpesvirus subfamily-specific glycoproteins to cellular receptors is thought to trigger activation of the conserved fusion machinery. However, the exact molecular mechanism of this process remains to be elucidated. According to the current model, the entry glycoproteins are activated in a cascade-like fashion, beginning with binding of, e.g., alphaherpesvirus gD to a cellular receptor. Receptor binding was shown to lead to a conformational change in the C-terminal region of gD, presumably enabling gD to interact with gH/gL (3, 4). gH/gL in turn is thought to activate gB by direct interaction of their respective ectodomains (5–9). gB then inserts its two fusion loops (FL) into the target membrane to subsequently merge the viral and cellular membranes by a large conformational change (5, 8). gB is a type I transmembrane protein and is considered the bona fide fusion protein, since crystal structures of gB homologs from pseudorabies virus (PrV) (10, 11), herpes simplex virus 1 (HSV-1) (12), human cytomegalovirus (HCMV) (13, 14), and Epstein-Barr virus (EBV) (15) resemble those of typical class III postfusion trimers. However, despite its homology to, e.g., the vesicular stomatitis virus fusion protein G (16) or baculovirus gp64 (17), gB is not able to mediate membrane fusion on its own but requires the conserved gH/gL complex.

Although the specific contribution of the gH/gL complex to herpesvirus membrane fusion remains largely unknown, functional analysis points to a regulatory role (5). In contrast to that of gB, the crystal structures of soluble gH/gL of HSV-2 (7), EBV (18), and varicella-zoster virus (VZV) (19) and of a core fragment of PrV gH (20) (Fig. 1) revealed no structural homology to any known viral fusion protein. However, despite poor sequence conservation, the crystallographic studies revealed a strikingly similar domain organization of the four gH homologs.

The least-conserved domain I, located at the N terminus of gH, is associated with gL, and the presence of both proteins seems to be critical for the tertiary structure of this domain in HSV and EBV (7, 18, 21). However, in PrV, *Bovine herpesvirus 4*, and *Murid herpesvirus* 4, gL is not required for correct folding, transport, or virion incorporation of gH (22–27). Moreover, infection by PrV can occur in the absence of gL and the gL-binding domain of gH when compensatory mutations in other glycoproteins are present (28–30). In addition, the absence of gL obviously facilitates maturation of certain N-glycans of PrV gH, which are possibly masked during wild-type (WT) replication (25). Interestingly, domain I of PrV gH, which was not included in the crystallized core fragment, contains one of the predicted N-glycosylation sites at an asparagine (N) at amino acid (aa) position 77 (Fig. 1).

Domain II contains two conserved elements (Fig. 1), the "fence," a sheet of antiparallel beta-chains, and a bundle of three alpha-helices which is tightly packed against the fence and was designated syntaxin-like bundle (SLB) due to its structural similarities to a specific domain of cellular syntaxins (20). The side of the fence which packs against the SLB is very hydrophobic, whereas the opposite side, including an N-glycosylation site at position 162, displays only polar residues (20). The integrity and flexibility of the SLB were recently shown to be relevant for the function of PrV gH in membrane fusion (31).

Domain III, which contains no N-glycosylation sites, is composed of eight alpha-helices (Fig. 1) and contains a highly conserved amino acid stretch (serine-proline-cysteine) which is important for regulation of membrane fusion (32).

The membrane-proximal domain IV is the most conserved domain of gH. It consists of a beta-sandwich comprising two opposed four-stranded beta-sheets, which in PrV contain one and two predicted N-glycosylation sites, respectively, at aa 554, 604, and 627 (Fig. 1). The two sheets are connected by an extended polypeptide chain, which is designated "flap" (20). Interestingly, the flap, supported by the N-glycan at position 627,

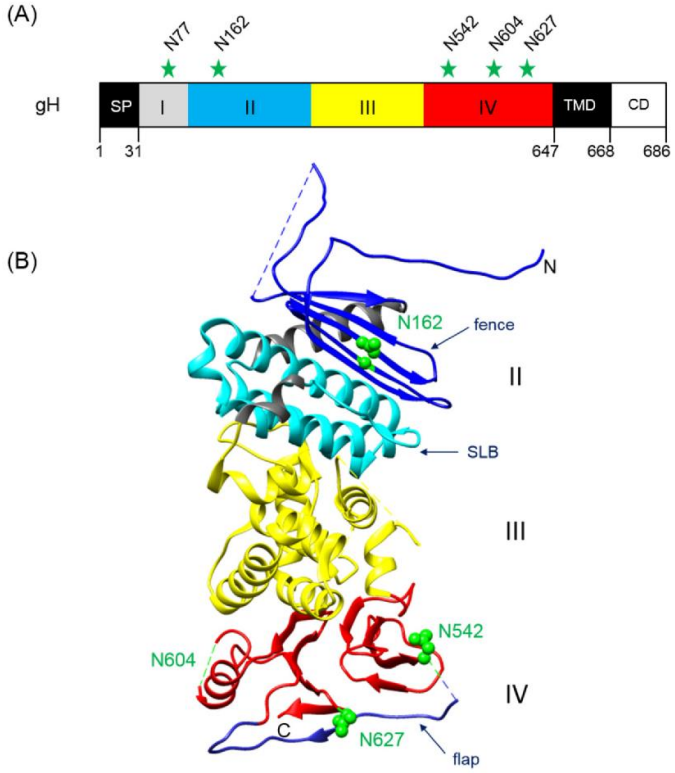

FIG 1 Positions of potential N-linked glycosylation sites in PrV gH. (A) The primary translation product of PrV gH (686 aa) is schematically shown. The first amino acids of the predicted signal peptide (SP), the ectodomain parts (I to IV), the transmembrane domain (TMD), and the cytoplasmic domain (CD), as well the modified asparagine (N) residues, are indicated. (B) Crystal structure of the gH core fragment (aa 107 to 639) (20). The N and C termini are labeled. In domain II, the fence (dark blue) and the syntaxin-like bundle (SLB) (light blue) are indicated. Domain III is colored yellow and domain IV red, with the flap highlighted in blue. Predicted glycosylation sites at N162, N542, and N627 are indicated by green spheres. N604 lies within a flexible region (dashed green line), which was not solved in the crystal structure. N77 was not included in the construct used for crystallization. The image was generated using the UCSF Chimera package (version 1.11.2) (65).

covers a patch of hydrophobic amino acid residues which is conserved in PrV, HSV, and EBV. Movement of the flap during a receptor-triggered conformational change of gH is thought to enable interaction of this underlying hydrophobic surface with the viral envelope (20, 33). This hypothesis was supported by studies revealing that disruption of conserved disulfide bonds important for positioning of the flap, prevention of flap movement by introduction of artificial disulfide bonds, or multiple alanine substitutions within the flap or the hydrophobic patch led to significant defects in gH function (33). Moreover, recent studies demonstrated functional conservation of domain IV by construction of a chimeric gH consisting of PrV domains I to III and HSV-1 domain IV. This chimera supported replication of gH-deleted PrV and was able to promote membrane fusion when coexpressed with HSV-1 or PrV gB and PrV gD and gL (34).

N-linked glycosylation is one of the most common types of membrane protein modification and involves the transfer of oligosaccharides to the asparagine residue of the sequon N-X-threonine (T) or serine (S) in the endoplasmic reticulum (ER), frequently followed by trimming and substitution of mannose residues by various other sugars in

the Golgi apparatus (35, 36). Unlike sugar chains of the complex type, the initially added high-mannose chains are sensitive to digestion with endoglycosidase H (endo H), which permits differentiation (37). Many viral envelope proteins contain N-linked glycans, which can play major roles in correct folding, physicochemical properties, intracellular transport, function during entry, and also immune evasion (38–40). Disruption of N-glycosylation sites from envelope proteins of a variety of viruses, such as HSV-2 (41), Ebola virus (40), influenza virus (42), respiratory syncytial virus (43) Zika virus (44), or Hendra and Nipah viruses (45), has been shown to have a strong impact on viral entry, cell-cell fusion, or shielding from neutralizing antibodies. N-glycans on other envelope proteins, such as HSV-1 gD, were shown to be structurally important. In contrast, N-glycosylation of gD was not required for its function during virus entry or spread (46–48).

While PrV gH contains five potential N-linked glycosylation sites (49) (Fig. 1), its complex partner gL is modified only by O-linked carbohydrates (23). Earlier studies indicated that N-linked glycans contribute approximately 19 kDa to the molecular mass of mature PrV gH and provided no evidence for the presence of O-linked sugars (49). Occupation of two (N162 and N627) of the five potential N-linked glycosylation sites was confirmed by crystal structure analysis of the core fragment of PrV gH (20). The site at aa 627 is highly conserved among the *Herpesviridae* and was suggested to play a role in the fusion process by partially masking the highly conserved hydrophobic patch in domain IV (20, 33). Mutation of this site affected the function of gH, although it was not abolished (33). However, more-detailed studies on the relevance of this site and of the four other potential PrV gH N-glycosylation sites were required.

To this end, we have now inactivated all potential N-linked glycosylation sites singly or in various combinations by conservative amino acid replacements of N by glutamine (Q) using site-directed mutagenesis of the plasmid-cloned PrV gH gene. The resulting gH expression plasmids were tested in a virus-free transfection-based cell fusion assay. Furthermore, the mutated gH genes were transferred into the PrV genome. Protein expression and glycosylation as well as *in vitro* replication properties, including penetration, growth kinetics, and plaque formation, of the obtained virus mutants were investigated.

RESULTS

Effect of N-glycosylation site mutations on gH expression and transport. The deduced amino acid sequence of PrV gH contains five potential N-linked glycosylation sites matching the consensus motif N-X-T/S, where X can represent any amino acid except proline (36). They are all located within the gH ectodomain at aa 77, 162, 542, 604, and 627 (Fig. 1). To investigate their occupation and functional relevance, the codons encoding asparagine were replaced by glutamine codons via site-directed mutagenesis of the expression plasmid-cloned gH gene of PrV strain Kaplan (PrV-Ka). The resulting plasmids, containing one to five mutations, were used for *in vitro* expression studies and fusion assays, as well as for generation of virus recombinants by mutagenesis of the PrV genome cloned as a bacterial artificial chromosome (BAC) in *Escherichia coli* (31).

Western blot (not shown) and indirect immunofluorescence (IIF) analyses (Fig. 2A) of rabbit kidney (RK13) cells cotransfected with gH and gL expression plasmids demonstrated that all generated gH mutants were stably expressed at similar levels. However, comparative IIF tests of permeabilized and nonpermeabilized RK13 cells revealed that whereas wild-type (WT) gH and most of the gH mutants were readily found at the cell surface, gH mutants containing the amino acid substitution N627Q were barely detectable on nonpermeabilized cells (Fig. 2A). These findings were confirmed by fluorescence-activated cell sorter (FACS) analysis of cotransfected cells showing that significantly decreased proportions of gHN627Q and gHN77/162/542/604/627Q were present on the cell surface compared to wild-type gH (Fig. 2B).

Analysis of the distribution of gH in the cytoplasm of plasmid transfected cells by laser scanning confocal microscopy revealed wild-type-like speckled patterns for

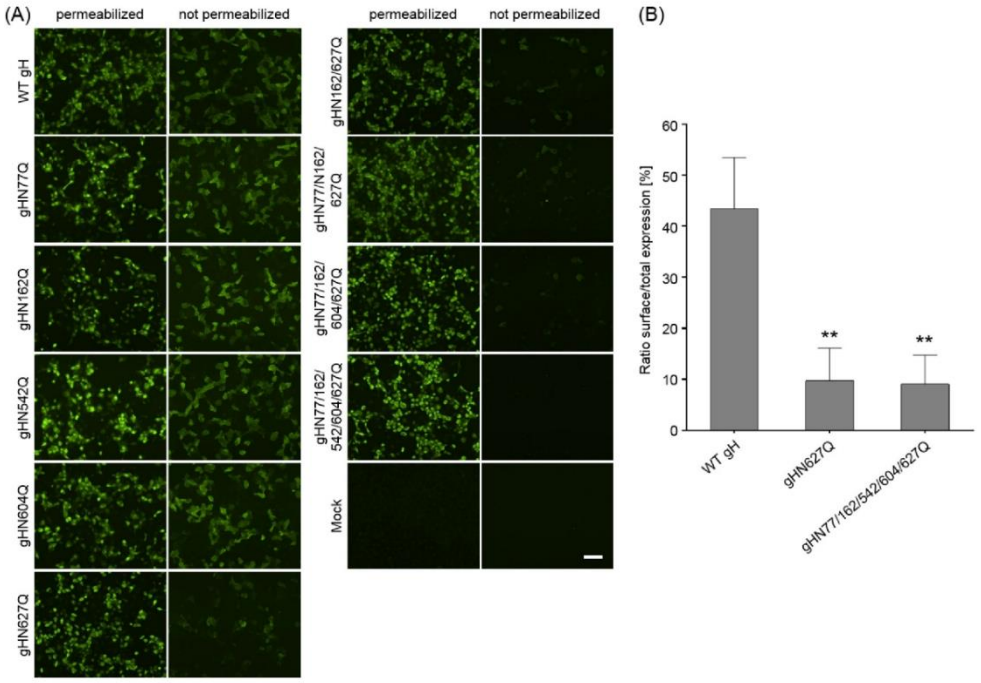

FIG 2 Expression and surface localization of gH. RK13 cells were cotransfected with expression plasmids for either wild-type (WT) or mutant gH in combination with gL. After 24 h, cells were either permeabilized or not and were stained with a gH-specific rabbit antiserum and Alexa Fluor 488-conjugated secondary antibodies. Total and cell surface expression of gH was analyzed either by fluorescence microscopy (Nikon Eclipse Ti-S) (A) or by flow cytometry (B). Bars represent the ratio between cells expressing gH at the surface and total gH-positive cells. Mean values and standard deviations from three independent experiments are shown, and the significance of differences from results obtained with wild-type gH is marked. (**, $P \leq 0.01$). Size bar in panel A, 100 μm.

most of the gH single-site mutants (Fig. 3). However, all variants, including that with the mutation N627Q showed a more perinuclear localization indicative of the endoplasmic reticulum (ER). For confirmation, colocalization of gH with an ER marker (pmTurquoise2ER; Addgene) was analyzed. As shown in Fig. 4, both gHN627Q and the quintuple mutant colocalized with the ER marker, whereas wild-type gH was found mainly in speckles distinct from the ER, indicating that N627Q impaired ER export of PrV gH to the plasma membrane.

Effects of gH N-glycosylation site mutations on *in vitro* fusion activity. To analyze the impact of the gH N-glycosylation sites on *in vitro* fusion activity, the different gH mutants were tested in transient-transfection-based fusion assays (Fig. 5). RK13 cells were cotransfected with expression plasmids encoding wild-type or mutated gH in combination with gB, gD, and gL of PrV-Ka as described previously (50). In addition, an enhanced green fluorescent protein (EGFP) expression plasmid was cotransfected to facilitate evaluation of the syncytium formation by fluorescence microscopy (51). The results of assays with wild-type gH were set as 100%. While fusion activities of mutants gHN77Q and gHN162Q were reduced by around 20% and 10%, respectively, no significant reduction was observed for gHN542Q (Fig. 5A). Interestingly, mutation of the N-glycosylation site at position 604, which is conserved in members of the *Varicellovirus* genus of alphaherpesviruses, led to a significant increase in *in vitro* fusion activity of approximately 30% compared to that with WT gH. In contrast, disruption of the highly conserved N627 completely abolished fusion activity. In line, the double, triple, quadruple, and quintuple mutants, which all contain mutation N627Q, exhibited no fusogenic potential (Fig. 5A).

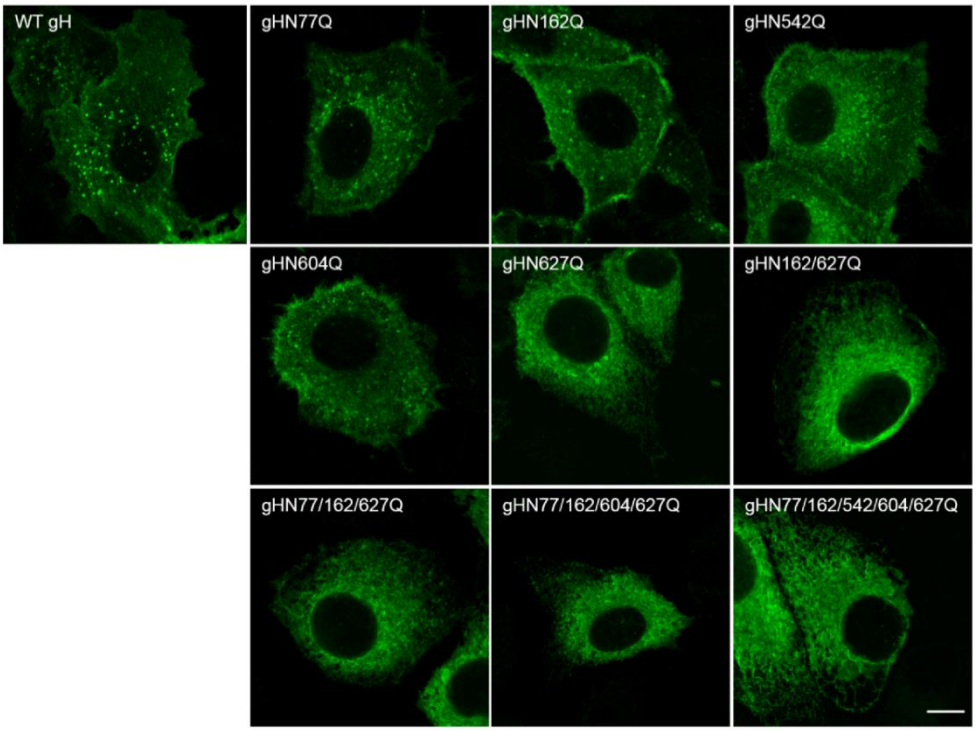

FIG 3 Subcellular localization of gH. RK13 cells were cotransfected with plasmids encoding wild-type (WT) or mutated gH in combination with gL. One day after transfection, cells were fixed with 3% paraformaldehyde and permeabilized with 0.1% Triton X-100. gH was detected using a monospecific rabbit antiserum and Alexa Fluor 488-conjugated secondary antibodies. Green fluorescence was excited at 488 nm and recorded with a laser scanning confocal microscope (Leica SP5). Size bar, 10 μm.

To investigate whether the gH mutants with an inactivated glycosylation site at position 627 are able to trigger fusion in combination with a more fusogenic gB, we replaced native gB with a C-terminally truncated protein (gB-008). In comparison to fusion assays with the WT glycoproteins, replacement of WT gB by gB-008 leads to a 3-fold increase in fusion activity (52) (Fig. 5B). Assays with plasmids encoding WT gH, gB-008, gL, and gD served as positive controls, and results were set as 100%. Assays conducted with the empty expression vector (pcDNA3) instead of a gH plasmid served as negative controls.

In relative terms, fusion activities obtained for gHN77Q, gHN162Q, gHN542Q, and gHN604Q in combination with the hyperfusogenic gB-008 (Fig. 5B) were similar to those obtained with wild-type gB (Fig. 5A). However, in contrast to fusion assays with wild-type gB, in which no activity could be observed for gH N627Q mutants, assays with gB-008 revealed that all these mutants mediated cell-cell fusion, although at ≥70% lower levels than WT gH (Fig. 5B). These results indicate that the carbohydrate moiety on N627 plays an important role in fusion or proper localization of gH.

Effects of N-glycosylation site mutations on processing and virion incorporation of gH. To investigate the relevance of the N-glycosylation sites for processing and virion incorporation of gH and virus replication, the mutated gH genes were introduced into the PrV genome by BAC mutagenesis in *E. coli* as described previously (31). PCR amplification and subsequent sequencing of the entire gH open reading frames (ORF) of all virus recombinants confirmed that neither reversions of the desired mutations nor additional mutations elsewhere in the gene had occurred.

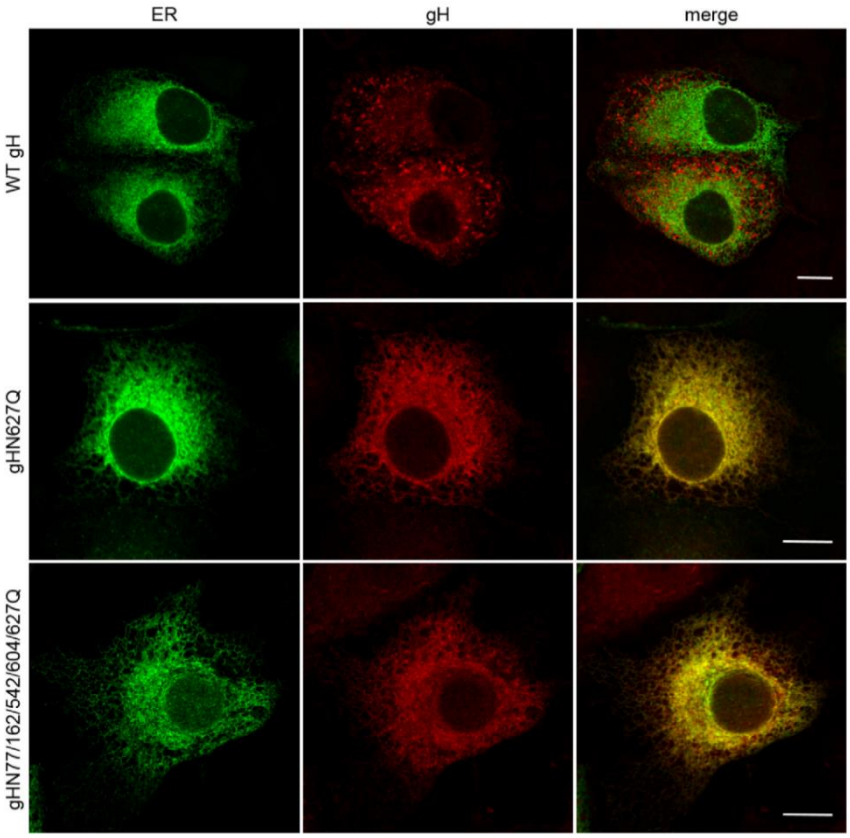

FIG 4 Colocalization of gH mutants with the endoplasmic reticulum. RK13 cells were cotransfected with expression plasmids for wild-type (WT) or mutated gH in combination with gL and the ER marker pmTurquoise2ER (Addgene). At 24 h posttransfection, cells were fixed with 3% paraformaldehyde and permeabilized with 0.1% Triton X-100. gH was detected using a monospecific rabbit antiserum and Alexa Fluor 633-conjugated secondary antibodies. Green (ER) and red (gH) fluorescence was excited at 488 nm and 633 nm, respectively, and recorded with a laser scanning confocal microscope (Leica SP5). Channels were merged to visualize ER localization of gH. Size bars, 10 μm.

None of the analyzed N-glycosylation site mutations of gH abrogated formation of infectious PrV (see below), and Western blot analyses of purified virions revealed that all mutated proteins were incorporated into virus particles (Fig. 6A). Moreover, no obvious reduction of gH amounts compared to those of other envelope glycoproteins such as gB (not shown) or gD (Fig. 6B) could be observed. As expected, all glycosylation site mutants of gH exhibited higher electrophoretic mobilities than WT gH, which possessed an apparent molecular mass of approximately 90 kDa (Fig. 6A, first lane). Considerable differences could be observed between the apparent masses of the single mutants, indicating that the sizes of carbohydrate chains of gH differ site specifically. Interestingly, removal of the highly conserved glycosylation site at gH position 627 had the least effect on electrophoretic mobility (Fig. 6A and 7F). The apparent molecular masses of the double (gHN162/627Q), triple (gHN77/162/627Q), quadruple (gHN77/162/604/627Q), and quintuple (gHN77/162/542/604/627Q) mutants gradually decreased as expected (Fig. 6A). These results demonstrate that all five predicted N-glycosylation sites are occupied by carbohydrates in PrV gH. Since N77 is located in PrV gH domain I, which was recently confirmed to be required for gL binding and virion

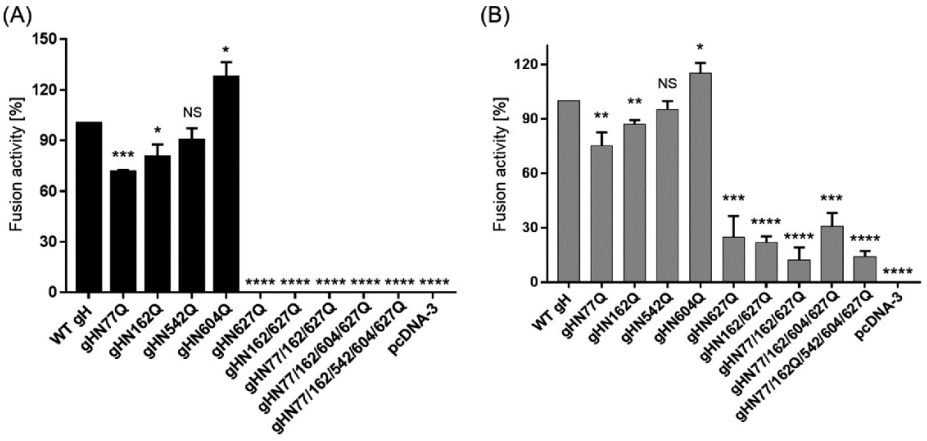

FIG 5 *In vitro* fusion activity of gH mutants. RK13 cells were cotransfected with expression plasmids for EGFP, gD, gL, wild-type (WT) or mutated gH, and wild-type gB (A) or C-terminally truncated gB-008 (B). Assays without gH served as negative controls. One day after transfection, the relative fusion activity was determined by multiplication of the mean syncytium area by the number of syncytia in 10 fields of view. Fusion activities in assay mixtures containing wild-type gH were set as 100%. Shown are the mean relative values and corresponding standard deviations from four independent experiments. Results significantly differing from those obtained with WT gH are marked (*, $P \leq 0.05$; **, $P \leq 0.01$, ***, $P \leq 0.001$; ****, $P \leq 0.0001$). NS, not significant.

incorporation (30), virus particles were also analyzed for the presence of gL (Fig. 6C). Despite moderate variations in signal strength, gL was detectable in virions of all investigated gH mutants, including the N77Q substitution mutants. Thus, N-glycosylation of gH is not required for interaction with gL.

To further analyze the glycosylation state of gH, purified virions of the different mutants were treated with either endo H to remove only high-mannose-type N-glycans (Fig. 7, lanes 3) or peptide-*N*-glycosidase F (PNGase F) to cleave off all N-linked carbohydrates (Fig. 7, lanes 2). As expected, WT gH and all gH mutants, except the quintuple mutant, were sensitive to digestion with PNGase F, which resulted in a shift from the different sizes of the untreated proteins (Fig. 7, lanes 1 and 4) to a similar apparent molecular mass of approximately 70 kDa (Fig. 7, lanes 2). This size corresponded to that of the glycosidase-resistant quintuple mutant of gH (Fig. 7H) and was close to the 69-kDa calculated molecular mass of the unmodified polypeptide after removal of the predicted signal peptide. These results confirmed that all predicted N-glycosylation sites on wild-type gH are occupied and that they are inactivated in the quintuple mutant.

As shown previously (49), PrV wild-type virions still contain endo H-sensitive carbohydrates (Fig. 7A). To investigate which of the five glycosylation sites of mature wild-type gH might be modified by high mannose N-glycans, virions of the gH mutants were also treated with endo H. All mutants containing deletions of only one N-glycosylation site were found to be sensitive, and faster-migrating gH species were detected (Fig. 7, lanes 3). However, the shifts compared to untreated gH (Fig. 7, lanes 1 and 4) were different, and least in pPrV-gHN162Q and pPrV-gHN627Q virions (Fig. 7C and F, arrows). Western blot analysis of virions of the double mutant pPrV-gHN162/627Q revealed that this gH mutant was no longer sensitive to endo H digestion (Fig. 7G, arrow). These results strongly suggest that high-mannose-type N-glycans are retained only at aa 162 and 627 of mature gH.

Effect of gH N-glycosylation site mutations on virus entry and spread. To determine the effect of N-glycosylation in PrV gH on virus replication, the penetration and growth kinetics, as well as direct viral cell-to-cell spread of all obtained virus mutants, were analyzed in RK13 cells. Penetration kinetics studies revealed that entry of WT gH-expressing PrV (pPrV-gHK) and pPrV-gHN162Q occurred at a similar high

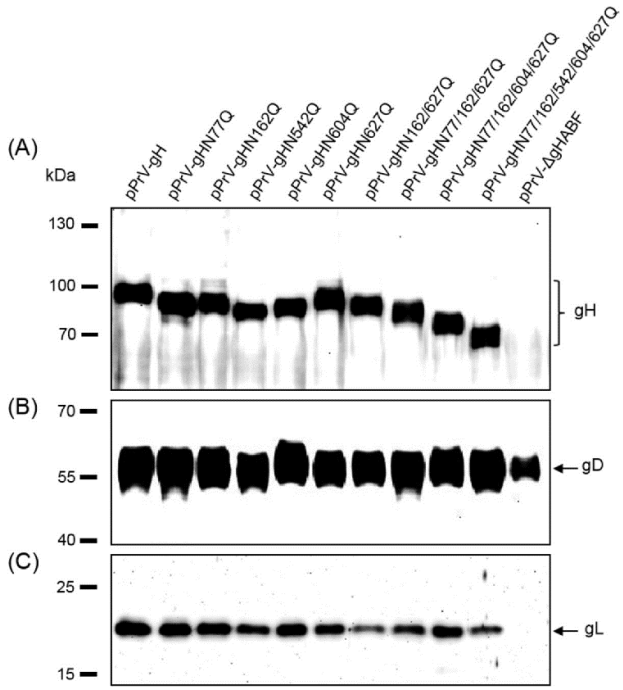

FIG 6 Western blot analyses of purified PrV particles. Virion proteins of the indicated gH mutants were separated by SDS-PAGE. Blots were probed with monospecific rabbit antisera against gH (A), gD (B), or gL (C). Molecular masses of marker proteins are indicated.

velocity, with almost 100% of infectious input virus protected from inactivation by low-pH treatment after 10 min at 37°C (Fig. 8). Penetration of pPrV-gHN77Q, pPrV-gHN542Q, and pPrV-gHN604Q was slightly delayed, with approximately 80% of virions being internalized within 10 min. However, after 30 min, almost complete penetration was achieved. In contrast, only 70% of infectious pPrV-gHN627Q and pPrV-gHN162/627Q particles were able to penetrate within 10 min, and 2 h was required for complete penetration (Fig. 8). The defect in entry was even more pronounced for the triple, quadruple, and quintuple virus mutants, of which only 30% of the infectious particles were internalized within 10 min. However, after 2 h, almost complete penetration was observed for all mutants (Fig. 8).

In contrast to the effects of N-glycosylation site mutations on the kinetics of virus entry, the impact on total replication was less striking (Fig. 9). Multistep growth analyses performed after infection at a multiplicity of infection (MOI) of 0.01 revealed no significant effects on maximum titers of any of the virus recombinants possessing single gH mutations compared to WT gH-rescued pPrV-gHK, demonstrating that none of the N-glycosylation sites is essential for efficient production of infectious virions. The multiply mutated viruses exhibited an approximately 5- to maximum 10-fold reduction of final titers compared to pPrV-gHK (Fig. 9). Moreover, the quintuple mutant showed a delayed increase of virus titers (Fig. 9). These results indicate that although none of the N-glycosylation sites is essential, complete absence of N-glycosylation impairs gH function during productive viral replication.

The most striking differences between the investigated virus mutants were observed in direct cell-to-cell spread, and the results from plaque assays generally paralleled the findings from transient-transfection fusion assays (Fig. 5). Whereas

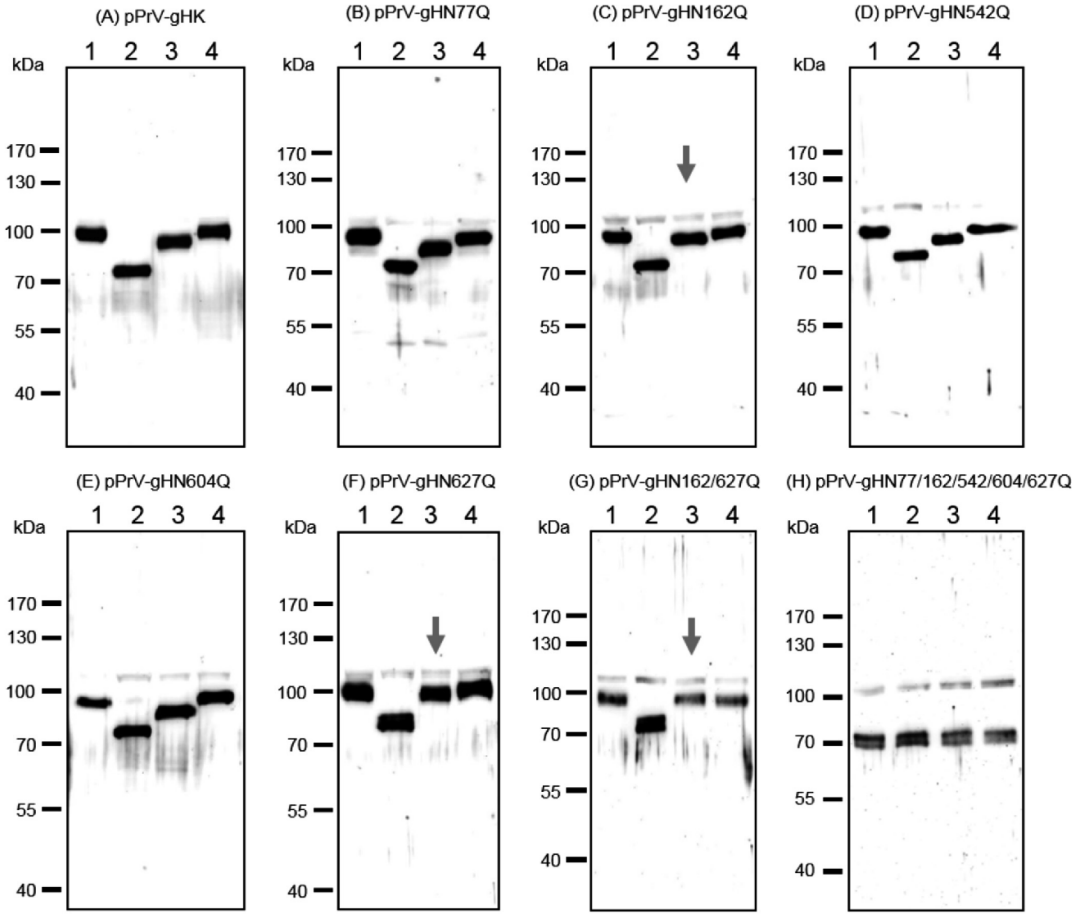

FIG 7 Analysis of N-linked carbohydrates in gH. Purified virion proteins of the indicated PrV recombinants were either left untreated (lanes 1), digested with PNGase F (lanes 2) or endo H (lanes 3), or incubated with reaction buffer without enzymes (lanes 4). Samples were separated by SDS-PAGE, and blots were tested with a gH-specific rabbit antiserum. Molecular masses of marker proteins are indicated. Arrows indicate gH mutants exhibiting reduced or no endo H sensitivity.

plaque sizes of pPrV-gHN162Q and pPrV-gHN542Q were similar to those of WT gH-expressing pPrV-gHK, plaque areas of pPrV-gHN604Q were significantly enlarged to 135% (Fig. 10). In contrast, pPrV-gHN77Q (65%) and pPrV-gHN627Q (45%) formed significantly smaller plaques than wild-type virus. Deletion of multiple glycosylation sites further reduced plaque sizes, and the quintuple mutant pPrV-gHN77/162/542/604/627Q formed only very tiny plaques reaching 20% of the pPrV-gHK size (Fig. 10).

In summary, the results indicate that the N-glycosylation of the partially conserved site at position 77, positioned in the gL binding domain, and of the highly conserved site at position 627, located within the hydrophobic patch in domain IV, is important but not absolutely required for gH function during virus entry and cell-to-cell spread. In contrast, deletion of the PrV-specific glycosylation site at gH position 604 seems to be beneficial for virus spread in cell culture, like for *in vitro* membrane fusion.

DISCUSSION

N-linked glycosylation of envelope glycoproteins of a variety of viruses, such as, e.g., gB from HSV-2 (41), has been shown to play an important role in viral infection.

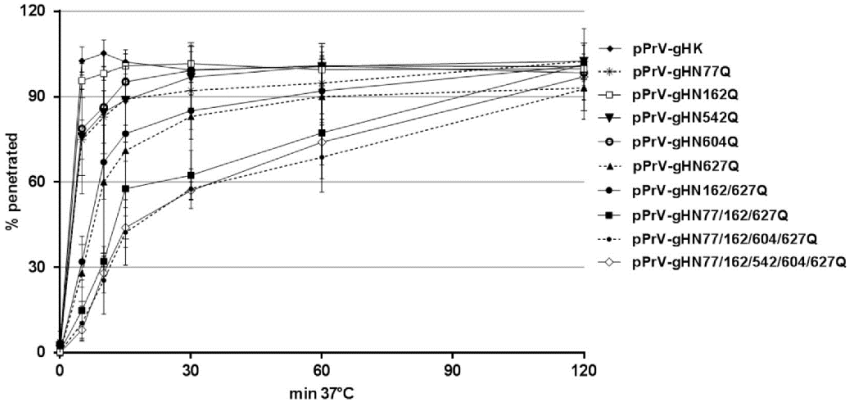

FIG 8 Penetration kinetics of PrV gH mutants. RK13 cells grown in 6-well plates were infected with approximately 250 PFU/well of pPrV-gHK or the different gH mutants. After adsorption at 4°C, the cells were incubated for 0, 5, 10, 15, 30, 60, and 120 min at 37°C, followed by acid inactivation of nonpenetrated virus. After 48 h at 37°C under semisolid medium, plaques were counted and compared to plaque numbers found without inactivation. Mean percentages from three independent experiments and corresponding standard deviations are shown.

However, little is known about the role of N-linked glycosylation in the function of herpesvirus gH. In the present study, we investigated the role of N-linked glycosylation of the alphaherpesvirus PrV gH for its function during entry and spread. To this end, the five predicted N-glycosylation sites in PrV gH (N77, N162, N542, N604, and N627) (Fig. 1) were inactivated singly or in combination by introduction of conservative amino acid substitutions (N→Q). The effect of the mutations on protein expression, maturation, virion incorporation, and, in particular, function in membrane fusion was investigated.

Western blot analysis of purified virions showed that the apparent molecular masses of all mutated gH variants were lower than that of wild type, demonstrating that the five potential glycosylation sites are indeed modified by N-glycans in PrV gH. Furthermore, gH of a quintuple mutant was no longer sensitive to N-glycosidases (Fig. 7H) and showed a molecular mass as predicted for the nonglycosylated precursor protein. This demonstrates that no other (e.g., O-linked) glycans are present in gH, which is in line

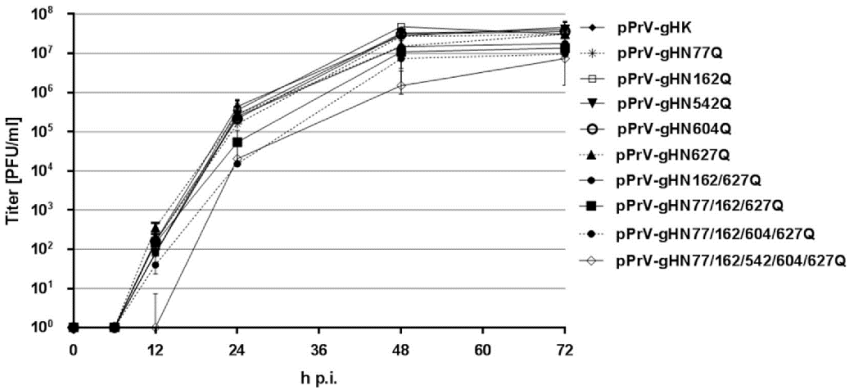

FIG 9 *In vitro* growth kinetics of PrV gH mutants. RK13 cells were infected with pPrV-gHK or the different gH mutants at an MOI of 0.01. Cells and supernatants were harvested after 0, 6, 12, 24, 48, and 72 h at 37°C and lysed by freeze-thawing. Progeny virus titers were determined on RK13 cells. Shown are mean values from four independent experiments and corresponding standard deviations.

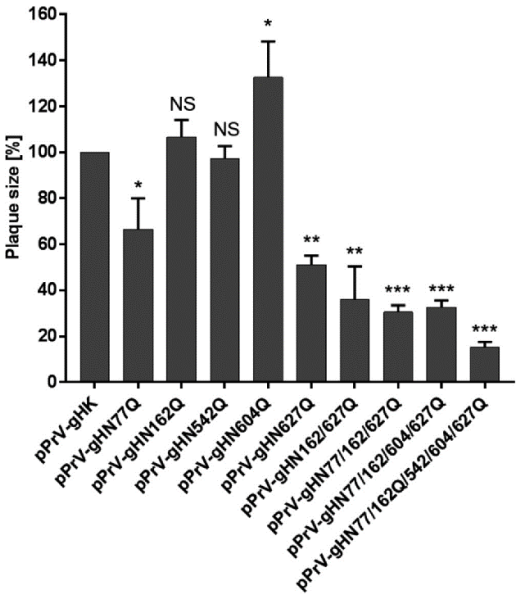

FIG 10 Plaque sizes of PrV gH mutants. RK13 cells were infected with the indicated PrV recombinants and subsequently incubated under plaque assay conditions. After 48 h, areas of 30 plaques per virus were measured. Plaque areas of wild-type gH-expressing pPrV-gHK were set as 100%. Mean values and standard deviations from four independent experiments are shown. Results significantly differing from those obtained with pPrV-gHK are marked (*, $P \leq 0.05$; **, $P \leq 0.01$, ***, $P \leq 0.001$). NS, not significant.

with previous results (49). Only two of the sites (N162 and N627) were found to be glycosylated in the crystallized gH core fragment, because they were either absent from the analyzed protein (N77) or located in insufficiently resolved parts of the determined structure (N542 and N604) (20). Interestingly, the five single mutants exhibited apparent molecular masses that were different from each other (Fig. 7A to F), which could be due to differences between the oligosaccharide chains attached to the individual N-glycosylation sites. It has been reported that other glycoproteins containing more than one N-X-T/S sequon per molecule are also often heterogeneous with respect to their content of complex N-glycans on different sequons (53, 54). It is conceivable that the glycans attached to the different glycosylation sites in gH are site specific and that the observed N-glycan diversity is caused by the surrounding amino acid sequence or conformation affecting substrate availability for Golgi glycosidases or glycosyltransferases (53).

Previous studies revealed that mature PrV gH, as found in virions, is still sensitive to endo H digestion, indicating that N-linked carbohydrates on gH are not completely processed to complex structures in the Golgi apparatus (49). Here, we show that only the two glycosylation sites at N162 and N627 carry high-mannose sugars. N162 is located in gH domain II (Fig. 1) and is part of the "fence," a sheet of antiparallel beta-chains. The side of the fence which includes glycan N162 displays only polar residues (20). In HSV-2 gH, which contains no equivalent glycosylation site, the corresponding side of the fence is partly covered by gL, which was not crystallized with the PrV gH core fragment (7, 20). Thus, N162 in PrV gH may also be covered by gL, which limits accessibility for glycosidases or glycosyltransferases in the Golgi apparatus, leading to incomplete modification of this glycosylation site and endo H sensitivity. This is in line with previous data showing that the carbohydrates incorporated into gH of PrV-ΔgL virions are completely endo H resistant (25).

The N-glycosylation site at aa 627 in PrV gH is located within a highly conserved hydrophobic patch which is covered by a negatively charged surface loop, designated the "flap" (20). Therefore, it is conceivable that the flap might interfere with glycosylation at position N627, leading to endo H sensitivity of the respective glycans in mature gH.

N-glycans on other entry glycoproteins, such as, e.g., gB from HSV-2, were shown to be important for correct intracellular trafficking and maturation (41). N-glycans on HSV-1 gD were found to be critical for the formation and maintenance of the gD structure. However, in contrast to what was observed for gB, no effect on protein processing or trafficking could be observed for HSV-1 gD N-glycosylation site mutants. Moreover, none of the investigated N-glycans on HSV-1 gD were required for gD function during entry and spread (46–48).

In PrV gH, the introduced N-glycosylation site mutations had no effect on expression level, and the subcellular localization of most single mutants was similar to that of wild-type gH. However, inactivation of the highly conserved N627 greatly affected efficient transport, resulting in ER retention and reduced cell surface expression as demonstrated by colocalization of gHN627Q with an ER marker as well as by IIF and FACS analysis of nonpermeabilized cells cotransfected with gH and gL expression plasmids (Fig. 2 to 4). Moreover, in transient-transfection assays no fusion activity could be observed for gH N627 mutants in combination with wild-type gB, gD, and gL (Fig. 5A), and surface expression of mutant gH was still barely detectable (data not shown). This indicates that none of the entry glycoproteins is able to assist gHN627Q in efficient trafficking to the cell surface. However, in contrast to the results of fusion assays conducted with wild-type gB, gHN627Q exhibited moderate fusion activity with hyperfusogenic gB-008 (Fig. 5B), as reported earlier (33). Thus, due to the enhanced surface expression of the C-terminally truncated gB-008 (52), smaller amounts of gH might be sufficient to trigger membrane fusion.

Although a great majority of gHN627Q seemed to be retained in the ER of transfected cells, Western blot analysis of corresponding PrV recombinants demonstrated that gHN627Q, as well as multiplex mutants including this amino acid substitution, is efficiently incorporated into virus particles (Fig. 6A). Thus, intracellular transport of gH during virus infection may differ from the situation after plasmid transfection, e.g., due to concomitant transport of other membrane proteins to the secondary envelopment site in the trans-Golgi network (55). For HSV and EBV it was shown that gL is critical for correct folding, transport, and virion incorporation of gH (7, 18). However, in PrV, gL is not required for these processes (21–27), and other protein interactions involved in gH transport remain to be analyzed.

As demonstrated by *in vitro* replication studies, none of the introduced single or multiple glycosylation site mutations abolished gH function in the viral context (Fig. 8 to 10). Most PrV recombinants reached maximum titers similar to those of wild-type PrV, and only the multiple mutants exhibited 5- to 10-fold reductions in final titers and a slight delay in replication kinetics (Fig. 9). Whereas formation of infectious progeny was barely affected, cell-to-cell spread of several of the PrV mutants was significantly impaired (Fig. 10). Plaque sizes of PrV-gHN77Q and PrV-gHN627Q were reduced by approximately 30% and 50%, respectively, while plaque sizes of the triple, quadruple, and quintuple mutants including both amino acid substitutions were further reduced by 70% to 85% compared to that of wild-type PrV. Consistently, mutations N77Q and N627Q led to reduced fusion activity in transfected cells, and simultaneous removal of both sites decreased fusion activity even further (Fig. 5B). N77 is located in the structurally uncharacterized gH domain I, which is important for binding of gL (30). Removal of the carbohydrates from this site might affect optimal interaction of gH with gL and thus interfere with efficient membrane fusion. However, Western blot analysis of purified pPrV-gHN77Q virions showed that gL was efficiently incorporated into particles (Fig. 6A), demonstrating that gH/gL binding *per se* is not disturbed.

N627 is located within a highly conserved hydrophobic patch of domain IV which

was suggested to play a role in membrane fusion by temporally regulated interaction with the viral envelope (20, 33). In line with our previous results (33), N-glycosylation of gH at position 627 was found to be important, although not essential, for PrV-mediated membrane fusion. The homologous glycosylation site in HSV-1 gH was also shown to be nonessential for its function (56). Thus, in the absence of the carbohydrates, the underlying hydrophobic patch might still be sufficiently masked by the charged "flap" to prevent its premature movement into the membrane. However, as outlined above, inactivation of the glycosylation site at position N627 severely affected gH transport and surface expression, which might also contribute to the observed spreading defects of the virus mutants. However, we cannot completely exclude that the mutation of the amino acid rather than the absence of the glycan is relevant for the observed phenotype.

Whereas mutations N77Q and N627Q led to a decrease in plaque sizes, an increase in plaque size by 30% was observed after substitution of N604, and, consistent with this, the *in vitro* fusion activity of gHN604Q was enhanced (Fig. 5). The N-glycosylation site N604 is located in gH domain IV (Fig. 1) and is conserved between members of the *Varicellovirus* genus, whereas members of the *Simplexvirus* genus lack a corresponding site (20). Previous studies using chimeric proteins consisting of domains of PrV and the simplexvirus HSV-1 gH demonstrated functional conservation of domain IV and indicated species-specific interactions of this domain with gB (34). Possibly, the absence of the carbohydrate at aa 604 positively influences this interaction between gH and gB, resulting in the observed phenotype.

In line with the observed defects in cell-to-cell spread and *in vitro* fusion activity, penetration of the triple, quadruple, and quintuple PrV mutants was significantly delayed (Fig. 8). pPrV-gHN627Q showed a less pronounced but also significant lag in penetration, whereas penetration of the single mutants with substitutions of N77, N162, N542, and N604 was not or only marginally affected. Although gHN604Q resulted in a significantly increased fusogenicity and plaque size, it exhibited a slight delay in penetration, again indicating that the mechanisms of membrane fusion during entry of free virus particles and direct viral cell-to-cell spread are similar but not identical. This is also highlighted by the different protein requirements for the two membrane fusion events. Whereas PrV gD is dispensable for plaque formation, it is required for entry, functionally separating the two events (50, 57, 58).

In summary, our results demonstrate that all five predicted N-glycosylation sites in PrV gH are modified by N-glycans, which play a modulating role in proper localization and function of PrV gH during membrane fusion. However, even simultaneous inactivation of all five sites did not severely inhibit formation of infectious virus particles, demonstrating that modification of gH by N-glycans is not necessary for efficient PrV replication. Although *in vitro* replication of the mutants was not severely affected, the relevance of the N-glycosylation sites *in vivo* remains to be determined. N-linked glycosylation of viral proteins expressed on the surface of virions may interfere with the host antibody response (59). For influenza and human immunodeficiency viruses, it is well documented that glycan modifications can serve as a "shield" which covers essential viral epitopes, thereby protecting the viruses from antibody-mediated neutralization (60, 61). The same might apply to PrV gH, but we cannot exclude that the N-glycans in PrV gH represent parts of epitopes, which can be targeted by neutralizing antibodies.

MATERIALS AND METHODS

Cells and viruses. Rabbit kidney (RK13) cells were grown in Eagle's minimum essential medium (MEM) supplemented with 10% fetal bovine serum (FBS) at 37°C and 5% CO_2. The viruses described in this study were derived from pPrV-ΔgHABF (31), which is a gH deletion mutant of PrV strain Kaplan (PrV-Ka) cloned as a bacterial artificial chromosome (BAC) (33). The gH-rescued viruses were propagated on RK13 cells, while pPrV-ΔgHABF was cultivated on RK13-gH/gL (62).

Mutagenesis of the cloned gH gene and generation of PrV N-glycosylation mutants. The expression plasmid pcDNA-gHKDE (31) containing the gH ORF (UL22) of PrV-Ka was used for site-directed mutagenesis (QuikChange II XL kit; Agilent). The oligonucleotide primers used for mutagenesis leading to inactivation of the potential N-glycosylation sites are indicated in Table 1. The resulting expression

TABLE 1 Oligonucleotide primers for mutagenesis, PCR, and sequence analyses[a]

Primer name	Sequence (5′ to 3′)[b]	Nucleotide positions[c]
PGHN77Q-F	CTGGGGGCGCTC**CAG**GACACGCGCATC	60986–61012
PGHN162Q-F	GCGGCCGTCTTC**CA**G**G**TGACGCTGGGC	61241–61267
PGHN542Q-F	GCCATCGTCAGC**CAG**GACAGCGCCGCG	62381–62407
PGHN604Q-F	CATGGCCGGCGCC**CA**G**T**CCACCATCCC	62566–62592
PGHN627Q-F	TGATGCTCTTCCCC**CAA**GGCACCGTGGTC	62634–62662
PgH-PSF	TTCACGTCGGAGATGGGG	60611–60628
PgH-PSF2	GGAAGCCCTTCGACCAG	61875–61891
PgHK-PSR	CGCGAGCCCATTTATACCC	(Kan^r)
PgH-PSR2	GTCGAGCAGGCTGAAGG	62055–62071 (r)
PgH-WH3	TGCACGAGAGCGACGACTACC	61479–61499

[a]Only forward-strand mutagenesis primers (F) are listed, since the reverse-strand primers were exactly complementary.

[b]Nonmatching nucleotides are shown in boldface.

[c]Nucleotide positions in the PrV-Ka genome refer to GenBank accession number JQ809328 (66), and a reverse-strand sequencing primer is indicated (r). PgHK-PSR binds to the inserted kanamycin resistance gene (Kan^r) of the PrV recombinants.

plasmids were digested with DrdI, and a 3,461-bp fragment containing the modified gH gene together with a downstream kanamycin resistance (Kan^r) gene was purified from an agarose gel and used for Red-mediated mutagenesis of pPrV-ΔgH in *E. coli* as described previously (30, 31, 33). Desired BAC recombinants were selected on LB agar plates supplemented with kanamycin (50 μg/ml) and chloramphenicol (30 μg/ml). DNA was prepared from overnight liquid cultures of single bacterial colonies by alkaline lysis, phenol-chloroform extraction, isopropanol precipitation, and RNase treatment. BAC DNA was used for transfection (FuGene HD transfection reagent; Promega) of RK13 cells, and progeny virus isolated from single plaques was propagated and characterized. Correct mutagenesis and recombination were verified by sequencing using the primers listed in Table 1, the BigDye Terminator v1.1 cycle sequencing kit, and a 3130 genetic analyzer (Applied Biosystems).

IIF analysis. For IIF analyses, RK13 cell monolayers grown in 24-well plates were cotransfected with 200 ng of wild-type or mutant gH and gL expression plasmids in 50 μl Opti-MEM using 1 μl Lipofectamine 2000 (Thermo Fisher Scientific). For colocalization studies, cells were additionally transfected with 200 μl of the ER marker pmTurquoise2ER (Addgene). The transfection mixture was incubated for 20 min at room temperature and added to the cells. After 3 h at 37°C, the cells were washed with phosphate-buffered saline (PBS) and incubated in MEM supplemented with 2% FBS for another 24 h at 37°C. The cells were fixed with 3% paraformaldehyde (PFA) in PBS for 20 min and, optionally, permeabilized in PBS containing 0.1% Triton X-100 for 10 min at room temperature. Afterwards, cells were washed with PBS, blocked with 0.25% fat-free powdered milk in PBS, and incubated with the rabbit antiserum specific for PrV gH (28) at a dilution of 1:200 in PBS. After 1 h at room temperature, bound antibody was detected with Alexa 488- or 633-conjugated goat anti-rabbit antibodies (Invitrogen) at a dilution of 1:1,000 in PBS. After each step, cells were washed repeatedly with PBS. Green fluorescence was excited at 488 nm and red fluorescence at 633 nm, and the cells were analyzed with an Eclipse Ti-S fluorescence microscope (Nikon) or with a laser scanning confocal microscope (SP5; Leica, Mannheim, Germany).

Flow cytometry. RK13 cells cotransfected with gH and gL expression plasmids were detached after 24 h with 2 mM EDTA in PBS for 1 h at 4°C. Thereafter, cells were fixed with 4% PFA for 20 min at 4°C and subsequently washed with PBS supplemented with 2% bovine serum albumin (BSA) and 2 mM EDTA. Each sample was split into two FACS tubes. One aliquot was permeabilized with 0.5% saponin in PBS with 0.2% BSA for 30 min at 4°C, while the second was incubated without saponin. Cells were probed with the monoclonal antibody 13c2 directed against gH (28) at a dilution of 1:5 in PBS with 2% BSA for 1 h at 4°C. After a washing step with 2 mM EDTA in PBS, cells were incubated for 1 h at 4°C with a secondary antibody (Alexa Fluor 488, goat anti-mouse IgG; Invitrogen) at a dilution of 1:1,000 in PBS with 2% BSA. Samples were analyzed using a MACSQuant analyzer (Miltenyi Biotec). Surface expression of gH was quantified as follows: percent fluorescein isothiocyanate (FITC)-positive, nonpermeabilized cells/percent FITC-positive permeabilized cells × 100. Mean values and standard deviations from three independent assays were determined.

Western blot analyses. RK13 cells were harvested 2 days after PrV infection at an MOI of 2, and virions were purified from culture supernatants as described previously (25). Protein samples (5 μg protein per lane) were separated by discontinuous sodium dodecyl sulfate-polyacrylamide gel electrophoresis (SDS-PAGE), transferred to nitrocellulose membranes, and incubated with antibodies (63). Monospecific rabbit antisera against PrV gD (62), gH (28), and gL (25) were used at a dilution of 1:1,000 (gL) or 1:10,000 (gD and gH).

Enzymatic deglycosylation. Purified PrV particles were incubated in 1% SDS and 10% β-mercaptoethanol for 10 min at 100°C. The pretreated purified virion preparations (15 μg each) were digested either with 500 U of endo H to remove high-mannose or hybrid forms of N-linked glycans, with 500 U of PNGase F to remove all N-linked glycans, or without enzymes for 2 h at 37°C under buffer conditions according to the manufacturer's (New England BioLabs) instructions. After digestion, samples (5 μg/lane) were separated by SDS-PAGE and analyzed by Western blotting.

***In vitro* fusion assays.** The fusogenic properties of the gH mutants were analyzed using a transient-transfection-based cell fusion assay (30, 51). Briefly, approximately 3×10^5 RK13 cells per well were seeded onto 12-well cell culture plates and after 20 h at 37°C transfected with 400 ng each of expression plasmids for EGFP (pEGFP-N1; Clontech) and PrV-Ka glycoproteins gB (or C-terminally truncated gB-008), gD, gL, and wild-type or mutagenized gH (29, 31, 50, 52) in 100 μl Opti-MEM using 2 μl Lipofectamine 2000 as described above. The empty expression vector (pcDNA3; Thermo Fisher Scientific) served as a negative control. After 24 h at 37°C, the cells were washed with PBS and fixed with 3% PFA for 20 min. An Eclipse Ti-S fluorescence microscope and the NIS-Elements imaging software (Nikon) were used to analyze syncytium formation. Total fusion activity was determined by multiplication of the area of syncytia with three or more nuclei by the number of syncytia counted within 10 fields of view (5.5 mm^2 each). Mean values and standard deviations from four independent assays were determined.

***In vitro* replication studies.** For analysis of growth kinetics, confluent monolayers of RK13 cells in 96-well plates were infected with the wild-type gH revertant pPrV-gHK (31) or the different PrV gH mutants at an MOI of 0.01 and were subsequently incubated for 1 h on ice to permit virus adsorption. After 2 h at 37°C, the inoculum was removed and nonpenetrated virus was inactivated by low-pH treatment (64). The cells were then washed with PBS, and fresh medium was added. Immediately thereafter and after 6, 12, 24, 48, and 72 h at 37°C, cells were harvested together with the supernatants and lysed by freeze-thawing (−70°C and 37°C). Progeny virus titers were determined by plaque assays on RK13 cells. After 48 h at 37°C under semisolid medium containing 6 g/liter methylcellulose, areas of 30 plaques were measured microscopically, and percentages of wild-type (pPrV-gHK) sizes were calculated. Mean results and standard deviations from four independent growth kinetic studies and comparative plaque assays were determined.

***In vitro* penetration kinetics.** For determination of penetration kinetics, confluent monolayers of RK13 cells in in 6-well plates were infected on ice with approximately 250 PFU of PrV-gHK or the different PrV gH mutants. After 1 h, the inoculum was replaced by prewarmed MEM supplemented with 5% FBS, and cells were incubated at 37°C. Before and 5, 10, 15, 30, 60, and 120 min after the temperature shift, remaining extracellular virus particles were inactivated by low-pH treatment. Cells were washed two times with PBS and overlaid with semisolid medium containing 6 g/liter methylcellulose. For 100% penetration controls, infected cells were washed with PBS only after 2 h at 37°C and overlaid with semisolid medium. After 48 h at 37°C, plaques were counted, and the penetration rate was calculated by comparison with corresponding controls. The experiment was repeated four times, and mean values and standard deviations were determined.

Statistical analyses. The statistical significance of differences observed in FACS analyses, transient fusion assays, and *in vitro* replication studies was evaluated using an unpaired *t* test with Welch correction provided by GraphPad Prism 7 software (GraphPad Software, Inc., San Diego, CA).

ACKNOWLEDGMENTS

These studies were supported by the Deutsche Forschungsgemeinschaft (DFG grant Me 854/11-2). Molecular graphics were obtained with the UCSF Chimera package; Chimera is developed by the Resource for Biocomputing, Visualization, and Informatics at the University of California, San Francisco, supported by the National Institutes of Health (NIGMS P41-GM103311).

We thank B. Wanner for providing plasmids for BAC mutagenesis and G. Strebelow for performing sequence analyses. The technical assistance of A. Landmesser and K. Biebl is greatly appreciated.

REFERENCES

1. Harrison SC. 2015. Viral membrane fusion. Virology 479-480:498–507. https://doi.org/10.1016/j.virol.2015.03.043.
2. Eisenberg RJ, Atanasiu D, Cairns TM, Gallagher JR, Krummenacher C, Cohen GH. 2012. Herpes virus fusion and entry: a story with many characters. Viruses 4:800–832. https://doi.org/10.3390/v4050800.
3. Di Giovine P, Settembre EC, Bhargava AK, Luftig MA, Lou H, Cohen GH, Eisenberg RJ, Krummenacher C, Carfi A. 2011. Structure of herpes simplex virus glycoprotein D bound to the human receptor nectin-1. PLoS Pathog 7:e1002277. https://doi.org/10.1371/journal.ppat.1002277.
4. Lazear E, Whitbeck JC, Zuo Y, Carfi A, Cohen GH, Eisenberg RJ, Krummenacher C. 2014. Induction of conformational changes at the N-terminus of herpes simplex virus glycoprotein D upon binding to HVEM and nectin-1. Virology 448:185–195. https://doi.org/10.1016/j.virol.2013.10.019.
5. Atanasiu D, Saw WT, Cohen GH, Eisenberg RJ. 2010. Cascade of events governing cell-cell fusion induced by herpes simplex virus glycoproteins gD, gH/gL, and gB. J Virol 84:12292–12299. https://doi.org/10.1128/JVI.01700-10.
6. Gianni T, Amasio M, Campadelli-Fiume G. 2009. Herpes simplex virus gD forms distinct complexes with fusion executors gB and gH/gL in part through the C-terminal profusion domain. J Biol Chem 284:17370–17382. https://doi.org/10.1074/jbc.M109.005728.
7. Chowdary TK, Cairns TM, Atanasiu D, Cohen GH, Eisenberg RJ, Heldwein EE. 2010. Crystal structure of the conserved herpesvirus fusion regulator complex gH-gL. Nat Struct Mol Biol 17:882–888. https://doi.org/10.1038/nsmb.1837.
8. Cooper RS, Heldwein EE. 2015. Herpesvirus gB: a finely tuned fusion machine. Viruses 7:6552–6569. https://doi.org/10.3390/v7122957.
9. Atanasiu D, Whitbeck JC, de Leon MP, Lou H, Hannah BP, Cohen GH, Eisenberg RJ. 2010. Bimolecular complementation defines functional regions of herpes simplex virus gB that are involved with gH/gL as a necessary step leading to cell fusion. J Virol 84:3825–3834. https://doi.org/10.1128/JVI.02687-09.
10. Vallbracht M, Brun D, Tassinari M, Vaney MC, Pehau-Arnaudet G, Guardado-Calvo P, Haouz A, Klupp BG, Mettenleiter TC, Rey FA, Backovic M. 18 October 2017. Structure-function dissection of the pseudorabies virus glycoprotein B fusion loops. J Virol https://doi.org/10.1128/JVI.01203-17.
11. Li X, Yang F, Hu X, Tan F, Qi J, Peng R, Wang M, Chai Y, Hao L, Deng J, Bai C, Wang J, Song H, Tan S, Lu G, Gao GF, Shi Y, Tian K. 2017. Two

classes of protective antibodies against pseudorabies virus variant glycoprotein B: implications for vaccine design. PLoS Pathog 13:e1006777. https://doi.org/10.1371/journal.ppat.1006777.
12. Heldwein EE, Lou H, Bender FC, Cohen GH, Eisenberg RJ, Harrison SC. 2006. Crystal structure of glycoprotein B from herpes simplex virus 1. Science 313:217–220. https://doi.org/10.1126/science.1126548.
13. Chandramouli S, Ciferri C, Nikitin PA, Calo S, Gerrein R, Balabanis K, Monroe J, Hebner C, Lilja AE, Settembre EC, Carfi A. 2015. Structure of HCMV glycoprotein B in the postfusion conformation bound to a neutralizing human antibody. Nat Commun 6:8176. https://doi.org/10.1038/ncomms9176.
14. Burke HG, Heldwein EE. 2015. Crystal structure of the human cytomegalovirus glycoprotein B. PLoS Pathog 11:e1005227. https://doi.org/10.1371/journal.ppat.1005227.
15. Backovic M, Longnecker R, Jardetzky TS. 2009. Structure of a trimeric variant of the Epstein-Barr virus glycoprotein B. Proc Natl Acad Sci U S A 106:2880–2885. https://doi.org/10.1073/pnas.0810530106.
16. Roche S, Bressanelli S, Rey FA, Gaudin Y. 2006. Crystal structure of the low-pH form of the vesicular stomatitis virus glycoprotein G. Science 313:187–191. https://doi.org/10.1126/science.1127683.
17. Kadlec J, Loureiro S, Abrescia NG, Stuart DI, Jones IM. 2008. The postfusion structure of baculovirus gp64 supports a unified view of viral fusion machines. Nat Struct Mol Biol 15:1024–1030. https://doi.org/10.1038/nsmb.1484.
18. Matsuura H, Kirschner AN, Longnecker R, Jardetzky TS. 2010. Crystal structure of the Epstein-Barr virus (EBV) glycoprotein H/glycoprotein L (gH/gL) complex. Proc Natl Acad Sci U S A 107:22641–22646. https://doi.org/10.1073/pnas.1011806108.
19. Xing Y, Oliver SL, Nguyen T, Ciferri C, Nandi A, Hickman J, Giovani C, Yang E, Palladino G, Grose C, Uematsu Y, Lilja AE, Arvin AM, Carfi A. 2015. A site of varicella-zoster virus vulnerability identified by structural studies of neutralizing antibodies bound to the glycoprotein complex gHgL. Proc Natl Acad Sci U S A 112:6056–6061. https://doi.org/10.1073/pnas.1501176112.
20. Backovic M, DuBois RM, Cockburn JJ, Sharff AJ, Vaney MC, Granzow H, Klupp BG, Bricogne G, Mettenleiter TC, Rey FA. 2010. Structure of a core fragment of glycoprotein H from pseudorabies virus in complex with antibody. Proc Natl Acad Sci U S A 107:22635–22640. https://doi.org/10.1073/pnas.1011507107.
21. Hutchinson L, Browne H, Wargent V, Davis-Poynter N, Primorac S, Goldsmith K, Minson AC, Johnson DC. 1992. A novel herpes simplex virus glycoprotein, gL, forms a complex with glycoprotein H (gH) and affects normal folding and surface expression of gH. J Virol 66:2240–2250.
22. Kaye JF, Gompels UA, Minson AC. 1992. Glycoprotein H of human cytomegalovirus (HCMV) forms a stable complex with the HCMV UL115 gene product. J Gen Virol 73:2693–2698. https://doi.org/10.1099/0022-1317-73-10-2693.
23. Klupp BG, Baumeister J, Karger A, Visser N, Mettenleiter TC. 1994. Identification and characterization of a novel structural glycoprotein in pseudorabies virus, gL. J Virol 68:3868–3878.
24. Liu DX, Gompels UA, Nicholas J, Lelliott C. 1993. Identification and expression of the human herpesvirus 6 glycoprotein H and interaction with an accessory 40K glycoprotein. J Gen Virol 74:1847–1857. https://doi.org/10.1099/0022-1317-74-9-1847.
25. Klupp BG, Fuchs W, Weiland E, Mettenleiter TC. 1997. Pseudorabies virus glycoprotein L is necessary for virus infectivity but dispensable for virion localization of glycoprotein H. J Virol 71:7687–7695.
26. Lete C, Machiels B, Stevenson PG, Vanderplasschen A, Gillet L. 2012. Bovine herpesvirus type 4 glycoprotein L is nonessential for infectivity but triggers virion endocytosis during entry. J Virol 86:2653–2664. https://doi.org/10.1128/JVI.06238-11.
27. Gillet L, May JS, Colaco S, Stevenson PG. 2007. Glycoprotein L disruption reveals two functional forms of the murine gammaherpesvirus 68 glycoprotein H. J Virol 81:280–291. https://doi.org/10.1128/JVI.01616-06.
28. Klupp BG, Mettenleiter TC. 1999. Glycoprotein gL-independent infectivity of pseudorabies virus is mediated by a gD-gH fusion protein. J Virol 73:3014–3022.
29. Schröter C, Vallbracht M, Altenschmidt J, Kargoll S, Fuchs W, Klupp BG, Mettenleiter TC. 2015. Mutations in pseudorabies virus glycoproteins gB, gD, and gH functionally compensate for the absence of gL. J Virol 90:2264–2272. https://doi.org/10.1128/JVI.02739-15.
30. Vallbracht M, Rehwaldt S, Klupp BG, Mettenleiter TC, Fuchs W. 2017. Functional relevance of the N-terminal domain of pseudorabies virus envelope glycoprotein H and its interaction with glycoprotein L. J Virol 91:e00061-17. https://doi.org/10.1128/JVI.00061-17.
31. Böhm SW, Eckroth E, Backovic M, Klupp BG, Rey FA, Mettenleiter TC, Fuchs W. 2015. Structure-based functional analyses of domains II and III of pseudorabies virus glycoprotein H. J Virol 89:1364–1376. https://doi.org/10.1128/JVI.02765-14.
32. Schröter C, Klupp BG, Fuchs W, Gerhard M, Backovic M, Rey FA, Mettenleiter TC. 2014. The highly conserved proline at position 438 in pseudorabies virus gH is important for regulation of membrane fusion. J Virol 88:13064–13072. https://doi.org/10.1128/JVI.01204-14.
33. Fuchs W, Backovic M, Klupp BG, Rey FA, Mettenleiter TC. 2012. Structure-based mutational analysis of the highly conserved domain IV of glycoprotein H of pseudorabies virus. J Virol 86:8002–8013. https://doi.org/10.1128/JVI.00690-12.
34. Böhm SW, Backovic M, Klupp BG, Rey FA, Mettenleiter TC, Fuchs W. 2016. Functional characterization of glycoprotein H chimeras composed of conserved domains of the pseudorabies virus and herpes simplex virus 1 homologs. J Virol 90:421–432. https://doi.org/10.1128/JVI.01985-15.
35. Cherepanova N, Shrimal S, Gilmore R. 2016. N-linked glycosylation and homeostasis of the endoplasmic reticulum. Curr Opin Cell Biol 41:57–65. https://doi.org/10.1016/j.ceb.2016.03.021.
36. Kornfeld R, Kornfeld S. 1985. Assembly of asparagine-linked oligosaccharides. Annu Rev Biochem 54:631–664. https://doi.org/10.1146/annurev.bi.54.070185.003215.
37. Maley F, Trimble RB, Tarentino AL, Plummer TH, Jr. 1989. Characterization of glycoproteins and their associated oligosaccharides through the use of endoglycosidases. Anal Biochem 180:195–204. https://doi.org/10.1016/0003-2697(89)90115-2.
38. Helenius A, Aebi M. 2004. Roles of N-linked glycans in the endoplasmic reticulum. Annu Rev Biochem 73:1019–1049. https://doi.org/10.1146/annurev.biochem.73.011303.073752.
39. Helle F, Vieyres G, Elkrief L, Popescu CI, Wychowski C, Descamps V, Castelain S, Roingeard P, Duverlie G, Dubuisson J. 2010. Role of N-linked glycans in the functions of hepatitis C virus envelope proteins incorporated into infectious virions. J Virol 84:11905–11915. https://doi.org/10.1128/JVI.01548-10.
40. Lennemann NJ, Walkner M, Berkebile AR, Patel N, Maury W. 2015. The role of conserved N-linked glycans on Ebola virus glycoprotein 2. J Infect Dis 212(Suppl 2):S204–S209. https://doi.org/10.1093/infdis/jiv201.
41. Luo S, Hu K, He S, Wang P, Zhang M, Huang X, Du T, Zheng C, Liu Y, Hu Q. 2015. Contribution of N-linked glycans on HSV-2 gB to cell-cell fusion and viral entry. Virology 483:72–82. https://doi.org/10.1016/j.virol.2015.04.005.
42. Kobayashi Y, Suzuki Y. 2012. Evidence for N-glycan shielding of antigenic sites during evolution of human influenza A virus hemagglutinin. J Virol 86:3446–3451. https://doi.org/10.1128/JVI.06147-11.
43. McDonald TP, Jeffree CE, Li P, Rixon HW, Brown G, Aitken JD, MacLellan K, Sugrue RJ. 2006. Evidence that maturation of the N-linked glycans of the respiratory syncytial virus (RSV) glycoproteins is required for virus-mediated cell fusion: the effect of alpha-mannosidase inhibitors on RSV infectivity. Virology 350:289–301. https://doi.org/10.1016/j.virol.2006.01.023.
44. Annamalai AS, Pattnaik A, Sahoo BR, Muthukrishnan E, Natarajan SK, Steffen D, Vu HLX, Delhon G, Osorio FA, Petro TM, Xiang SH, Pattnaik AK. 20 September 2017. Zika virus encoding nonglycosylated envelope protein is attenuated and defective in neuroinvasion. J Virol https://doi.org/10.1128/JVI.01348-17.
45. Bradel-Tretheway BG, Liu Q, Stone JA, McInally S, Aguilar HC. 2015. Novel functions of Hendra virus G N-glycans and comparisons to Nipah virus. J Virol 89:7235–7247. https://doi.org/10.1128/JVI.00773-15.
46. Sodora DL, Cohen GH, Eisenberg RJ. 1989. Influence of asparagine-linked oligosaccharides on antigenicity, processing, and cell surface expression of herpes simplex virus type 1 glycoprotein D. J Virol 63:5184–5193.
47. Sodora DL, Cohen GH, Muggeridge MI, Eisenberg RJ. 1991. Absence of asparagine-linked oligosaccharides from glycoprotein D of herpes simplex virus type 1 results in a structurally altered but biologically active protein. J Virol 65:4424–4431.
48. Sodora DL, Eisenberg RJ, Cohen GH. 1991. Characterization of a recombinant herpes simplex virus which expresses a glycoprotein D lacking asparagine-linked oligosaccharides. J Virol 65:4432–4441.
49. Klupp BG, Visser N, Mettenleiter TC. 1992. Identification and characterization of pseudorabies virus glycoprotein H. J Virol 66:3048–3055.
50. Klupp BG, Nixdorf R, Mettenleiter TC. 2000. Pseudorabies virus glycopro-

tein M inhibits membrane fusion. J Virol 74:6760–6768. https://doi.org/10.1128/JVI.74.15.6760-6768.2000.
51. Vallbracht M, Schröter C, Klupp BG, Mettenleiter TC. 2017. Transient transfection-based fusion assay for viral proteins. Bio-protocol 7:e2162. https://doi.org/10.21769/BioProtoc.2162.
52. Nixdorf R, Klupp BG, Karger A, Mettenleiter TC. 2000. Effects of truncation of the carboxy terminus of pseudorabies virus glycoprotein B on infectivity. J Virol 74:7137–7145. https://doi.org/10.1128/JVI.74.15.7137-7145.2000.
53. Stanley PSH, Taniguchi N. 2009. N-glycans, essentials of glycobiology. Cold Spring Harbor Laboratory Press, Cold Spring Harbor, NY.
54. Bieberich E. 2014. Synthesis, processing, and function of N-glycans in N-glycoproteins. Adv Neurobiol 9:47–70. https://doi.org/10.1007/978-1-4939-1154-7_3.
55. Mettenleiter TC. 2006. Intriguing interplay between viral proteins during herpesvirus assembly or: the herpesvirus assembly puzzle. Vet Microbiol 113:163–169. https://doi.org/10.1016/j.vetmic.2005.11.040.
56. Galdiero M, Whiteley A, Bruun B, Bell S, Minson T, Browne H. 1997. Site-directed and linker insertion mutagenesis of herpes simplex virus type 1 glycoprotein H. J Virol 71:2163–2170.
57. Rauh I, Mettenleiter TC. 1991. Pseudorabies virus glycoproteins gII and gp50 are essential for virus penetration. J Virol 65:5348–5356.
58. Peeters B, de Wind N, Hooisma M, Wagenaar F, Gielkens A, Moormann R. 1992. Pseudorabies virus envelope glycoproteins gp50 and gII are essential for virus penetration, but only gII is involved in membrane fusion. J Virol 66:894–905.
59. Vigerust DJ, Shepherd VL. 2007. Virus glycosylation: role in virulence and immune interactions. Trends Microbiol 15:211–218. https://doi.org/10.1016/j.tim.2007.03.003.
60. Wanzeck K, Boyd KL, McCullers JA. 2011. Glycan shielding of the influenza virus hemagglutinin contributes to immunopathology in mice. Am J Respir Crit Care Med 183:767–773. https://doi.org/10.1164/rccm.201007-1184OC.
61. Wei X, Decker JM, Wang S, Hui H, Kappes JC, Wu X, Salazar-Gonzalez JF, Salazar MG, Kilby JM, Saag MS, Komarova NL, Nowak MA, Hahn BH, Kwong PD, Shaw GM. 2003. Antibody neutralization and escape by HIV-1. Nature 422:307–312. https://doi.org/10.1038/nature01470.
62. Klupp B, Altenschmidt J, Granzow H, Fuchs W, Mettenleiter TC. 2008. Glycoproteins required for entry are not necessary for egress of pseudorabies virus. J Virol 82:6299–6309. https://doi.org/10.1128/JVI.00386-08.
63. Pavlova SP, Veits J, Keil GM, Mettenleiter TC, Fuchs W. 2009. Protection of chickens against H5N1 highly pathogenic avian influenza virus infection by live vaccination with infectious laryngotracheitis virus recombinants expressing H5 hemagglutinin and N1 neuraminidase. Vaccine 27:773–785. https://doi.org/10.1016/j.vaccine.2008.11.033.
64. Mettenleiter TC. 1989. Glycoprotein gIII deletion mutants of pseudorabies virus are impaired in virus entry. Virology 171:623–625. https://doi.org/10.1016/0042-6822(89)90635-1.
65. Pettersen EF, Goddard TD, Huang CC, Couch GS, Greenblatt DM, Meng EC, Ferrin TE. 2004. UCSF Chimera—a visualization system for exploratory research and analysis. J Comput Chem 25:1605–1612. https://doi.org/10.1002/jcc.20084.
66. Grimm KS, Klupp BG, Granzow H, Muller FM, Fuchs W, Mettenleiter TC. 2012. Analysis of viral and cellular factors influencing herpesvirus-induced nuclear envelope breakdown. J Virol 86:6512–6521. https://doi.org/10.1128/JVI.00068-12.

(VI) Structure-Function Dissection of Pseudorabies Virus Glycoprotein B Fusion Loops

Melina Vallbracht, Delphine Brun, Matteo Tassinari, Marie-Christine Vaney, Gérard Pehau-Arnaudetd, Pablo Guardado-Calvo, Ahmed Haouze, Barbara G. Klupp, Thomas C. Mettenleiter, Felix A. Rey, Marija Backovic

Journal of Virology

Volume 92, Issue 1

January 2018

doi: 10.1128/JVI.01203-17

VI

AMERICAN SOCIETY FOR MICROBIOLOGY | Journal of Virology®

SPOTLIGHT

Articles of Significant Interest Selected from This Issue by the Editors

Insight into Herpesvirus Glycoprotein B Interactions with Membranes

Glycoprotein B (gB) of herpesviruses catalyzes fusion of viral and cellular membranes. Prior to the merger, gB must be inserted into target membranes. Vallbracht et al. (e01203-17) report the X-ray structure of the pseudorabies virus (PrV) gB ectodomain together with structure-directed mutagenesis of its membrane-interacting fusion loops (FLs), suggesting a model of initial interactions between gB and the target membrane. Comparative analyses indicate that the membrane interaction model is valid for other herpesvirus gB proteins, even though the FLs are poorly conserved in sequence and vary significantly in hydrophobicity across the herpesvirus family.

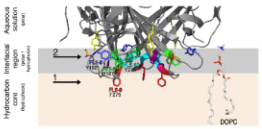

Model for PrV gB fusion loop insertion into membranes.

Rubella Virus Entry Requires Host Cell Membrane Sphingomyelin and Cholesterol

Rubella virus (RuV) causes systemic infection, and transplacental fetal infection induces congenital rubella syndrome. Otsuki et al. (e01130-17) discovered that RuV has two distinct binding mechanisms. One is Ca^{2+}-dependent and the other Ca^{2+}-independent. Ca^{2+}-dependent binding is directed to lipid membranes enriched in sphingomyelin (SM) and cholesterol (Chol) and observed in erythrocytes, liposomes, and most cell lines. Ca^{2+}-dependent binding is required but not sufficient for RuV infection. Ca^{2+}-independent binding is SM/Chol independent and occurs only in adherent nonlymphoid cell lines, which suggests that RuV receptors remain to be identified.

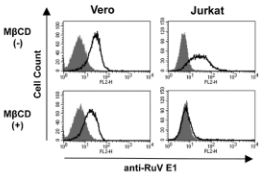

Effects of methyl-β-cyclodextrin on RuV binding to mammalian cell lines.

RNA Sequences Involved in Genome Packaging of Foot-and-Mouth Disease Virus

Genome packaging in the picornavirus family of nonenveloped RNA viruses is not well understood. The picornavirus foot-and-mouth disease virus (FMDV) is a significant pathogen of livestock. Logan et al. (e01159-17) identified multiple sequences in the FMDV genome that are involved in RNA packaging. These sequences are predicted to form conserved stem-loops, and disruption of these features results in reduced assembly of mature virions. This study provides evidence for the involvement of predicted RNA structures in picornavirus packaging and offers a readily transferable methodology for identifying packaging requirements in other viruses.

Predicted RNA stem-loop structures involved in FMDV packaging.

Viperin Diminishes Flavivirus Virulence by Inducing Assembly of Noninfectious Capsid Particles

The antiviral response targets almost every aspect of viral replication. However, little is known about its effects on flavivirus assembly. Vonderstein et al. (e01751-17) discovered that interferon, via the action of viperin, disrupts assembly of tick-borne encephalitis virus (TBEV). Viperin induces release of noninfectious capsid particles by interacting with and inhibiting the function of the cellular protein Golgi brefeldin A-resistant guanine nucleotide exchange factor 1. This antiviral mechanism highlights a new target for therapeutic intervention.

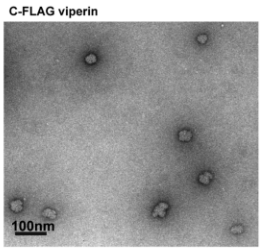

Viperin induces the release of noninfectious TBEV capsid particles.

https://doi.org/10.1128/JVI.01908-17

AMERICAN SOCIETY FOR MICROBIOLOGY | Journal of Virology®

VIRUS-CELL INTERACTIONS

Structure-Function Dissection of Pseudorabies Virus Glycoprotein B Fusion Loops

Melina Vallbracht,[a] Delphine Brun,[b,c] Matteo Tassinari,[b,c]* Marie-Christine Vaney,[b,c] Gérard Pehau-Arnaudet,[d,e] Pablo Guardado-Calvo,[b,c] Ahmed Haouz,[e,f] Barbara G. Klupp,[a] Thomas C. Mettenleiter,[a] Felix A. Rey,[b,c] Marija Backovic[b,c]

[a]Institute of Molecular Virology and Cell Biology, Friedrich-Loeffler-Institut, Greifswald-Insel Riems, Germany
[b]Institut Pasteur, Unité de Virologie Structurale, Département de Virologie, Paris, France
[c]CNRS UMR3569, Paris, France
[d]Institut Pasteur, Ultrapole, Département de Biologie Cellulaire et Infection, Paris, France
[e]CNRS UMR3528, Paris, France
[f]Institut Pasteur, Plate-Forme de Cristallographie, Paris, France

ABSTRACT Conserved across the family *Herpesviridae*, glycoprotein B (gB) is responsible for driving fusion of the viral envelope with the host cell membrane for entry upon receptor binding and activation by the viral gH/gL complex. Although crystal structures of the gB ectodomains of several herpesviruses have been reported, the membrane fusion mechanism has remained elusive. Here, we report the X-ray structure of the pseudorabies virus (PrV) gB ectodomain, revealing a typical class III postfusion trimer that binds membranes via its fusion loops (FLs) in a cholesterol-dependent manner. Mutagenesis of FL residues allowed us to dissect those interacting with distinct subregions of the lipid bilayer and their roles in membrane interactions. We tested 15 gB variants for the ability to bind to liposomes and further investigated a subset of them in functional assays. We found that PrV gB FL residues Trp187, Tyr192, Phe275, and Tyr276, which were essential for liposome binding and for fusion in cellular and viral contexts, form a continuous hydrophobic patch at the gB trimer surface. Together with results reported for other alphaherpesvirus gBs, our data suggest a model in which Phe275 from the tip of FL2 protrudes deeper into the hydrocarbon core of the lipid bilayer, while the side chains of Trp187, Tyr192, and Tyr276 form a rim that inserts into the more superficial interfacial region of the membrane to catalyze the fusion process. Comparative analysis with gBs from beta- and gammaherpesviruses suggests that this membrane interaction model is valid for gBs from all herpesviruses.

IMPORTANCE Herpesviruses are common human and animal pathogens that infect cells by entering via fusion of viral and cellular membranes. Central to the membrane fusion event is glycoprotein B (gB), which is the most conserved envelope protein across the herpesvirus family. Like other viral fusion proteins, gB anchors itself in the target membrane via two polypeptide segments called fusion loops (FLs). The molecular details of how gB FLs insert into the lipid bilayer have not been described. Here, we provide structural and functional data regarding key FL residues of gB from pseudorabies virus, a porcine herpesvirus of veterinary concern, which allows us to propose, for the first time, a molecular model to understand how the initial interactions by gBs from all herpesviruses with target membranes are established.

KEYWORDS alphaherpesvirus, class III fusion protein, entry, fusion loops, fusion protein, glycoprotein B, herpesvirus, membrane fusion, pseudorabies virus

Received 20 July 2017 **Accepted** 3 October 2017

Accepted manuscript posted online 18 October 2017

Citation Vallbracht M, Brun D, Tassinari M, Vaney M-C, Pehau-Arnaudet G, Guardado-Calvo P, Haouz A, Klupp BG, Mettenleiter TC, Rey FA, Backovic M. 2018. Structure-function dissection of pseudorabies virus glycoprotein B fusion loops. J Virol 92:e01203-17. https://doi.org/10.1128/JVI.01203-17.

Editor Richard M. Longnecker, Northwestern University

Address correspondence to Marija Backovic, marija@pasteur.fr.

* Present address: Matteo Tassinari, Institut Pasteur, Unité de Microbiologie Structurale, Département de Biologie Structurale et Chimie, Paris, France.

The family *Herpesviridae* contains a large number of enveloped, double-stranded DNA viruses, which are classified into alpha-, beta-, and gammaherpesvirus subfamilies based on their evolutionary relationships and biological properties (1). Pseudorabies virus (PrV) (suid alphaherpesvirus 1), the etiological agent of Aujeszky's disease in swine (2), belongs to the *Alphaherpesvirinae*, which also includes human pathogens, such as herpes simplex virus 1 (HSV-1) and HSV-2 and varicella-zoster virus (VZV). PrV has become a useful model for studying the biology of alphaherpesviruses in general (3).

Herpesviruses enter cells by fusion of their envelope with the host cell plasma membrane or with the membrane of an endocytic vesicle, depending on the virus and the cell type (4, 5). While many enveloped viruses require only one or two proteins to mediate receptor binding and entry, herpesviruses rely on the concerted actions of at least four glycoproteins. Distinct viral proteins first engage specific cellular receptors in an interaction that provides a trigger for membrane fusion (e.g., glycoprotein D [gD] in HSV-1/2 and PrV, gO in the betaherpesvirus human cytomegalovirus [HCMV], and gp42 in the gammaherpesvirus Epstein-Barr virus [EBV]) (6–9). The merger of the viral and cellular membranes is then catalyzed by fusion machinery that is conserved across the herpesvirus family and consists of gB and a heterodimeric complex of membrane-bound gH, in association with the anchorless gL (gH/gL) (reviewed in references 10 and 11).

The molecular basis of the entry mechanism has been best described for alphaherpesviruses. In HSV-1, the cascade begins with gD binding to cellular receptors, such as herpesvirus entry mediator (HVEM), nectin-1, or 3-O-sulfonated heparin sulfate (reviewed in reference 12). This interaction leads to a conformational change in gD (13, 14) that is believed to enable its interaction with the gH/gL complex, which in turn triggers gB to carry out membrane fusion (15, 16). It should be noted that unlike HSV-1, PrV does not require gD for direct viral cell-cell spread and gB-induced cell-cell fusion (17–19). Moreover, PrV virions can acquire the ability to infect cells in the absence of gD, gL, or the N-terminal domain of gH by compensatory mutations in other envelope glycoproteins (20, 21).

gB was proposed to be the bona fide fusion protein of herpesviruses due to its structural homology with the fusogenic G protein of the otherwise unrelated vesicular stomatitis virus (VSV) (22). Together with VSV G and the baculovirus fusion protein gp64 (23), gB was classified as a class III fusion protein. Viral fusion proteins are in general presented in a metastable prefusion state on the viral membrane. Upon an activation signal, they undergo conformational rearrangements unmasking the initially buried hydrophobic regions (fusion peptide [FP] or fusion loops [FLs]) for interactions with the target membrane, resulting in simultaneous anchorage of the fusion protein in the viral and cellular membrane at opposite ends of the protein. This extended intermediate is unstable and rapidly folds back into a "hairpin," an energetically more favorable postfusion conformation (24, 25).

gB is the most conserved envelope glycoprotein of herpesviruses, although only ~5% of its residues are identical across the entire herpesvirus family. The level of conservation is higher within each subfamily, and PrV and HSV-1 gBs share 50% amino acid sequence identity. The X-ray structures determined for the postfusion gB ectodomains from HSV-1 (26), EBV (27), and HCMV (28, 29) demonstrate conservation of the three-dimensional structural organization. Although the crystal structure of gB in a prefusion state has not yet been determined, a low-resolution structure of full-length HSV-1 gB in a state different from the postfusion conformation was obtained by cryo-electron tomography (30). VSV G protein has been crystallized in both pre- and postfusion conformations. The former revealed a trimeric molecule with the FLs pointing toward the viral membrane and with a different spatial organization of domains than the postfusion, low-pH form (31). Hypothetical models of the prefusion gB using the VSV G conformation as a template have been proposed (27, 32), but supporting structural data are still lacking. The high structural conservation observed for gB also applies to the gH/gL complex, as illustrated by the X-ray structures of the gH/gL

ectodomains from HSV-2, EBV, VZV, and a core domain of PrV gH (33–36), which revealed a common fold despite low sequence conservation (37). gH/gL has no structural resemblance to any known fusion protein but was shown to play a role in regulation of the fusion activity of gB (16, 37).

Membrane-interacting regions of fusion proteins are typically well conserved within the virus family and are rich in hydrophobic and aromatic residues that insert into the outer leaflet of a cell membrane (38). In class I fusion proteins, they are called FPs, which can be N-terminal peptides or an internal loop near the N terminus, as in the Ebola virus envelope glycoprotein GP2, for example (39) (to avoid confusion, we reserve the term FL for the loops of class II and III fusion proteins, and we refer to all class I membrane-interacting regions as fusion peptides, even when they correspond to an internal loop). FPs were shown to adopt a different structure upon insertion into target membranes (reviewed in reference 40). The FLs of class II and class III fusion proteins, in contrast, are conformationally constrained by being part of a larger structured β-barrel domain and appear to largely maintain their structure upon membrane insertion. In class II fusion proteins, the membrane-interacting surface can be composed of residues from one (flaviviruses and alphaviruses [41, 42]), two (rubella virus and phleboviruses [43, 44]), or three (hantaviruses [45]) FLs, while the known class III fusion proteins use two FLs to interact with membranes. FLs of herpesviruses are unusual because their amino acid sequences are poorly conserved even within subfamilies. Therefore, their identification was impossible until structural data became available. Residues exposed at the tips of the recombinant crystallized HSV-1 gB ectodomain (26) were proposed to form the FLs based on structural homology with the well-defined FLs of the VSV G protein (46, 47). A similar organization of the FLs was observed in the reported gB structures, with the difference that the aromatic and apolar residues are predominantly presented at the sides of the HSV-1 FLs while they protrude from the tips of the EBV and HCMV FLs. These exposed hydrophobic residues in EBV and HCMV gBs caused the recombinant ectodomains to aggregate, forming rosette-like structures (48, 49). Mutagenesis of the hydrophobic residues within the FL, while abolishing their fusion function, was essential for solubility of these proteins for structure determination (49, 50). In contrast, HSV-1 gB (51) and PrV gB (this study) exhibit less hydrophobic tips, form soluble trimers, and can be studied and crystallized as functional wild-type (WT) proteins.

Extensive mutagenesis studies have been performed on HSV-1 gB, demonstrating that the hydrophobic residues Trp174, Phe175, and Tyr179 in FL1 and Ala261 in FL2, as well as polar and charged residues, such as His263 and Arg264, presented at the sides of FL2, play an important role in fusion (51–54). The hydrophobic residues were proposed to form a patch that inserts into the membrane, while the His and Arg side chains were speculated to interact with phospholipid head groups without penetrating deeper into the membrane. In support of this model, the low-resolution structure of HSV-1 gB ectodomains bound to liposomes and obtained by cryo-electron tomography showed that the interactions of the HSV-1 gB ectodomains are limited to the outer membrane leaflet. This model predicted that the FLs would insert into the bilayer at an oblique angle, indicating that the residues from β-strands leading to the FLs may be involved in the interactions with lipids (55). HSV-1 gB FL residues Trp174, Tyr179, His263, and Arg264, furthermore, were shown to be the contact sites for interactions of the ectodomain with liposomes (54).

Cholesterol (CH) is a lipid that is ubiquitously present in mammalian cell membranes, where it plays an important role in the entry of many viruses (56), including PrV and HSV-1 (reviewed in references 57 to 59). The HSV-1 gB ectodomain was shown to bind to liposomes only in the presence of cholesterol (54), and full-length HSV-1 gB expressed in cells was found to associate with lipid rafts (60).

While the current HSV-1 model has provided an important step forward in understanding how gB binds to membranes, it has been unclear whether a similar model of insertion would hold true for other gB proteins due to the poor conservation of the FLs, highlighting the need to study each gB individually and to perform comparative analyses. With this in mind, we sought to enlarge the structural and functional

repertoire available for alphaherpesviruses by carrying out studies on PrV gB. We report here the X-ray crystal structure of the PrV gB ectodomain at 2.7-Å resolution and demonstrate that the recombinant ectodomains bind to liposomes in a cholesterol-dependent fashion. The association with liposomes occurs via the trimer tip that contains the FLs, resembling the shallow insertion observed for HSV-1 gB. We designed the PrV gB mutagenesis to complement what had already been reported for HSV-1 gB and to target all aromatic and hydrophobic residues within the FLs, some that are unique to PrV and some that are conserved in HSV-1 gB, as well. The resulting pattern of active and inactive FL mutants matches in part what had been observed previously for HSV-1 gB, but with some interesting differences that shine new light on the way the FLs insert into membranes. Based on our results, we propose a model in which the tip of FL2 penetrates deeper into the lipid bilayer, reaching into the hydrophobic core, while residues on the sides of the FL1 and FL2 tips position their side chains within the same plane, inserting into the amphipathic, interfacial region of the membrane. Comparative analysis with the FLs of HCMV and EBV gBs further suggests that, in spite of considerable sequence divergence, this model could be used to describe in general the way herpesvirus gBs interact with membranes.

RESULTS

PrV gB expression, crystallization, and structure determination. The ectodomain expression construct of PrV gB (suid alphaherpesvirus 1, strain Kaplan [PrV-Ka]; GenBank accession number AEM64049.1) encodes gB residues 59 to 756 (Fig. 1A). The construct was designed to exclude the gB signal sequence (residues 1 to 58), which was replaced by the *Drosophila* Bip signal peptide, present in the expression vector and known to drive efficient expression of heterologous proteins (61). The expression construct ends with double Strep-tag II, as described in Materials and Methods, added just before the hydrophobic membrane-proximal region (MPR) (residues 757 to 800), which is followed by the transmembrane region (residues 801 to 821) and the cytoplasmic domain (residues 822 to 916) in the intact protein.

The PrV gB ectodomain was expressed using the stably transfected *Drosophila* Schneider 2 (S2) cell line, as described previously (62). After affinity and size exclusion chromatography (SEC), we obtained 8 to 12 mg of pure protein from 1 liter of cell culture. The protein eluted as a single peak from a SEC column and exhibited no signs of aggregation. Sodium dodecyl sulfate-polyacrylamide gel electrophoresis (SDS-PAGE) analysis of the purified ectodomain showed a single band migrating just below the 100-kDa marker under nonreducing conditions (Fig. 1B, lane 1). PrV gB contains a furin cleavage site, ^{501}RRARR^{505}, and the recombinant protein is cleaved in S2 cells, as demonstrated by the presence of two protein bands of lower molecular mass under reducing conditions (~60-kDa and ~40-kDa fragments labeled, respectively, gB^{b} and gB^{c}) (Fig. 1B, lane 3).

Compared to its 100-kDa apparent molecular mass, the polypeptide chain of the gB ectodomain has a calculated mass of 82 kDa, corresponding to the 49-kDa N-terminal and 33-kDa C-terminal furin cleavage products, which indicates the presence of posttranslational modifications in the mature protein. There are six predicted N-glycosylation sites (four in the N-terminal and two in the C-terminal fragments), and a shift to a lower molecular mass is indeed observed for both fragments upon treatment with a deglycosidase (Fig. 1B, lanes 2 and 4). *Drosophila* S2 cells add 1- to 2-kDa simple mannose core structures to form N-linked sugars (63), accounting for the presence of several N-linked sugars in the expressed protein.

The purified gB ectodomains crystallized easily under numerous conditions, but the crystals were fragile and of poor diffraction quality. Upon enzymatic deglycosylation with endo-β-*N*-acetylglucosaminidase (Endo D), we obtained diffraction quality crystals in 0.1 M Tris, pH 8.5, 7% polyethylene glycol (PEG) 4000, 0.6 M LiCl. Diffraction data were collected and processed as described in Materials and Methods. The crystals belong to the H3 space group (a = 99.9 Å, b = 99.9 Å, c = 272.9 Å; $\alpha = \beta = 90°$; $\gamma = 120°$), with

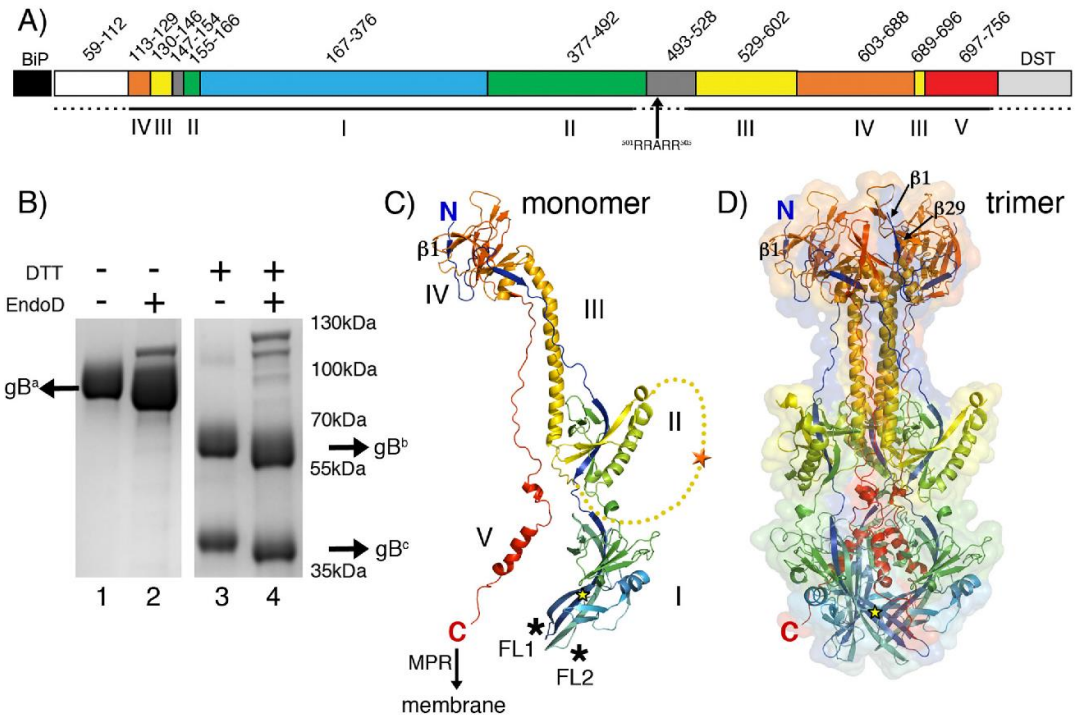

FIG 1 PrV gB ectodomain structure. (A) Schematic representation of the PrV gB expression construct. The PrV gB signal peptide (residues 1 to 58) was replaced by the *Drosophila* BiP secretion signal, which was cleaved off and not part of the secreted protein. The secreted PrV gB ectodomain used for crystallization contains residues 59 to 756, followed by a double Strep-tag II (DST). Regions forming the five gB domains are labeled with Roman numbers I to V below the bar and are colored as follows: domain I, blue; domain II, green; domain III, yellow; domain IV, orange; and domain V, red. Two linker regions (residues 147 to 154 and 493 to 528) are shown in gray. The dashed lines mark the regions that were unresolved in the gB structure. The location of the furin cleavage site (RRARR; residues 501 to 505) is indicated. (B) SDS-PAGE analysis of the recombinant PrV gB. The Coomassie blue-stained 4 to 20% SDS-PAGE gel shows the purified PrV gB ectodomain under nonreducing (lanes 1 and 2) and reducing (lanes 3 and 4) conditions. The samples in lanes 2 and 4 were treated with Endo D. The N-terminal and C-terminal fragments generated by furin cleavage are labeled gB^b and gB^c, and the uncleaved gB is marked gB^a. DTT, dithiothreitol. (C) Structure of the PrV gB monomer. The molecule is colored from blue (N terminus) to red (C terminus). The locations of the N and C termini are indicated, and domains are labeled with Roman numbers I to V. The C terminus is followed by the 50-residue-long MPR, not present in the expression construct, leading to the transmembrane anchor; the anticipated location of the membrane is indicated by the arrow. Fusion loops presented by domain I are marked by asterisks. The extra N-terminal residues that were resolved for the first time in this structure form a strand labeled $\beta1$. The linker connecting domains II and III, which is not visible in our structure, is plotted as a yellow dotted line to indicate the putative location of the furin cleavage site (orange star). The location of the glycosylation site Asn264, to which a single NAG residue is attached, is indicated by the yellow star. (D) Structure of the PrV gB trimer. The colors of the protomers are the same as in panel C. Ribbon and molecular-surface representations are shown. The N and C termini of the same protomer represented in panel B are labeled. Strand $\beta29$, which runs antiparallel to strand $\beta1$, is indicated (domain IV). PyMOL (103) was used to create the structures shown in panels C and D.

one gB protomer per asymmetric unit. Crystallographic statistics of data processing and structure refinement are given in Table 1.

PrV gB forms a typical class III postfusion trimer. The PrV gB ectodomain folds into an ~16-nm by ~8-nm trimeric spike, resembling the structures reported for the postulated postfusion conformation of the HSV-1 (26), EBV (27), and HCMV (28, 29) gB ectodomains. Briefly, the N terminus of the protein (amino acid 113) is located at the top end of the trimer, with the polypeptide chain running down along the entire length of the spike, folding into domain I, which carries the FLs exposed at the base of the molecule (Fig. 1C). Domain II is positioned laterally, adopting a fold reminiscent of the pleckstrin homology domains. The furin cleavage site is located in the flexible linker that connects domains II and III and could not be resolved in our structure. Domain III contains the prominent, centrally located helix that extends to the top of the molecule, followed by domain IV, also known as the "top" or "crown" domain. Residues 697 to 750

TABLE 1 X-ray diffraction data collection and refinement for PrV gB

Parameter	Value[a]
X-ray data processing	
Beamline	ESRF ID29
Space group	H3
Cell constants	99.89 Å, 99.89 Å, 272.89 Å
a, b, c, α, β, γ	90.00°, 90.00°, 120.00°
Resolution (Å)	46.15–2.69 (2.85–2.69)
No. of reflections	147,396 (23,196)
Multiplicity	5.3
$<I/\sigma(I)>$	14.99 (2.33)
Completeness (%)	99.6 (98.3)
R_{merge} (%)	7.4 (52.3)
R_{pim} (%)	5.5 (38.6)
$CC_{1/2}$	0.98 (0.82)
Wilson B factor (Å^2)	55.7
Refinement	
Program	BUSTER 2.10.2
Resolution (Å)	46.15–2.70 (2.80–2.70)
No. of reflections	27,695 (2,738)
R_{work}/R_{free}[b]	0.193/0.236
No. of atoms[c]	4,759/92
B atomic factors (Å^2)[d]	73/73.8/59.6
Geometry	
RMSD bond lengths (Å)	0.010
RMSD bond angles (°)	1.16
Ramachandran plot[e] (%)	95.25/4.24/0.51

[a]Outer-shell values are given in parentheses.
[b]The R_{free} test set was composed of 5% randomly chosen reflections.
[c]Number of protein/water atoms.
[d]Overall/protein/water B factors.
[e]Preferred/allowed/outliers as calculated by Coot (109).

form a stretched chain that packs tightly into the crevice formed by the other two protomers. This so-called "domain V" has the appearance of a zipper that seals the trimer (Fig. 1D), resulting in the C terminus of the ectodomain (amino acid 750) being brought into close proximity to the FLs.

Although the expression construct encodes gB residues 59 to 756, the first residue resolved in the crystal structure was Arg113, consistent with the highly flexible N-terminal end of the protein, which is rich in glycine and proline residues. The same applies to HSV-1, EBV, and HCMV gBs, in which the N-terminal region of the crystallized construct also was not resolved. The other PrV gB regions that were not built into the structure are the above-mentioned unstructured segment that contains the furin cleavage site and connects domains II and III (residues 478 to 521) and the C-terminal 6 residues of the ectodomain (residues 750 to 756), which are followed by the double Strep-tag II in the expression construct. The PrV gB structure, however, does reveal 3 residues at the very N terminus (residues 113 to 116), which had not been observed in the other gB structures. This segment forms a short β-strand (β1) in domain IV that packs against β29 in an antiparallel fashion (Fig. 1C and D).

Of six potential N-glycosylation sites, we observed densities for the sugar moieties attached to Asn264 (domain I), Asn444 (domain II), and Asn636 (domain IV). The electron density was of sufficient quality to allow building of one *N*-acetylglucosamine (NAG) residue only to Asn264 (Fig. 1C and D).

As anticipated, PrV gB showed higher structural conservation with the HSV-1 homolog than with the more distant gBs of EBV or HCMV. The root mean square deviation (RMSD) for the superposition of the PrV and HSV-1 structures is 1.04 Å for C-α atoms (Table 2). The main difference between the PrV and HSV-1 ectodomains regards the gross organization of the spike resides in the position of domain IV, which appears slightly rotated when the structures are superimposed on domains I and II. The domain IV disposition is even more evident compared to those of HCMV and EBV gBs (Fig. 2).

TABLE 2 Sequence and structural comparison of PrV and HSV-1/HCMV/EBV gB ectodomains

Comparison	Sequence identity (%)[a]	n_A/n_T[b]	RMSD (Å)[c]
PrV vs HSV-1	50.1	524/568	1.04
PrV vs HCMV	25.6	508/535	3.39
PrV vs EBV	25.3	496/530	3.72

[a]Percent identity was calculated using the shorter sequence as the denominator.
[b]n_A and n_T, numbers of aligned and total atoms, respectively.
[c]The RMSDs were calculated for C-α atoms in PyMOL (103).

The PrV gB ectodomain requires cholesterol in the membrane for binding. The recombinant PrV gB ectodomain used for crystallization was tested for binding to liposomes with different compositions in coflotation experiments in density gradients, as described in detail in Materials and Methods. Briefly, the protein-liposome mixture, adjusted to 36% iodixanol (OptiPrep), was loaded below the 20% iodixanol layer, which was then overlaid with buffer and subjected to ultracentrifugation. Liposomes float and are found at the top of the gradient, while the protein alone sediments and remains at the bottom of the tube. Protein bound to liposomes cofloats with liposomes and in this case partitions to the top of the gradient. All the gradient fractions were analyzed for the presence of the protein in the control experiments, demonstrating that gB was

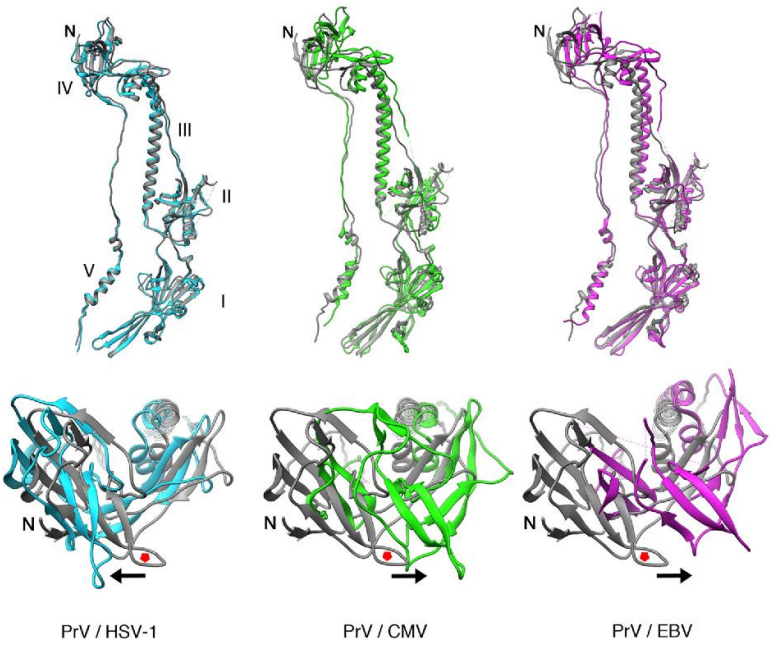

FIG 2 Structural comparison of gB ectodomains. The PrV gB ectodomain structure, shown in gray cartoon representation, was superimposed on those of HSV-1 (PDB accession number 2GUM; light blue), HCMV (PDB accession number 5C6T; green), and EBV (PDB accession number 3FVC; purple) gBs, using the residue range that corresponds to domains I and II of PrV, HSV-1, HCMV, and EBV gBs (residues 167 to 458, 154 to 473, 89 to 388, and 133 to 415, respectively). The alignment was done by superimposing domains I and II to highlight the disposition of the top, domain IV, which is not as obvious when the superimposition is applied to the entire molecule. The alignments were done in PyMOL (103). Domains are labeled with Roman numbers. Each superimposition is shown in two orientations, looking at the monomer from the front (top) and at domain IV from the top of the spike (bottom). The red pentagons are placed in the same loop of the PrV gBs to serve as a reference point for the movement of the superimposed domain IV, the direction of which is indicated by the arrows.

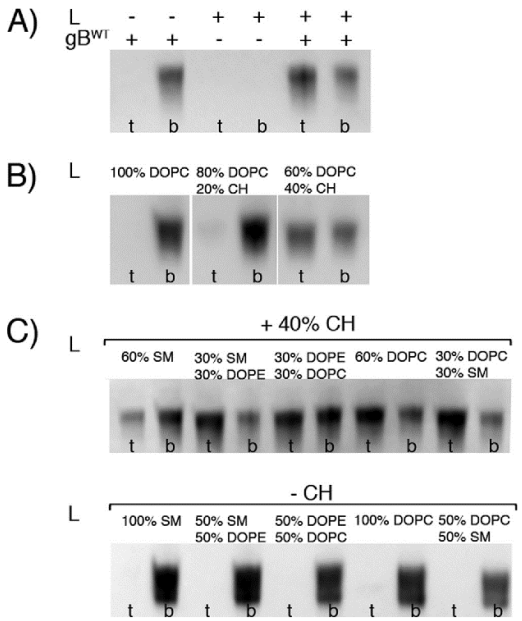

FIG 3 WT PrV gB ectodomain interactions with liposomes. (A) WT gB ectodomains bind to the DOPC-CH liposomes. The presence (+) of liposomes (L) and protein is indicated. Aliquots of the top (t), i.e., liposome, and bottom (b), i.e., unbound protein, fractions were analyzed by SDS-PAGE, and the Strep-tag present on gB was detected by WB using Streptactin-HRP conjugate. The WT protein is found in the top fraction only in the presence of liposomes with 60% DOPC and 40% CH. (B) Coflotation of WT gB and DOPC liposomes with increasing amounts of cholesterol. The liposome composition is indicated at the top. gB is detected in the top fraction only when 40% CH is present. (C) Coflotation of WT gB and liposomes made of combinations of lipids found in the plasma membrane. The CH concentration was fixed at 40% or 0% (top and bottom, respectively), and one or two more lipids were added, resulting in a total of 5 lipid compositions. The protein was detected bound to all of the CH-containing liposomes, while it was found in the unbound fraction in the absence of CH.

found either at the top or the bottom of the gradient, which is why only these two fractions were analyzed further.

Liposomes containing 60% 1,2-dioleoyl-*sn*-glycero-3-phosphocholine (DOPC) and 40% CH were prepared. This is the same composition used for testing HSV-1 gB ectodomain interactions with membranes (54, 64). The top and bottom factions were analyzed by Western blotting (WB) with a reagent that specifically binds to the Strep affinity tag. The WT PrV gB ectodomain was found in the top fraction only when liposomes were present and sedimented to the bottom of the tube in the absence of liposomes (Fig. 3A). Complexes made of the WT PrV gB ectodomain and liposomes containing DOPC and increasing molar amounts of CH (100% DOPC, 80% DOPC plus 20% CH, or 60% DOPC plus 40% CH) were prepared and tested next. gB ectodomains bound only to the latter type of liposomes (Fig. 3B), suggesting that there is a threshold CH concentration required for the association. To determine if the lack of binding at lower CH concentrations was due to the requirement for another lipid rather than insufficient CH concentration, a series of liposomes made of mixtures of DOPC, 1,2-dioleoyl-sn-glycero-3-phosphoethanolamine (DOPE), and sphingomyelin (SM) was prepared in the presence of 40% CH or without CH. DOPE alone or mixed with CH does not form liposomes but assembles into lipid nanotubes due to its inverted hexagonal shape (65), which is why these lipid mixtures were omitted. The results of the flotation experiments showed that WT gB was present in the top fraction, i.e., bound to the

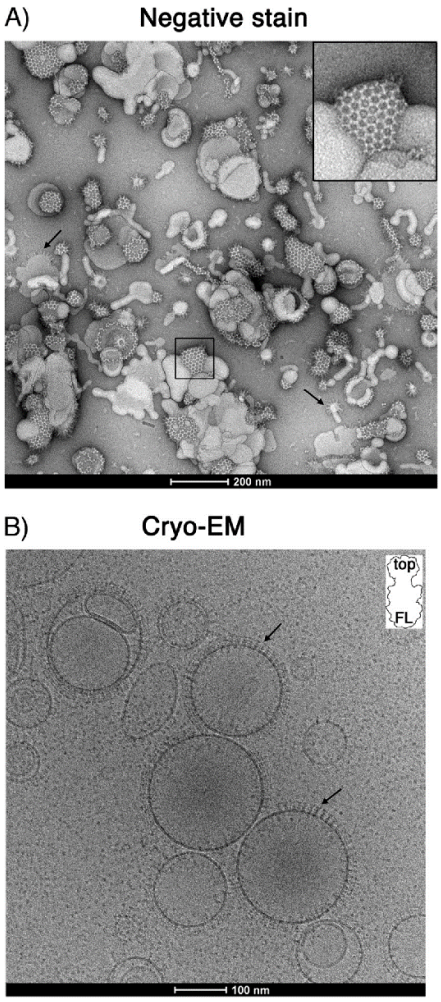

FIG 4 (A) Negative-stain EM image of liposomes incubated with PrV gB ectodomains. Characteristic hexagonal structures made of gB covering the liposomes (60% DOPC, 40% CH) are observed, representing the top view on the gB spikes. Individual trimers establish an extensive network of lateral interactions, giving rise to the array appearance of the protein coat. Liposomes showing side views of the gB trimers projecting away from the liposome surface are marked by arrows. An enlarged view of the boxed area is shown in the upper right corner. (B) Cryo-EM of PrV gB ectodomains bound to liposomes. The arrows indicate individual gB trimers in which the top end of the spike is better resolved, indicating that the molecule binds to the liposomes via the other end, i.e., the one carrying the FLs. (Inset) Shape of a gB trimer, with "top" representing the domain IV end of the spike and "FL" marking the base of domain I and the location of FLs.

liposomes only in the presence of CH (Fig. 3C), reinforcing the conclusion that CH is essential for PrV gB ectodomain interactions with liposomes.

A sample of gB mixed with liposomes was visualized by negative-stain electron microscopy (EM) (Fig. 4A), revealing liposomes decorated by protein arrays, forming honeycomb-like structures in which the individual trimers appeared to be in contact with each other. Cryo-EM images of the same sample (Fig. 4B) showed individual gB

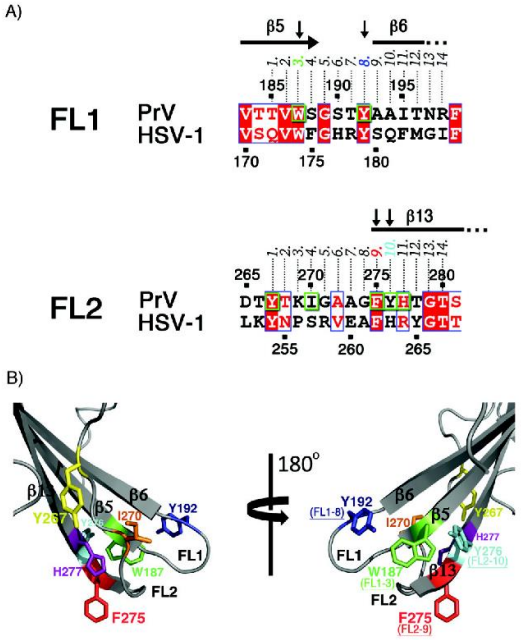

FIG 5 (A) Sequence alignment of PrV and HSV-1 gB fusion loop regions. Identical residues are shown as white letters on a red background and residues with similar physicochemical properties in red on a white background. Residues mutated in this study (Trp187, Tyr192, Tyr267, Ile270, Phe275, Tyr276, and His277) are boxed in green. The numbers 1 to 14 above the alignment indicate the position of each residue in FL1 or FL2. The residues found to be important for binding to liposomes are indicated by vertical arrows, and their corresponding numbers (3 and 8 in FL1 and 9 and 10 in FL2) are colored according to the scheme used in panel B. (B) Structural representation of the mutated PrV gB FL residues. The aromatic residues in FL1 and FL2 are indicated with their side chains in stick representation. These residues were individually mutated as shown in Table 3. For clarity, two views of the FLs are presented, and the remainder of the protein is omitted. The residues shown to be required for binding to liposomes are also indicated, with their corresponding positions within FL1 and FL2.

trimers packing tightly and inserting into the liposomes via the spike end that contains the FLs (domain I), as was observed for the HSV-1 protein (55).

Selection of PrV gB FL residues and design of mutagenesis studies. The side chains of Trp and Phe, as well as smaller hydrophobic residues, such as Leu or Ile, have favorable energies for penetration into the hydrophobic membrane core, made exclusively of lipid tails (66), while amphipathic Tyr and His side chains preferentially partition in the interfacial membrane region, localized between the hydrocarbon core and the aqueous phase (66, 67). Trp is also often found in this region (68). The interfacial membrane region is amphipathic itself due to the presence of carbons from the beginnings of the apolar lipid tails and of polar phosphate and glycerol groups (69). A Phe side chain can penetrate into the membrane core and could thus be emulated by Trp, but not by Tyr, due to the presence of a polar hydroxyl group at the distal tip of the side chain. The interfacial region, on the other hand, would be expected to accommodate aromatic residues, such as Tyr, Trp, Phe, or His (the last in its unprotonated form).

To shed light on how the side chains of individual FL residues interact with membranes, several changes were introduced. Each of the aromatic or hydrophobic residues found in PrV gB FLs (Trp187, Tyr192, Tyr267, Ile270, Phe275, Tyr276, and His277) (Fig. 5) was individually mutated to Ala, a change that resulted in the replacement of the bulky hydrophobic side chain with a methyl group, or to a different

TABLE 3 PrV gB mutants with single mutations in fusion loops in liposome binding and functional assays

PrV gB variant[a]	Binding to 2L[b] liposomes	Cell-cell fusion	*trans*-complement[e]	Binding to 4L[c] liposomes	Ectodomain yield/ protein purity[d]
FL1					
W187A	−	−	−	−	NC
W187H	−	NT[f]	NT	−	NC
W187F	−	NT	NT	−	NC
Y192A	−	−	±	−	NC
Y192F	±	+	+	+	NC
Y267A	±	+	+	+	NC
Y267F	+	NT	NT	+	NC
I270A	+	+	+	+	NC
F275A	−	−	±	−	NC
FL2					
F275W	+	+	+	+	NC
F275Y	−	−	±	−	NC
Y276A	−	−	±	−	NC
Y276F	±	+	+	+	NC
H277A	+	+	+	+	NC
H277W	+	NT	NT	+	NC

[a]Single point mutations introduced in FL1 and FL2 of PrV gB are indicated. The variants containing mutations to alanine are shaded.
[b]2L indicates that liposomes were made of 2 lipids: 60% DOPC and 40% CH. ± indicates the presence of a faint band in the liposome fraction (Fig. 7A), indicating weak binding of the protein to liposomes.
[c]4L indicates that liposomes were made of 4 lipids: 20% DOPC, 20% DOPE, 20% SM, and 40% CH.
[d]The expression yield and purity of the recombinant ectodomains are indicated relative to those of the WT protein; NC, no change.
[e]± indicates marginal complementation of PrV-ΔgB virus (Fig. 9A).
[f]NT, not tested.

aromatic residue with similar chemical structure: Trp was changed to Phe or His, Phe to Trp or Tyr, His to Trp, and Tyr to Phe (Table 3). This was done to probe if the residue was more likely to insert more deeply into the hydrocarbon core or to remain in the polar region of the membrane. Three of the mutagenized residues are unique to PrV gB (Ile270, Tyr276, and His277), Tyr267 is conserved but has not been mutated, and the changes introduced at the conserved positions were not analyzed previously in HSV-1 gB.

Side chains of PrV gB FL residues Trp187, Tyr192, Phe275, and Tyr276 mediate binding to liposomes and form a hydrophobic patch. To facilitate generation of mutant proteins, recombinant PrV gB ectodomains were expressed after transient transfection of Expi293F mammalian cells, and the same type of liposomes (60% DOPC and 40% CH) as reported for the HSV-1 gB ectodomain variants were used in the liposome flotation assay (54). The variants did not differ from the WT protein in terms of expression yields, behavior during affinity and size exclusion chromatography, and cleavage by cellular furin (Fig. 6).

Replacement of the selected residues with alanine had three consequences (Table 3 and Fig. 7A). The W187A, Y192A, F275A, and Y276A variants completely lost the ability to bind to liposomes and were present exclusively in the bottom fraction. I270A and H277A floated like the WT protein, indicating that the mutation exerted no effect on liposome binding. Y267A showed intermediate behavior, with very low binding to liposomes, at the limit of WB detection.

Mutation to other aromatic residues also had different outcomes. Trp187 was essential for association of the ectodomain with liposomes, and changes to Phe or His yielded a protein that did not cofloat with liposomes. Y192F was only weakly detected in the liposome fraction, similar to what was observed for Y267A, while Y267F and F275W bound to liposomes comparably to WT gB. Interestingly, in contrast to F275W, F275Y did not associate with liposomes, indicating that the presence of the hydroxyl group in F275Y may impair the ability of the protein to interact with lipids. Y276F showed very weak binding, resembling that of Y192F and Y267A. The amino acid at

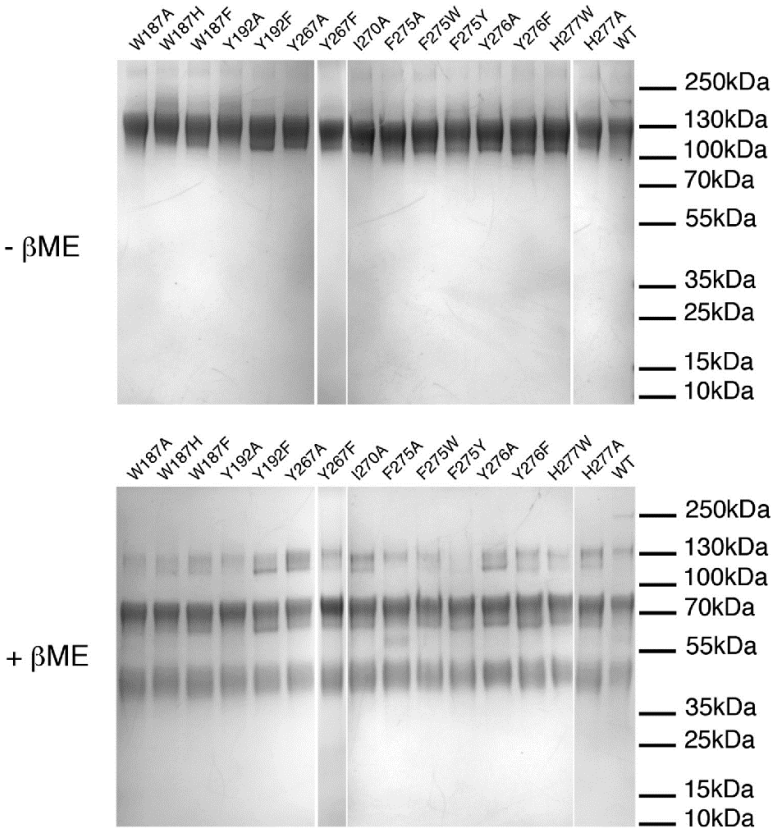

FIG 6 SDS-PAGE analysis of purified PrV gB ectodomain variants. Shown is SDS-PAGE analysis of the PrV gB recombinant ectodomains under nonreducing (top) and reducing (bottom) conditions. Two micrograms of each purified protein was loaded on a 4 to 20% gradient gel. The proteins were stained with Coomassie blue. The three bands resolved under reducing conditions correspond to the uncleaved protein and the N-terminal and C-terminal fragments produced by furin cleavage. There were no observable differences in purity and cleavage patterns between the FL variants and the WT PrV gB.

position 277 does not seem to be important for liposome binding, since the substitutions H277A and H277W had no effect (Fig. 7A).

The four residues Trp187, Tyr192, Phe275, and Tyr276, which did not tolerate substitutions to alanine and must have a bulky aromatic side chain in order to bind to liposomes, form a continuous hydrophobic and electrostatically neutral patch at the surface of the trimeric postfusion spike, as shown in Fig. 7B. The phenyl group of Phe275 appears protrude the most, while Trp187, Tyr192, and Tyr276 form a rim above (Fig. 5B).

PrV gB FL variant binding to liposomes correlates with fusion activity. The fusogenic potentials of a subset of PrV gB FL mutants, including all the Ala variants, were assessed in eukaryotic cells using the corresponding full-length gB constructs, generated by site-directed mutagenesis of pcDNA-gB. Correct mutagenesis was verified by sequencing, and protein expression and processing were analyzed, respectively, by indirect immunofluorescence of permeabilized gB-expressing cells (Fig. 8A) and WB of whole-cell lysates (Fig. 8B). The PrV gB FL variants revealed WT-like behavior in both subcellular localization and processing by furin, with the exception of W187A and

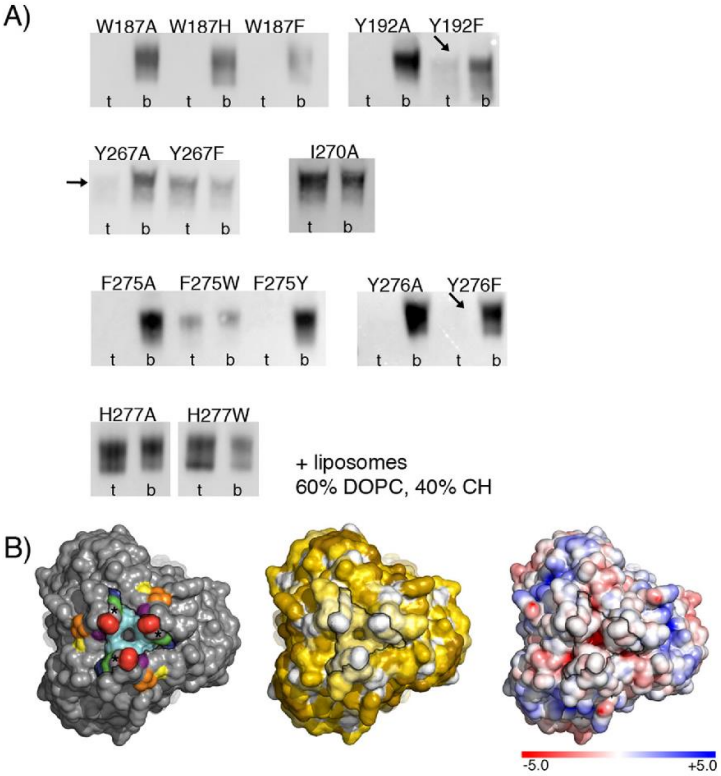

FIG 7 (A) Liposome binding of PrV gB FL variants. Shown is the WB analysis of gradient fractions. t, top fraction (liposomes and bound gB); b, bottom fraction (unbound protein). The liposomes were made of 60% DOPC and 40% CH. The arrows indicate the presence of very weak signals in the top fractions observed for Y192F, Y267A, and Y276F. Streptactin-HRP conjugate was used for gB detection. (B) Solvent-accessible surface representation of the bottom tip of the PrV gB spike carrying fusion loops. (Left) The FL residues mutated in this study are shown in the same colors as in Fig. 5B. The stars indicate the positions of the conserved Gly274. The black contour indicates the edges of the continuous hydrophobic surface formed by the side chains of Trp187, Tyr192, Gly274, Phe275, and Tyr276. (Middle) Solvent-accessible surface colored according to hydrophobicity. The same PrV gB surface is shown, with the colors corresponding to the hydrophobicity of the individual side chains calculated using the Eisenberg hydrophobicity scale (104), with white corresponding to the most hydrophobic and dark yellow to the most hydrophilic/charged side chains. (Right) Electrostatic solvent-accessible surface. The same surface is shown, colored according to the electrostatic potential calculated with the ABPS tool (105), with blue and red corresponding to negative and positive potentials, respectively. All the images were generated in PyMOL (103).

Y192A gBs. These two variants accumulated in larger structures in the cytoplasm and showed impaired furin cleavage, as indicated by lower levels of the furin-cleaved subunit (gB^b) and more abundant uncleaved gB (gB^a) (Fig. 8B).

To test the fusogenic potential of the mutated gB proteins, RK13 cells were cotransfected with plasmids encoding WT gB (Ka) or the mutated gB and gH/gL, as described previously (70, 71). In addition, an enhanced green fluorescent protein (EGFP) expression plasmid was cotransfected to facilitate evaluation of the assays by fluorescence microscopy (72). Transfection with plasmids encoding the WT proteins served as a positive control, and the results were set as 100%, while the empty expression vector pcDNA3 was used as a negative control.

Fusion assays revealed good correlation between the ability of the protein to bind to liposomes *in vitro* and its activity in fusion (Table 3 and Fig. 9A). Most of the variants

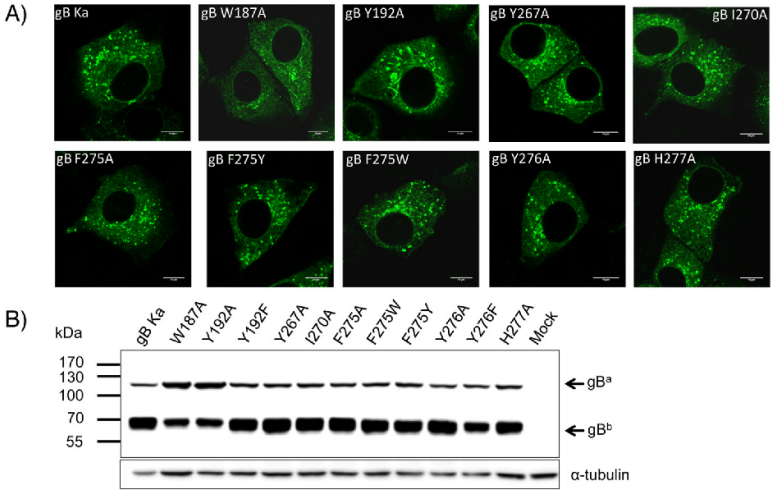

FIG 8 Expression of full-length PrV gB variants in RK13 cells. (A) Subcellular localization. RK13 cells were transfected with expression plasmids for wild-type gB (gB Ka) or the PrV gB FL mutants and analyzed by indirect immunofluorescence. One day after transfection, the cells were fixed with 3% paraformaldehyde and permeabilized with 0.1% Triton X-100. gB was detected using a gB-specific rabbit antiserum and Alexa Fluor 488-conjugated secondary antibodies. Green fluorescence was excited at 488 nm and recorded with a laser scanning confocal microscope (SP5; Leica, Mannheim, Germany). (B) Western blot analyses. Lysates of RK13 cells transfected with expression plasmids for gB Ka or gB variants containing FL single mutations were separated by SDS-PAGE under reducing conditions. Cells transfected with the empty vector pcDNA3 served as a negative control (Mock). The blots were incubated with the gB-specific monoclonal antibody C15-b1. Signals of uncleaved gB (gB^a) or a furin-cleaved gB subunit (gB^b) are labeled by arrows, and the molecular masses of marker proteins are indicated. As a loading control, the blot was incubated with an anti-alpha-tubulin monoclonal antibody.

that did not show association with liposomes were unable to induce cell-cell fusion, and all the variants with liposome binding properties supported efficient cell-cell fusion. Surprisingly, the three variants that showed only weak binding to liposomes, Y192F, Y267A, and Y276F, mediated fusion to an extent similar to that of WT gB.

To test whether this discrepancy was due to the liposome composition used in the *in vitro* experiments (60% DOPC and 40% CH, referred to as "2L," for two lipids present), the coflotation experiments were repeated with liposomes whose composition more closely resembled the composition of the plasma membrane (20% DOPC, 20% DOPE, 20% SM, and 40% cholesterol, referred to as "4L," for four lipids present) (73–75). The three variants Y192F, Y267A, and Y276 indeed floated with 4L liposomes, like the WT protein (Fig. 9B), demonstrating that the previously observed weak association was due to the inadequate liposome composition and not the mutated protein. The association of the other FL variants did not change as a function of liposome composition (Fig. 9C). These data demonstrate for the first time significant differences in the capabilities of gB mutants to bind to liposomes as a function of lipid composition, underlining the importance of testing different liposome compositions and cross-checking biochemical data with functional data.

Since W187A and Y192A variants were inactive and showed impaired furin cleavage, we wanted to establish whether furin processing was important for the function of PrV gB in the particular functional assays used in this study. A gB variant with a 5-residue (RRARR) deletion in the furin site (gB-Δfurin) was created. WB analysis of gB-Δfurin expressed in RK13 cells confirmed that the protein was not cleaved, as indicated by a prominent band for uncleaved gB (gB^a) and absence of bands corresponding to the furin-cleaved subunits (Fig. 10). gB-Δfurin was functional in cell-cell fusion assays and was able to complement gB-negative PrV to levels comparable to those of WT-gB (Fig. 10C). These data demonstrate that furin cleavage of PrV gB is not necessary for its

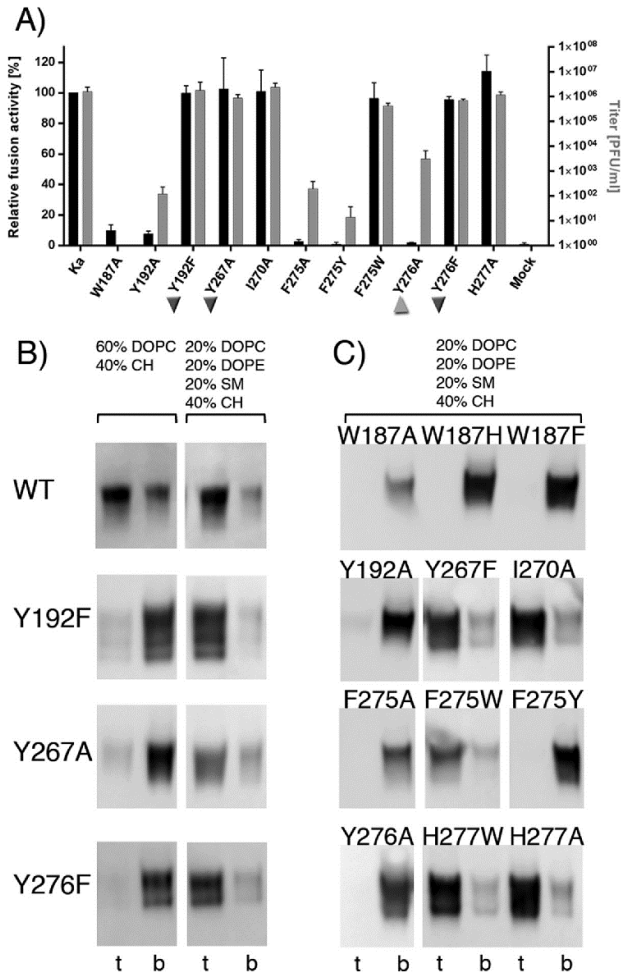

FIG 9 (A) Functional data obtained for the PrV gB FL variants. The results of the cell-cell fusion assay are plotted as black bars and expressed as percentages of the activity of the WT gB in combination with gH/gL, which was set to 100% (left *y* axis). Viral titers obtained in the *trans*-complementation assay are shown as gray bars (right *y* axis). Ka, PrV strain Kaplan, the WT protein, was used as a positive control. The inverted triangles mark the three variants that showed poor binding to liposomes while being functional in fusion and complementation assays. The triangle labels Y276A, which had a fusion-null phenotype in the cell-cell assay but was partially functional in the virus complementation assay. The error bars indicate standard deviations from three independent experiments. (B) Effect of liposome composition on binding of the WT and the Y192F, Y267A, and Y276F PrV gB variants. Two types of liposomes were used, 2L (60% DOPC and 40% CH) (left) and 4L (20% DOPC, 20% DOPE, 20% SM, and 40% CH) (right), and the top and bottom fractions were analyzed by WB, showing larger amounts of all the variants bound to the more complex 4L liposomes. (C) Flotation of PrV gB variants whose binding to liposomes is not affected by lipid composition. These variants showed the same pattern of binding to 4L liposomes as to 2L liposomes (Fig. 7A). Aliquots from the top and bottom fractions were analyzed by WB.

function in cell-cell fusion and complementation. The observed fusion deficiency of the W187A and Y192A variants thus cannot be attributed to the reduced furin cleavage alone but could still be caused by impaired trafficking and low surface expression. Unlike HSV-1 gB, which is highly abundant at the cell surface, WT PrV gB exhibits rather low surface expression. Only around 4% of WT PrV gB is targeted to the plasma

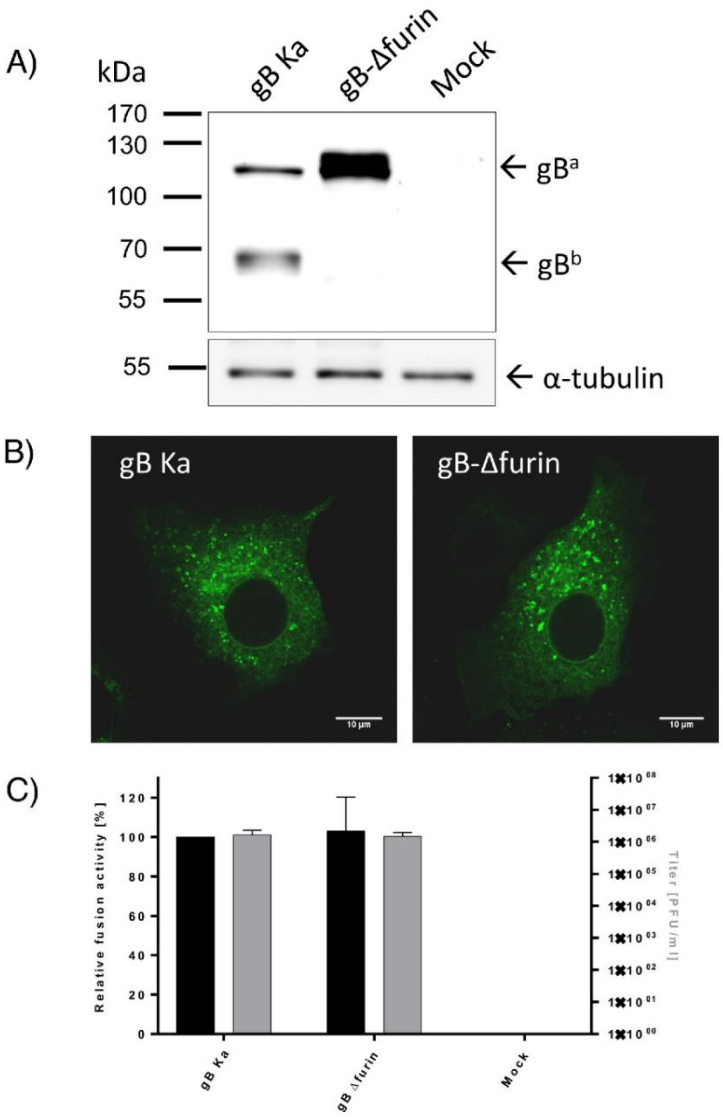

FIG 10 Functional characterization of gB-Δfurin. (A) Western blot analysis. Lysates of RK13 cells transfected with expression plasmids for wild-type gB (gB Ka) or the gB furin deletion mutant (gB-Δfurin) were separated by SDS-PAGE under reducing conditions. Cells transfected with the empty vector pcDNA3 served as a negative control (Mock). The blots were incubated with the gB-specific monoclonal antibody C15-b1. Signals of uncleaved gB (gB^a) or a furin-cleaved gB subunit (gB^b) are labeled by arrows, and the molecular masses of marker proteins are indicated. Signals of α-tubulin served as a loading control. (B) Subcellular localization. RK13 cells were transfected with expression plasmids for gB Ka or gB-Δfurin mutants and analyzed by indirect immunofluorescence. gB was detected using a gB-specific rabbit antiserum and Alexa Fluor 488-conjugated secondary antibodies. Green fluorescence was excited at 488 nm and recorded with a laser scanning confocal microscope (SP5; Leica, Mannheim, Germany). (C) Functional data. Results from the cell-cell fusion assay are plotted as black bars and expressed as the percentage of the signal measured for the WT protein, set to 100% (left *y* axis). The viral titers obtained in the *trans*-complementation assay are shown as gray bars (right *y* axis). PrV strain Kaplan (Ka) was used as a control. pcDNA-3-transfected cells were used as a negative control (Mock). The error bars indicate standard deviations from three independent experiments.

membrane, as determined by fluorescence-activated cell sorting (FACS) analysis (data not shown), making robust quantification complicated.

Next, the functions of the mutated proteins during virus entry were tested in a *trans*-complementation assay. RK13 cells were transfected with the different gB expression plasmids and infected 1 day later with a PrV mutant lacking the gB gene (PrV-ΔgB) (76). Cells and supernatant were harvested 24 h postinfection (p.i.), and progeny virus titers were determined on RK13-gB cells (Fig. 9A). Cells transfected with expression plasmids for gBs that efficiently mediated cell-cell fusion also complemented the defect of PrV-ΔgB during entry comparably to WT gB. In contrast, no infectious progeny was derived from cells transfected with the empty vector. Infectious progeny was also not produced after infection of cells transfected with the expression plasmid for W187A, indicating that this gB mutant is not functional. Surprisingly, Y192A, F275A, and F275Y gB mutants, which were unable to mediate cell-cell fusion, supported production of a low titer of infectious virions (10^2 PFU/ml), while expression of Y276A resulted in titers of 10^4 PFU/ml, indicating that the presence of other viral proteins might have partially compensated for the impairment in membrane binding and fusion.

DISCUSSION

Comparison with available gB structures from other herpesviruses. The structural alignment of PrV gB with the homologous HSV-1, EBV, and HCMV proteins demonstrated that the postfusion conformation is well preserved, with the main difference residing in the positioning of domain IV relative to the rest of the protein (Fig. 2). The low-resolution structure obtained for the full-length HSV-1 gB in a conformation distinct from the postfusion conformation localizes domain IV to the interior of the spike (30), implying that a large movement occurs during the conformational change. Insertion of a foot-and-mouth disease virus (FMDV) epitope in PrV gB domain IV, right after the residue Arg685, resulted in high titers of neutralizing antibodies against FMDV (77), suggesting that at least some of the antigenic determinants on PrV gB domain IV are presented at the surface when the protein is expressed in its prefusion form. It is also possible, however, that the epitope is available because a fraction of gB at the virion surface may have adopted the postfusion conformation.

Cholesterol dependence. HSV-1 gB binding to membranes was previously concluded to be cholesterol dependent based on experiments using binary liposomes made of DOPC and CH (54). As we show in this study, the ability of PrV gB to bind to liposomes is influenced not only by its FL residues, but also by the lipid membrane composition. The WT PrV gB ectodomains, as well as Y192F, Y267A, and Y276F variants, showed increased binding to 4L compared to 2L liposomes (Fig. 9B), whose composition does not emulate a real biological membrane well. We show here that liposomes, either 2L or 4L, need to contain at least 40% CH for gB to bind (Fig. 3C), which is in agreement with 30 to 40% CH being present in the plasma membrane and secretory vesicles (75) and with PrV entering cells via fusion with the plasma membrane. In the case of herpesviruses that enter cells by endocytosis, the requirement for a high CH concentration might also indicate that the fusion would occur within the internal compartments enriched in CH. A possible role for CH could be to fill the voids in the leaflet introduced by displacement of the bulkier head groups of the other lipids upon insertion of the FLs.

Cholesterol has been shown previously to induce lipid curvature and to promote formation of lipid stalks in fusion intermediates (25). While CH depletion was reported not to affect PrV attachment to cells, the virus was observed to be stalled at the plasma membrane, and entry was significantly reduced (58). It was speculated that the particles might have been blocked due to an inability to resolve the hemifusion intermediate in the absence of cholesterol, which is contrary to our observation that CH is required for the initial insertion of FLs into the membrane, i.e., for an early event that must take place prior to reaching the hemifusion state.

HSV-1 gB full-length protein expressed on cells was shown to associate specifically with CH- and SM-enriched lipid rafts (60), in which the two lipids are organized in the

so-called ordered lipid domains (Lo) (78). The borders between these Lo and the more fluid, disordered membrane domains (Ld) were identified as the preferred sites for insertion of the HIV Env class I fusion protein FP (79), presumably because they impose the smallest energy penalty for insertion due to the line tension caused by the discontinuity between the domains. Desplanques et al. had previously observed a significant fraction of PrV virions juxtaposed with the lipid raft marker GM1 (58), which could, in the light of the Env insertion mode, indicate that PrV may use Lo-Ld boundaries as sites of attachment, as well. Although the FP of HIV Env is a short hydrophobic sequence that has a free N terminus, in contrast to the bipartite internal FLs of gB, it is tempting to speculate that despite the different natures of the inserted segments, similar energetic constraints might apply to membrane insertion of these divergent proteins. Further experimental studies on herpesvirus gB are needed to test these hypotheses and to establish if CH is required for binding of herpesviruses to membranes, for membrane fusion, or for both. It is worth noting that our EM data show an even distribution of the PrV gB ectodomains bound to liposomes, opposing the idea of gB having preferred membrane insertion sites. This could be due to the properties of the liposomes used for EM, which were made of 60% DOPC and 40% CH, a binary mixture that would be expected to form the Lo phase only (80).

Furin processing. Proteolytic cleavage by cellular furin had been previously reported to be dispensable for gB function in herpesviruses encoding cleavable gBs, as its absence did not have an effect on viral replication or penetration kinetics, although smaller syncytia were detected (81–85). A similar observation was made when gB was expressed in LoVo cells, which are naturally deficient in furin, suggesting that PrV gB cleavage may play a role in cell-cell fusion (83). Our data demonstrate that furin cleavage of PrV gB was not required for its activity in cell-cell fusion and the virus transcomplementation assays used in this study (Fig. 10). The discrepancy between our results regarding the gB-Δfurin variant function in cell-cell fusion and those reported by Okazaki (83) could be due to the different cell types used for fusion.

PrV gB FL variants in liposome binding and functional assays. The liposome binding experiments performed with the 15 recombinant gB ectodomain variants studied here allowed the selection of a subset of variants to be followed up by studies in the context of the full-length protein, both in cell-cell fusion and after incorporation into virus particles. The gB ectodomains in interaction with liposomes provided snapshots of the protein already in the postfusion form (Fig. 7A and 9B and C). The functional assays, on the other hand, illuminated the functions of full-length protein mutants expressed at the cell surface or incorporated into virus particles in their prefusion state (Fig. 9A). This may explain certain discrepancies, for instance, with variants that were expressed well as recombinant ectodomains but that failed to be folded and transported to the cell surface in cells. The selected variants of full-length gB were assessed for the ability to mediate fusion in two functional assays: a virus-free cell-cell fusion assay and *trans*-complementation of gB-negative PrV (18, 19, 21, 71).

To simplify comparisons with gBs from other herpesviruses, we numbered the FL residues from 1 to 14 (Fig. 5A). Our mutagenesis data are consistent with a model in which the residues Trp187 (FL1-3), Tyr192 (FL1-8), and Tyr276 (FL2-10) form an aromatic surface compatible with insertion into the polar region of the membrane, establishing an interfacial rim structure that would provide multiple interactions with the lipid head groups, while Phe275 (FL2-9) would reach deeper into the hydrocarbon core (Fig. 11A). gB sequence conservation in alphaherpesviruses shows that residues with similar membrane-partitioning preferences are found at these four positions (see Fig. S1 in the supplemental material). Hydrophobic residues compatible with insertion into the membrane core (Phe, Val, Leu, and Trp) are present at FL2-9, while amphipathic side chains that would favor the interfacial region (Tyr, His, and Trp) are found at positions FL1-3, FL1-8, and FL2-10. This suggests that a common mode of gB insertion into membranes may have evolved within the alphaherpesvirus subfamily, although the residues interacting with lipids may not be identical. Charged residues, such as Arg and Glu, are

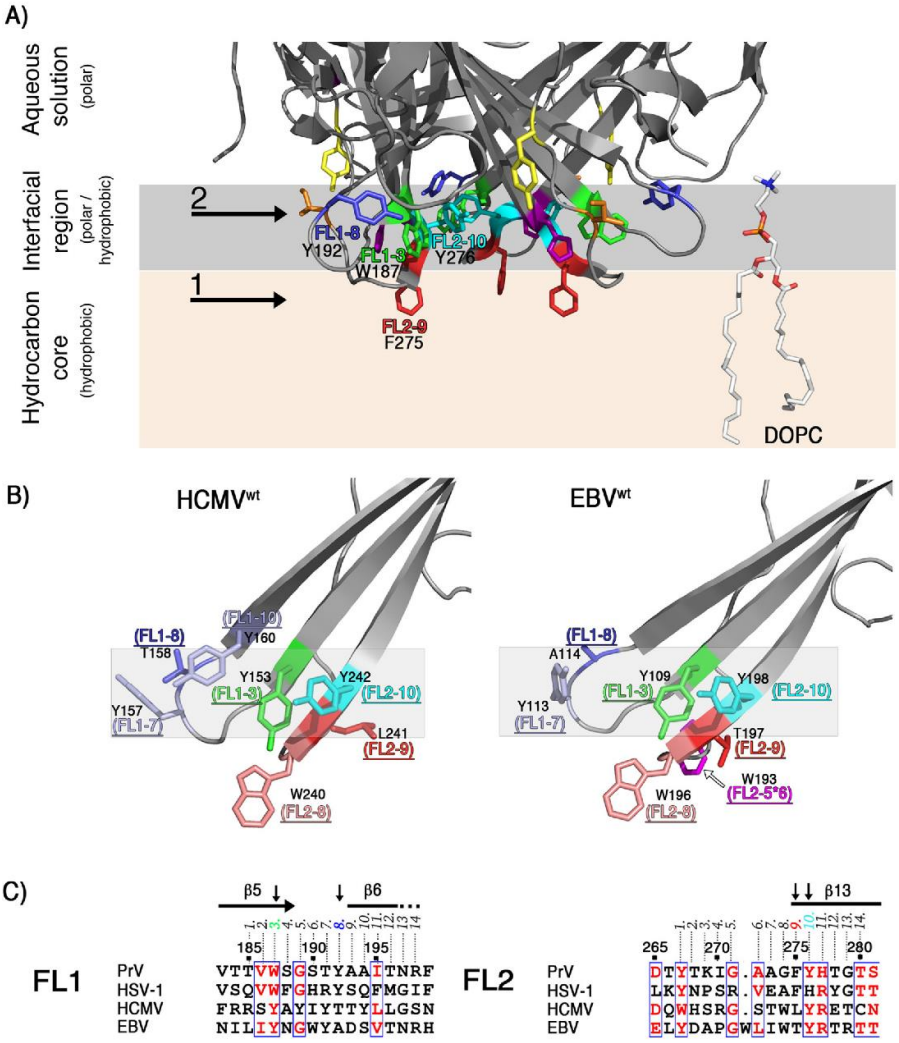

FIG 11 (A) Model of PrV gB ectodomain interactions with membranes. The model displays the base of the PrV gB trimer, illustrating putative locations of the FL residues investigated in this study, shown with their side chains as sticks and colored as in Fig. 5B. The arrows and numbers are used to indicate the deeper insertion of Phe275 (FL2-9) into the apolar region containing the lipid tails (1) and the interfacial rim made of Tyr192, Trp187, Tyr276 (2) (FL1-8, FL1-3, and FL2-10) that would be located within the more polar part of the membrane. A single molecule of DOPC and its putative localization in the membrane are shown in stick representation on the right. Carbon, oxygen, phosphorus, and nitrogen atoms are colored white, red, orange, and blue, respectively. (B) Model of HCMV and EBV gB interactions with membranes. HCMV (PDB accession number 5CXF), and EBV (PDB accession number 3FVC) gB structures were superimposed on the PrV structure using the Dali pairwise alignment algorithm (106). The last two structures contain WT residues (YIY$^{155–157}$ and WLY$^{240–242}$ in HCMV gB; WY$^{112–113}$ and WLIW$^{193–196}$ in EBV gB) that were modeled back onto the FL residues that had been mutated in the crystallized constructs (GHR$^{155–157}$ and ATH$^{240–242}$ in HCMV and HR$^{112–113}$ and RVEA$^{193–196}$ in EBV). The residues at positions FL1-8, FL1-3, FL2-10, and FL2-9 are indicated and colored as in Fig. 5B, with their side chains shown as sticks. Trp residues found at FL2-8 in HCMV and EBV gB are colored salmon, and Tyr side chains at positions FL1-10 and FL1-7 in HCMV and EBV gBs are colored light blue. The gray shading highlights the putative interfacial rim in each structure. The side chain of Trp^{193} inserted between residues FL2-5 and FL2-6 in EBV gB is labeled FL2-5*6 and colored magenta. Other hydrophobic residues are not shown as sticks for clarity. (C) Sequence alignment of the FL regions. Residues with similar physicochemical properties that are 75% or more conserved are colored red. Secondary-structure elements corresponding to the PrV gB ectodomain structure are displayed at the top, and residues identified as membrane contact sites in PrV gB (FL1-3, FL1-8, FL2-9, and FL2-10) are indicated with black arrows. The numbering at the top corresponds to that of the PrV gB protein. The alignment was generated in Clustal Omega (107) and displayed using ESPript (108).

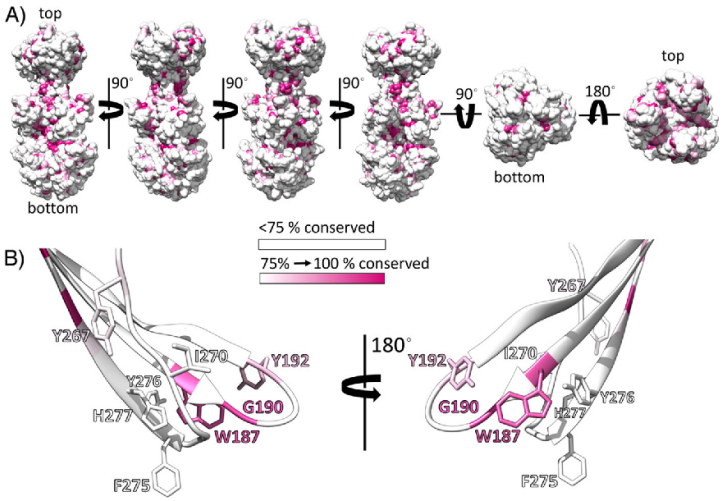

FIG 12 Conservation of gB in alphaherpesviruses plotted on the PrV gB ectodomain structure. (A) Solvent-accessible surface of PrV gB in multiple orientations. Residues showing identity lower than 75% are colored white, while the residues that are strictly conserved in more than 75% of the analyzed sequences are colored in an increasing purple gradient. The alignment shown in Fig. S1 in the supplemental material was used. (B) PrV gB FLs. Fusion loop residues investigated in this study are shown with the side chains in stick representation. Two orientations are presented for clarity.

present in the FLs of HSV-1 but not of PrV gB (Fig. 5A), highlighting intrinsic differences that exist despite potentially shared principles for insertion of aromatic and hydrophobic residues.

The FL2-9 position is always occupied by a hydrophobic side chain, such as Phe275 in PrV gB. Mutation of the corresponding residue in HSV-1 gB (Phe262) to Asp or Leu resulted, respectively, in a poorly expressed protein and a protein that could mediate fusion at 70% of the level measured for the WT protein (51, 54). The tolerance for Leu (but not for Asp) in HSV-1 gB and for Trp (but not for Tyr) in PrV gB indicates that FL2-9 has the potential to insert into the membrane core, i.e., deeper than the interfacial region.

Positions FL1-3 (Trp187), FL1-5 (Gly189), and FL1-8 (Tyr192) are occupied by the best-conserved residues in FL1 of alphaherpesviruses (Fig. 12; see Fig. S1 in the supplemental material). FL1-5 Gly has already been shown to be important for the function of HSV-1 gB (54) and was not tested here. Mutation of HSV-1 gB FL1-3 (Trp) to Tyr resulted in a protein that was 50% active in fusion (51). When the same residue was changed to Phe in PrV gB, the resulting ectodomain did not cofloat with liposomes. It is possible that the FL1-3 position requires Trp because its indole ring may be involved in interactions with a specific lipid and/or because its central location between FL1-8 and FL2-10 might be important for the structural integrity and docking of the trio of rim residues into the membrane interface. HSV-1 gB variants containing Ser and Arg at positions FL1-3 and FL1-8, respectively, were shown to be defective in fusion and in liposome binding (54). These variants were subsequently crystallized, demonstrating that the mutations did not introduce any structural changes in FL1 and that the loss of binding to liposomes was solely due to the elimination of the hydrophobic side chains (86). While we anticipate that the same is true for the PrV gB ectodomains with mutations in FL1-3 and FL1-8, it is important to note that when expressed in cells as full-length proteins, W187A and Y192A accumulated in intracellular compartments and showed impaired processing (Fig. 8). We speculate that the furin sites in the misfolded gB variants may not be accessible for cleavage, giving rise to the observed decrease in

the amount of cleaved protein. The possibility therefore remains that these two FL1 variants were not active in functional assays due to the altered cellular localization, even though production of ectodomains with the same mutations in insect cells led to efficient protein secretion into the medium, suggesting that these residues are at least not important for correct folding of the postfusion ectodomain.

The FL2-10 residue is predicted to insert into the interfacial region, and while PrV gB Y276F was functional, Y276A did not associate with liposomes and failed to mediate cell-cell fusion, although it unexpectedly partially rescued gB-null virus in the complementation assay. This result emphasizes distinct functional requirements for cell-cell fusion and viral entry processes and that the two do not follow identical mechanisms. This is highlighted by the requirement for gD in PrV entry but not for cell-cell spread (18, 87). The presence of other viral proteins during infection may compensate for the reduced membrane binding activity, and/or the protein may be present at higher density in the virion envelope than at the cell surface, favoring the fusion function.

FL2-1 is the most conserved FL2 residue in alphaherpesviruses, being Tyr in 75% of the sequences (Fig. 12; see Fig. S1 in the supplemental material). This residue was not mutagenized in HSV-1 gB but was analyzed here for PrV gB, revealing, to our surprise, that changes to Ala or Phe had no effect. This suggests that Tyr267 is not directly involved in interactions with liposomes and is not essential for the protein function in fusion. Interestingly, Y267F bound indiscriminately to 2L and 4L liposomes, while Y267A was sensitive to the lipid composition and associated better with the 4L liposomes. Membrane composition has been shown to also influence binding of fusion proteins of flaviviruses (88, 89), bunyaviruses (90), influenza virus (91), and HIV (92). In the last case, the FP of gp41 was shown to adopt an α-helical or β-strand structure, depending on the CH concentration, indicating alternative modes of insertion into membranes of the same protein.

Position FL2-11 is occupied by Arg in most alphaherpesviruses and by His in PrV gB. The substitution of this residue for Ala or the larger Trp in PrV gB resulted in a functional protein that associated with liposomes, indicating that the aromatic side chain is not important for interactions with lipids. In contrast, Arg present at the same position in HSV-1 gB and in 26 other analyzed sequences (see Fig. S1 in the supplemental material) was implicated in binding to liposomes, possibly by interacting with the negatively charged phosphate head groups of membrane lipids (54). The His and Arg side chains present at position FL2-11 obviously play different roles in binding to lipids.

Model of PrV gB interactions with lipids. We show here that PrV gB residues Trp187, Tyr192, Gly274, Phe275, and Tyr276 form a continuous, electrostatically neutral hydrophobic surface (Fig. 7B) reminiscent of the hydrophobic patch reported for HSV-1 gB (54). EBV and HCMV gB ectodomains used for crystallization had polar and charged residues inserted in place of the hydrophobic WT FL residues, but similar hydrophobic patches at the base of the trimers were observed when the WT residues were modeled back on the structure (data not shown). This strongly suggests functional conservation of the areas involved in membrane interactions. Closer inspection of the HCMV and EBV gB FL residues found at the positions identified as the membrane contact sites in PrV gB revealed that two of the three rim positions, FL1-3 and FL2-10, are occupied by Tyr, similar to gBs of alphaherpesviruses, while Thr and Ala are found at FL1-8 in HCMV and EBV gBs, respectively (Fig. 11B and C). The Tyr residues at FL1-3 and FL2-10 are highly conserved in beta- and gammaherpesviruses (data not shown), while FL1-8 is not. In addition, the side chain of Tyr, found at the neighboring FL1-10 in HCMV and at FL1-7 in HCMV and EBV gBs, could reach the plane in which FL1-3 and FL2-10 side chains insert, contributing to formation of the interfacial rim. FL2-9, which according to our model inserts more deeply, is Leu in HCMV gB and Thr in EBV gB, while Trp is found at FL2-8 in both proteins. This Trp is strictly conserved within betaherpesviruses and partially within gammaherpesviruses, while the latter have in addition a well-conserved Trp inserted between FL2-5 and FL2-6 (designated FL2-5*6 in Fig. 11B). There are also other hydrophobic residues in the FLs on HCMV and EBV gBs whose side chains could

insert into the lipid bilayer (FL1-4, FL1-5, and FL1-6 in HCMV and FL1-6, FL2-6, and FL2-7 in EBV gB) (not shown in Fig. 11B for clarity). Thus, although they have more hydrophobic residues at the tips of the FLs, our model suggests that beta- and gammaherpesvirus gBs interact with the membranes similarly to alphaherpesvirus gB, with exposed hydrophobic residues in FL2 penetrating into the hydrocarbon core (FL2-9 and/or FL2-8 and/or FL2-5*6), while the rim formed by residues from both FLs (FL1-3, FL1-7, and FL2-10) would secure protein insertion into the interface. The exact molecular mechanisms through which this is achieved may vary, pointing to differences between the herpesvirus subfamilies that might be related to the different host cells and the specific compositions of the target membranes.

MATERIALS AND METHODS

Expression and purification of the PrV gB ectodomain in insect cells for crystallization studies. The synthetic gene encoding gB of suid herpesvirus 1 strain Kaplan (GenBank accession number AEM64049.1) was codon optimized for protein expression in *Drosophila* S2 cells and was purchased from GenScript. The gene segment encoding the ectodomain (PrV gB residues 59 to 756) was cloned into the expression vector pT350 (61) so that the ectodomain was flanked by the *Drosophila* Bip secretion signal, driving efficient protein secretion (93) at the N terminus, and the enterokinase-cleavable double Strep-tag II (sequence SRFESDDDDKAGWSHPQFEKGGGSGGGSGGGSWSHPQFEK) at the C terminus. Protein expression was induced by the addition of 0.5 mM $CuSO_4$, and the protein was harvested from the culture supernatant 7 days postinduction (the detailed protocol is available in reference 62). Standard protocols were applied to purify the protein by affinity (Streptactin resin; IBA Technologies) and then by size exclusion chromatography using 10 mM Tris, 50 mM NaCl, pH 8, buffer and a Superdex S200 column. An extinction coefficient of 1.2 ml/mg for protein absorbance at 280 nm was used for calculation of the protein concentration.

Crystallization and structure determination of the PrV gB ectodomain. Purified PrV gB ectodomains were deglycosylated with Endo D from *Streptococcus pneumoniae* (94) by overnight incubation of gB and Endo D in a 10:1 (wt/wt) ratio in 50 mM sodium-phosphate buffer, pH 7.5, at 25°C. The reaction mixture was then loaded onto a Superdex S200 column to separate deglycosylated gB from Endo D, using 10 mM Tris, 50 mM NaCl, pH 8, buffer. Fractions corresponding to gB were pooled, and the protein was concentrated to 9.2 mg/ml in a 50-kDa-cutoff Vivaspin concentrator.

Crystals were grown by vapor diffusion in hanging drops in 0.1 M Tris, pH 8.5, 7% PEG 4000, 0.6 M LiCl and then flash frozen in liquid nitrogen using 20% glycerol as the cryoprotectant. Data were collected at the European Synchrotron Radiation Facility (ESRF) synchrotron source ID29 beamline and processed using XDS (95). Molecular replacement was done with Phaser (96) using HSV-1 gB structure (Protein Data Bank [PDB] accession number 2GUM) as a search model. The structure was refined using BUSTER (97).

Electron microscopy. Samples for negative-stain EM were prepared by mixing 0.5 μM protein and 1 mM liposomes as described in more detail under "Liposome Flotation Assay" below. Liposomes were made of 60% DOPC and 40% CH. Staining was done with 2% uranyl acetate, and images were collected on a Tecnai G2 Spirit Biotwin microscope 5 (FEI) operating at an accelerating voltage of 120 kV. Samples for cryo-EM analysis were made by incubating 4 μM protein and 2 mM liposomes. Cryofixation was done using Lacey grids (Leica EMGP, Austria). Data were recorded on a Tecnai F20 operating at 200 kV, equipped with a Falcon II direct detector (FEI) under low-dose conditions.

Generation of expression constructs and production of PrV gB recombinant ectodomains in mammalian cells. The gene encoding PrV gB ectodomain residues 59 to 756, followed by a double Strep-tag II, was cloned into the pcDNA4 (Invitrogen) expression vector using Gibson Assembly master mix (New England BioLabs). QuikChange mutagenesis was applied to introduce single point mutations in the FLs, following the standard protocols (Agilent Technologies; QuikChange II site-directed mutagenesis kit). The presence of desired mutations was confirmed by DNA sequencing. The expression constructs were transfected into Expi293F mammalian cells (Thermo Fisher Scientific) using Expifectamine transfection agent as described in the manufacturer's manual (Thermo Fisher Scientific). Cell supernatants were collected 5 days posttransfection, and the protein was purified by affinity chromatography on Streptactin resin (IBA Technologies), followed by SEC.

Liposome flotation assay. Lipids, DOPC, DOPE, SM (from bovine brain), and CH (from ovine wool) were purchased from Avanti Polar Lipids. Liposomes were prepared by the freeze-thaw and extrusion method (98), using 200-nm membranes for extrusion. 2L liposomes were made of 60 mol% DOPC and 40 mol% CH, and 4L liposomes were 20 mol% DOPC, 20 mol% DOPE, 20 mol% SM, and 40 mol% CH. Recombinant 0.5 μM gB ectodomains were mixed with 1 mM liposomes in phosphate-buffered saline (PBS) in a 100-μl volume, incubated overnight (12 to 15 h) at 4°C and then at 37°C for 15 min (the overnight incubation can be omitted and was done for convenience). OptiPrep medium (Axis-Shield PoC AS, Oslo, Norway) was used for density gradient preparation. Protein-liposome samples were adjusted to a volume of 300 μl by addition of 30 μl of PBS and 170 μl of 60% OptiPrep (final OptiPrep concetration, 36%) and deposited with a syringe on the bottom of the ultracentrifuge tube already containing 4.5 ml of 20% OptiPrep solution in PBS. Two hundred microliters of PBS was added to the top, and the samples were centrifuged for 1 h at 40,000 $\times$ *g* and 4°C in an SWTi 55 swinging-bucket rotor in a Beckman Coulter ultracentrifuge. The 5-ml gradients were fractionated into two 400-μl fractions (the first one representing the top fraction), three 1.2-ml fractions, and one 600-μl (bottom) fraction. Thirty-microliter aliquots of the

top and bottom fractions were analyzed on SDS-PAGE 4 to 20% gradient gels (GenScript), and Western blotting to detect the Strep-tag II on gB was done with a Streptactin-horseradish peroxidase (HRP) conjugate (IBA Technologies) following the manufacturer's instructions.

Viruses and cells. Rabbit kidney (RK13) and RK13-gB cells were grown in Dulbecco's modified Eagle's minimum essential medium (MEM) supplemented with 10% fetal calf serum (FCS) at 37°C and 5% CO_2. A PrV mutant lacking gB (PrV-ΔgB) (76), which was derived from PrV strain Kaplan (PrV-Ka), was propagated in RK13-gB cells.

Expression plasmids for cell-cell fusion assays. Generation of expression plasmids for PrV-Ka gB, gH, and gL has been described previously (70). The expression plasmid pcDNA-gB^{Ka} containing the gB open reading frame (ORF UL27) was used for site-directed mutagenesis (QuikChange II XL kit; Agilent) with the complementary pair of oligonucleotide primers. Correct mutagenesis was verified by sequencing.

***In vitro* cell-cell fusion assays.** Fusion activities of the different gB mutants were analyzed after transient transfection of RK13 cells as described recently (72). Briefly, approximately 1.8×10^5 RK13 cells per well were seeded onto 24-well cell culture plates. On the following day, the cells were transfected with 200 ng each of expression plasmids for EGFP (pEGFP-N1; Clontech) and for PrV glycoprotein gB^{Ka} or mutant gB, gL^{Ka}, and gH^{Ka} (21, 70, 99) in 100 μl Opti-MEM using 1 μl Lipofectamine 2000 (Thermo Fisher Scientific). An empty vector (pcDNA3) served as a negative control. The mixture was incubated for 20 min at room temperature and added to the cells. After 3 h, the cells were washed with PBS and incubated in MEM supplemented with 2% FCS for another 24 h at 37°C. Thereafter, the cells were fixed with 3% paraformaldehyde (PFA). Syncytium formation was analyzed using an Eclipse Ti-S fluorescence microscope and NIS Elements imaging software (Nikon). Total fusion activity was determined by multiplication of the area of cells with three or more nuclei by the number of syncytia within 10 fields of view (5.5 mm² each). The experiment was repeated three times, and average percent values of positive-control transfections, as well as standard deviations, were calculated.

***trans*-complementation assay.** The functions of the different gB mutants in virus entry were determined by *trans*-complementation of PrV-ΔgB (76). Approximately 1.8×10^5 RK13 cells per well were seeded onto 24-well cell culture plates. On the following day, the cells were transfected with 200 ng of the corresponding gB expression plasmid as described above. One day posttransfection, the cells were infected with phenotypically gB-complemented PrV-ΔgB at a multiplicity of infection (MOI) of 3 and consecutively incubated on ice for 1 h and at 37°C for 1 h. Subsequently, the inoculum was removed, nonpenetrated virus was inactivated by low-pH treatment (100), and 1 ml fresh medium was added. After 24 h at 37°C, the cells were harvested together with the supernatants and lysed by freeze-thawing (−80°C and 37°C). Progeny virus titers were determined on PrV gB-expressing cells (RK13-gB) (76). The mean values of three independent experiments with the corresponding standard deviations are shown.

Indirect immunofluorescence tests. To test for subcellular localization of the mutated proteins, RK13 cells were transfected with the gB expression plasmids as described above. After 24 h, the cells were fixed with 3% PFA for 20 min and permeabilized in PBS containing 0,1% Triton X-100 for 10 min at room temperature. Subsequently, the cells were incubated with a rabbit antiserum specific for PrV gB (101), which was diluted 1:1,000 in PBS. After 1 h at room temperature, bound antibody was detected with Alexa 488-conjugated goat anti-rabbit antibodies (1:1,000 in PBS; Invitrogen). After each step, the cells were washed repeatedly with PBS. Green fluorescence was excited at 488 nm and recorded with a laser scanning confocal microscope (SP5; Leica, Mannheim, Germany).

Western blot analyses. RK13 cells were harvested 24 h after transfection with the different gB expression plasmids, as described above. The cells were lysed, and protein samples were separated by SDS-PAGE and transferred to a nitrocellulose membrane. The membrane was incubated with a monoclonal gB antibody (C15-b1 at 1:500 dilution) (101, 102). Binding of peroxidase-conjugated secondary antibody (Jackson ImmunoResearch) was detected with Clarity Western ECL substrate (Bio-Rad) and recorded with a VersaDoc 4000 MP imager (Bio-Rad).

Accession number(s). The PrV gB coordinates have been deposited in the RCSB Protein Data Bank (PDB) under accession code 6ESC.

SUPPLEMENTAL MATERIAL

Supplemental material for this article may be found at https://doi.org/10.1128/JVI.01203-17.

SUPPLEMENTAL FILE 1, PDF file, 9.4 MB.

ACKNOWLEDGMENTS

Work done by M.B., D.B., M.-C.V., P.G.-C., and F.A.R. was supported by Institut Pasteur and CNRS recurrent funding and the Pasteur-Weizmann/Servier International Prize (F.A.R., 2015). Work done by M.V., B.G.K., and T.C.M. was supported by DFG, grant Me 854/11-2.

We acknowledge assistance of the core facilities for crystallization and microscopy at Institut Pasteur and also thank M. Nilges and the Equipex CACSICE for providing the Falcon II direct detector. We thank the European Synchrotron Radiation Facility for help during data collection.

REFERENCES

1. Pellet PE, Roizman B. 2014. Herpesviridae, p 1802–1822. *In* Knipe DM, Howley PM (ed), Fields virology, 6th ed, vol 2. Lippincott Williams & Wilkins, New York, NY.
2. Mettenleiter TC. 1996. Immunobiology of pseudorabies (Aujeszky's disease). Vet Immunol Immunopathol 54:221–229. https://doi.org/10.1016/S0165-2427(96)05695-4.
3. Pomeranz LE, Reynolds AE, Hengartner CJ. 2005. Molecular biology of pseudorabies virus: impact on neurovirology and veterinary medicine. Microbiol Mol Biol Rev 69:462–500. https://doi.org/10.1128/MMBR.69.3.462-500.2005.
4. Eisenberg RJ, Atanasiu D, Cairns TM, Gallagher JR, Krummenacher C, Cohen GH. 2012. Herpes virus fusion and entry: a story with many characters. Viruses 4:800–832. https://doi.org/10.3390/v4050800.
5. Nicola AV. 2016. Herpesvirus entry into host cells mediated by endosomal low pH. Traffic 17:965–975. https://doi.org/10.1111/tra.12408.
6. Li A, Lu G, Qi J, Wu L, Tian K, Luo T, Shi Y, Yan J, Gao GF. 2017. Structural basis of nectin-1 recognition by pseudorabies virus glycoprotein D. PLoS Pathog 13:e1006314. https://doi.org/10.1371/journal.ppat.1006314.
7. Spear PG. 2004. Herpes simplex virus: receptors and ligands for cell entry. Cell Microbiol 6:401–410. https://doi.org/10.1111/j.1462-5822.2004.00389.x.
8. Vanarsdall AL, Chase MC, Johnson DC. 2011. Human cytomegalovirus glycoprotein gO complexes with gH/gL, promoting interference with viral entry into human fibroblasts but not entry into epithelial cells. J Virol 85:11638–11645. https://doi.org/10.1128/JVI.05659-11.
9. Mullen MM, Haan KM, Longnecker R, Jardetzky TS. 2002. Structure of the Epstein-Barr virus gp42 protein bound to the MHC class II receptor HLA-DR1. Mol Cell 9:375–385. https://doi.org/10.1016/S1097-2765(02)00465-3.
10. Krummenacher C, Carfi A, Eisenberg RJ, Cohen GH. 2013. Entry of herpesviruses into cells: the enigma variations. Adv Exp Med Biol 790:178–195. https://doi.org/10.1007/978-1-4614-7651-1_10.
11. Sathiyamoorthy K, Chen J, Longnecker R, Jardetzky TS. 2017. The COMPLEXity in herpesvirus entry. Curr Opin Virol 24:97–104. https://doi.org/10.1016/j.coviro.2017.04.006.
12. Agelidis AM, Shukla D. 2015. Cell entry mechanisms of HSV: what we have learned in recent years. Future Virol 10:1145–1154. https://doi.org/10.2217/fvl.15.85.
13. Di Giovine P, Settembre EC, Bhargava AK, Luftig MA, Lou H, Cohen GH, Eisenberg RJ, Krummenacher C, Carfi A. 2011. Structure of herpes simplex virus glycoprotein D bound to the human receptor nectin-1. PLoS Pathog 7:e1002277. https://doi.org/10.1371/journal.ppat.1002277.
14. Lazear E, Whitbeck JC, Zuo Y, Carfi A, Cohen GH, Eisenberg RJ, Krummenacher C. 2014. Induction of conformational changes at the N-terminus of herpes simplex virus glycoprotein D upon binding to HVEM and nectin-1. Virology 448:185–195. https://doi.org/10.1016/j.virol.2013.10.019.
15. Gianni T, Amasio M, Campadelli-Fiume G. 2009. Herpes simplex virus gD forms distinct complexes with fusion executors gB and gH/gL in part through the C-terminal profusion domain. J Biol Chem 284:17370–17382. https://doi.org/10.1074/jbc.M109.005728.
16. Atanasiu D, Saw WT, Cohen GH, Eisenberg RJ. 2010. Cascade of events governing cell-cell fusion induced by herpes simplex virus glycoproteins gD, gH/gL, and gB. J Virol 84:12292–12299. https://doi.org/10.1128/JVI.01700-10.
17. Schmidt J, Klupp BG, Karger A, Mettenleiter TC. 1997. Adaptability in herpesviruses: glycoprotein D-independent infectivity of pseudorabies virus. J Virol 71:17–24.
18. Rauh I, Mettenleiter TC. 1991. Pseudorabies virus glycoproteins gII and gp50 are essential for virus penetration. J Virol 65:5348–5356.
19. Peeters B, de Wind N, Broer R, Gielkens A, Moormann R. 1992. Glycoprotein H of pseudorabies virus is essential for entry and cell-to-cell spread of the virus. J Virol 66:3888–3892.
20. Klupp BG, Fuchs W, Weiland E, Mettenleiter TC. 1997. Pseudorabies virus glycoprotein L is necessary for virus infectivity but dispensable for virion localization of glycoprotein H. J Virol 71:7687–7695.
21. Schröter C, Vallbracht M, Altenschmidt J, Kargoll S, Fuchs W, Klupp BG, Mettenleiter TC. 2015. Mutations in pseudorabies virus glycoproteins gB, gD, and gH functionally compensate for the absence of gL. J Virol 90:2264–2272. https://doi.org/10.1128/JVI.02739-15.
22. Roche S, Bressanelli S, Rey FA, Gaudin Y. 2006. Crystal structure of the low-pH form of the vesicular stomatitis virus glycoprotein G Science 313:187–191.
23. Kadlec J, Loureiro S, Abrescia NG, Stuart DI, Jones IM. 2008. The postfusion structure of baculovirus gp64 supports a unified view of viral fusion machines. Nat Struct Mol Biol 15:1024–1030. https://doi.org/10.1038/nsmb.1484.
24. Harrison SC. 2015. Viral membrane fusion. Virology 479-480:498–507. https://doi.org/10.1016/j.virol.2015.03.043.
25. Chernomordik LV, Kozlov MM. 2008. Mechanics of membrane fusion. Nat Struct Mol Biol 15:675–683. https://doi.org/10.1038/nsmb.1455.
26. Heldwein EE, Lou H, Bender FC, Cohen GH, Eisenberg RJ, Harrison SC. 2006. Crystal structure of glycoprotein B from herpes simplex virus 1. Science 313:217–220. https://doi.org/10.1126/science.1126548.
27. Backovic M, Longnecker R, Jardetzky TS. 2009. Structure of a trimeric variant of the Epstein-Barr virus glycoprotein B. Proc Natl Acad Sci U S A 106:2880–2885. https://doi.org/10.1073/pnas.0810530106.
28. Chandramouli S, Ciferri C, Nikitin PA, Calo S, Gerrein R, Balabanis K, Monroe J, Hebner C, Lilja AE, Settembre EC, Carfi A. 2015. Structure of HCMV glycoprotein B in the postfusion conformation bound to a neutralizing human antibody. Nat Commun 6:8176. https://doi.org/10.1038/ncomms9176.
29. Burke HG, Heldwein EE. 2015. Crystal structure of the human cytomegalovirus glycoprotein B. PLoS Pathog 11:e1005227. https://doi.org/10.1371/journal.ppat.1005227.
30. Zeev-Ben-Mordehai T, Vasishtan D, Hernandez Duran A, Vollmer B, White P, Prasad Pandurangan A, Siebert CA, Topf M, Grunewald K. 2016. Two distinct trimeric conformations of natively membrane-anchored full-length herpes simplex virus 1 glycoprotein B. Proc Natl Acad Sci U S A 113:4176–4181. https://doi.org/10.1073/pnas.1523234113.
31. Roche S, Rey FA, Gaudin Y, Bressanelli S. 2007. Structure of the prefusion form of the vesicular stomatitis virus glycoprotein G. Science 315:843–848. https://doi.org/10.1126/science.1135710.
32. Gallagher JR, Atanasiu D, Saw WT, Paradisgarten MJ, Whitbeck JC, Eisenberg RJ, Cohen GH. 2014. Functional fluorescent protein insertions in herpes simplex virus gB report on gB conformation before and after execution of membrane fusion. PLoS Pathog 10:e1004373. https://doi.org/10.1371/journal.ppat.1004373.
33. Chowdary TK, Cairns TM, Atanasiu D, Cohen GH, Eisenberg RJ, Heldwein EE. 2010. Crystal structure of the conserved herpesvirus fusion regulator complex gH-gL. Nat Struct Mol Biol 17:882–888. https://doi.org/10.1038/nsmb.1837.
34. Matsuura H, Kirschner AN, Longnecker R, Jardetzky TS. 2010. Crystal structure of the Epstein-Barr virus (EBV) glycoprotein H/glycoprotein L (gH/gL) complex. Proc Natl Acad Sci U S A 107:22641–22646. https://doi.org/10.1073/pnas.1011806108.
35. Xing Y, Oliver SL, Nguyen T, Ciferri C, Nandi A, Hickman J, Giovani C, Yang E, Palladino G, Grose C, Uematsu Y, Lilja AE, Arvin AM, Carfi A. 2015. A site of varicella-zoster virus vulnerability identified by structural studies of neutralizing antibodies bound to the glycoprotein complex gHgL. Proc Natl Acad Sci U S A 112:6056–6061. https://doi.org/10.1073/pnas.1501176112.
36. Backovic M, DuBois RM, Cockburn JJ, Sharff AJ, Vaney MC, Granzow H, Klupp BG, Bricogne G, Mettenleiter TC, Rey FA. 2010. Structure of a core fragment of glycoprotein H from pseudorabies virus in complex with antibody. Proc Natl Acad Sci U S A 107:22635–22640. https://doi.org/10.1073/pnas.1011507107.
37. Heldwein EE. 2016. gH/gL supercomplexes at early stages of herpesvirus entry. Curr Opin Virol 18:1–8. https://doi.org/10.1016/j.coviro.2016.01.010.
38. White JM, Delos SE, Brecher M, Schornberg K. 2008. Structures and mechanisms of viral membrane fusion proteins: multiple variations on a common theme. Crit Rev Biochem Mol Biol 43:189–219. https://doi.org/10.1080/10409230802058320.
39. Ito H, Watanabe S, Sanchez A, Whitt MA, Kawaoka Y. 1999. Mutational analysis of the putative fusion domain of Ebola virus glycoprotein. J Virol 73:8907–8912.
40. Apellaniz B, Huarte N, Largo E, Nieva JL. 2014. The three lives of viral fusion peptides. Chem Phys Lipids 181:40–55. https://doi.org/10.1016/j.chemphyslip.2014.03.003.
41. Bressanelli S, Stiasny K, Allison SL, Stura EA, Duquerroy S, Lescar J, Heinz FX, Rey FA. 2004. Structure of a flavivirus envelope glycoprotein in its

low-pH-induced membrane fusion conformation. EMBO J 23:728–738. https://doi.org/10.1038/sj.emboj.7600064.
42. Voss JE, Vaney MC, Duquerroy S, Vonrhein C, Girard-Blanc C, Crublet E, Thompson A, Bricogne G, Rey FA. 2010. Glycoprotein organization of Chikungunya virus particles revealed by X-ray crystallography. Nature 468:709–712. https://doi.org/10.1038/nature09555.
43. DuBois RM, Vaney MC, Tortorici MA, Kurdi RA, Barba-Spaeth G, Krey T, Rey FA. 2013. Functional and evolutionary insight from the crystal structure of rubella virus protein E1. Nature 493:552–556. https://doi.org/10.1038/nature11741.
44. Dessau M, Modis Y. 2013. Crystal structure of glycoprotein C from Rift Valley fever virus. Proc Natl Acad Sci U S A 110:1696–1701. https://doi.org/10.1073/pnas.1217780110.
45. Guardado-Calvo P, Bignon EA, Stettner E, Jeffers SA, Perez-Vargas J, Pehau-Arnaudet G, Tortorici MA, Jestin JL, England P, Tischler ND, Rey FA. 2016. Mechanistic insight into bunyavirus-induced membrane fusion from structure-function analyses of the hantavirus envelope glycoprotein Gc. PLoS Pathog 12:e1005813. https://doi.org/10.1371/journal.ppat.1005813.
46. Sun X, Belouzard S, Whittaker GR. 2008. Molecular architecture of the bipartite fusion loops of vesicular stomatitis virus glycoprotein G, a class III viral fusion protein. J Biol Chem 283:6418–6427. https://doi.org/10.1074/jbc.M708955200.
47. Baquero E, Albertini AA, Gaudin Y. 2015. Recent mechanistic and structural insights on class III viral fusion glycoproteins. Curr Opin Struct Biol 33:52–60. https://doi.org/10.1016/j.sbi.2015.07.011.
48. Backovic M, Leser GP, Lamb RA, Longnecker R, Jardetzky TS. 2007. Characterization of EBV gB indicates properties of both class I and class II viral fusion proteins. Virology 368:102–113. https://doi.org/10.1016/j.virol.2007.06.031.
49. Sharma S, Wisner TW, Johnson DC, Heldwein EE. 2013. HCMV gB shares structural and functional properties with gB proteins from other herpesviruses. Virology 435:239–249. https://doi.org/10.1016/j.virol.2012.09.024.
50. Backovic M, Jardetzky TS, Longnecker R. 2007. Hydrophobic residues that form putative fusion loops of Epstein-Barr virus glycoprotein B are critical for fusion activity. J Virol 81:9596–9600. https://doi.org/10.1128/JVI.00758-07.
51. Hannah BP, Heldwein EE, Bender FC, Cohen GH, Eisenberg RJ. 2007. Mutational evidence of internal fusion loops in herpes simplex virus glycoprotein B. J Virol 81:4858–4865. https://doi.org/10.1128/JVI.02755-06.
52. Lin E, Spear PG. 2007. Random linker-insertion mutagenesis to identify functional domains of herpes simplex virus type 1 glycoprotein B. Proc Natl Acad Sci U S A 104:13140–13145. https://doi.org/10.1073/pnas.0705926104.
53. Atanasiu D, Saw WT, Gallagher JR, Hannah BP, Matsuda Z, Whitbeck JC, Cohen GH, Eisenberg RJ. 2013. Dual split protein-based fusion assay reveals that mutations to herpes simplex virus (HSV) glycoprotein gB alter the kinetics of cell-cell fusion induced by HSV entry glycoproteins. J Virol 87:11332–11345. https://doi.org/10.1128/JVI.01700-13.
54. Hannah BP, Cairns TM, Bender FC, Whitbeck JC, Lou H, Eisenberg RJ, Cohen GH. 2009. Herpes simplex virus glycoprotein B associates with target membranes via its fusion loops. J Virol 83:6825–6836. https://doi.org/10.1128/JVI.00301-09.
55. Maurer UE, Zeev-Ben-Mordehai T, Pandurangan AP, Cairns TM, Hannah BP, Whitbeck JC, Eisenberg RJ, Cohen GH, Topf M, Huiskonen JT, Grunewald K. 2013. The structure of herpesvirus fusion glycoprotein B-bilayer complex reveals the protein-membrane and lateral protein-protein interaction. Structure 21:1396–1405. https://doi.org/10.1016/j.str.2013.05.018.
56. Yang ST, Kreutzberger AJ, Lee J, Kiessling V, Tamm LK. 2016. The role of cholesterol in membrane fusion. Chem Phys Lipids 199:136–143. https://doi.org/10.1016/j.chemphyslip.2016.05.003.
57. Ren X, Yin J, Li G, Herrler G. 2011. Cholesterol dependence of pseudorabies herpesvirus entry. Curr Microbiol 62:261–266. https://doi.org/10.1007/s00284-010-9700-8.
58. Desplanques AS, Nauwynck HJ, Vercauteren D, Geens T, Favoreel HW. 2008. Plasma membrane cholesterol is required for efficient pseudorabies virus entry. Virology 376:339–345. https://doi.org/10.1016/j.virol.2008.03.039.
59. Wudiri GA, Pritchard SM, Li H, Liu J, Aguilar HC, Gilk SD, Nicola AV. 2014. Molecular requirement for sterols in herpes simplex virus entry and infectivity. J Virol 88:13918–13922. https://doi.org/10.1128/JVI.01615-14.
60. Bender FC, Whitbeck JC, Ponce de Leon M, Lou H, Eisenberg RJ, Cohen GH. 2003. Specific association of glycoprotein B with lipid rafts during herpes simplex virus entry. J Virol 77:9542–9552. https://doi.org/10.1128/JVI.77.17.9542-9552.2003.
61. Krey T, d'Alayer J, Kikuti CM, Saulnier A, Damier-Piolle L, Petitpas I, Johansson DX, Tawar RG, Baron B, Robert B, England P, Persson MA, Martin A, Rey FA. 2010. The disulfide bonds in glycoprotein E2 of hepatitis C virus reveal the tertiary organization of the molecule. PLoS Pathog 6:e1000762. https://doi.org/10.1371/journal.ppat.1000762.
62. Backovic M, Krey T. 2016. Stable Drosophila cell lines: an alternative approach to exogenous protein expression. Methods Mol Biol 1350:349–358. https://doi.org/10.1007/978-1-4939-3043-2_17.
63. Culp JS, Johansen H, Hellmig B, Beck J, Matthews TJ, Delers A, Rosenberg M. 1991. Regulated expression allows high level production and secretion of HIV-1 gp120 envelope glycoprotein in Drosophila Schneider cells. Biotechnology 9:173–177.
64. Gianni T, Fato R, Bergamini C, Lenaz G, Campadelli-Fiume G. 2006. Hydrophobic alpha-helices 1 and 2 of herpes simplex virus gH interact with lipids, and their mimetic peptides enhance virus infection and fusion. J Virol 80:8190–8198. https://doi.org/10.1128/JVI.00504-06.
65. Sugihara K, Chami M, Derenyi I, Voros J, Zambelli T. 2012. Directed self-assembly of lipid nanotubes from inverted hexagonal structures. ACS Nano 6:6626–6632. https://doi.org/10.1021/nn300557s.
66. Wimley WC, White SH. 1996. Experimentally determined hydrophobicity scale for proteins at membrane interfaces. Nat Struct Biol 3:842–848. https://doi.org/10.1038/nsb1096-842.
67. MacCallum JL, Bennett WF, Tieleman DP. 2008. Distribution of amino acids in a lipid bilayer from computer simulations. Biophys J 94:3393–3404. https://doi.org/10.1529/biophysj.107.112805.
68. Yau WM, Wimley WC, Gawrisch K, White SH. 1998. The preference of tryptophan for membrane interfaces. Biochemistry 37:14713–14718. https://doi.org/10.1021/bi980809c.
69. White SH, Wimley WC. 1999. Membrane protein folding and stability: physical principles. Annu Rev Biophys Biomol Struct 28:319–365. https://doi.org/10.1146/annurev.biophys.28.1.319.
70. Klupp BG, Nixdorf R, Mettenleiter TC. 2000. Pseudorabies virus glycoprotein M inhibits membrane fusion. J Virol 74:6760–6768. https://doi.org/10.1128/JVI.74.15.6760-6768.2000.
71. Turner A, Bruun B, Minson T, Browne H. 1998. Glycoproteins gB, gD, and gHgL of herpes simplex virus type 1 are necessary and sufficient to mediate membrane fusion in a Cos cell transfection system. J Virol 72:873–875.
72. Vallbracht M, Schröter C, Klupp BG, Mettenleiter TC. 2017. Transient transfection-based fusion assay for viral proteins. Bio-protocol 7(5):e2162. https://doi.org/10.21769/BioProtoc.2162.
73. Dodge JT, Phillips GB. 1967. Composition of phospholipids and of phospholipid fatty acids and aldehydes in human red cells. J Lipid Res 8:667–675.
74. Virtanen JA, Cheng KH, Somerharju P. 1998. Phospholipid composition of the mammalian red cell membrane can be rationalized by a superlattice model. Proc Natl Acad Sci U S A 95:4964–4969. https://doi.org/10.1073/pnas.95.9.4964.
75. Kalvodova L, Sampaio JL, Cordo S, Ejsing CS, Shevchenko A, Simons K. 2009. The lipidomes of vesicular stomatitis virus, Semliki Forest virus, and the host plasma membrane analyzed by quantitative shotgun mass spectrometry. J Virol 83:7996–8003. https://doi.org/10.1128/JVI.00635-09.
76. Nixdorf R, Klupp BG, Karger A, Mettenleiter TC. 2000. Effects of truncation of the carboxy terminus of pseudorabies virus glycoprotein B on infectivity. J Virol 74:7137–7145. https://doi.org/10.1128/JVI.74.15.7137-7145.2000.
77. Dory D, Remond M, Beven V, Cariolet R, Backovic M, Zientara S, Jestin A. 2009. Pseudorabies virus glycoprotein B can be used to carry foot and mouth disease antigens in DNA vaccination of pigs. Antiviral Res 81:217–225. https://doi.org/10.1016/j.antiviral.2008.11.005.
78. Rog T, Vattulainen I. 2014. Cholesterol, sphingolipids, and glycolipids: what do we know about their role in raft-like membranes? Chem Phys Lipids 184:82–104. https://doi.org/10.1016/j.chemphyslip.2014.10.004.
79. Yang ST, Kiessling V, Tamm LK. 2016. Line tension at lipid phase boundaries as driving force for HIV fusion peptide-mediated fusion. Nat Commun 7:11401. https://doi.org/10.1038/ncomms11401.

80. Feigenson GW. 2006. Phase behavior of lipid mixtures. Nat Chem Biol 2:560–563. https://doi.org/10.1038/nchembio1106-560.
81. Oliver SL, Sommer M, Zerboni L, Rajamani J, Grose C, Arvin AM. 2009. Mutagenesis of varicella-zoster virus glycoprotein B: putative fusion loop residues are essential for viral replication, and the furin cleavage motif contributes to pathogenesis in skin tissue in vivo. J Virol 83:7495–7506. https://doi.org/10.1128/JVI.00400-09.
82. Sorem J, Longnecker R. 2009. Cleavage of Epstein-Barr virus glycoprotein B is required for full function in cell-cell fusion with both epithelial and B cells. J Gen Virol 90:591–595. https://doi.org/10.1099/vir.0.007237-0.
83. Okazaki K. 2007. Proteolytic cleavage of glycoprotein B is dispensable for in vitro replication, but required for syncytium formation of pseudorabies virus. J Gen Virol 88:1859–1865. https://doi.org/10.1099/vir.0.82610-0.
84. Strive T, Borst E, Messerle M, Radsak K. 2002. Proteolytic processing of human cytomegalovirus glycoprotein B is dispensable for viral growth in culture. J Virol 76:1252–1264. https://doi.org/10.1128/JVI.76.3.1252-1264.2002.
85. Kopp A, Blewett E, Misra V, Mettenleiter TC. 1994. Proteolytic cleavage of bovine herpesvirus 1 (BHV-1) glycoprotein gB is not necessary for its function in BHV-1 or pseudorabies virus. J Virol 68:1667–1674.
86. Stampfer SD, Lou H, Cohen GH, Eisenberg RJ, Heldwein EE. 2010. Structural basis of local, pH-dependent conformational changes in glycoprotein B from herpes simplex virus type 1. J Virol 84:12924–12933. https://doi.org/10.1128/JVI.01750-10.
87. Peeters B, de Wind N, Hooisma M, Wagenaar F, Gielkens A, Moormann R. 1992. Pseudorabies virus envelope glycoproteins gp50 and gII are essential for virus penetration, but only gII is involved in membrane fusion. J Virol 66:894–905.
88. Stiasny K, Koessl C, Heinz FX. 2003. Involvement of lipids in different steps of the flavivirus fusion mechanism. J Virol 77:7856–7862. https://doi.org/10.1128/JVI.77.14.7856-7862.2003.
89. Zaitseva E, Yang ST, Melikov K, Pourmal S, Chernomordik LV. 2010. Dengue virus ensures its fusion in late endosomes using compartment-specific lipids. PLoS Pathog 6:e1001131. https://doi.org/10.1371/journal.ppat.1001131.
90. Guardado-Calvo P, Rey FA. 2017. The envelope proteins of the Bunyavirales. Adv Virus Res 98:83–118. https://doi.org/10.1016/bs.aivir.2017.02.002.
91. Domanska MK, Wrona D, Kasson PM. 2013. Multiphasic effects of cholesterol on influenza fusion kinetics reflect multiple mechanistic roles. Biophys J 105:1383–1387. https://doi.org/10.1016/j.bpj.2013.08.003.
92. Lai AL, Moorthy AE, Li Y, Tamm LK. 2012. Fusion activity of HIV gp41 fusion domain is related to its secondary structure and depth of membrane insertion in a cholesterol-dependent fashion. J Mol Biol 418:3–15. https://doi.org/10.1016/j.jmb.2012.02.010.
93. Kirkpatrick RB, Ganguly S, Angelichio M, Griego S, Shatzman A, Silverman C, Rosenberg M. 1995. Heavy chain dimers as well as complete antibodies are efficiently formed and secreted from Drosophila via a BiP-mediated pathway. J Biol Chem 270:19800–19805. https://doi.org/10.1074/jbc.270.34.19800.
94. Fan SQ, Huang W, Wang LX. 2012. Remarkable transglycosylation activity of glycosynthase mutants of endo-D, an endo-beta-N-acetylglucosaminidase from Streptococcus pneumoniae. J Biol Chem 287:11272–11281. https://doi.org/10.1074/jbc.M112.340497.
95. Kabsch W. 2010. XDS. Acta Crystallogr D Biol Crystallogr 66:125–132. https://doi.org/10.1107/S0907444909047337.
96. McCoy AJ, Grosse-Kunstleve RW, Adams PD, Winn MD, Storoni LC, Read RJ. 2007. Phaser crystallographic software. J Appl Crystallogr 40:658–674. https://doi.org/10.1107/S0021889807021206.
97. Bricogne G, Blanc E, Brandl M, Flensburg C, Keller P, Paciorek W, Roversi P, Smart OS, Vonrhein C, Womack TO. 2009. BUSTER, v2.8.0. Global Phasing Ltd., Cambridge, United Kingdom.
98. Castile JD, Taylor KM. 1999. Factors affecting the size distribution of liposomes produced by freeze-thaw extrusion. Int J Pharm 188:87–95. https://doi.org/10.1016/S0378-5173(99)00207-0.
99. Böhm SW, Eckroth E, Backovic M, Klupp BG, Rey FA, Mettenleiter TC, Fuchs W. 2015. Structure-based functional analyses of domains II and III of pseudorabies virus glycoprotein H. J Virol 89:1364–1376. https://doi.org/10.1128/JVI.02765-14.
100. Mettenleiter TC. 1989. Glycoprotein gIII deletion mutants of pseudorabies virus are impaired in virus entry. Virology 171:623–625. https://doi.org/10.1016/0042-6822(89)90635-1.
101. Kopp M, Granzow H, Fuchs W, Klupp BG, Mundt E, Karger A, Mettenleiter TC. 2003. The pseudorabies virus UL11 protein is a virion component involved in secondary envelopment in the cytoplasm. J Virol 77:5339–5351. https://doi.org/10.1128/JVI.77.9.5339-5351.2003.
102. Pavlova SP, Veits J, Keil GM, Mettenleiter TC, Fuchs W. 2009. Protection of chickens against H5N1 highly pathogenic avian influenza virus infection by live vaccination with infectious laryngotracheitis virus recombinants expressing H5 hemagglutinin and N1 neuraminidase. Vaccine 27:773–785. https://doi.org/10.1016/j.vaccine.2008.11.033.
103. DeLano WL. 2002. The PyMOL Molecular Graphics System, DeLano Scientific, San Carlos, CA, USA.
104. Eisenberg D, Schwarz E, Komaromy M, Wall R. 1984. Analysis of membrane and surface protein sequences with the hydrophobic moment plot. J Mol Biol 179:125–142. https://doi.org/10.1016/0022-2836(84)90309-7.
105. Baker NA, Sept D, Joseph S, Holst MJ, McCammon JA. 2001. Electrostatics of nanosystems: application to microtubules and the ribosome. Proc Natl Acad Sci U S A 98:10037–10041. https://doi.org/10.1073/pnas.181342398.
106. Hasegawa H, Holm L. 2009. Advances and pitfalls of protein structural alignment. Curr Opin Struct Biol 19:341–348. https://doi.org/10.1016/j.sbi.2009.04.003.
107. Sievers F, Wilm A, Dineen D, Gibson TJ, Karplus K, Li W, Lopez R, McWilliam H, Remmert M, Soding J, Thompson JD, Higgins DG. 2011. Fast, scalable generation of high-quality protein multiple sequence alignments using Clustal Omega. Mol Syst Biol 7:539. https://doi.org/10.1038/msb.2011.75.
108. Gouet P, Courcelle E, Stuart DI, Metoz F. 1999. ESPript: analysis of multiple sequence alignments in PostScript. Bioinformatics 15:305–308. https://doi.org/10.1093/bioinformatics/15.4.305.
109. Emsley P, Cowtan K. 2004. Coot: model-building tools for molecular graphics. Acta Crystallogr D Biol Crystallogr 60:2126–2132. https://doi.org/10.1107/S0907444904019158.

SUPPLEMENTAL MATERIALS

Figure S1. Sequence alignment of gB sequences of 35 alphaherpesviruses. The alignment was generated using Clustal Omega (2-4), and represented in ESPript 3.x program (5), with the residues colored according to their conservation. Identical residues are shown in white letters on red background, while the residues conserved more than 75% are shown as red letters on white background. PrV gB sequence is shown on the top, with the corresponding numbering and secondary structure elements plotted above the alignment. FL1 and FL2 regions are indicated. Predicted N-glycosylation sites in PrV gB are marked with blue star symbols on the top, and the cysteine residues involved in formation of five disulfide bridges are shown in green numbers at the bottom of the alignment. Purple, vertical arrows indicate the boundaries of the expression construct, and dotted line shows regions not resolved in the structure. The FL residues investigate in this study are underlined in green.

35 sequences of gB of alphaherpesviruses used for the alignment (GenBank accession codes are given in brackets) correspond to gB of: **Suid alphaherpesvirus 1** (AEM64049), Human alphaherpesvirus 1 (AAF04615.1), Human alphaherpesvirus 2 (ADG45133.1), Human alphaherpesvirus 3 (AAP32845.1), Saimiriine alphaherpesvirus 1 (YP_003933812.1), Macropodid alphaherpesvirus 1 (AAD11960.1), Macropodid herpesvirus 4 (AGC54689.1), Macropodid alphaherpesvirus 2 (AAD11961.1), Leporid alphaherpesvirus 4 (YP_009230158.1), Macacine alphaherpesvirus 1 (BAC58067.1), Papiine alphaherpesvirus 2 (AAA85648.1), Cercopithecine alphaherpesvirus 2 (AAA88010.1), Chimpanzee alpha-1 herpesvirus (BAE47051.1), Spheniscid herpesvirus 2 (YP_009342376.1), Anatid herpesvirus 1

(YP_003084394.1), Falconid herpesvirus 1 (YP_009046525.1), Meleagrid alphaherpesvirus 1 (NP_073321.1), Gallid alphaherpesvirus 2 (YP_001033956.1), Cercopithecine alphaherpesvirus 9 (NP_077446.1), Lagenorhynchus alphaherpesvirus 1 (BAM99305.1), Caprine alphaherpesvirus 1 (AAD46114.2), Rangiferine herpesvirus 1 (AAD46113.2), Cervid alphaherpesvirus 1 (AAD46115.2), Bovine alphaherpesvirus 1 (AFB76670.1), Bovine alphaherpesvirus 5 (AAD46112.2), Bubaline alphaherpesvirus 1 (APO15888.1), Felid alphaherpesvirus 1 (ANG65542.1), Canid alphaherpesvirus 1 (AEK27122.1), Phocid alphaherpesvirus 1 (CAA92272.1), Equid alphaherpesvirus 3 (YP_009054936.1), Equid alphaherpesvirus 4 (AMB16237.1), Equid alphaherpesvirus 8 (YP_006273012.1), Equid alphaherpesvirus 9 (YP_002333514.1), Equid alphaherpesvirus 1 (AII81366.1), and Testudinid herpesvirus 3 (YP_009176910.1).


AEM64049.1
1 10 20 30 40
AEM64049.1 .....MPAGGG..LWRGPRGHRPGHHGGAGLGRLWPAPHHAA.....AARGA....
AAF04615.1 .....MRQGAPARGCR.....
ADG45133.1 .....MRG.....
AAP32845.1 .....
YP_003933812.1 .....MA..PPAAKSR.....
AAD11960.1 .....MAVHPPLRPRL.....
AGC54689.1 .....HQL.....
AAD11961.1 .....MTTHSPPKRQR.....
YP_009230158.1 .....
BAC58067.1 .....MRPR.....
AAA85648.1 .....MRPR....GAR.....
AAA88010.1 .....MRPR....GTP.....
BAE47051.1 .....MRDGAPAHGRG.....
YP_009342376.1 .....
YP_003084394.1 MYRRTICYLRDRMPAYFCNS.SGPEWRNNPRDVGCDRQGRLLYALYGASTTGSR.....NGGA..C
YP_009046525.1 MQGRDLHHLRDRLPSDGRPG.SGSGREDRSGHDSYLRLGRVFSLVRGAPAAGAGHRRKSQGGG..G
NP_073321.1 .....
YP_001033956.1 .....
NP_077446.1 .....MSPDCSIT.QQYCRYNYKRHDCNLRRRRFLFIVYSNSAACSGRTKTY.....
BAM99305.1 .....MSLGSG..LKQHLRANRRQYSCHIRPGRIFYAIYNFTTT.....GPRIQ....
AAD46114.2 .....MPPRGSAERRAGPGDRQRGQRCHLRPGRVFPALRGLAAPGAG...GPRAA....
AAD46113.2 .....MAARGRAERAAGAGDGRRGQRGHLRPGRVLAALRGAAAPGAGRDGGGGPR....
AAD46115.2 .....MAARGGAERAAGPGDGRRGQRRHPGPGRVLAALRGPAAPGAA.G..ARAA....
AFB76670.1 .....MAARGGAERAAGAGDGRRGQRRHLRPGRVLAALRGPAAPGAG.G..ARAA....
AAD46112.2 .....MATRGGAEPAAGAGYGRRGQRRHLRPGRVLAALRGPAAPGAGGG..ARAA....
APO15888.1 .....MAARGGAEPAAGAGDGRRGQRRHLRPGRVLAALRGPAAPGAGGG..ARAA....
ANG65542.1 .....MSTRGDLG.KRRRGSRWQGHSGYFRQRCFFPSLLGIAATGSRHGNGSS.....
AEK27122.1 .....
CAA92272.1 .....
YP_009054936.1 .....MSSRGGVV.AGPGGYGPGGDRCHLRRRRVLSPLRGPAADGSGVWGELGAIGDRC
AMB16079.1 .....MSTCCRAI.CGPQRCYWRRDCGNLRQRRVLASIHRTPAAGSWLWSQLGNVNLPA
YP_006273012.1 .....
YP_002333514.1 .....
AII81366.1 .....MSSGCRSV.GGSKWGHWRGDGGYLRQRRVLAPVCSAPAAGSWIGSQLGNVGNLL
YP_009176910.1 .....
AEM64049.1
50 60
AEM64049.1 .....V.....ALALLLLALA.AA.....P..PCGAAAVTRAASA.
AAF04615.1 .....WFVVWAL.....LGLTLGVLVASAA.....PSSPGTPGV
ADG45133.1 .....GGLICAL.....VVGALVAAVASAA.....PAAPRASGG
AAP32845.1 .....MFV..TAVV...SVSPSS.
YP_003933812.1 .....ASRVAP.....LTSLVSMLAAAAAAAVALCAAFAEAARGVTPVYSDDAD.
AAD11960.1 .....WLTRFWY.....MFIVGGIL.....VDTGGN
AGC54689.1 .....RLTRLWY.....IFLACGVF.....GGTTGH
AAD11961.1 .....QITRLWY.....IFLAWGVF.....GGPTGH
YP_009230158.1 .....M.....RLTMRGILVILVVAVPLLAAAA....STRAAAPRRARPEGR
BAC58067.1 .....AGPLPLPSPLVPLLALAL.....LA.ATRPLG
AAA85648.1 .....ALPIPIPIPI.....PIPIPIPIPLPPPALLALALLL.....AA.AGRAGP
AAA88010.1 .....PSF.....LPLPVLLALAV.I.....AA.AGRAAP
BAE47051.1 .....GGLICAL.....VVGTLMAAVVLAA.....PSPSGA
YP_009342376.1 .....MIG.....SVNTNVVIVLTFLLVS....LVRSEDPGDNS.
YP_003084394.1 TTAVR.RK.....EFDRMNRARRVSALHLTAPRRS..RFVL.SLIMVSV.....LFRPIQPQPIV.
YP_009046525.1 ERGARKRERLSSRAFVPMSPDVYV...PTTSPCVQLVAFVVMHLLLGSLP....MVSSQTAAPAA.
NP_073321.1 .....MLMTPT.....MKYFN...RSLFIFLTP....ILS.....
YP_001033956.1 .....MHYFR...RNCIFFLIV....ILY.....
NP_077446.1 .....L.....NVCYITSFA..ILFA...CVHPSL.
BAM99305.1 .....Y.....PASLMWLEYS.LLCVCLLIY..PGGAAREYP.PSS.
AAD46114.2 .....L.....AAALLWAAWA.L..LLA..A..PAAALPTAP.PSA.
AAD46113.2 .....A.....ALALLWPLLL.LLPLLA..P..PAAAAPVTP.APP.
AAD46115.2 .....L.....AAALLWAAWA.L..LLA..A..PAAGLPATP.APP.
AFB76670.1 .....L.....AAALLWATWA.L..LLA..A..PAAGRPATT.PPA.
AAD46112.2 .....L.....AAALLWAAWA.L..LLA..A..PAAGRPTTP.PVP.
APO15888.1 .....L.....AAALLWAAWA.L..LLA..A..PAAGRPTTP.QVP.
ANG65542.1 .....G....L.....TRLARYVSFI....WIVLF...LVGPRPVEGQSGS.
AEK27122.1 .....M.....FSLYLYIFFI....IYTLI...ICDPTTPES.....
CAA92272.1 .....MYLITLVFFI....NILVI...QCVPTTQPT.....
YP_009054936.1 SPGAVAGARPPPH....F.....KPWTLLVLVL.LSGLLAAG...RCGAT..PTSPPA.
AMB16079.1 ASPMS.KDSTSLG....V.....RTI.....V.IACLVLLG...CCIVEAVPTTPSS.
YP_006273012.1 .....
YP_002333514.1 .....
AII81366.1 AAPHPLGKQASSR....V.....GTI.....V.LACLLLFG...SCVVRAVPTTPSP.
YP_009176910.1 .....MIMWLSFMMTLWSLSLVY....GQTIVPP..T..

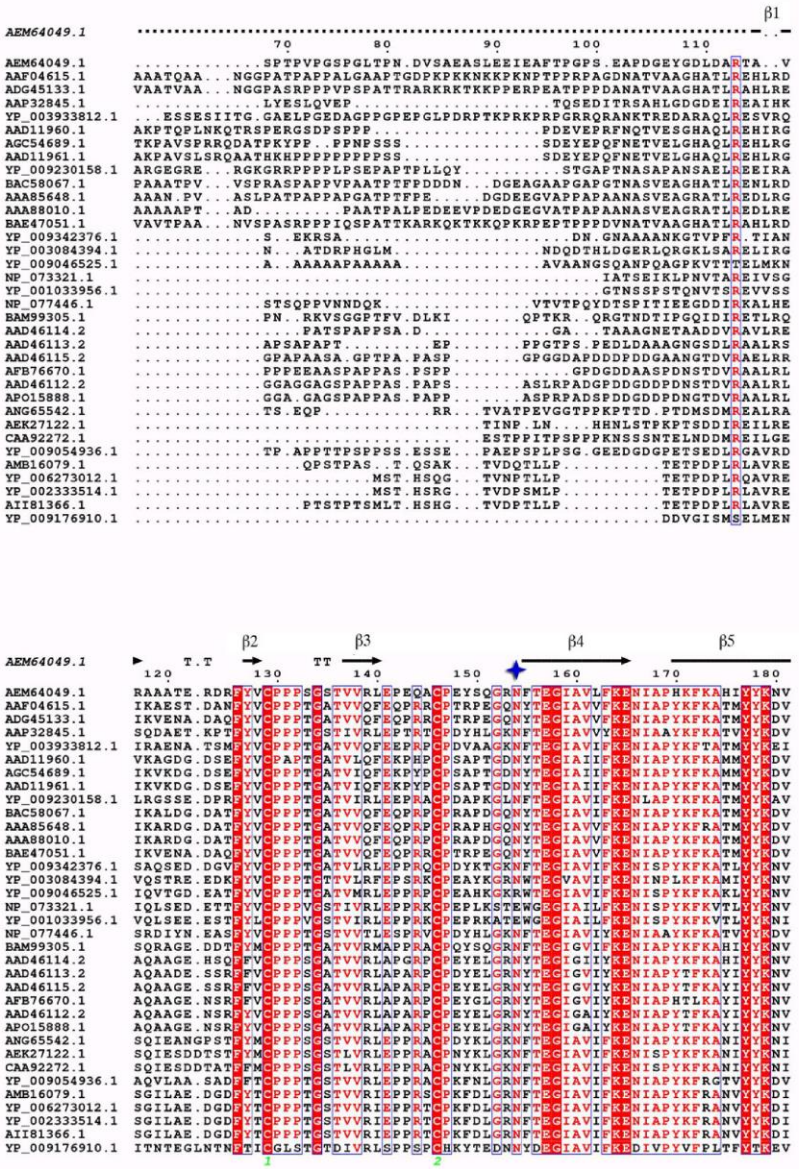
β1
β2
β3
β4
β5
AEM64049.1
AEM64049.1
AAF04615.1
ADG45133.1
AAP32845.1
YP_003933812.1
AAD11960.1
AGC54689.1
AAD11961.1
YP_009230158.1
BAC58067.1
AAA85648.1
AAA88010.1
BAE47051.1
YP_009342376.1
YP_003084394.1
YP_009046525.1
NP_073321.1
YP_001033956.1
NP_077446.1
BAM99305.1
AAD46114.2
AAD46113.2
AAD46115.2
AFB76670.1
AAD46112.2
APO15888.1
ANG65542.1
AEK27122.1
CAA92272.1
YP_009054936.1
AMB16079.1
YP_006273012.1
YP_002333514.1
AII81366.1
YP_009176910.1

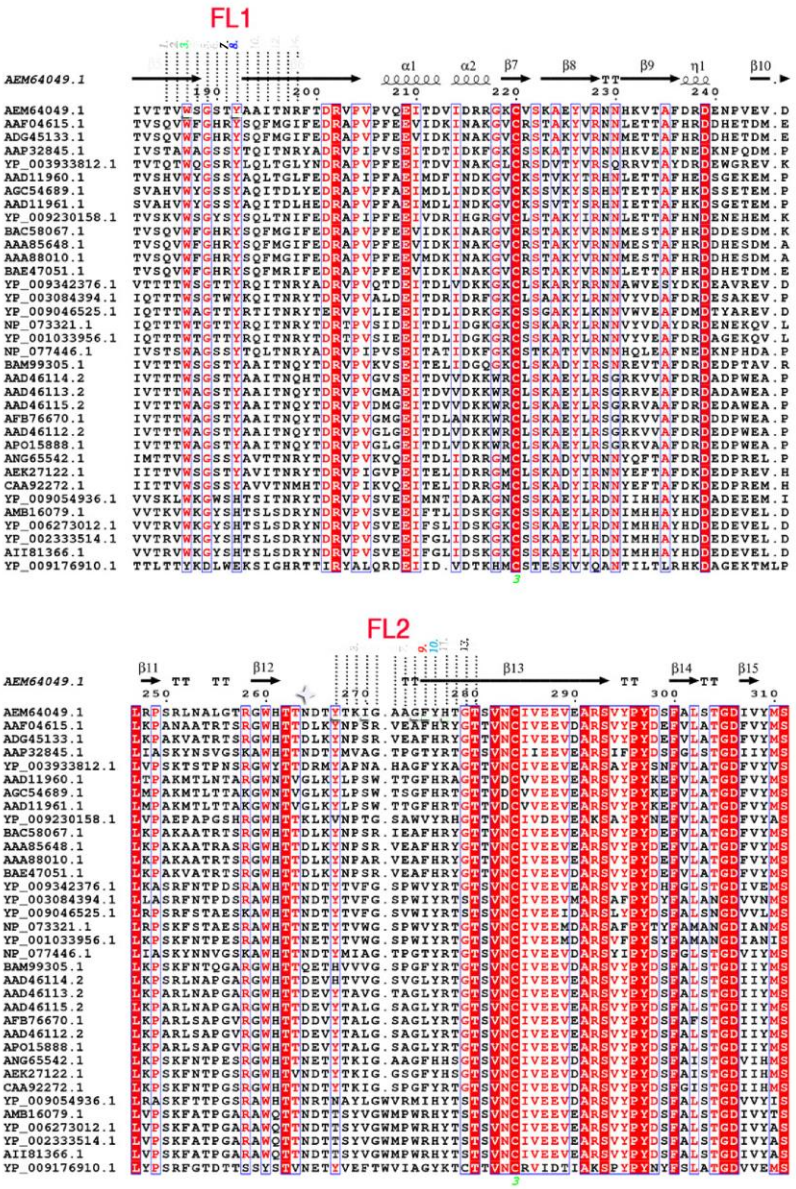
FL1
AEM64049.1
α1 α2 β7 β8 β9 η1 β10
190 200 210 220 230 240
AEM64049.1 IVTTVWSGSTYAAITNRFTDRVPFVPVQEITDVIDRRGKGVSKAEYVRNNHKVTAFDRDENPVEV.D
AAF04615.1 TVSQVWFGHRYSQFMGIFEDRAPVPFEEVIDKINAKGVGRSTAKYVRNNLETTAFHRDDHETDM.E
ADG45133.1 TVSQVWFGHRYSQFMGIFEDRAPVPFEEVIDKINAKGVGRSTAKYVRNNMETTAFHRDDHETDM.E
AAP32845.1 IVSTAWAGSSYTQITNRYADRVPIPVSEITDTIDKFGKGSSKATYVRNNHKVEAFNEDKNPQDM.P
YP_003933812.1 TVTQTWQGSRYLQLTGLYNDRAPVPFEEITDVINAKGLGRSDVTYVRSQRRVTAYDRDEWGREV.K
AAD11960.1 TVSHVWYGSSYAQLTGLFEDRAPIPFAEIMDFINDKGVGKSTVKYTRNNLETTAFHEDSGEKEM.P
AGC54689.1 SVAHVWYGSSYAQITDLYEDRAPVPFAEIMDLINDKGVGKSSVKYSRHNTETTAFHKDSSETEM.P
AAD11961.1 SVAHVWYGSSYAQITDLHEDRAPVPFAEIMDLINDKGVGKSSVTYSRHNIETTAFHKDSGETEM.P
YP_009230158.1 TVSKVWSGYSYSQLTNIFEDRAPIPFEEIVDRIHGRGVGLSTAKYIRNNLETTAFHNDENEHEM.K
BAC58067.1 TVSQVWFGHRYSQFMGIFEDRAPVPFEEVIDKINARGVGRSTAKYVRNNMESTAFHRDDDESDM.K
AAA85648.1 TVSQVWFGHRYSQFMGIFEDRAPVPFEEVIDKINAKGVGRSTAKYVRNNMESTAFHRDDHESDM.A
AAA88010.1 TVSQVWFGHRYSQFMGIFEDRAPVPFEEVMDKINAKGVGRSTAKYVRNNMESTAFHRDDHESDM.A
BAE47051.1 TVSQVWFGHRYSQFMRIFEDRAPVPFEEVIDKINAKGVGRSTAKYVRNNLETTAFHRDDHETDM.E
YP_009342376.1 VTTTTWSGTTYRQITNRYADRVPVQTDEITDLVDKKGKGLSKARYRRNNAWVESYDKDEAVREV.D
YP_003084394.1 IQTTTWSGTWYKQITNRYTDRVPVALDEITDRIDRFGKGLSAAKYLRNNVYVDADFDRDESAKEV.P
YP_009046525.1 IQTTTWAGTTYRTITNRYTERVPVLIEEITDLIDRKGKGSSGAKYLKNNVWVEAFDMDTYAREV.D
NP_073321.1 IQTTTWTGTTYRQITNRYTDRTPVSIDEITDLIDGKGKGSSKARYLRNNVYVDAYDRDENEKQV.L
YP_001033956.1 IQTTTWTGTTYRQITNRYTDRTPVSIEEITDLIDGKGRGSSKARYLRNNVYVEAFDRDAGEKQV.L
NP_077446.1 IVSTSWAGSSYTQLTNRYADRVPIPVSEITATIDKFGKGSTKATYVRNNHQLEAFNEDKNPHDA.P
BAM99305.1 IVTTTWSGSTYAAITNQYTDRVPVKVSEITELIDGQGKGLSKADYIRSNREVTAFDRDEDPTAV.R
AAD46114.2 IVTTTWSGSTYAAITNQHTDRVPVGVSEITDVVDKKWRGLSKAEYLRSGRKVVAFDRDADPWEA.P
AAD46113.2 IVTTTWAGSTYAAITNQYTDRVPVGMAEITDVVDKKWRGLSKAEYLRSGRRVEAFDRDADAWEA.P
AAD46115.2 IVTTTWAGSTYAAITNQYTDRVPVDMGEITDVVDKKWRGLSKAEYLRSGRRVAAFDRDEDAWEA.P
AFB76670.1 IVTTTWAGSTYAAITNQYTDRVPVGMGEITDLANKKWRGLSKAEYLRSGRKVVAFDRDDDPWEA.P
AAD46112.2 IVTTTWAGSTYAAITNQYTDRVPVGLGEITDLVDKKWRGLSKAEYLRSGRKVVAFDRDEDPWEA.P
APO15888.1 IVTTTWAGSTYAAITNQYTDRVPVGLGEITDLVDKKWRGLSKADYLRSGRKVAAFDRDEDPWEA.P
ANG65542.1 IMTTTWSGSSYAVTTNRYTDRVPVKVQEITDLIDRRGMGLSKADYVRNNYQFTAFDRDEDPREL.P
AEK27122.1 IITTTWSGSTYAVITNRYTDRVPIGVPEITELIDRRGMGLSKADYIRNNYEFTAFDKDEDPREV.H
CAA92272.1 IITTTWSGSSYAVVTNMHTDRVPIKVQEITELIDRRGMGLSKADYIRNNYEFTAFDKDEDPREM.H
YP_009054936.1 VVSKLWKGWSHTSITNRYTDRVPVSVEEIMNTIDAKGNGSSKAEYLRDNIIHHAYHKDADEEEM.I
AMB16079.1 VVTKVWKGYSHTSLSDRYNDRVPVSVEEIFTLIDSKGKGSSKAEYLRDNIMHHAYHDDEDEVEL.D
YP_006273012.1 VVTRVWKGYSHTSLSDRYNDRVPVSVEEIFSLIDSKGKGSSKAEYLRDNIMHHAYHDDEDEVEL.D
YP_002333514.1 VVTRVWKGYSHTSLSDRYNDRVPVSVEEIFGLIDSKGKGSSKAEYLRDNIMHHAYHDDEDEVEL.D
AII81366.1 VVTRVWKGYSHTSLSDRYNDRVPVSVEEIFGLIDSKGKGSSKAEYLRDNIMHHAYHDDEDEVEL.D
YP_009176910.1 TTLTTYKDLWEKSIGHRTTIRYALQRDEIID.VDTKHMGSTESKVYQANTILTLRHKDAGEKTMLP
FL2
AEM64049.1
β11 β12 β13 β14 β15
250 260 270 280 290 300 310
AEM64049.1 LRPSRLNALGTRGWHTTNDTYTKIG.AAGFYHTGTSVNGIVEEVEARSVYPYDSFALSTGDIVYMS
AAF04615.1 LKPANAATRTSRGWHTTDLKYNPSR.VEAFHRYGTTVNGIVEEVDARSVYPYDEFVLATGDFVYMS
ADG45133.1 LKPAKVATRTSRGWHTTDLKYNPSR.VEAFHRYGTTVNGIVEEVDARSVYPYDEFVLATGDFVYMS
AAP32845.1 LIASKYNSVGSKAWHTTNDTYMVAG.TPGTYRTGTSVNGIIEEVEARSIFPYDSFGLSTGDIIYMS
YP_003933812.1 LVPSKTSTPNSRGWYTTDRMYAPNA.HAGFYKAGTTVNGIVEEVEARSAYPYSNFVLATGDFVYVS
AAD11960.1 LTPAKMTLNTARGWNTVGLKYLPSW.TTGFHRAGTTVDGVVEEVEARSVYPYKEFVLATGDFVYMS
AGC54689.1 LMPAKMTLTTAKGWNTVGLKYLPSW.TSGFHRTGTTVDGVVEEVEARSVYPYKEFVLATGDFVYMS
AAD11961.1 LMPAKMTLTTAKGWNTVGLKYLPSW.TTGFHRTGTTVDGVVEEVEARSVYPYKEFVLATGDFVYMS
YP_009230158.1 LVPAEPAPGSHRGWHTTKLKVNPTG.SAWVYRHGTTVNGIVDEVEAKSAYPYNEFVLATGDFVYAS
BAC58067.1 LKPAKAATRTSRGWHTTDLKYNPSR.IEAFHRYGTTVNGIVEEVEARSVYPYDEFVLATGDFVYMS
AAA85648.1 LKPAKAATRASRGWHTTDLKYNPSR.VEAFHRYGTTVNGIVEEVEARSVYPYDEFVLATGDFVYMS
AAA88010.1 LKPAKAATRTSRGWHTTDLKYNPAR.VEAFHRYGTTVNGIVEEVEARSVYPYDEFVLATGDFVYMS
BAE47051.1 LKPAKVATRTSRGWHTTDLKYNPSR.VEAFHRYGTTVNGIVEEVDARSVYPYDEFVLATGDFVYMS
YP_009342376.1 LKASRFNTPDSRAWHTTNDTYTVFG.SPWVYRTGTSVNGIVEEVEARSVYPYDHFGLSTGDIVEMS
YP_003084394.1 LLASRFNTPDSRAWHTTNDTYTVFG.SPWIYRTSTSVNGIVEEVMARSAFPYDYFALANGDVVNMS
YP_009046525.1 LRPSRFSTAESKAWHTTNDTYTVFG.SVWIYRTSTSVNGIVEEIDARSLYPYDSFALSNGDVVLMS
NP_073321.1 LRPSKFSTAESRAWHTTNETYTVWG.SPWVYRTGTSVNGIVEEMDARSAFPYTYFAMANGDIANMS
YP_001033956.1 LKPSKFNTPESRAWHTTNETYTVWG.SPWIYRTGTSVNGIVEEMDARSVFPYSYFAMANGDIANIS
NP_077446.1 LIASKYNNVGSKAWHTTNDTYMIAG.TPGTYRTGTSVNGIVEEVDARSYIPYDSFGLSTGDVIYMS
BAM99305.1 LKPSKFNTQGARGWHTTQETHVVVG.SPGFYRTGTSVNGIVEEVDARSVYPYDSFALSTGDIIYMS
AAD46114.2 LKPSRLNAPGARGWHTTDEVHTVVG.SVGLYRTGTSVNGIVEEVEARSVYPYDSFALSTGDIIYMS
AAD46113.2 LKPARLNAPGARGWHTTDEVYTAVG.TAGLYRTGTSVNGIVEEVEARSVYPYDSFALSTGDIIYMS
AAD46115.2 LKPARLNAPGARGWHTTDEVYTALG.SAGLYRTGTSVNGIVEEVEARSVYPYDSFALSTGDIIYMS
AFB76670.1 LKPARLSAPGVRGWHTTDDVYTALG.SAGLYRTGTSVNGIVEEVEARSVYPYDSFAFSTGDIIYMS
AAD46112.2 LKPARLSAPGVRGWHTTDEVYTALG.SAGLYRTGTSVNGIVEEVEARSVYPYDSFALSTGDIIYMS
APO15888.1 LKPARLSAPGVRGWHTTDEVYTALG.SAGLYRTGTSVNGIVEEVEARSVYPYDSFALSTGDIIYMS
ANG65542.1 LKPSKFNTPESRGWHTTNETYTKIG.AAGFHHSGTSVNGIVEEVDARSVYPYDSFAISTGDVIHMS
AEK27122.1 LKPSKFNTPGSRGWHTVNDTYTKIG.GSGFYHSGTSVNGIVEEVDARSVYPYDSFAISTGDIIHMS
CAA92272.1 LKPSKFNTPGSRGWHTTNDTYTKIG.SPGFYRTGTSVNGIVEEVDARSVYPYDSFGISTGDIIHMS
YP_009054936.1 LRASKFTTPGSRAWHTTNRTNAYLGWVRMIHYTSTSVNGIVEEVDARSVYPYDSFALSTGDVVYIS
AMB16079.1 LVPSKFATPGARAWQTTNDTTSYVGWMPWRHYTSTSVNGIVEEVEARSVYPYDSFALSTGDIVYTS
YP_006273012.1 LVPSKFATPGARAWQTTNDTTSYVGWMPWRHYTSTSVNGIVEEVEARSVYPYDSFALSTGDIVYAS
YP_002333514.1 LVPSKFATPGARAWQTTNDTTSYVGWMPWRHYTSTSVNGIVEEVEARSVYPYDSFALSTGDIVYAS
AII81366.1 LVPSKFATPGARAWQTTNDTTSYVGWMPWRHYTSTSVNGIVEEVEARSVYPYDSFALSTGDIVYAS
YP_009176910.1 LYPSRFGTDTTSSYSTVNETYVEFTWVIAGYKTCTTVNGRVIDTIAKSPYPYNYFSLATGDVVEMS

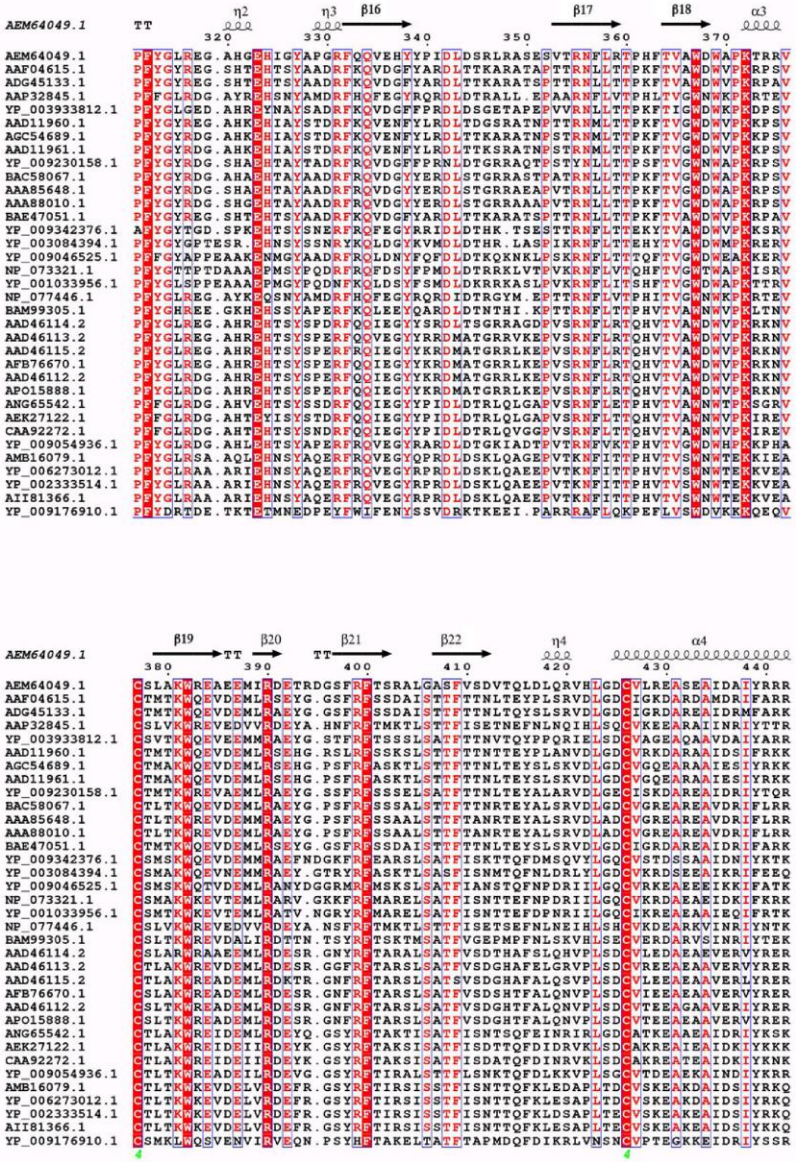

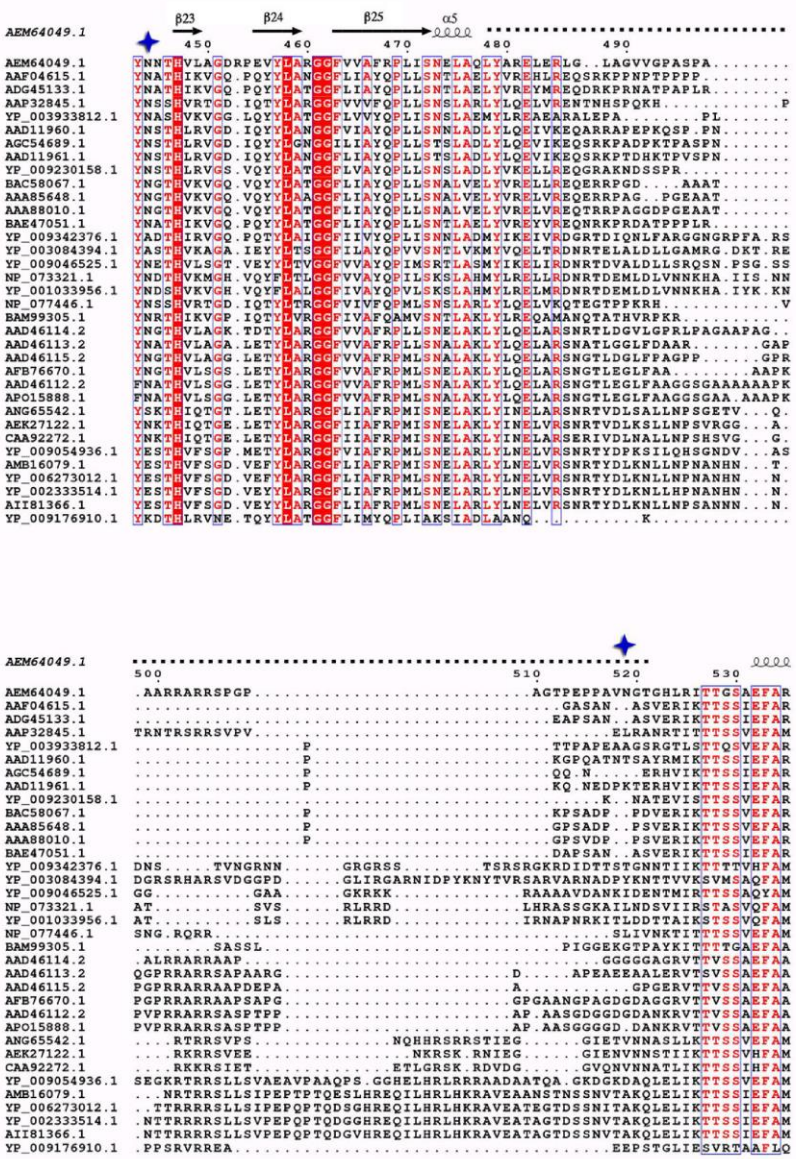
β23
β24
β25
α5
AEM64049.1
450
460
470
480
490
AEM64049.1
AAF04615.1
ADG45133.1
AAP32845.1
YP_003933812.1
AAD11960.1
AGC54689.1
AAD11961.1
YP_009230158.1
BAC58067.1
AAA85648.1
AAA88010.1
BAE47051.1
YP_009342376.1
YP_003084394.1
YP_009046525.1
NP_073321.1
YP_001033956.1
NP_077446.1
BAM99305.1
AAD46114.2
AAD46113.2
AAD46115.2
AFB76670.1
AAD46112.2
APO15888.1
ANG65542.1
AEK27122.1
CAA92272.1
YP_009054936.1
AMB16079.1
YP_006273012.1
YP_002333514.1
AII81366.1
YP_009176910.1
AEM64049.1
500
510
520
530
AEM64049.1
AAF04615.1
ADG45133.1
AAP32845.1
YP_003933812.1
AAD11960.1
AGC54689.1
AAD11961.1
YP_009230158.1
BAC58067.1
AAA85648.1
AAA88010.1
BAE47051.1
YP_009342376.1
YP_003084394.1
YP_009046525.1
NP_073321.1
YP_001033956.1
NP_077446.1
BAM99305.1
AAD46114.2
AAD46113.2
AAD46115.2
AFB76670.1
AAD46112.2
APO15888.1
ANG65542.1
AEK27122.1
CAA92272.1
YP_009054936.1
AMB16079.1
YP_006273012.1
YP_002333514.1
AII81366.1
YP_009176910.1

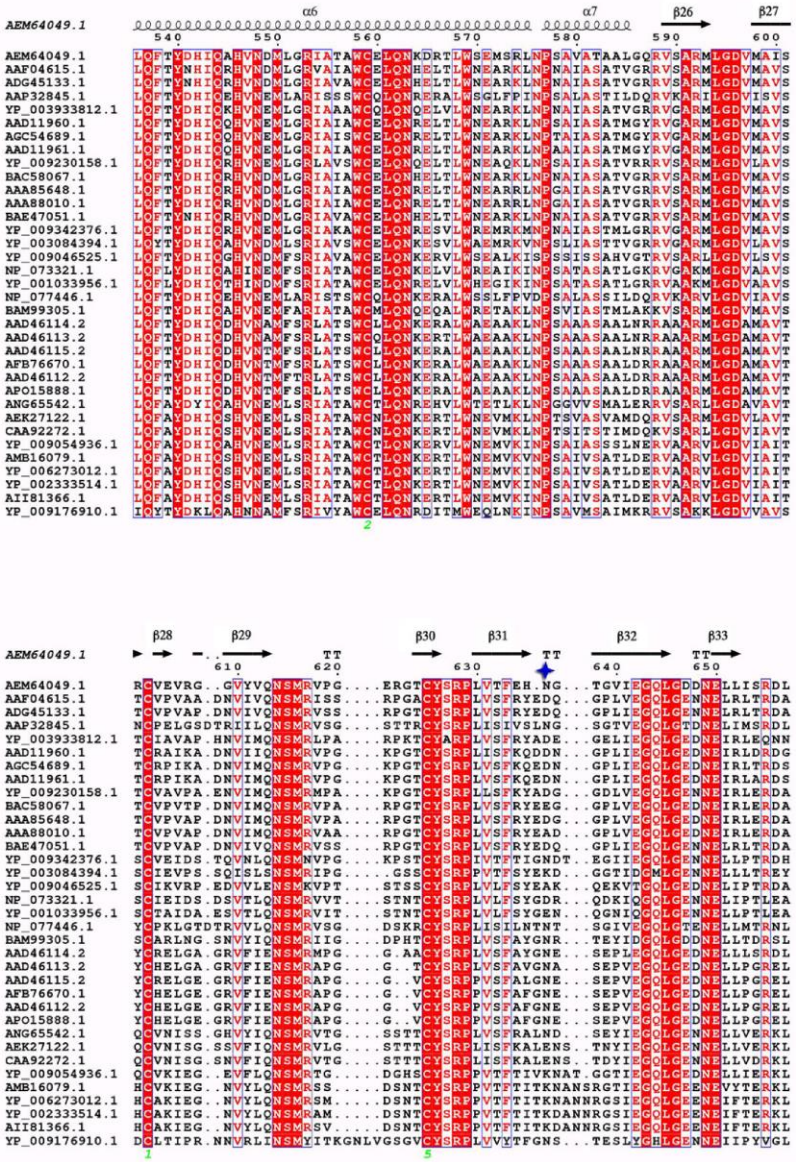
α6
α7
β26
β27
AEM64049.1
540
550
560
570
580
590
600
AEM64049.1
AAF04615.1
ADG45133.1
AAP32845.1
YP_003933812.1
AAD11960.1
AGC54689.1
AAD11961.1
YP_009230158.1
BAC58067.1
AAA85648.1
AAA88010.1
BAE47051.1
YP_009342376.1
YP_003084394.1
YP_009046525.1
NP_073321.1
YP_001033956.1
NP_077446.1
BAM99305.1
AAD46114.2
AAD46113.2
AAD46115.2
AFB76670.1
AAD46112.2
APO15888.1
ANG65542.1
AEK27122.1
CAA92272.1
YP_009054936.1
AMB16079.1
YP_006273012.1
YP_002333514.1
AII81366.1
YP_009176910.1
β28
β29
β30
β31
β32
β33
AEM64049.1
610
620
630
640
650
AEM64049.1
AAF04615.1
ADG45133.1
AAP32845.1
YP_003933812.1
AAD11960.1
AGC54689.1
AAD11961.1
YP_009230158.1
BAC58067.1
AAA85648.1
AAA88010.1
BAE47051.1
YP_009342376.1
YP_003084394.1
YP_009046525.1
NP_073321.1
YP_001033956.1
NP_077446.1
BAM99305.1
AAD46114.2
AAD46113.2
AAD46115.2
AFB76670.1
AAD46112.2
APO15888.1
ANG65542.1
AEK27122.1
CAA92272.1
YP_009054936.1
AMB16079.1
YP_006273012.1
YP_002333514.1
AII81366.1
YP_009176910.1

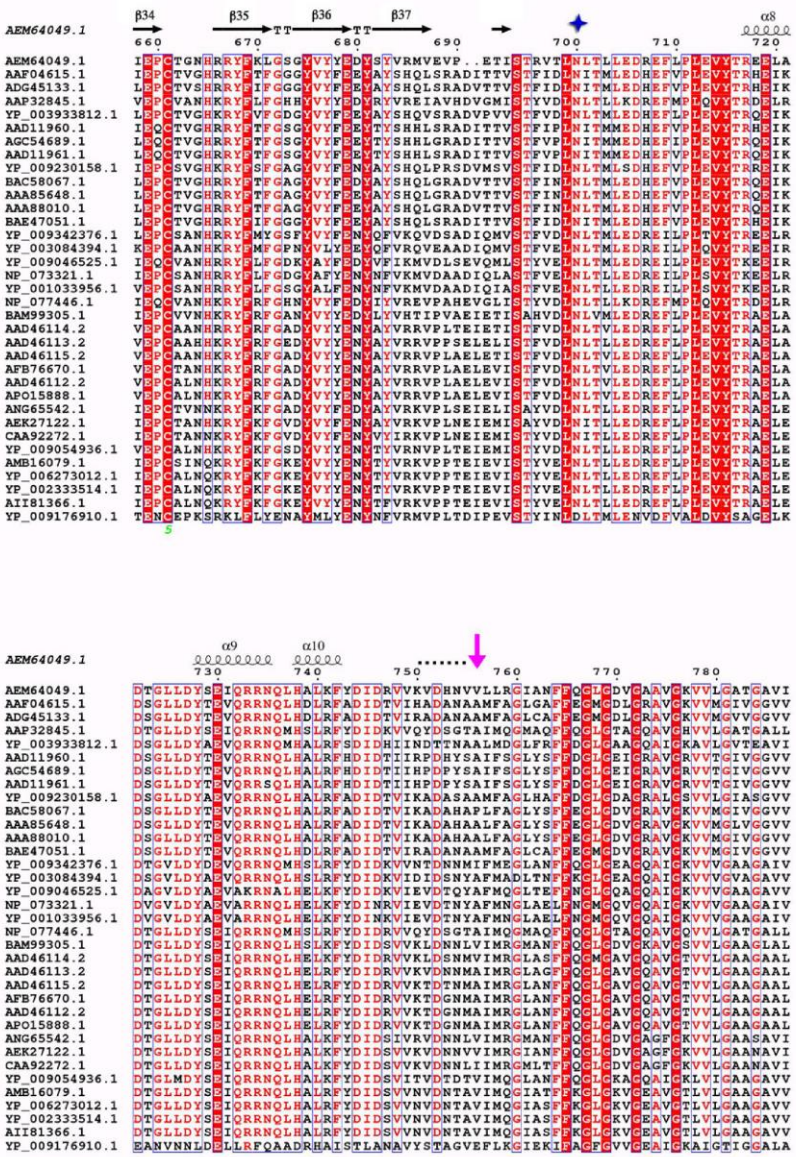
β34
β35
β36
β37
α8
AEM64049.1
660
670
680
690
700
710
720
AEM64049.1
AAF04615.1
ADG45133.1
AAP32845.1
YP_003933812.1
AAD11960.1
AGC54689.1
AAD11961.1
YP_009230158.1
BAC58067.1
AAA85648.1
AAA88010.1
BAE47051.1
YP_009342376.1
YP_003084394.1
YP_009046525.1
NP_073321.1
YP_001033956.1
NP_077446.1
BAM99305.1
AAD46114.2
AAD46113.2
AAD46115.2
AFB76670.1
AAD46112.2
APO15888.1
ANG65542.1
AEK27122.1
CAA92272.1
YP_009054936.1
AMB16079.1
YP_006273012.1
YP_002333514.1
AII81366.1
YP_009176910.1
α9
α10
AEM64049.1
730
740
750
760
770
780
AEM64049.1
AAF04615.1
ADG45133.1
AAP32845.1
YP_003933812.1
AAD11960.1
AGC54689.1
AAD11961.1
YP_009230158.1
BAC58067.1
AAA85648.1
AAA88010.1
BAE47051.1
YP_009342376.1
YP_003084394.1
YP_009046525.1
NP_073321.1
YP_001033956.1
NP_077446.1
BAM99305.1
AAD46114.2
AAD46113.2
AAD46115.2
AFB76670.1
AAD46112.2
APO15888.1
ANG65542.1
AEK27122.1
CAA92272.1
YP_009054936.1
AMB16079.1
YP_006273012.1
YP_002333514.1
AII81366.1
YP_009176910.1

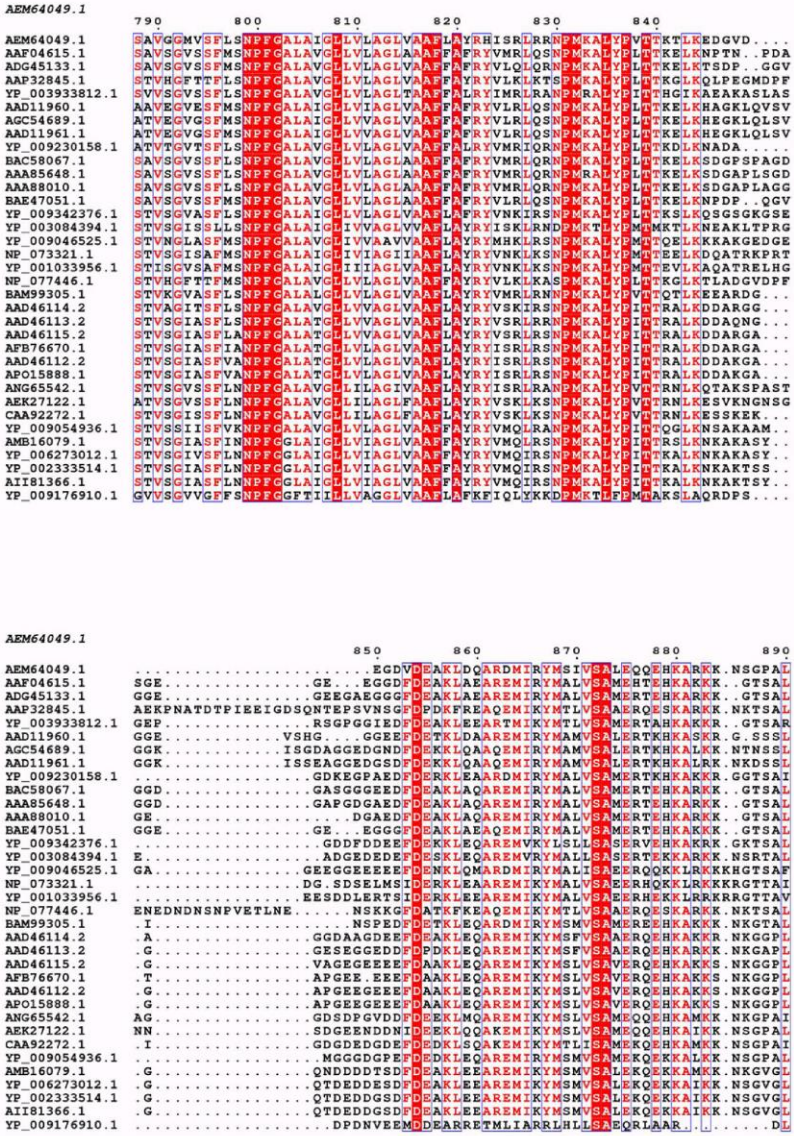
AEM64049.1
790 800 810 820 830 840
AEM64049.1 SAVGGMVSFLSNPFGALAIGLVLAGLVAAELAYRHISRLRRNPMKAFYPVTTKTLKEDGVD....
AAF04615.1 SAVSGVSSFMSNPFGALAVGLVLAGLAAAEFAFRYVMRLQSNPMKAFYPLTTKELKNPTN..PDA
ADG45133.1 SAVSGVSSFMSNPFGALAVGLVLAGLVAAEFAFRYVLQLQRNPMKAFYPLTTKELKTSDP..GGV
AAP32845.1 STVHGFTTFLSNPFGALAVGLVLAGLVAAEFAYRYVLKLKTSPMKAFYPLTTKGLKQLPEGMDPF
YP_003933812.1 SVVSGVSSFLSNPFGALAVGLVLAGLTAAEFALRYIMRLRANPMRAFYPITTHGIKAEAKASLAS
AAD11960.1 AAVEGVESFMSNPFGALAIGLVLIAGLVAAEFAFRYVLRLQSNPMKAFYPLTTKELKHAGKLQVSV
AGC54689.1 ATVEGVGSFMSNPFGALAIGLVVAGLVAAEFAFRYVLRLQSNPMKAFYPLTTKELKHEGKLQLSV
AAD11961.1 ATVEGVGSFMSNPFGALAIGLVVAGLVAAEFAFRYVLRLQSNPMKAFYPLTTKELKHEGKLQLSV
YP_009230158.1 ATVTGVTSFLSNPFGALAVGLVLAGLVAAEFALRYVMRIQRNPMKAFYPLTTKDLKNADA.....
BAC58067.1 SAVSGVSSFLSNPFGALAVGLVLAGLAAAEFAFRYVMRLQRNPMKAFYPLTTKELKSDGPSPAGD
AAA85648.1 SAVSGVSSFLSNPFGALAVGLVLAGLAAAEFAFRYVMRLQRNPMRAFYPLTTKELKSDGAPLSGD
AAA88010.1 SAVSGVSSFLSNPFGALAVGLVLAGLAAAEFAFRYVMRLQRNPMKAFYPLTTKELKSDGAPLAGG
BAE47051.1 SAVSGVSSFMSNPFGALAVGLVLAGLAAAEFAFRYVLRLQSNPMKAFYPLTTKELKNPDP..QGV
YP_009342376.1 STVSGVASFLSNPFGALAIGLVLAGLVAAELAFRYVNKIRSNPMKAFYPLTTKSLKQSGSGKGSE
YP_003084394.1 STVSGISSLLSNPFGALAIGLIVVAGLVVAELAYRYISKLRNDPMKTFYPMTMKTLKNEAKLTPRG
YP_009046525.1 STVNGLASFMSNPFGALAVGLIVVAAVVAAELAYRYMHKLRSNPMKAFYPMTTQELKKKAKGEDGE
NP_073321.1 STVSGISAFMSNPFGALAIGLIVIAGIIAAELAYRYVNKLKSNPMKAFYPMTTEELKDQATRKPRT
YP_001033956.1 STISGVSAFMSNPFGALAIGLIIIAGLVAAELAYRYVNKLKSNPMKAFYPMTTEVLKAQATRELHG
NP_077446.1 STVHGFTTFMSNPFGALAVGLVLAGLVAAEFAYRYVLKLKASPMKAFYPLTTKGLKTLADGVDPF
BAM99305.1 STVKGVASFLSNPFGALALGLVLAGLVAAELAYRYVMRLRNNPMKAFYPVTTQTLKEEARDG...
AAD46114.2 STVAGITSFLSNPFGALAVGLVVAGLVAAELAYRYVSKIRSNPMKAFYPITTRALKDDARGG...
AAD46113.2 STVSGIASFLSNPFGALATGLVVAGLVAAELAYRYVSRLRRNPMKAFYPITTRALKDDAQNG...
AAD46115.2 STVSGIASFLANPFGALATGLVVAGLVAAELAYRYVSRLRSNPMKAFYPITTRALKDDARGA...
AFB76670.1 STVSGIASFIANPFGALATGLVLAGLVAAELAYRYISRLRSNPMKAFYPITTRALKDDARGA...
AAD46112.2 STVSGIASFVANPFGALATGLVLAGLVAAELAYRYISRLRSNPMKAFYPITTRALKDDAKGA...
APO15888.1 STVSGIASFVANPFGALATGLVLAGLVAAELAYRYISRLRSNPMKAFYPITTRALKDDAKGA...
ANG65542.1 STVSGVSSFLNNPFGALAVGLILAGIVAAELAYRYISRLRANPMKAFYPVTTRNLKQTAKSPAST
AEK27122.1 ATVSGVSSFLNNPFGALAVGLILAGLFAAELAYRYVSKLKSNPMKAFYPVTTRNLKESVKNGNSG
CAA92272.1 STVSGISSFLNNPFGALAVGLILAGLFAAELAYRYVSKLKSNPMKAFYPVTTRNLKESSKEK...
YP_009054936.1 STVSSIISFVKNPFGALAVGLVLAGLVAAEFAYRYVMQLRANPMKAFYPITTQGLKNSAKAAM..
AMB16079.1 STVSGIASFINNPFGGLAIGLVLIAGLVAAEFAYRYVMQLRSNPMKAFYPITTRSLKNKAKASY..
YP_006273012.1 STVSGIVSFLNNPFGGLAIGLVLIAGLVAAEFAYRYVMQIRSNPMKAFYPITTKALKNKAKASY..
YP_002333514.1 STVSGIASFLNNPFGGLAIGLVLIAGLVAAEFAYRYVMQIRSNPMKAFYPITTKALKNKAKTSS..
AII81366.1 STVSGIASFLNNPFGGLAIGLVLIAGLVAAEFAYRYVMQIRSNPMKAFYPITTKALKNKAKTSY..
YP_009176910.1 GVVSGVVGFFSNPFGGFTIILLVAGGLVAAELAFKFIQLYKKDPMKTFFPMTAKSLAQRDPS....

AEM64049.1
850 860 870 880 890
AEM64049.1 .....EGDVDEAKLDQARDMIRYMSIVSALEQQEHKARKK.NSGPAL
AAF04615.1 SGE.....EGGDFDEAKLAEAREMIRYMALVSAMEHTEHKAKKK..GTSAL
ADG45133.1 GGE.....GEEGAEGGGFDEAKLAEAREMIRYMALVSAMERTEHKARKK..GTSAL
AAP32845.1 AEKPNATDTPIEEIGDSQNTEPSVNSGFDPDKFREAQEMIKYMTLVSAAERQESKARKK.NKTSAL
YP_003933812.1 GEP.....RSGPGGIEDFDEAKLEEARTMIKYMTLVSAMERTAHKAKKR..GTSAR
AAD11960.1 GGE.....VSHG....GGEEFDETKLDAAREMIRYMAMVSALERTKHKASKR.G.SSSL
AGC54689.1 GGK.....ISGDAGGEDGNDFDEKKLQAAQEMIRYMAMVSALERTKHKALKK.NTNSSL
AAD11961.1 GGK.....ISSEAGGEDGSDFDEKKLQAAQEMIRYMAMVSALERTKHKALRK.NKDSSL
YP_009230158.1 .....GDKEGPAEDFDERKLEAARDMIRYMALVSAMERTKHKAKKR.GGTSAI
BAC58067.1 GGD.....GASGGGEEDFDEAKLAQAREMIRYMALVSAMERTEHKARKK..GTSAL
AAA85648.1 GGD.....GAPGDGAEDFDEAKLAQAREMIRYMALVSAMERTEHKARKK..GTSAL
AAA88010.1 GE.....DGAEDFDEAKLAQAREMIRYMALVSAMERTEHKARKK..GTSAL
BAE47051.1 GGE.....GE...EGGGFDEAKLAEAQEMIRYMALVSAMERTEHKAKKK..GTSAL
YP_009342376.1 .....GDDFDDEEFDEKKLEQAREMVKYLSLLSASERVEHKAKRK.GKTSAL
YP_003084394.1 E.....ADGEDEDEFDESKLEQAREMVRYMALLSASERTEKKARKK.NSRTAL
YP_009046525.1 GA.....GEEGGEEEEEFDENKLQMARDMIRYMALISAEERQQKKLRKKKHGTSAF
NP_073321.1 .....DG.SDSELMSIDERKLEAAREMIKYMALVSAEERHQKKLRKKKRGTTAI
YP_001033956.1 .....EESDDLERTSIDERKLEEAREMIKYMALVSAEERHEKKLRRKRRGTTAV
NP_077446.1 ENEDNDNSNPVETLNE.....NSKKGFDATKFKEAQEMIKYMTLVSAAERQESKARKK.NKTSAL
BAM99305.1 .I.....NSPEDFDETKLEQARDMIRYMSMVSAMEREEHKAKKK.NKGTAL
AAD46114.2 .A.....GGDAAGDEEFDEAKLEQAREMIKYMSFVSAAERQEHKAKKR.NKGGPL
AAD46113.2 .G.....GESEGGEDDFDPDKLEQAREMIKYMSFVSAAERQEHKARKK.NKGAPL
AAD46115.2 .G.....VAGEGEEEEFDAAKLEQAREMIKYMSLVSAVERQEHKAKKS.NKGGPL
AFB76670.1 .T.....APGEE.EEEFDAAKLEQAREMIKYMSLVSAVERQEHKAKKS.NKGGPL
AAD46112.2 .G.....APGEEGEEEFDAAKLEQAREMIKYMSLVSAVERQEHKAKKS.NKGGPL
APO15888.1 .G.....APGEEGEEEFDAAKLEQAREMIKYMSLVSAVERQEHKAKKS.NKGGPL
ANG65542.1 AG.....GDSDPGVDDFDEEKLMQAREMIKYMSLVSAMEQQEHKAMKK.NKGPAI
AEK27122.1 NN.....SDGEENDDNIDEEKLQQAKEMIKYMSLVSAMEQQEHKAIKK.NSGPAL
CAA92272.1 .I.....GDGDEDGDEFDEDKLSQAKEMIKYMTLISAMEKQEHKAMKK.NSGPAI
YP_009054936.1 .....MGGGDGPEFDEDKLEQAREMIRYMSMVSAMEKQEKKALKK.NSGPAL
AMB16079.1 .G.....QNDDDDTSDFDEAKLEEAREMIKYMSMVSALEKQEKKAMKK.NKGVGL
YP_006273012.1 .G.....QTDEDDESDFDEAKLEEAREMIKYMSMVSALEKQEKKAIKK.NSGVGL
YP_002333514.1 .G.....QTDEDDGSDFDEAKLEEAREMIKYMSMVSALEKQEKKAIKK.NSGVGL
AII81366.1 .G.....QTDEDDGSDFDEAKLEEAREMIKYMSMVSALEKQEKKAIKK.NSGVGL
YP_009176910.1 .....DPDNVEEMDDEARRETMLIARRLHLLSAEQRLAAR.....DL

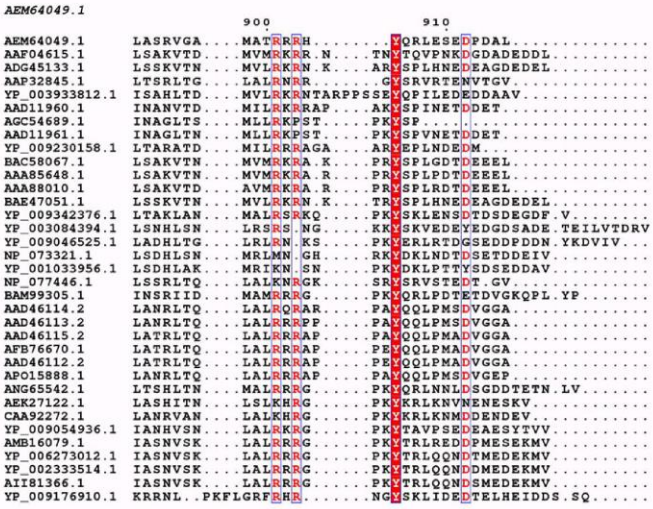
AEM64049.1
900
910
AEM64049.1 LASRVGA....MATRRRH.....KQRLESEDPDAL.....
AAF04615.1 LSAKVTD....MVMRKRR.N....TNKTQVPNKDGADEDDL.....
ADG45133.1 LSSKVTN....MVLRKRN.K....ARKSPLHNEDEAGDEDEL.....
AAP32845.1 LTSRLTG....LALRNRR.....GKKSRVRTENVTGV.....
YP_003933812.1 ISAHLTD....MVLRKRNTARPPSSEKQPILEDEDDAAV.....
AAD11960.1 INANVTD....MILRKRRAP....AKKSPINETDDET.....
AGC54689.1 INAGLTS....MLLRKPST.....PKKSP.....
AAD11961.1 INAGLTN....MLLRKPST.....PKKSPVNETDDET.....
YP_009230158.1 LTARATD....MILRRRAGA....ARKEPLNDEDM.....
BAC58067.1 LSAKVTN....MVMRKRA.K....PRKSPLGDTDEEEL.....
AAA85648.1 LSAKVTN....MVMRKRA.R....PRKSPLPDTDEEEL.....
AAA88010.1 LSAKVTD....AVMRKRA.R....PRKSPLRDTDEEEL.....
BAE47051.1 LSSKVTN....MVLRKRN.K....TRKSPLHNEDEAGDEDEL.....
YP_009342376.1 LTAKLAN....MALRSRKQ.....PKKSKLENSDTDSDEGDF.V.....
YP_003084394.1 LSNHLSN....LRSRS.NG.....KKKSKVEDEYEDGDSADE.TEILVTDRV
YP_009046525.1 LADHLTG....LRLRN.KS.....PKKERLRTDGSEDDPDDN.YKDVIV...
NP_073321.1 LSDHLSN....MRLMN.GH.....RKKDKLNDTDSETDDEIV.....
YP_001033956.1 LSDHLAK....MRIKN.SN.....PKKDKLPTTYSDSEDDAV.....
NP_077446.1 LSSRLTQ....LALKNRGK.....SRKSRVSTEDT.GV.....
BAM99305.1 INSRIID....MAMRRRG.....PKKQRLPDTETDVGKQPL.YP.....
AAD46114.2 LANRLTQ....LALRQRAR.....PAKQQLPMSDVGGA.....
AAD46113.2 LANRLTQ....LALRRRPP.....PAKQQLPMSDVGGA.....
AAD46115.2 LATRLTQ....LALRRRAP.....PAKQQLPMADVGGA.....
AFB76670.1 LATRLTQ....LALRRRAP.....PEKQQLPMADVGGA.....
AAD46112.2 LATRLTQ....LALRRRAP.....PEKQQLPMADVGGA.....
APO15888.1 LANRLTQ....LALRRRAP.....PAKQQLPMSDVGEP.....
ANG65542.1 LTSHLTN....MALRRRG.....PKKQRLNNLDSGDDTETN.LV.....
AEK27122.1 LASHITN....LSLKHRG.....PKKKRLKNVNENESKV.....
CAA92272.1 LANRVAN....LALKHRG.....PKKKRLKNMDDENDEV.....
YP_009054936.1 IANHVSN....LALRKRG.....PKKTAVPSEDEAESYTVV.....
AMB16079.1 IASNVSK....LALRRRG.....PKKTRLREDDPMESEKMV.....
YP_006273012.1 IASNVSK....LALRRRG.....PKKTRLQQNDTMEDEKMV.....
YP_002333514.1 IASNVSK....LALRRRG.....PKKTRLQQNDDMEDEKMV.....
AII81366.1 IASNVSK....LALRRRG.....PKKTRLQQNDSMEDEKMV.....
YP_009176910.1 KRRNL..PKFLGRFRHR.....NGKSKLIDEDTELHEIDDS.SQ.....

4 Own contribution to publications

(I) **Vallbracht M, Schröter C, Klupp BG, Mettenleiter TC.** 2017. Transient Transfection-based Fusion Assay for Viral Proteins. Bio-protocol **7**.

Melina Vallbracht:	Design of the study; Optimization of the protocol for the transient transfection-based fusion assay; Main preparation and correction of the manuscript plus figures and movies.
Christina Schröter:	Preliminary work important for the comparison of different fusion assay systems.
Barbara G. Klupp:	Design of the study; Participation in the preparation and correction of the manuscript plus figures.
Thomas C. Mettenleiter:	Design of the study; Participation in the preparation and correction of the manuscript plus figures; Corresponding author.

(II) **Schröter C, Vallbracht M, Altenschmidt J, Kargoll S, Fuchs W, Klupp BG, Mettenleiter TC.** 2016. Mutations in Pseudorabies Virus Glycoproteins gB, gD, and gH Functionally Compensate for the Absence of gL. J Virol **90**:2264-2272.

Christina Schröter:	Plaque assay of PrV-ΔgLPassB4.1; Sequencing of PrV-ΔgLPassB4.1; Generation of $gB^{B4.1}$ truncation and site specific gB mutants; Functional characterization of gB and $gB^{B4.1}$ using transient transfection-based fusion assay; Interpretation of data; Main participation in the preparation and correction of the manuscript plus figures.
Melina Vallbracht:	Growth kinetics of PrV-ΔgLPassB4.1; Generation of plasmid cloned gD mutants plus sequencing. Characterization of gD mutants by transient transfection-based fusion assay and Western blot analysis. Interpretation of data. Participation in the preparation and correction of the manuscript plus figures.
Jan Altenschmidt:	Reversion analysis of the gL-negative PrV virus mutant and isolation of PrV-ΔgLPassB4.1; Generation of expression plasmids pcDNA-$gB^{B4.1}$ and pcDNA-$gH^{B4.1}$.
Sabrina Kargoll:	Generation of expression plasmid pcDNA-$gD^{B4.1}$; Sequencing of PrV-ΔgLPassB4.1 and plasmid cloned genes.
Walter Fuchs:	Participation in the preparation and correction of the manuscript plus figures.
Barbara G. Klupp:	Design of the study; Interpretation of data; Main participation in the preparation and correction of the manuscript plus figures.
Thomas C. Mettenleiter:	Design of the study; Interpretation of data; Participation in the preparation and correction of the manuscript plus figures; Corresponding author.

(III) **Vallbracht M, Rehwaldt S, Klupp BG, Mettenleiter TC, Fuchs W.** 2017. Functional Relevance of the N-Terminal Domain of Pseudorabies Virus Envelope Glycoprotein H and Its Interaction with Glycoprotein L. J Virol **91**.

Melina Vallbracht:	Characterization of plasmid cloned gH-genes by transient transfection-based fusion assay. Generation and functional characterization of virus mutants including growth and penetration kinetics and plaque assays. Sequencing and Western blot analysis of virus mutants; Design of the study; Interpretation of all data. Main participation in the preparation and correction of the manuscript plus figures.
Sascha Rehwald:	Generation and preliminary characterization of virus mutants and plasmid cloned gH-genes.
Barbara G. Klupp:	Participation in the preparation and correction of the manuscript plus figures.
Thomas C. Mettenleiter:	Design of the study; Participation in the preparation and correction of the manuscript plus figures; Corresponding author.
Walter Fuchs:	Design of the study; Generation of virus mutants and preliminary characterization of virus mutants and plasmid cloned gH-genes; Participation in the preparation and correction of the manuscript plus figures.

(IV) **Vallbracht M, Rehwaldt S, Klupp BG, Mettenleiter TC, Fuchs W.** 2018. Functional Role of N-linked Glycosylation in Pseudorabies Virus Glycoprotein gH. J Virol doi:10.1128/JVI.00084-18.

Melina Vallbracht:	Characterization of plasmid cloned gH-genes by transient transfection-based fusion assay, FACS analysis, indirect immunofluorescence analysis and laser scanning confocal microscopy. Functional characterization of virus mutants including growth kinetics, penetration kinetics and plaque assays; Sequencing and Western blot analysis of virus mutants. Interpretation of all data; Design of the study; Main participation in the preparation and correction of the manuscript plus figures.
Sascha Rehwald:	Generation and preliminary characterization of virus mutants and plasmid cloned gH-genes.
Barbara G. Klupp:	Participation in the preparation and correction of the manuscript plus figures.
Thomas C. Mettenleiter:	Design of the study; Participation in the preparation and correction of the manuscript plus figures; Corresponding author.
Walter Fuchs:	Generation and preliminary characterization of virus mutants and plasmid cloned gH-genes; Design of the study; Participation in the preparation and correction of the manuscript plus figures.

(V) **Vallbracht M, Fuchs W, Klupp BG, Mettenleiter TC.** 2018. Functional Relevance of the Transmembrane Domain and Cytoplasmic Tail of Pseudorabies Virus Glycoprotein H for Membrane Fusion. J Virol 92.

Melina Vallbracht:	Generation of the expression constructs; Sequencing of the plasmids; Characterization of the mutagenized proteins including FACS analysis, indirect immunofluorescence analysis, Western blot analysis, transfection-based cell-cell fusion assay, complementation assay; Interpretation of all data; Design of the study; Main participation in the preparation and correction of the manuscript plus figures.
Walter Fuchs:	Participation in the correction of the manuscript plus figures.
Barbara G. Klupp:	Design of the study; Interpretation of data; Participation in the preparation and correction of the manuscript plus figures.
Thomas C. Mettenleiter:	Design of the study; Interpretation of data; Participation in the preparation and correction of the manuscript plus figures; Corresponding author.

(VI) **Vallbracht M, Brun D, Tassinari M, Vaney MC, Pehau-Arnaudet G, Guardado-Calvo P, Haouz A, Klupp BG, Mettenleiter TC, Rey FA, Backovic M.** 2017. Structure-Function Dissection of Pseudorabies Virus Glycoprotein B Fusion Loops. J Virol doi:10.1128/JVI.01203-17.

Melina Vallbracht:	Generation and sequencing of gB expression plasmids; Functional characterization of gB mutants including Western blot and indirect immunofluorescence analysis, transient transfection-based fusion assay, transcomplementation assay; Analysis of subcellular expression of the different mutants by laser scanning confocal microscopy; Interpretation of functional data; Participation in the preparation and correction of the manuscript plus figures.
Delphine Brun:	Generation of gB constructs used for production of recombinant proteins in mammalian cells; purification of gB recombinant proteins
Matteo Tassinari:	Generation of the gB expression plasmid for production of recombinant ectodomains in insect cells; Generation of first gB crystals
Marie-Christine Vaney:	Assistance with X-ray diffraction data processing, structure model refinement and building.
Gérard Pehau-Arnaudet:	Electron microscopy of gB-liposome complexes.
Pablo Guardado-Calvo:	Assistance with design of the study; Participation in correction of the manuscript plus figures.
Ahmed Haouz:	Assistance with crystal optimization and freezing.
Barbara G. Klupp:	Participation in the preparation and correction of the manuscript plus figures.
Thomas C. Mettenleiter:	Design of the study; Participation in the preparation and correction of the manuscript plus figures.
Felix A. Rey:	Design of the study; Participation in the preparation and correction of the manuscript plus figures
Marija Backovic:	Design of the study; Main participation in the preparation and correction of the manuscript plus figures; Optimization of PrV gB crystals, X-ray data collection, data processing and structure refinement; Structure model building; Liposome floatation assays; Corresponding author.

Obige Angaben (Publikationen I-VI) werden bestätigt:

…… ……

Prof. Dr. Dr. h.c. Thomas C. Mettenleiter Melina Vallbracht

5 Results and discussion

Herpesviruses must fuse their envelope with the host cell plasma membrane for productive infection. Whereas other enveloped viruses can employ only a single protein to mediate the fusion process, herpesviruses require the cooperative action of at least three envelope glycoproteins for entry and direct viral cell-to-cell spread. The core fusion machinery is composed of the *bona fide* fusion gB, the presumably gB activating gH/gL heterodimer, plus other species-specific receptor binding proteins like alphaherpesvirus gD (Eisenberg, Atanasiu *et al.* 2012). However, although crystal structures are available for all four components, the molecular details of the fusion mechanism remain as yet elusive.

In this thesis, the functional relevance of individual components of the essential gH/gL complex of the alphaherpesvirus PrV were investigated. The approaches applied in this thesis to investigate gH/gL function ranged from single amino acid substitutions, to removal of individual domains and deletion of a whole gene (**papers II-V**). In addition to the functional analysis of the fusion regulator gH/gL, the structure and nature of how the *bona fide* fusion protein gB of PrV interacts with membranes to accomplish fusion was investigated in **paper VI**. As basis to assess the fusogenic potential of the PrV entry glycoproteins a robust infection-free, transfection-based cell-cell fusion assay was established (**paper I**).

5.1 Establishment of a transient transfection-based fusion assay for viral fusion proteins (Paper I)

Cell-cell fusion assays are a valuable surrogate for all fusion mechanisms. In **paper I**, an improved protocol for an infection-free, transient transfection-based cell-cell fusion assay was established and described. The fusion assay is based on the ability of the PrV core fusion machinery components, represented by gB and gH/gL, to induce cell-cell fusion in the absence of other viral proteins, when expressed in cells *in vitro* (Klupp, Nixdorf *et al.* 2000; Nixdorf, Klupp *et al.* 2000). Similar reductionist approaches have been developed for *e.g.*, HSV-1 and 2, which are also utilized to quantitate membrane fusion (Turner, Bruun *et al.* 1998; Muggeridge 2000; McShane and Longnecker 2005). Typically, quantitation or evaluation of fusion activity in these systems is based on counting the number of nuclei of a formed syncytium, which is a very time consuming process. Here, we aimed at optimizing the current protocol by facilitating and accelerating the evaluation process. Measurement of fusion activity was facilitated by cotransfection of enhanced green fluorescent protein (EGFP), allowing easy visualization of the formed syncytia using fluorescence microscopy. To obtain more robust and comparable data, important factors like the size and the number of formed syncytia were combined. Thus, 24 h

after transfection, the fusion activity was determined by multiplication of the area of cells with three or more nuclei with the number of formed syncytia within 10 fields of view (5.5 mm^2 each), using the computer software NIS-Elements (Nikon, Düsseldorf, Germany). This robust transient transfection-based cell-cell fusion assay was utilized to study the ability and requirements of the PrV entry glycoproteins to induce membrane fusion (**paper II-VI**).

5.2 Identification and characterization of compensatory mutations in a novel infectious gL-negative mutant PrV-ΔgLPassB4.1 (Paper II)

In **paper II**, the role of the conserved gH/gL complex for membrane fusion was investigated by reversion analysis of a gL-deficient PrV mutant. In contrast to the closely related HSV-1 (Fan, Lin *et al.* 2009), PrV gL is dispensable for virion incorporation of gH (Klupp, Fuchs *et al.* 1997). Moreover, gL-deleted PrV is capable of limited cell-to-cell spread in culture (Klupp and Mettenleiter 1999). Thus, PrV provides the unique opportunity to investigate gH/gL function by reversion analysis of gL-deleted virus mutants by serial cell-culture passages. This approach already resulted in a gL-independently replicating PrV mutant, in which the function of gL was compensated by formation of a gDgH hybrid protein (Klupp and Mettenleiter 1999). In **paper II**, a second independent experiment was carried out, in which the infectious, gL-independently replicating PrV-ΔgLPassB4.1 was isolated and subsequently analyzed to identify the requirements for its gL-independent infectivity.

Sequence analysis of the genes encoding the fusion-associated glycoproteins gH, gB, and gD revealed mutations in each of them. The mutated genes were cloned into a eukaryotic expression vector, and used for the transient transfection-based fusion assay to analyze the impact of the different mutations on membrane fusion.

The mutations in $gH^{B4.1}$ affected the gL binding domain I (L70P, W103R) and were found to be sufficient to compensate for the lack of gL in the fusion assays. Unfortunately, the exact location of the mutations and their influence on the gH-structure could not be specified since domain I was not included in the PrV-gH crystal structure (Backovic, DuBois *et al.* 2010). It is conceivable that the absence of gL resulted in selection of compensatory mutations in the gL-interacting domain of gH. However, trans-complementation assays revealed that these two mutations are not completely sufficient to compensate for all functions of gL, which was reflected by lower final titers.

Two of the three mutations which had occurred in $gB^{B4.1}$ (G672R; ΔK883) strongly enhanced fusogenicity in the transient transfection fusion assays, which was further augmented by truncation of the C-terminal 29 aa of $gB^{B4.1}$ ($gB^{B4.1}$008). The fusion enhancing effect of ΔK883 and the truncation of the C-terminally cytosolic 29 aa of gB support the idea, that the gB CD

negatively regulates fusion (Klupp, Nixdorf *et al.* 2000; Nixdorf, Klupp *et al.* 2000; Rogalin and Heldwein 2015). Thus, the PrV gB CD may function in a similar manner as proposed for the HSV CD, namely by acting as a clamp which braces against the viral or cellular membranes and thereby stabilizes the prefusion form (Vitu, Sharma *et al.* 2013; Cooper and Heldwein 2015; Rogalin and Heldwein 2015). Only recently, the crystal structures of the HSV-1 gB TMD and CD were solved, indicating that in analogy, K883 in PrV gB is part of a conserved belt of basic aa, which was suggested to be involved in interactions of the CD with the membrane (Cooper, Georgieva *et al.* 2018). Possibly, deletion of K883 in $gB^{B4.1}$ could weaken the interaction of the CD with the membrane and, thus, lower the energy required for gB refolding from pre- to postfusion conformation. In line, artificially introduced point mutations at the corresponding site in HSV-1 gB (K865) led to a hyperfusogenic phenotype (Rogalin and Heldwein 2015), indicating a similar function of these aa in the two viruses.

Although fusion activity of $gB^{B4.1}$008 was strongly enhanced, gH was still required for membrane fusion. In contrast to the cytosolic ΔK883, the second mutation in $gB^{B4.1}$, resulting in the substitution of G at position 672 to R, is located in the "crown" domain IV of PrV gB (see section 1.3.2.3, Fig. 5, orange). In addition to the known trimeric postfusion form of gB, a more condensed conformation, presumably a prefusion or intermediate form, has been recently identified (Zeev-Ben-Mordehai, Vasishtan *et al.* 2016). In this conformation, domain IV is localized to the interior of the gB spike, implying an extensive conformational rearrangement during pre- to postfusion transition. Thus, the position and the observed hyperfusogenic effect of G672R in PrV gB suggest that this mutation reduces the kinetic energy barrier which must be overcome for the movement of domain IV during pre- to postfusion refolding.

Coexpression of $gH^{B4.1}$ and $gB^{B4.1}$ resulted in significantly enhanced gL-independent *in vitro* fusion activity. With respect to the observed synergism between $gH^{B4.1}$ and $gB^{B4.1}$ it is conceivable that both, $gH^{B4.1}$ and $gB^{B4.1}$ represent partially triggered and thus more "fusion prone" molecules, which can be further activated without the need for gL.

Surprisingly, $gD^{B4.1}$ had a strong dominant negative phenotype and completely abrogated fusion in the transient assay, even when hyperfusogenic $gH^{B4.1}$ and $gB^{B4.1}$ were coexpressed. This finding was unexpected since the PrV gD is not required for membrane fusion in transient fusion assays (Klupp, Nixdorf *et al.* 2000) or during direct viral cell-to-cell spread (Rauh and Mettenleiter 1991; Peeters, de Wind *et al.* 1992; Mulder, Pol *et al.* 1996). Remarkably, the observed inhibitory effect of $gD^{B4.1}$ could be attributed to a single point mutation resulting in the amino acid substitution A106V located in the ectodomain of $gD^{B4.1}$. Since the interaction between gD and gH/gL of the closely related HSV-1 was postulated to be weak or only transient (Atanasiu, Whitbeck *et al.* 2007; Avitabile, Forghieri *et al.* 2007; Fan, Longnecker *et al.* 2015), an

increase in binding affinity of $gD^{B4.1}$ to gH, resulting in inability of gH to efficiently activate gB, might explain the inhibitory effect of $gD^{B4.1}$. However, in the recently published crystal structure of PrV gD (Li, Lu *et al.* 2017), alanine at position 106 is not exposed on the surface of the protein and the exact molecular mechanism of fusion inhibition by $gD^{B4.1}$ remains enigmatic. Although alanine 106 is conserved in HSV-1 gD, unpublished data revealed that introduction of this mutation in HSV gD does not lead to fusion inhibition (Vallbracht *et al.*, unpublished data). This finding points to interesting additional differences in gD function between the two alphaherpesviruses.

In conclusion, the data suggest that the absence of gL resulted in selection for mutations in gH-domain I, which normally interacts with gL. The mutations in $gH^{B4.1}$ together with hyperfusogenic $gB^{B4.1}$ allowed for gL-independence but led to an excess fusion, which is detrimental to productive virus replication and thus may be counter-regulated by the fusion inhibiting mutations in $gD^{B4.1}$. The appearance of compensatory mutations in the fusion machinery components gH, gB and gD, support the notion that the interplay between the herpesviral entry glycoproteins to mediate fusion is very tightly regulated. Finally, the results demonstrate that, although gL is usually an essential component of the herpesvirus fusion machinery, its function can be compensated by mutations in gH (as in gDgH) or in gH plus gB (this study). Thus, gL appears not to be central to the fusion process but may have a regulatory role.

5.3 Functional relevance of the N-terminal domain of Pseudorabies virus envelope glycoprotein H and its interaction with glycoprotein L (Paper III)

In the gL-independently replicating PrV mutants, the N-terminal domain I of gH, including the proposed gL-binding site, was either affected by point mutations (see section 5.2, **paper II**) or replaced by the N-terminal part of gD, resulting in a gDgH hybrid protein (Klupp and Mettenleiter 1999). Therefore, in **paper III** we aimed at identifying the functional relevance of this structurally uncharacterized N-terminal part of gH by introducing a similar in-frame deletion of gH codons 32 to 97 ($gH^{32/98}$), as observed for the chimeric gDgH, lacking aa 1 to 96 of gH. gH residues 1 to 30 are predicted to represent an N-terminal signal peptide and were retained to enable translocation of gH into the endoplasmic reticulum (ER). Thus, the engineered $gH^{32/98}$ was similar to the gH-core fragment (aa 107 to 639), whose crystal structure has been solved at high resolution (Backovic, DuBois *et al.* 2010).

Targeted deletion of the predicted gL-binding domain did not affect expression or processing of gH as shown by Western blot analysis of purified virus particles. Whereas $gH^{32/98}$ was found to be efficiently incorporated into virus particles, gL could not be detected, indicating that $gH^{32/98}$

was unable to bind gL. These results corroborate that PrV gH, unlike HSV-1 or VZV gH (Roop, Hutchinson *et al.* 1993; Duus and Grose 1996), does not depend on gL or the gL binding domain for virion incorporation, confirming earlier studies (Klupp, Fuchs *et al.* 1997). Moreover, these findings indicate that the N-terminal residues missing in $gH^{32/98}$ indeed comprise the gL binding site of PrV gH, as has been shown for HSV-2 (Chowdary, Cairns *et al.* 2010) and EBV gH/gL (Matsuura, Kirschner *et al.* 2010). In contrast to $gH^{B4.1}$ and the chimeric gDgH, which have been shown to exhibit wild-type like function in transient fusion assays (Klupp and Mettenleiter 1999; Klupp, Nixdorf *et al.* 2000), $gH^{32/98}$ was found to be non-functional in the fusion assay and in the viral context, as demonstrated by *in vitro* replication studies after insertion of the mutated gH gene into the BAC (bacterial artificial chromosome)-cloned PrV genome. These results suggest that the gD moiety in the gDgH hybrid protein may not only provide receptor binding capacity, but also is essential for proper function of the gH-core fragment. It is conceivable that the gD moiety of gDgH exerts a stabilizing or modulating influence on gH structure, which is normally executed by gL and important for interaction with wild-type gB. Strikingly, in the fusion assays $gH^{32/98}$ was able to trigger hyperfusogenic $gB^{B4.1}$ obtained from the passaged gL-deletion mutant PrV-ΔgLPassB4.1 described in **paper II**, indicating that $gB^{B4.1}$ is adapted to interaction with "gL-less" gH. In line, $gB^{B4.1}$ was also able to restore function of $gH^{32/98}$ in the viral context. Thus, simultaneous substitution of gB by $gB^{B4.1}$ and gH by $gH^{32/98}$ rescued infectivity and plaque formation independent of gL.

In conclusion, the results demonstrate that gL and the gL-binding domain are not strictly required for membrane fusion during virus entry and spread provided that compensatory mutations in gH and gB are present. These findings strongly emphasize the notion that a functional gH-gB interaction, presumably between their ectodomains, is crucial for the fusion process and that gL in the wild-type situation may control complex formation.

5.4 Functional relevance of the transmembrane domain and cytoplasmic tail of the Pseudorabies virus glycoprotein H for membrane fusion (Paper IV)

Interactions between gH and gB, in particular between their cytoplasmic domains, have been proposed to be important for fusion in HSV-1, VZV and EBV (Browne, Bruun *et al.* 1996; Harman, Browne *et al.* 2002; Pasieka, Maresova *et al.* 2003; Suenaga, Satoh *et al.* 2010; Yang, Arvin *et al.* 2014; Rogalin and Heldwein 2015; Chen, Jardetzky *et al.* 2016). While studies on HSV support a model in which the gH CD would directly interact with the gB CD by acting as a "wedge" to release the fusion restricting gB CD "clamp" to allow membrane fusion (Rogalin and Heldwein 2015), the gH CD of VZV was hypothesized to act as a "gatekeeper" to control access to functional domains of neighboring proteins, thereby allowing or preventing phosphorylation of

the gB CD (Yang, Arvin *et al.* 2014). However, the studies on the role of the CD and also the TMD of gH from different herpesviruses for membrane fusion are partially contradictory. Although an important function was ascribed to the TMD and CD of the closely related HSV-1 gH (Harman, Browne *et al.* 2002; Jones and Geraghty 2004), soluble HSV-1 gH/gL lacking the CD and membrane anchor, has been found to be sufficient to promote low levels of membrane fusion in transient assays (Atanasiu, Saw *et al.* 2010). In contrast, a soluble form of EBV gH/gL was not sufficient to trigger membrane fusion (Kirschner, Omerovic *et al.* 2006; Rowe, Connolly *et al.* 2013). Because of the apparent fundamental differences in the requirement for the gH TMD in different herpesviruses, we aimed at determining whether the requirements for fusion activation vary for members of different subfamilies or even between the closely related alphaherpesviruses HSV-1 and PrV. Thus, in **paper IV** we elucidated whether the CD of PrV gH is essential to promote membrane fusion and whether gH needs to be firmly anchored in the membrane to fulfil its role, by generation of C-terminally truncated and soluble gH variants. In addition, the PrV gH TMD was substituted by a glycosylphosphatidylinositol (gpi)-anchor and different chimeras with substitution of the CD and TMD were generated.

While approximately half of the PrV gH CD (10 of 19 aa as in PrV gHΔ678) was found to be sufficient for full function in the fusion assays and trans-complementation of gH-deficient PrV (PrV-ΔgH), as was observed for HSV-1 (8 of 14 aa) (Rogalin and Heldwein 2015) and EBV gH (4 of 8 aa) (Chen, Jardetzky *et al.* 2016), further deletion resulted in a significant reduction in fusion activity and complementation of PrV-ΔgH. These results point to a regulatory role for the membrane proximal part of the PrV gH CD. In different alphaherpesviruses, the membrane proximal gH CD residues are partially conserved, comprising a basic residue (K or R; the only exception is VZV), followed by two neutral non-aromatic residues (M, V, L) (**paper III**, Fig. 1, page 64). The first two amino acids have been shown to be important for correct trafficing of HSV-1 gH, presumably by involvement in lipid interactions in the plasma membrane or the viral envelope (Wilson, Davis-Poynter *et al.* 1994). The CD of type I transmembrane proteins is often involved in correct trafficking. Thus, whereas the truncation mutant PrV-gHΔ670, retaining only the first two membrane proximal residues, was efficiently processed and transported to the cell surface, gHΔ668 completely lacking the CD, was predominantly detected in its immature form. Nevertheless, cell surface expression of this mutant was only slightly reduced and gHΔ668 still complemented PrV-ΔgH to around 10-fold reduced titers. These results demonstrate that the PrV gH CD, in contrast to the HSV-1 gH CD (Harman, Browne *et al.* 2002; Rogalin and Heldwein 2015), is not required for gH incorporation into the virus envelope to function during entry.

Since gHΔ670 and gHΔ668 showed reduced *in vitro* fusion levels the PrV gH CD, although not essential, may modulate fusion in a similar manner as proposed for HSV (Rogalin and Heldwein

2015). However, it can also not be excluded that truncations in PrV gH may affect the conformation of the gH ectodomain, thereby influencing interactions between the gB and gH ectodomains, as was shown for C-terminal truncation of EBV gH altering binding of gp42 to the gH ectodomain (Yang, Arvin *et al.* 2014; Rogalin and Heldwein 2015; Chen, Jardetzky *et al.* 2016).

Whereas the gH CD was found to be dispensable for gH function during virus infection, deletion of the TMD (and CD) or substitution by a lipid-anchor (gH-gpi) or the PrV gD TMD resulted in proteins, which were nonfunctional in the cell-cell fusion assays or complementation of a gH-negative virus, despite efficient cell surface expression. Thus, membrane anchorage by the gH TMD is essential for PrV gH function. Accordingly, studies on the TMD of HSV-1 gH revealed that the TMD of HSV-1 gD or other type I membrane proteins such as CD8 and influenza HA were not sufficient to functionally substitute for the HSV-1 gH TMD (Harman, Browne *et al.* 2002). Interestingly, despite low sequence conservation, we found that the HSV-1 gH TMD could functionally substitute for the PrV gH TMD in the fusion assays and in trans-complementation of PrV-ΔgH, pointing to functional conservation. Together, these data point to specific features within the membrane-spanning domain of herpesvirus gH, which are apparently not present in *e.g.*, the PrV gD TMD.

A highly conserved glycine in the HSV-1 gH TMD, which is also present in PrV (aa 812 in HSV-1; aa 655 in PrV) is crucial for efficient fusion (Harman, Browne *et al.* 2002). However, sequence analysis revealed that this particular glycine is also present in the PrV gD TMD (aa 362) indicating that this residue alone is not sufficient for functional complementation of gH. However, three additional aa were found to be conserved between the PrV and HSV-1 gH TMD, which are absent from PrV gD. Interestingly, two of them (A808 and S809 in HSV; A651 and S652 in PrV gH) are essential for HSV gH function during membrane fusion (Harman, Browne *et al.* 2002). Since the HSV-1 gH TMD can functionally substitute for the corresponding domain in PrV gH, a similar significance of these aa for fusion seems likely. Intriguingly, an alpha helical-wheel plot places those four residues which are conserved between PrV and HSV-1 gH, on one face of the helix (Harman, Browne *et al.* 2002), suggesting that the gH TMD has an intrinsic property to specifically interact with lipids or other molecules in the membrane, involving these residues. In influenza HA specific TMD residues are essential for the oligomeric state and function of the protein (Kemble, Henis *et al.* 1993; Melikyan, Lin *et al.* 1999; Melikyan, Markosyan *et al.* 2000). Moreover, recent studies demonstrated trimeric interactions between isolated TMDs of class I and III fusion proteins from a variety of viruses including paramyxoviruses, Ebola virus, influenza virus, and rabies virus, suggesting that TMD-TMD interactions could play an important role in the fusion process (Smith, Smith *et al.* 2013; Webb, Smith *et al.* 2018), possibly, also in herpesviruses.

While the predicted TMDs of PrV and HSV-1 comprise 21 aa, which is close to the lower limit for a transmembrane spanning helix (Harman, Browne *et al.* 2002), the TMD of gD consists of 23 aa. Therefore, it cannot be excluded that the difference in length and not the aa composition accounts for the nonfunctional phenotype observed with PrV gH containing the gD TMD.

In summary, in paper IV we could identify the TMD of PrV gH as an essential component of the fusion machinery, while the PrV gH CD was found to play a modulatory but non-essential role. As observed for EBV (Kirschner, Omerovic *et al.* 2006), but unlike HSV (Atanasiu, Saw *et al.* 2010), soluble forms of PrV gH/gL are unable to trigger gB mediated membrane fusion. Based on our findings and previous studies on the closely related HSV-1 gH TMD (Harman, Browne *et al.* 2002), which was able to functionally substitute for the PrV gH TMD, we hypothesize that the gH TMD has an intrinsic property to interact with membrane components such as lipids or other molecules as a prerequisite for promoting membrane fusion.

5.5 Functional role of N-linked glycosylation in Pseudorabies virus glycoprotein H (Paper V)

Many viral envelope proteins are modified by N-linked glycosylation, which is one of the most abundant and important posttranslational modifications, known to play major roles in correct folding of proteins, their physiochemical properties, intracellular transport and also function during entry (Helenius and Aebi 2004; Helle, Vieyres *et al.* 2010; Lennemann, Walkner *et al.* 2015). Inactivation of N-glycosylation sites from envelope proteins of a variety of viruses including gB of the closely related HSV-2 (Luo, Hu *et al.* 2015), has been shown to have a strong impact on viral infection. However, little is known about the requirement of herpesvirus gH N-glycosylation for its function during virus infection. Thus, in the present **paper V**, the functional role of N-linked glycans on PrV gH was systematically investigated. To this end, all five potential N-linked glycosylation sites (N77, N162, N542, N604, and N627) were inactivated by introduction of conservative amino acid substitutions of N by glutamine (Q) singly or in various combination. The proteins were characterized with respect to their *in vitro* fusion activity. Furthermore, the engineered gH genes were inserted into the BAC-cloned PrV genome for investigation of the protein expression, maturation, glycosylation state and *in vitro* replication properties of the resulting virus mutants in cell culture.

Western blot analysis of purified virus particles revealed that all five sites in PrV gH are modified by N-linked carbohydrates. gH of a PrV mutant, in which all five glycosylation sites were mutated, was no longer sensitive to N-glycosidases and showed a molecular mass as predicted for the non-glycosylated precursor protein. This demonstrated that no other larger modifications are present in gH, which is in line with earlier reports (Klupp, Visser *et al.* 1992).

While proper N-glycosylation was shown to be critical for correct intracellular trafficking and maturation of the core fusion machinery component gB of HSV-2 (Luo, Hu *et al.* 2015), inactivation of most of the glycosylation sites in PrV gH had no effect on protein expression or subcellular localization. However, mutation of glycosylation site N627, which is highly conserved among the *Herpesviridae,* severely affected intracellular transport of PrV gH, resulting in ER retention and reduced surface expression. Moreover, glycosylation at N627 was found to be important for gH function during membrane fusion, since all mutants with inactivation of this site were unable to mediate membrane fusion in combination with wild-type gB, gD, and gL. Nonetheless, in line with earlier studies, gHN627Q was able to trigger a C-terminally truncated, hyperfusogenic variant of gB (gB-008) (Fuchs, Backovic *et al.* 2012). Since gB-008 is highly expressed on the surface of transfected cells due to truncation of an endocytosis motif (Nixdorf, Klupp *et al.* 2000), it is conceivable that smaller amounts of gH are sufficient to trigger membrane fusion.

gHN627Q as well as multiple mutants exhibiting this aa substitution were efficiently incorporated into virus particles, suggesting that other viral components may influence the intracellular transport of gH during viral infection. EBV and HSV-1 gH for example are highly dependent on gL for correct transport and virion incorporation (Hutchinson, Browne *et al.* 1992; Chowdary, Cairns *et al.* 2010; Matsuura, Kirschner *et al.* 2010), whereas PrV gH is efficiently transported and incorporated into virus particles without gL (**paper II-III**, (Klupp, Baumeister *et al.* 1994; Klupp and Mettenleiter 1999)).

Although formation of infectious progeny was barely affected by mutation of N627, in line with the observed defect in *in vitro* fusion activity, N627Q led to a significant decrease in plaque sizes, used as a read-out for cell-to-cell spread, and a delay in penetration kinetics, confirming previous results (Fuchs, Backovic *et al.* 2012). N627 is part of a conserved hydrophobic patch in domain IV (see section 1.3.2.2, Fig. 4). This hydrophobic patch was suggested to play a role in membrane fusion by interacting with the viral envelope after a receptor-triggered conformational change of gH (Backovic, DuBois *et al.* 2010). Therefore, N627 together with the "flap" were proposed to partially cover this patch to prevent premature interactions with the membrane (Backovic, DuBois *et al.* 2010; Fuchs, Backovic *et al.* 2012). Accordingly, N627 was found to be important, although non-essential for membrane fusion, indicating that presence of the basic "flap" may be sufficient to cover the underlying hydrophobic patch. In line, N-glycosylation of HSV-1 gH at this site was also shown to be non-essential for gH function (Galdiero, Whiteley *et al.* 1997). Nevertheless, PrV gH trafficking was greatly affected by mutation N627Q, which might also contribute to the spreading defects of the corresponding recombinants.

In addition to N627, glycosylation at PrV-specific N77 was also found to be important in *in vitro* fusion assays and direct viral cell-to-cell spread. Simultaneous inactivation of N77 and N627 further reduced *in vitro* fusion activity and cell-to-cell spread as shown by plaque assays. N77 is located within the structurally uncharacterized PrV gH domain I, which was shown to be important for gL-binding (**paper II-III**), suggesting that the N-glycan attached at this site may modulate interaction between gH and gL. Thus, inactivation of this site may interfere with efficient membrane fusion. However, gH/gL binding per se was not impaired as demonstrated by Western Blot analysis of purified virus particles, revealing that gL was efficiently incorporated into pPrV-gHN77Q particles. Interestingly, in contrast to N77 and N627, removal of N604 was found to enhance *in vitro* fusion activity and cell-to-cell spread. N604 is conserved between members of the *Varicellovirus* genus but is not present in members belonging to the *Simplexvirus* genus (Backovic, DuBois *et al.* 2010). However, N604 is also located in the most conserved gH domain IV. Interestingly, substitution of this domain in PrV gH by the corresponding domain of HSV-1 gH resulted in a functional protein, which is capable of activating both, PrV and HSV-1 gB, indicating functional conservation and species-specific interactions of gH domain IV with gB (Böhm, Backovic *et al.* 2016). Removal of the carbohydrate at position N604 could impact positively on this gH-gB interaction, leading to enhanced fusion activity. However, despite the apparent hyperfusogenic phenotype during cell-to-cell spread, pPrVgHN604Q exhibited a slight delay in penetration, indicating mechanistic differences between membrane fusion during entry of free virus particles and direct viral cell-to-cell spread. As outlined above (section 5.2, **paper II**), this differences in the two fusion events is also highlighted by the protein requirements, as presence of PrV gD is essential for entry but dispensable for plaque formation (Rauh and Mettenleiter 1991; Peeters, de Wind *et al.* 1992; Klupp, Nixdorf *et al.* 2000).

In conclusion, the results demonstrate a modulatory role of N-glycans in proper localization and function of PrV gH during membrane fusion. However, even simultaneous inactivation of all five N-glycosylation sites did not substantially impair formation of infectious virus particles, suggesting a nonessential role for N-glycans in PrV gH for efficient replication. It should be noted, however, that N-glycans can function as a “shield” to cover essential viral epitopes protecting the virus from antibody-mediated neutralization, as was shown for influenza virus and HIV (Wei, Decker *et al.* 2003; Wanzeck, Boyd *et al.* 2011). Thus, N-glycans on PrV gH may mask epitopes, which can otherwise be targeted by neutralizing antibodies.

5.6 Structure function dissection of Pseudorabies virus gB fusion loops (Paper VI)

Within the framework of this thesis it was elaborated that gL and the gL binding domain of PrV gH are dispensable for maturation and virion incorporation of gH, and, conditionally, also for membrane fusion in transient assays and during viral entry and spread (**paper II and III**). Moreover, it has been demonstrated that PrV gD is not required for membrane fusion in the transient assays (**paper II**, (Klupp, Nixdorf *et al.* 2000)), reducing the complexity of cell-cell fusion from four proteins, as necessary in HSV-1 (Turner, Bruun *et al.* 1998), to only two proteins in PrV (Klupp, Nixdorf *et al.* 2000). By comparison with other class III fusion proteins, herpesvirus gB appears to contain all features necessary to effect fusion (Backovic and Jardetzky 2011), raising the question whether gB can be transformed into an autonomous fusion protein. In this context, we could show that truncation of the C-terminal 29 aa of the already highly fusogenic $gB^{B4.1}$ ($gB^{B4.1}$008) could even further enhance gB fusogenicity to around 350% when compared to wild-type gB (**paper II**). However, even this extremely fusogenic gB was still reliant on activation via gH. Thus, hyperfusogenicity per se appears to be insufficient to substitute for activation by gH. Interestingly, exposure to heat has been shown to act as a surrogate trigger for gH/gL to activate EBV gB (Chesnokova, Ahuja *et al.* 2014), and several other class III and I fusion proteins (Ruigrok, Martin *et al.* 1986). However, heat-induced fusion has not been reported for HSV gB (Fan, Kopp *et al.* 2017), and elevated temperatures could not trigger PrV gB (Vallbracht *et al.*, unpublished data). Other external stimuli which could act as potential triggers, such as low-pH treatment were found to induce structural changes in HSV gB, which, however, were unable to trigger fusogenicity of HSV gB (Dollery, Delboy *et al.* 2010; Stampfer, Lou *et al.* 2010), or PrV gB (Vallbracht *et al.*, unpublished data). These findings strongly support the hypothesis that structural interactions between gH and gB are essential for gB activation but also raise questions regarding the evidence that PrV gB is indeed the actual fusion protein.

Entry of enveloped viruses relies on the insertion of nonpolar residues, termed fusion peptides or fusion loops, of the viral fusion protein into the outer leaflet of the host cell membrane (White, Delos *et al.* 2008). In **paper VI** the crystal structure of the ectodomain of PrV gB was determined at 2.7-Å resolution, revealing a typical class III postfusion trimer, which can associate with membranes via its FLs. Despite the structural data available for the ectodomains of gB from several herpesviruses, such as HSV-1 (Heldwein, Lou *et al.* 2006), EBV (Backovic, Longnecker *et al.* 2009) and HCMV (Burke and Heldwein 2015; Chandramouli, Ciferri *et al.* 2015), the molecular details of how gB FLs insert into the lipid bilayer, remained unclear. Thus, based on the structural data for PrV gB, we performed functional analyses including liposome binding experiments, cell-cell fusion and complementation assays to identify key residues in the gB FLs, essential for membrane binding and fusion induction.

All class III fusion proteins identified so far utilize bipartite FLs to interact with the target membrane (Backovic and Jardetzky 2011). However, despite their structural homology, the amino acid sequence of FLs of herpesviruses is only poorly conserved, even within the same subfamily. PrV gB was found to contain two putative fusion loops (FL1 and FL2), which are exposed at the tip of the molecule in domain I (see section 1.3.2.3., Fig 5, black asterisks). Whereas the FL tips of EBV and HCMV gB are predominantly hydrophobic and had to be mutated for protein crystallization, since they caused the recombinant ectodomains to aggregate, PrV and HSV gB FLs tips are less hydrophobic and the ectodomains form soluble trimers, providing the opportunity to crystallize and study them as wild-type forms.

Liposome flotation assays demonstrated that the PrV wild-type gB ectodomain is able to associate with liposomes of different compositions, which could be visualized by cryo-electron microscopy (EM), demonstrating that the gB postfusion ectodomain trimers indeed insert into the synthetic membranes via domain I containing the FLs. In line, the recombinant ectodomain of HSV-1 gB was likewise shown to associate with liposomes via domain I (Hannah, Cairns *et al.* 2009). To identify residues in the PrV gB FLs, which are essential for membrane binding and fusion, all seven aromatic and hydrophobic residues, present in the PrV gB FLs, were systematically substituted to alanine, resulting in replacement of the bulky hydrophobic side chain with a methyl group. Additionally, the residues were changed to a different aromatic residue with a similar chemical structure to determine whether the residue would insert into the more polar interfacial region of the membrane or even deeper into the hydrocarbon core. The resulting mutants were tested in liposome coflotation experiments and for their ability to mediate membrane fusion in cell-cell fusion assays and to complement a gB-negative PrV mutant (Nixdorf, Klupp *et al.* 2000). Four residues in PrV gB, namely tryptophan (W)187 and tyrosine (Y)192, which are located in FL1, as well as phenylalanine (F)275 and Y276, present in FL2, were demonstrated to be crucial for liposome binding and for membrane fusion in the cellular and viral context, since substitution of these residues to alanine resulted in non-functional proteins. Interestingly, PrV gB with substitution of Y276 or Y192 to F was able to mediate membrane fusion and associated with liposomes, indicating that gB requires bulky, aromatic site chains at these positions to retain functionality. Residue F275 in FL2 tolerated substitution to W but not to Y, suggesting that the presence of a hydrophilic moiety at this position affects functionality. The tolerance for W but not for Y indicates that F275 likely inserts more deeply into the membrane core, *i.e.*, deeper than the amphipathic, interfacial region. Together with the structural information, the functional data suggest a model in which the side chains of PrV gB residues W187, Y192, F275 and Y276 form a continuous hydrophobic and electrostatically neutral patch at the surface of the trimeric postfusion spike. Whereas F275 from

the tip of FL2 would protrude deeper into the hydrocarbon core, the side chains of W187, Y192, and Y276 appear to form an aromatic surface, which would enable insertion into the polar region of the membrane, establishing an interfacial rim structure which provides multiple interactions with the lipid head groups. Sequence comparison of different alphaherpesvirus gBs reveals that residues with similar membrane-partitioning preferences are present at these four positions. Thus, residues which correspond to F275 of PrV gB FL2 were found to be hydrophobic (F, W, V, and L) in all analyzed sequences, allowing insertion into the hydrocarbon core of the membrane. Positions corresponding to W187, Y192, and Y276 are occupied by residues with amphipathic side chains (W, Y, and H), which are compatible with insertion into the interfacial region. Moreover, the results from functional analyses of PrV gB FLs obtained here are mostly in line with reports on the HSV-1 gB FLs (Hannah, Heldwein *et al.* 2007; Hannah, Cairns *et al.* 2009). Together, these findings indicate that a common mode of gB FL insertion into membranes may have evolved within the alphaherpesvirus subfamily. More importantly, structural and sequence comparison of alphaherpesvirus gB FLs with those of beta- and gammaherpesviruses suggest that the mode of membrane interaction may be similar. Thus, although beta- and gammaherpesviruses exhibit more hydrophobic residues at the tips of their FLs, hydrophobic residues exposed in FL2 may penetrate into the core of the lipid bilayer, while residues from both FL1 and 2 form a rim above, which would insert into the region between the hydrocarbon core and the aqueous phase to catalyze the fusion process.

Not only the amino acids, but also the lipid composition was found to influence the function of PrV gB. Binding of PrV gB to liposomes, used as surrogate for a host cell membrane, was highly dependent on the presence of cholesterol (CH). For the PrV gB ectodomain to bind, at least 40 % CH were required, which correlates with the amount of 30 to 40% CH being present in the plasma membrane and secretory vesicles (Lange, Swaisgood *et al.* 1989). CH has been demonstrated to induce lipid curvature, facilitate formation of lipid stalks, and also to stabilize fusion pores (Yang, Kreutzberger *et al.* 2016). The results obtained here for PrV coincide with the growing evidence that enveloped viruses, including HSV (Bender, Whitbeck *et al.* 2003; Hannah, Cairns *et al.* 2009), HIV (Liao, Cimakasky *et al.* 2001; Yang, Kiessling *et al.* 2016) and Influenza virus (Sun and Whittaker 2003) exploit CH-rich membrane regions to efficiently enter host cells.

In conclusion, this study demonstrated that the PrV gB ectodomain forms a typical class III postfusion trimer, which is able to insert into membranes with its FLs in a CH-dependent manner via a mode of action, which is likely to be conserved throughout the *Herpesviridae* family. Finally, these findings support the hypothesis that gB is indeed the *bona fide* fusion protein.

6 Summary

Herpesviruses are a fascinating group of enveloped DNA viruses, which rely on membrane fusion for infectious entry and direct cell-to-cell spread. Compared with many other enveloped viruses, they utilize a remarkably complex fusion machinery. Three conserved virion proteins, the *bona fide* fusion protein gB, and the presumably gB activating gH/gL heterodimer constitute the conserved core fusion machinery and are believed to drive membrane fusion in a cascade-like fashion. Activation of this cascade in most alphaherpesviruses is proposed to be triggered by binding of gD to specific host cell receptors. The molecular details of this fusion process, however, remain largely elusive. Yet, a detailed mechanistic knowledge of this process would be greatly beneficial for the development of efficient countermeasures against a variety of diseases.

In this thesis, the functional relevance of individual components of the essential gH/gL complex of the alphaherpesvirus PrV has been assessed by two different approaches: by reversion analysis (**paper II**) and site-directed mutagenesis (**papers III-V**). In contrast to other herpesviruses, gL-deleted PrV is able to perform limited cell-to-cell spread, providing the unique opportunity to passage the entry-deficient virus in cell culture to select for PrV revertants capable of infecting cells gL-independently. This approach already resulted in an infectious gL-negative PrV mutant (PrV-ΔgLPass), in which the function of gL was compensated by formation of a gDgH hybrid protein. Here, the requirements for gL-independent infectivity of a second independent revertant (PrV-ΔgLPassB4.1), were analyzed. Sequencing of the genes encoding for gB, gH and gD, revealed mutations in each of them. By means of a robust infection-free, transfection-based cell-cell fusion assay (**paper I**), we identified two amino acid substitutions in the gL-binding domain I of $gH^{B4.1}$ (L70P, W103R) as sufficient to compensate for lack of gL. Two mutations in gB (G672R, ΔK883) were found to enhance fusogenicity, probably by lowering the energy, required for gB refolding from pre- to postfusion conformation. Coexpression of $gH^{B4.1}$ and $gB^{B4.1}$ led to an excess fusion, which was completely suppressed by $gD^{B4.1}$ in the fusion assays. This was surprising since PrV gD is normally not required for *in vitro* fusion or direct viral cell-to-cell spread, clearly separating this process from fusion during entry, for which PrV gD is essential. The fusion inhibiting effect of $gD^{B4.1}$ could be attributed to a single point mutation resulting in an amino acid substitution within the ectodomain (A106V). In conclusion, these results indicated that gL is not central to the fusion process, as its function can be compensated for. As found so far, gL-independent infectivity can be realized by compensatory mutations in gH (as in PrV-ΔgLPass) or in gH plus gB (as in PrV-ΔgLPassB4.1). Excessive fusion induced by $gH^{B4.1}$ and $gB^{B4.1}$ was counter-regulated by $gD^{B4.1}$, indicating that the interplay between these proteins is precisely

regulated and further implies that gL and gD, despite being not absolutely essential for the fusion process, have important regulatory functions on gH and/or gB.

Both PrV-ΔgLPass mutants had acquired compensatory mutations in gH affecting the predicted gL-binding domain I in gH. By construction of an artificial $gH^{32/98}$, which lacked the predicted gL-binding domain and was similar to the recently crystallized gH-core fragment present in the gDgH hybrid protein, we identified the N-terminal part of PrV gH as essential for gH function during fusion (**paper III**). $gH^{32/98}$ was unable to promote fusion of wild-type gB in fusion assays and led to a total loss of function in the viral context. These results indicated that the gD moiety, present in gDgH, is critical for proper function of the gH-core fragment. We hypothesize that the gD moiety may adopt a stabilizing or modulating influence on the gH structure, which is normally executed by gL and important for interaction of gH with wild-type gB. Remarkably, substitution of wild-type gB by $gB^{B4.1}$ rescued function of $gH^{32/98}$ in the cellular and viral contexts. These findings suggest that $gB^{B4.1}$ has been selected for interaction with "gL-less" gH. In conclusion, these results demonstrated that gL and the gL-binding domain are not strictly required for membrane fusion during virus entry and spread but that compensatory mutations must be present in gB to restore a fully functional fusion machinery. These results strongly support the notion of a functional gH-gB interaction as a prerequisite for membrane fusion.

In addition to the N-terminal domain, we identified the transmembrane domain of PrV gH as an essential component of the fusion machinery, while the cytoplasmic domain was demonstrated to play a modulatory but nonessential role (**paper IV**). Whereas truncation or substitution of the PrV gH TMD by a gpi-anchor or the analogous sequence from PrV gD rendered gH non-functional, the HSV-1 gH TMD was found to functionally substitute for the PrV gH TMD in cell-cell fusion and complementation assays. Since residues in the TMD which are conserved between HSV and PrV gH but absent in PrV gD, are placed on one face of an α-helical wheel plot, we hypothesize that the gH TMD has an intrinsic property to interact with membrane components such as lipids or other molecules as a requirement for promoting membrane fusion.

In a final study focusing on the function of gH, we identified the N-glycosylation sites utilized by PrV gH, and determined their individual role in viral infection (**paper V**). PrV gH was found to be modified by N-glycans at five potential glycosylation sites. N-glycans at PrV specific N77 and the highly conserved site N627 were found to be critical for efficient membrane fusion in the fusion assays, and during viral entry and cell-to-cell spread. N627 was further shown to be crucial for proper gH transport and maturation. In contrast, inactivation of N604, conserved in the *Varicellovirus* genus, enhanced *in vitro* fusion activity and viral cell-to-cell spread. These findings demonstrated a role of the N-glycans in proper localization and function of PrV gH.

While we were able to demonstrate that gL and gL-binding domain are dispensable for membrane fusion, a surrogate trigger for gH to activate gB could not be identified. Thus, despite all effort made to transform PrV gB into an autonomous fusion protein *e.g.*, by introduction of fusion enhancing mutations into the already highly fusogenic $gB^{B4.1}$ ($gB^{B4.1}$008) or exposure to external stimuli such as heat or low pH, gH was still required. These results strongly support the notion that physical interactions with gH are necessary for triggering gB but also raise questions regarding the evidence that PrV gB is the actual fusion protein. The final study presented in this thesis (**paper VI**) provided evidence that gB is indeed the fusogen of PrV. In this study, the crystal structure of PrV gB was solved at 2.7 Å resolution, revealing a class III postfusion trimer, which is able to bind to membranes via its bipartite fusion loops in a cholesterol-dependent manner. By mutagenesis studies we could identify the key residues in the PrV gB FLs, essential for membrane binding and fusion in cellular and viral contexts. These residues form a continuous hydrophobic patch, compatible with insertion into membranes. Based on the structural and functional data combined with comparative analysis with gBs from beta- and gammaherpesviruses, we propose for the first time a molecular model on how the initial interaction of gB with the target membrane is established, which may be valid not only for alphaherpesviruses but for all members of the *Herpesviridae* family.

In conclusion, this thesis significantly expanded the current knowledge on the membrane fusion mechanism utilized by this fascinating family of viruses. The mutagenesis and structural studies yielded critical information on the fusion capabilities and functional requirements of the herpesvirus fusion machinery components and their interactions. Moreover, the study provides a comprehensive picture of common elements and differences in the fusion process of different herpesviruses, particularly on the interactions of gB with the membrane and the functional requirements for gH, providing an important basis for future research.

7 References

Abou-Hamdan A, Belot L, Albertini A and Gaudin Y (2018). "Monomeric Intermediates Formed by Vesiculovirus Glycoprotein during Its Low-pH-induced Structural Transition." *J Mol Biol*.

Aeffner S, Reusch T, Weinhausen B and Salditt T (2012). "Energetics of stalk intermediates in membrane fusion are controlled by lipid composition." *Proc Natl Acad Sci U S A* **109**(25): E1609-1618.

Atanasiu D, Cairns TM, Whitbeck JC, Saw WT, Rao S, Eisenberg RJ and Cohen GH (2013). "Regulation of herpes simplex virus gB-induced cell-cell fusion by mutant forms of gH/gL in the absence of gD and cellular receptors." *MBio* **4**(2).

Atanasiu D, Saw WT, Cohen GH and Eisenberg RJ (2010). "Cascade of events governing cell-cell fusion induced by herpes simplex virus glycoproteins gD, gH/gL, and gB." *J Virol* **84**(23): 12292-12299.

Atanasiu D, Saw WT, Eisenberg RJ and Cohen GH (2016). "Regulation of HSV glycoprotein induced cascade of events governing cell-cell fusion." *J Virol*.

Atanasiu D, Whitbeck JC, Cairns TM, Reilly B, Cohen GH and Eisenberg RJ (2007). "Bimolecular complementation reveals that glycoproteins gB and gH/gL of herpes simplex virus interact with each other during cell fusion." *Proc Natl Acad Sci U S A* **104**(47): 18718-18723.

Atanasiu D, Whitbeck JC, de Leon MP, Lou H, Hannah BP, Cohen GH and Eisenberg RJ (2010). "Bimolecular complementation defines functional regions of Herpes simplex virus gB that are involved with gH/gL as a necessary step leading to cell fusion." *J Virol* **84**(8): 3825-3834.

Avitabile E, Forghieri C and Campadelli-Fiume G (2007). "Complexes between herpes simplex virus glycoproteins gD, gB, and gH detected in cells by complementation of split enhanced green fluorescent protein." *J Virol* **81**(20): 11532-11537.

Avitabile E, Forghieri C and Campadelli-Fiume G (2009). "Cross talk among the glycoproteins involved in herpes simplex virus entry and fusion: the interaction between gB and gH/gL does not necessarily require gD." *J Virol* **83**(20): 10752-10760.

Babic N, Mettenleiter TC, Flamand A and Ugolini G (1993). "Role of essential glycoproteins gII and gp50 in transneuronal transfer of pseudorabies virus from the hypoglossal nerves of mice." *J Virol* **67**(7): 4421-4426.

Backovic M, DuBois RM, Cockburn JJ, Sharff AJ, Vaney MC, Granzow H, Klupp BG, Bricogne G, Mettenleiter TC and Rey FA (2010). "Structure of a core fragment of glycoprotein H from pseudorabies virus in complex with antibody." *Proc Natl Acad Sci U S A* **107**(52): 22635-22640.

Backovic M and Jardetzky TS (2009). "Class III viral membrane fusion proteins." *Curr Opin Struct Biol* **19**(2): 189-196.

Backovic M and Jardetzky TS (2011). "Class III viral membrane fusion proteins." *Adv Exp Med Biol* **714**: 91-101.

Backovic M, Longnecker R and Jardetzky TS (2009). "Structure of a trimeric variant of the Epstein-Barr virus glycoprotein B." *Proc Natl Acad Sci U S A* **106**(8): 2880-2885.

Baghian A, Huang L, Newman S, Jayachandra S and Kousoulas KG (1993). "Truncation of the carboxy-terminal 28 amino acids of glycoprotein B specified by herpes simplex virus type 1 mutant amb1511-7 causes extensive cell fusion." *J Virol* **67**(4): 2396-2401.

Baquero E, Albertini AA and Gaudin Y (2015). "Recent mechanistic and structural insights on class III viral fusion glycoproteins." *Curr Opin Struct Biol* **33**: 52-60.

Baquero E, Albertini AA, Vachette P, Lepault J, Bressanelli S and Gaudin Y (2013). "Intermediate conformations during viral fusion glycoprotein structural transition." *Curr Opin Virol* **3**(2): 143-150.

Bender FC, Whitbeck JC, Ponce de Leon M, Lou H, Eisenberg RJ and Cohen GH (2003). "Specific association of glycoprotein B with lipid rafts during herpes simplex virus entry." *J Virol* **77**(17): 9542-9552.

Blomberg N, Baraldi E, Nilges M and Saraste M (1999). "The PH superfold: a structural scaffold for multiple functions." *Trends Biochem Sci* **24**(11): 441-445.

Blumenthal R, Clague MJ, Durell SR and Epand RM (2003). "Membrane fusion." *Chem Rev* **103**(1): 53-69.

Böhm SW, Backovic M, Klupp BG, Rey FA, Mettenleiter TC and Fuchs W (2016). "Functional Characterization of Glycoprotein H Chimeras Composed of Conserved Domains of the Pseudorabies Virus and Herpes Simplex Virus 1 Homologs." *J Virol* **90**(1): 421-432.

Böhm SW, Eckroth E, Backovic M, Klupp BG, Rey FA, Mettenleiter TC and Fuchs W (2015). "Structure-based functional analyses of domains II and III of pseudorabies virus glycoprotein H." *J Virol* **89**(2): 1364-1376.

Booy FP, Newcomb WW, Trus BL, Brown JC, Baker TS and Steven AC (1991). "Liquid-crystalline, phage-like packing of encapsidated DNA in herpes simplex virus." *Cell* **64**(5): 1007-1015.

Boulant S, Stanifer M and Lozach PY (2015). "Dynamics of virus-receptor interactions in virus binding, signaling, and endocytosis." *Viruses* **7**(6): 2794-2815.

Browne HM, Bruun BC and Minson AC (1996). "Characterization of herpes simplex virus type 1 recombinants with mutations in the cytoplasmic tail of glycoprotein H." *J Gen Virol* **77 (Pt 10)**: 2569-2573.

Buchmann JP and Holmes EC (2015). "Cell Walls and the Convergent Evolution of the Viral Envelope." *Microbiol Mol Biol Rev* **79**(4): 403-418.

Bullough PA, Hughson FM, Skehel JJ and Wiley DC (1994). "Structure of influenza haemagglutinin at the pH of membrane fusion." *Nature* **371**(6492): 37-43.

Burke HG and Heldwein EE (2015). "Crystal Structure of the Human Cytomegalovirus Glycoprotein B." *PLoS Pathog* **11**(10): e1005227.

Cai WH, Gu B and Person S (1988). "Role of glycoprotein B of herpes simplex virus type 1 in viral entry and cell fusion." *J Virol* **62**(8): 2596-2604.

Cai WZ, Person S, DebRoy C and Gu BH (1988). "Functional regions and structural features of the gB glycoprotein of herpes simplex virus type 1. An analysis of linker insertion mutants." *J Mol Biol* **201**(3): 575-588.

Cairns TM, Fontana J, Huang ZY, Whitbeck JC, Atanasiu D, Rao S, Shelly SS, Lou H, Ponce de Leon M, Steven AC, Eisenberg RJ and Cohen GH (2014). "Mechanism of neutralization of herpes simplex virus by antibodies directed at the fusion domain of glycoprotein B." *J Virol* **88**(5): 2677-2689.

Cairns TM, Friedman LS, Lou H, Whitbeck JC, Shaner MS, Cohen GH and Eisenberg RJ (2007). "N-terminal mutants of herpes simplex virus type 2 gH are transported without gL but require gL for function." *J Virol* **81**(10): 5102-5111.

Cairns TM, Milne RS, Ponce-de-Leon M, Tobin DK, Cohen GH and Eisenberg RJ (2003). "Structure-function analysis of herpes simplex virus type 1 gD and gH-gL: clues from gDgH chimeras." *J Virol* **77**(12): 6731-6742.

Cairns TM, Whitbeck JC, Lou H, Heldwein EE, Chowdary TK, Eisenberg RJ and Cohen GH (2011). "Capturing the herpes simplex virus core fusion complex (gB-gH/gL) in an acidic environment." *J Virol* **85**(13): 6175-6184.

Campadelli-Fiume G and Menotti L (2007). Entry of alphaherpesviruses into the cell. Human Herpesviruses: Biology, Therapy, and Immunoprophylaxis. A. Arvin, G. Campadelli-Fiume, E. Mocarski *et al.* Cambridge.

Carfi A, Willis SH, Whitbeck JC, Krummenacher C, Cohen GH, Eisenberg RJ and Wiley DC (2001). "Herpes simplex virus glycoprotein D bound to the human receptor HveA." *Mol Cell* **8**(1): 169-179.

Chandramouli S, Ciferri C, Nikitin PA, Calo S, Gerrein R, Balabanis K, Monroe J, Hebner C, Lilja AE, Settembre EC and Carfi A (2015). "Structure of HCMV glycoprotein B in the postfusion conformation bound to a neutralizing human antibody." *Nat Commun* **6**: 8176.

Chen J, Jardetzky TS and Longnecker R (2016). "The Cytoplasmic Tail Domain of Epstein-Barr Virus gH Regulates Membrane Fusion Activity through Altering gH Binding to gp42 and Epithelial Cell Attachment." *MBio* **7**(6).

Chernomordik L, Kozlov MM and Zimmerberg J (1995). "Lipids in biological membrane fusion." *J Membr Biol* **146**(1): 1-14.

Chernomordik LV and Kozlov MM (2003). "Protein-lipid interplay in fusion and fission of biological membranes." *Annu Rev Biochem* **72**: 175-207.

Chernomordik LV and Kozlov MM (2005). "Membrane hemifusion: crossing a chasm in two leaps." *Cell* **123**(3): 375-382.

Chernomordik LV and Kozlov MM (2008). "Mechanics of membrane fusion." *Nat Struct Mol Biol* **15**(7): 675-683.

Chernomordik LV, Melikyan GB and Chizmadzhev YA (1987). "Biomembrane fusion: a new concept derived from model studies using two interacting planar lipid bilayers." *Biochim Biophys Acta* **906**(3): 309-352.

Cheshenko N, Pierce C and Herold BC (2018). "Herpes simplex viruses activate phospholipid scramblase to redistribute phosphatidylserines and Akt to the outer leaflet of the plasma membrane and promote viral entry." *PLoS Pathog* **14**(1): e1006766.

Chesnokova LS, Ahuja MK and Hutt-Fletcher LM (2014). "Epstein-Barr virus glycoprotein gB and gHgL can mediate fusion and entry in trans, and heat can act as a partial surrogate for gHgL and trigger a conformational change in gB." *J Virol* **88**(21): 12193-12201.

Chowdary TK, Cairns TM, Atanasiu D, Cohen GH, Eisenberg RJ and Heldwein EE (2010). "Crystal structure of the conserved herpesvirus fusion regulator complex gH-gL." *Nat Struct Mol Biol* **17**(7): 882-888.

Chowdary TK and Heldwein EE (2010). "Syncytial phenotype of C-terminally truncated herpes simplex virus type 1 gB is associated with diminished membrane interactions." *J Virol* **84**(10): 4923-4935.

Cocchi F, Menotti L, Dubreuil P, Lopez M and Campadelli-Fiume G (2000). "Cell-to-cell spread of wild-type herpes simplex virus type 1, but not of syncytial strains, is mediated by the immunoglobulin-like receptors that mediate virion entry, nectin1 (PRR1/HveC/HIgR) and nectin2 (PRR2/HveB)." *J Virol* **74**(8): 3909-3917.

Connolly SA and Longnecker R (2012). "Residues within the C-terminal arm of the herpes simplex virus 1 glycoprotein B ectodomain contribute to its refolding during the fusion step of virus entry." *J Virol* **86**(12): 6386-6393.

Connolly SA, Whitbeck JJ, Rux AH, Krummenacher C, van Drunen Littel-van den Hurk S, Cohen GH and Eisenberg RJ (2001). "Glycoprotein D homologs in herpes simplex virus type 1, pseudorabies virus, and bovine herpes virus type 1 bind directly to human HveC(nectin-1) with different affinities." *Virology* **280**(1): 7-18.

Cooper RS, Georgieva ER, Borbat PP, Freed JH and Heldwein EE (2018). "Structural basis for membrane anchoring and fusion regulation of the herpes simplex virus fusogen gB." *Nat Struct Mol Biol* **25**(5): 416-424.

Cooper RS and Heldwein EE (2015). "Herpesvirus gB: A Finely Tuned Fusion Machine." *Viruses* **7**(12): 6552-6569.

Davison AJ (2010). "Herpesvirus systematics." *Vet Microbiol* **143**(1): 52-69.

Davison AJ, Eberle R, Ehlers B, Hayward GS, McGeoch DJ, Minson AC, Pellett PE, Roizman B, Studdert MJ and Thiry E (2009). "The order Herpesvirales." *Arch Virol* **154**(1): 171-177.

Davison AJ and Scott JE (1986). "The complete DNA sequence of varicella-zoster virus." *J Gen Virol* **67 (Pt 9)**: 1759-1816.

Dessau M and Modis Y (2013). "Crystal structure of glycoprotein C from Rift Valley fever virus." *Proc Natl Acad Sci U S A* **110**(5): 1696-1701.

Di Giovine P, Settembre EC, Bhargava AK, Luftig MA, Lou H, Cohen GH, Eisenberg RJ, Krummenacher C and Carfi A (2011). "Structure of herpes simplex virus glycoprotein D bound to the human receptor nectin-1." *PLoS Pathog* **7**(9): e1002277.

Diakidi-Kosta A, Michailidou G, Kontogounis G, Sivropoulou A and Arsenakis M (2003). "A single amino acid substitution in the cytoplasmic tail of the glycoprotein B of herpes simplex virus 1 affects both syncytium formation and binding to intracellular heparan sulfate." *Virus Res* **93**(1): 99-108.

Dingwell KS, Brunetti CR, Hendricks RL, Tang Q, Tang M, Rainbow AJ and Johnson DC (1994). "Herpes simplex virus glycoproteins E and I facilitate cell-to-cell spread in vivo and across junctions of cultured cells." *J Virol* **68**(2): 834-845.

Dingwell KS, Doering LC and Johnson DC (1995). "Glycoproteins E and I facilitate neuron-to-neuron spread of herpes simplex virus." *J Virol* **69**(11): 7087-7098.

Dingwell KS and Johnson DC (1998). "The herpes simplex virus gE-gI complex facilitates cell-to-cell spread and binds to components of cell junctions." *J Virol* **72**(11): 8933-8942.

Dollery SJ, Delboy MG and Nicola AV (2010). "Low pH-induced conformational change in herpes simplex virus glycoprotein B." *J Virol* **84**(8): 3759-3766.

DuBois RM, Vaney MC, Tortorici MA, Kurdi RA, Barba-Spaeth G, Krey T and Rey FA (2013). "Functional and evolutionary insight from the crystal structure of rubella virus protein E1." *Nature* **493**(7433): 552-556.

Duus KM and Grose C (1996). "Multiple regulatory effects of varicella-zoster virus (VZV) gL on trafficking patterns and fusogenic properties of VZV gH." *J Virol* **70**(12): 8961-8971.

Eisenberg RJ, Atanasiu D, Cairns TM, Gallagher JR, Krummenacher C and Cohen GH (2012). "Herpes virus fusion and entry: a story with many characters." *Viruses* **4**(5): 800-832.

Engel JP, Boyer EP and Goodman JL (1993). "Two novel single amino acid syncytial mutations in the carboxy terminus of glycoprotein B of herpes simplex virus type 1 confer a unique pathogenic phenotype." *Virology* **192**(1): 112-120.

Enquist LW, Dubin J, Whealy ME and Card JP (1994). "Complementation analysis of pseudorabies virus gE and gI mutants in retinal ganglion cell neurotropism." *J Virol* **68**(8): 5275-5279.

Esiri MM and Tomlinson AH (1972). "Herpes Zoster. Demonstration of virus in trigeminal nerve and ganglion by immunofluorescence and electron microscopy." *J Neurol Sci* **15**(1): 35-48.

Fan Q, Kopp SJ, Connolly SA and Longnecker R (2017). "Structure-Based Mutations in the Herpes Simplex Virus 1 Glycoprotein B Ectodomain Arm Impart a Slow-Entry Phenotype." *MBio* **8**(3).

Fan Q, Lin E and Spear PG (2009). "Insertional mutations in herpes simplex virus type 1 gL identify functional domains for association with gH and for membrane fusion." *J Virol* **83**(22): 11607-11615.

Fan Q, Longnecker R and Connolly SA (2014). "Substitution of herpes simplex virus 1 entry glycoproteins with those of saimiriine herpesvirus 1 reveals a gD-gH/gL functional interaction and a region within the gD profusion domain that is critical for fusion." *J Virol* **88**(11): 6470-6482.

Fan Q, Longnecker R and Connolly SA (2015). "A Functional Interaction between Herpes Simplex Virus 1 Glycoprotein gH/gL Domains I and II and gD Is Defined by Using Alphaherpesvirus gH and gL Chimeras." *J Virol* **89**(14): 7159-7169.

Fan Z, Grantham ML, Smith MS, Anderson ES, Cardelli JA and Muggeridge MI (2002). "Truncation of herpes simplex virus type 2 glycoprotein B increases its cell surface expression and activity in cell-cell fusion, but these properties are unrelated." *J Virol* **76**(18): 9271-9283.

Farnsworth A and Johnson DC (2006). "Herpes simplex virus gE/gI must accumulate in the trans-Golgi network at early times and then redistribute to cell junctions to promote cell-cell spread." *J Virol* **80**(7): 3167-3179.

Field HJ and Vere Hodge RA (2013). "Recent developments in anti-herpesvirus drugs." *Br Med Bull* **106**: 213-249.

Fontana J, Atanasiu D, Saw WT, Gallagher JR, Cox RG, Whitbeck JC, Brown LM, Eisenberg RJ and Cohen GH (2017). "The Fusion Loops of the Initial Prefusion Conformation of Herpes Simplex Virus 1 Fusion Protein Point Toward the Membrane." *MBio* **8**(4).

Foster TP, Melancon JM and Kousoulas KG (2001). "An alpha-helical domain within the carboxyl terminus of herpes simplex virus type 1 (HSV-1) glycoprotein B (gB) is associated with cell fusion and resistance to heparin inhibition of cell fusion." *Virology* **287**(1): 18-29.

Fuchs W, Backovic M, Klupp BG, Rey FA and Mettenleiter TC (2012). "Structure-based mutational analysis of the highly conserved domain IV of glycoprotein H of pseudorabies virus." *J Virol* **86**(15): 8002-8013.

Fusco D, Forghieri C and Campadelli-Fiume G (2005). "The pro-fusion domain of herpes simplex virus glycoprotein D (gD) interacts with the gD N terminus and is displaced by soluble forms of viral receptors." *Proc Natl Acad Sci U S A* **102**(26): 9323-9328.

Gage PJ, Levine M and Glorioso JC (1993). "Syncytium-inducing mutations localize to two discrete regions within the cytoplasmic domain of herpes simplex virus type 1 glycoprotein B." *J Virol* **67**(4): 2191-2201.

Galdiero M, Whiteley A, Bruun B, Bell S, Minson T and Browne H (1997). "Site-directed and linker insertion mutagenesis of herpes simplex virus type 1 glycoprotein H." *J Virol* **71**(3): 2163-2170.

Galdiero S, Falanga A, Vitiello M, Browne H, Pedone C and Galdiero M (2005). "Fusogenic domains in herpes simplex virus type 1 glycoprotein H." *J Biol Chem* **280**(31): 28632-28643.

Galdiero S, Falanga A, Vitiello M, D'Isanto M, Collins C, Orrei V, Browne H, Pedone C and Galdiero M (2007). "Evidence for a role of the membrane-proximal region of herpes simplex virus type 1 glycoprotein H in membrane fusion and virus inhibition." *Chembiochem* **8**(8): 885-895.

Gallagher JR, Saw WT, Atanasiu D, Lou H, Eisenberg RJ and Cohen GH (2013). "Displacement of the C terminus of herpes simplex virus gD is sufficient to expose the fusion-activating interfaces on gD." *J Virol* **87**(23): 12656-12666.

Garcia NJ, Chen J and Longnecker R (2013). "Modulation of Epstein-Barr virus glycoprotein B (gB) fusion activity by the gB cytoplasmic tail domain." *MBio* **4**(1): e00571-00512.

Gatta V, Petrovic B and Campadelli-Fiume G (2015). "The Engineering of a Novel Ligand in gH Confers to HSV an Expanded Tropism Independent of gD Activation by Its Receptors." *PLoS Pathog* **11**(5): e1004907.

Geraghty RJ, Krummenacher C, Cohen GH, Eisenberg RJ and Spear PG (1998). "Entry of alphaherpesviruses mediated by poliovirus receptor-related protein 1 and poliovirus receptor." *Science* **280**(5369): 1618-1620.

Gianni T, Massaro R and Campadelli-Fiume G (2015). "Dissociation of HSV gL from gH by alphavbeta6- or alphavbeta8-integrin promotes gH activation and virus entry." *Proc Natl Acad Sci U S A* **112**(29): E3901-3910.

Gianni T, Salvioli S, Chesnokova LS, Hutt-Fletcher LM and Campadelli-Fiume G (2013). "alphavbeta6- and alphavbeta8-integrins serve as interchangeable receptors for HSV gH/gL to promote endocytosis and activation of membrane fusion." *PLoS Pathog* **9**(12): e1003806.

Gilbert R, Ghosh K, Rasile L and Ghosh HP (1994). "Membrane anchoring domain of herpes simplex virus glycoprotein gB is sufficient for nuclear envelope localization." *J Virol* **68**(4): 2272-2285.

Gillet L, May JS, Colaco S and Stevenson PG (2007). "Glycoprotein L disruption reveals two functional forms of the murine gammaherpesvirus 68 glycoprotein H." *J Virol* **81**(1): 280-291.

Granzow H, Weiland F, Jons A, Klupp BG, Karger A and Mettenleiter TC (1997). "Ultrastructural analysis of the replication cycle of pseudorabies virus in cell culture: a reassessment." *J Virol* **71**(3): 2072-2082.

Guirakhoo F, Heinz FX, Mandl CW, Holzmann H and Kunz C (1991). "Fusion activity of flaviviruses: comparison of mature and immature (prM-containing) tick-borne encephalitis virions." *J Gen Virol* **72 (Pt 6)**: 1323-1329.

Haan KM, Lee SK and Longnecker R (2001). "Different functional domains in the cytoplasmic tail of glycoprotein B are involved in Epstein-Barr virus-induced membrane fusion." *Virology* **290**(1): 106-114.

Halldorsson S, Li S, Li M, Harlos K, Bowden TA and Huiskonen JT (2018). "Shielding and activation of a viral membrane fusion protein." *Nat Commun* **9**(1): 349.

Han J, Pluhackova K and Bockmann RA (2017). "The Multifaceted Role of SNARE Proteins in Membrane Fusion." *Front Physiol* **8**: 5.

Hannah BP, Cairns TM, Bender FC, Whitbeck JC, Lou H, Eisenberg RJ and Cohen GH (2009). "Herpes simplex virus glycoprotein B associates with target membranes via its fusion loops." *J Virol* **83**(13): 6825-6836.

Hannah BP, Heldwein EE, Bender FC, Cohen GH and Eisenberg RJ (2007). "Mutational evidence of internal fusion loops in herpes simplex virus glycoprotein B." *J Virol* **81**(9): 4858-4865.

Harman A, Browne H and Minson T (2002). "The transmembrane domain and cytoplasmic tail of herpes simplex virus type 1 glycoprotein H play a role in membrane fusion." *J Virol* **76**(21): 10708-10716.

Harrison SC (2015). "Viral membrane fusion." *Virology* **479-480**: 498-507.

Harson R and Grose C (1995). "Egress of varicella-zoster virus from the melanoma cell: a tropism for the melanocyte." *J Virol* **69**(8): 4994-5010.

Heineman TC and Hall SL (2002). "Role of the varicella-zoster virus gB cytoplasmic domain in gB transport and viral egress." *J Virol* **76**(2): 591-599.

Heldwein EE, Lou H, Bender FC, Cohen GH, Eisenberg RJ and Harrison SC (2006). "Crystal structure of glycoprotein B from herpes simplex virus 1." *Science* **313**(5784): 217-220.

Helenius A and Aebi M (2004). "Roles of N-linked glycans in the endoplasmic reticulum." *Annu Rev Biochem* **73**: 1019-1049.

Helle F, Vieyres G, Elkrief L, Popescu CI, Wychowski C, Descamps V, Castelain S, Roingeard P, Duverlie G and Dubuisson J (2010). "Role of N-linked glycans in the functions of hepatitis C virus envelope proteins incorporated into infectious virions." *J Virol* **84**(22): 11905-11915.

Hernandez LD, Hoffman LR, Wolfsberg TG and White JM (1996). "Virus-cell and cell-cell fusion." *Annu Rev Cell Dev Biol* **12**: 627-661.

Herold BC, Visalli RJ, Susmarski N, Brandt CR and Spear PG (1994). "Glycoprotein C-independent binding of herpes simplex virus to cells requires cell surface heparan sulphate and glycoprotein B." *J Gen Virol* **75 (Pt 6)**: 1211-1222.

Hunter E (1997). Viral Entry and Receptors. Retroviruses. J. H. Coffin, SH.; Varmus, HE. (NY), Cold Spring Harbor (NY).

Hutchinson L, Browne H, Wargent V, Davis-Poynter N, Primorac S, Goldsmith K, Minson AC and Johnson DC (1992). "A novel herpes simplex virus glycoprotein, gL, forms a complex with glycoprotein H (gH) and affects normal folding and surface expression of gH." *J Virol* **66**(4): 2240-2250.

Jahn R, Lang T and Sudhof TC (2003). "Membrane fusion." *Cell* **112**(4): 519-533.

Johnson DC, Webb M, Wisner TW and Brunetti C (2001). "Herpes simplex virus gE/gI sorts nascent virions to epithelial cell junctions, promoting virus spread." *J Virol* **75**(2): 821-833.

Jones NA and Geraghty RJ (2004). "Fusion activity of lipid-anchored envelope glycoproteins of herpes simplex virus type 1." *Virology* **324**(1): 213-228.

Kadlec J, Loureiro S, Abrescia NG, Stuart DI and Jones IM (2008). "The postfusion structure of baculovirus gp64 supports a unified view of viral fusion machines." *Nat Struct Mol Biol* **15**(10): 1024-1030.

Karger A and Mettenleiter TC (1993). "Glycoproteins gIII and gp50 play dominant roles in the biphasic attachment of pseudorabies virus." *Virology* **194**(2): 654-664.

Kaye JF, Gompels UA and Minson AC (1992). "Glycoprotein H of human cytomegalovirus (HCMV) forms a stable complex with the HCMV UL115 gene product." *J Gen Virol* **73 (Pt 10)**: 2693-2698.

Kemble GW, Henis YI and White JM (1993). "GPI- and transmembrane-anchored influenza hemagglutinin differ in structure and receptor binding activity." *J Cell Biol* **122**(6): 1253-1265.

Kielian M (2006). "Class II virus membrane fusion proteins." *Virology* **344**(1): 38-47.

Kielian M (2014). "Mechanisms of Virus Membrane Fusion Proteins." *Annu Rev Virol* **1**(1): 171-189.

Kielian M and Rey FA (2006). "Virus membrane-fusion proteins: more than one way to make a hairpin." *Nat Rev Microbiol* **4**(1): 67-76.

Kim YH, Donald JE, Grigoryan G, Leser GP, Fadeev AY, Lamb RA and DeGrado WF (2011). "Capture and imaging of a prehairpin fusion intermediate of the paramyxovirus PIV5." *Proc Natl Acad Sci U S A* **108**(52): 20992-20997.

Kirschner AN, Omerovic J, Popov B, Longnecker R and Jardetzky TS (2006). "Soluble Epstein-Barr virus glycoproteins gH, gL, and gp42 form a 1:1:1 stable complex that acts like soluble gp42 in B-cell fusion but not in epithelial cell fusion." *J Virol* **80**(19): 9444-9454.

Klupp BG, Baumeister J, Karger A, Visser N and Mettenleiter TC (1994). "Identification and characterization of a novel structural glycoprotein in pseudorabies virus, gL." *J Virol* **68**(6): 3868-3878.

Klupp BG, Fuchs W, Weiland E and Mettenleiter TC (1997). "Pseudorabies virus glycoprotein L is necessary for virus infectivity but dispensable for virion localization of glycoprotein H." *J Virol* **71**(10): 7687-7695.

Klupp BG, Karger A and Mettenleiter TC (1997). "Bovine herpesvirus 1 glycoprotein B does not productively interact with cell surface heparan sulfate in a pseudorabies virion background." *J Virol* **71**(6): 4838-4841.

Klupp BG and Mettenleiter TC (1999). "Glycoprotein gL-independent infectivity of pseudorabies virus is mediated by a gD-gH fusion protein." *J Virol* **73**(4): 3014-3022.

Klupp BG, Nixdorf R and Mettenleiter TC (2000). "Pseudorabies virus glycoprotein M inhibits membrane fusion." *J Virol* **74**(15): 6760-6768.

Klupp BG, Visser N and Mettenleiter TC (1992). "Identification and characterization of pseudorabies virus glycoprotein H." *J Virol* **66**(5): 3048-3055.

Kopp A, Blewett E, Misra V and Mettenleiter TC (1994). "Proteolytic cleavage of bovine herpesvirus 1 (BHV-1) glycoprotein gB is not necessary for its function in BHV-1 or pseudorabies virus." *J Virol* **68**(3): 1667-1674.

Kozlov MM, McMahon HT and Chernomordik LV (2010). "Protein-driven membrane stresses in fusion and fission." *Trends Biochem Sci* **35**(12): 699-706.

Kozlovsky Y, Chernomordik LV and Kozlov MM (2002). "Lipid intermediates in membrane fusion: formation, structure, and decay of hemifusion diaphragm." *Biophys J* **83**(5): 2634-2651.

Kritas SK, Pensaert MB and Mettenleiter TC (1994). "Invasion and spread of single glycoprotein deleted mutants of Aujeszky's disease virus (ADV) in the trigeminal nervous pathway of pigs after intranasal inoculation." *Vet Microbiol* **40**(3-4): 323-334.

Krummenacher C, Baribaud I, Eisenberg RJ and Cohen GH (2003). "Cellular localization of nectin-1 and glycoprotein D during herpes simplex virus infection." *J Virol* **77**(16): 8985-8999.

Krummenacher C, Carfi A, Eisenberg RJ and Cohen GH (2013). "Entry of herpesviruses into cells: the enigma variations." *Adv Exp Med Biol* **790**: 178-195.

Krummenacher C, Supekar VM, Whitbeck JC, Lazear E, Connolly SA, Eisenberg RJ, Cohen GH, Wiley DC and Carfi A (2005). "Structure of unliganded HSV gD reveals a mechanism for receptor-mediated activation of virus entry." *EMBO J* **24**(23): 4144-4153.

Lamb RA and Jardetzky TS (2007). "Structural basis of viral invasion: lessons from paramyxovirus F." *Curr Opin Struct Biol* **17**(4): 427-436.

Lange Y, Swaisgood MH, Ramos BV and Steck TL (1989). "Plasma membranes contain half the phospholipid and 90% of the cholesterol and sphingomyelin in cultured human fibroblasts." *J Biol Chem* **264**(7): 3786-3793.

Laquerre S, Argnani R, Anderson DB, Zucchini S, Manservigi R and Glorioso JC (1998). "Heparan sulfate proteoglycan binding by herpes simplex virus type 1 glycoproteins B and C, which differ in their contributions to virus attachment, penetration, and cell-to-cell spread." *J Virol* **72**(7): 6119-6130.

Leabu M (2006). "Membrane fusion in cells: molecular machinery and mechanisms." *J Cell Mol Med* **10**(2): 423-427.

Leikin S, Parsegian VA, Rau DC and Rand RP (1993). "Hydration forces." *Annu Rev Phys Chem* **44**: 369-395.

Leikina E and Chernomordik LV (2000). "Reversible merger of membranes at the early stage of influenza hemagglutinin-mediated fusion." *Mol Biol Cell* **11**(7): 2359-2371.

Lemmon MA (2007). "Pleckstrin homology (PH) domains and phosphoinositides." *Biochem Soc Symp*(74): 81-93.

Lennemann NJ, Walkner M, Berkebile AR, Patel N and Maury W (2015). "The Role of Conserved N-Linked Glycans on Ebola Virus Glycoprotein 2." *J Infect Dis* **212 Suppl 2**: S204-209.

Lete C, Machiels B, Stevenson PG, Vanderplasschen A and Gillet L (2012). "Bovine herpesvirus type 4 glycoprotein L is nonessential for infectivity but triggers virion endocytosis during entry." *J Virol* **86**(5): 2653-2664.

Li A, Lu G, Qi J, Wu L, Tian K, Luo T, Shi Y, Yan J and Gao GF (2017). "Structural basis of nectin-1 recognition by pseudorabies virus glycoprotein D." *PLoS Pathog* **13**(5): e1006314.

Li Q, Krogmann T, Ali MA, Tang WJ and Cohen JI (2007). "The amino terminus of varicella-zoster virus (VZV) glycoprotein E is required for binding to insulin-degrading enzyme, a VZV receptor." *J Virol* **81**(16): 8525-8532.

Li X, Yang F, Hu X, Tan F, Qi J, Peng R, Wang M, Chai Y, Hao L, Deng J, Bai C, Wang J, Song H, Tan S, Lu G, Gao GF, Shi Y and Tian K (2017). "Two classes of protective antibodies against Pseudorabies virus variant glycoprotein B: Implications for vaccine design." *PLoS Pathog* **13**(12): e1006777.

Li Y and Modis Y (2014). "A novel membrane fusion protein family in Flaviviridae?" *Trends Microbiol* **22**(4): 176-182.

Liao Z, Cimakasky LM, Hampton R, Nguyen DH and Hildreth JE (2001). "Lipid rafts and HIV pathogenesis: host membrane cholesterol is required for infection by HIV type 1." *AIDS Res Hum Retroviruses* **17**(11): 1009-1019.

Lin E and Spear PG (2007). "Random linker-insertion mutagenesis to identify functional domains of herpes simplex virus type 1 glycoprotein B." *Proc Natl Acad Sci U S A* **104**(32): 13140-13145.

Litwin V, Jackson W and Grose C (1992). "Receptor properties of two varicella-zoster virus glycoproteins, gpI and gpIV, homologous to herpes simplex virus gE and gI." *J Virol* **66**(6): 3643-3651.

Liu DX, Gompels UA, Nicholas J and Lelliott C (1993). "Identification and expression of the human herpesvirus 6 glycoprotein H and interaction with an accessory 40K glycoprotein." *J Gen Virol* **74 (Pt 9)**: 1847-1857.

Lobigs M and Garoff H (1990). "Fusion function of the Semliki Forest virus spike is activated by proteolytic cleavage of the envelope glycoprotein precursor p62." *J Virol* **64**(3): 1233-1240.

Lu G, Zhang N, Qi J, Li Y, Chen Z, Zheng C, Gao GF and Yan J (2014). "Crystal structure of herpes simplex virus 2 gD bound to nectin-1 reveals a conserved mode of receptor recognition." *J Virol* **88**(23): 13678-13688.

Luo S, Hu K, He S, Wang P, Zhang M, Huang X, Du T, Zheng C, Liu Y and Hu Q (2015). "Contribution of N-linked glycans on HSV-2 gB to cell-cell fusion and viral entry." *Virology* **483**: 72-82.

Marsh M and Helenius A (1989). "Virus entry into animal cells." *Adv Virus Res* **36**: 107-151.

Martens S and McMahon HT (2008). "Mechanisms of membrane fusion: disparate players and common principles." *Nat Rev Mol Cell Biol* **9**(7): 543-556.

Mateo M, Generous A, Sinn PL and Cattaneo R (2015). "Connections matter--how viruses use cell-cell adhesion components." *J Cell Sci* **128**(3): 431-439.

Matsuura H, Kirschner AN, Longnecker R and Jardetzky TS (2010). "Crystal structure of the Epstein-Barr virus (EBV) glycoprotein H/glycoprotein L (gH/gL) complex." *Proc Natl Acad Sci U S A* **107**(52): 22641-22646.

Matsuyama S, Delos SE and White JM (2004). "Sequential roles of receptor binding and low pH in forming prehairpin and hairpin conformations of a retroviral envelope glycoprotein." *J Virol* **78**(15): 8201-8209.

Maurer UE, Zeev-Ben-Mordehai T, Pandurangan AP, Cairns TM, Hannah BP, Whitbeck JC, Eisenberg RJ, Cohen GH, Topf M, Huiskonen JT and Grunewald K (2013). "The structure of herpesvirus fusion glycoprotein B-bilayer complex reveals the protein-membrane and lateral protein-protein interaction." *Structure* **21**(8): 1396-1405.

McCarthy KM, Tank DW and Enquist LW (2009). "Pseudorabies virus infection alters neuronal activity and connectivity in vitro." *PLoS Pathog* **5**(10): e1000640.

McClain DS and Fuller AO (1994). "Cell-specific kinetics and efficiency of herpes simplex virus type 1 entry are determined by two distinct phases of attachment." *Virology* **198**(2): 690-702.

McGeoch DJ, Cook S, Dolan A, Jamieson FE and Telford EA (1995). "Molecular phylogeny and evolutionary timescale for the family of mammalian herpesviruses." *J Mol Biol* **247**(3): 443-458.

McShane MP and Longnecker R (2005). "Analysis of fusion using a virus-free cell fusion assay." *Methods Mol Biol* **292**: 187-196.

Melikyan GB, Lin S, Roth MG and Cohen FS (1999). "Amino acid sequence requirements of the transmembrane and cytoplasmic domains of influenza virus hemagglutinin for viable membrane fusion." *Mol Biol Cell* **10**(6): 1821-1836.

Melikyan GB, Markosyan RM, Roth MG and Cohen FS (2000). "A point mutation in the transmembrane domain of the hemagglutinin of influenza virus stabilizes a hemifusion intermediate that can transit to fusion." *Mol Biol Cell* **11**(11): 3765-3775.

Mendelsohn CL, Wimmer E and Racaniello VR (1989). "Cellular receptor for poliovirus: molecular cloning, nucleotide sequence, and expression of a new member of the immunoglobulin superfamily." *Cell* **56**(5): 855-865.

Mettenleiter TC (1989). "Glycoprotein gIII deletion mutants of pseudorabies virus are impaired in virus entry." *Virology* **171**(2): 623-625.

Mettenleiter TC (1994). "Pseudorabies (Aujeszky's disease) virus: state of the art. August 1993." *Acta Vet Hung* **42**(2-3): 153-177.

Mettenleiter TC (1996). "Immunobiology of pseudorabies (Aujeszky's disease)." *Vet Immunol Immunopathol* **54**(1-4): 221-229.

Mettenleiter TC (2002). "Herpesvirus assembly and egress." *J Virol* **76**(4): 1537-1547.

Mettenleiter TC (2008). Pseudorabies Virus. Encyclopedia of Virology. B. W. J. Mahy and M. H. V. Van Regenmortel. Oxford, Elsevier. **5:** 341-351.

Mettenleiter TC, Klupp BG and Granzow H (2009). "Herpesvirus assembly: an update." *Virus Res* **143**(2): 222-234.

Mettenleiter TC, Zsak L, Zuckermann F, Sugg N, Kern H and Ben-Porat T (1990). "Interaction of glycoprotein gIII with a cellular heparinlike substance mediates adsorption of pseudorabies virus." *J Virol* **64**(1): 278-286.

Miranda-Saksena M, Denes CE, Diefenbach RJ and Cunningham AL (2018). "Infection and Transport of Herpes Simplex Virus Type 1 in Neurons: Role of the Cytoskeleton." *Viruses* **10**(2).

Modis Y (2014). "Relating structure to evolution in class II viral membrane fusion proteins." *Curr Opin Virol* **5**: 34-41.

Modis Y, Ogata S, Clements D and Harrison SC (2004). "Structure of the dengue virus envelope protein after membrane fusion." *Nature* **427**(6972): 313-319.

Möhl BS, Schröter C, Klupp BG, Fuchs W, Mettenleiter TC, Jardetzky TS and Longnecker R (2015). "Comparative Mutagenesis of Pseudorabies Virus and Epstein-Barr Virus gH Identifies a Structural Determinant within Domain III of gH Required for Surface Expression and Entry Function." *J Virol* **90**(5): 2285-2293.

Moller-Tank S and Maury W (2015). "Ebola virus entry: a curious and complex series of events." *PLoS Pathog* **11**(4): e1004731.

Mondal Roy S and Sarkar M (2011). "Membrane fusion induced by small molecules and ions." *J Lipids* **2011**: 528784.

Montgomery RI, Warner MS, Lum BJ and Spear PG (1996). "Herpes simplex virus-1 entry into cells mediated by a novel member of the TNF/NGF receptor family." *Cell* **87**(3): 427-436.

Mothes W, Sherer NM, Jin J and Zhong P (2010). "Virus cell-to-cell transmission." *J Virol* **84**(17): 8360-8368.

Muggeridge MI (2000). "Characterization of cell-cell fusion mediated by herpes simplex virus 2 glycoproteins gB, gD, gH and gL in transfected cells." *J Gen Virol* **81**(Pt 8): 2017-2027.

Mulder W, Pol J, Kimman T, Kok G, Priem J and Peeters B (1996). "Glycoprotein D-negative pseudorabies virus can spread transneuronally via direct neuron-to-neuron transmission in its natural host, the pig, but not after additional inactivation of gE or gI." *J Virol* **70**(4): 2191-2200.

Nixdorf R, Klupp BG, Karger A and Mettenleiter TC (2000). "Effects of truncation of the carboxy terminus of pseudorabies virus glycoprotein B on infectivity." *J Virol* **74**(15): 7137-7145.

Ogle BM, Cascalho M and Platt JL (2005). "Biological implications of cell fusion." *Nat Rev Mol Cell Biol* **6**(7): 567-575.

Okazaki K (2007). "Proteolytic cleavage of glycoprotein B is dispensable for in vitro replication, but required for syncytium formation of pseudorabies virus." *J Gen Virol* **88**(Pt 7): 1859-1865.

Ozorowski G, Pallesen J, de Val N, Lyumkis D, Cottrell CA, Torres JL, Copps J, Stanfield RL, Cupo A, Pugach P, Moore JP, Wilson IA and Ward AB (2017). "Open and closed structures reveal allostery and pliability in the HIV-1 envelope spike." *Nature* **547**(7663): 360-363.

Pasieka TJ, Maresova L and Grose C (2003). "A functional YNKI motif in the short cytoplasmic tail of varicella-zoster virus glycoprotein gH mediates clathrin-dependent and antibody-independent endocytosis." *J Virol* **77**(7): 4191-4204.

Pasieka TJ, Maresova L, Shiraki K and Grose C (2004). "Regulation of varicella-zoster virus-induced cell-to-cell fusion by the endocytosis-competent glycoproteins gH and gE." *J Virol* **78**(6): 2884-2896.

Peeters B, de Wind N, Hooisma M, Wagenaar F, Gielkens A and Moormann R (1992). "Pseudorabies virus envelope glycoproteins gp50 and gII are essential for virus penetration, but only gII is involved in membrane fusion." *J Virol* **66**(2): 894-905.

Peng R, Zhang S, Cui Y, Shi Y, Gao GF and Qi J (2017). "Structures of human-infecting Thogotovirus fusogens support a common ancestor with insect baculovirus." *Proc Natl Acad Sci U S A* **114**(42): E8905-E8912.

Pertel PE, Fridberg A, Parish ML and Spear PG (2001). "Cell fusion induced by herpes simplex virus glycoproteins gB, gD, and gH-gL requires a gD receptor but not necessarily heparan sulfate." *Virology* **279**(1): 313-324.

Petrovic B, Gianni T, Gatta V and Campadelli-Fiume G (2017). "Insertion of a ligand to HER2 in gB retargets HSV tropism and obviates the need for activation of the other entry glycoproteins." *PLoS Pathog* **13**(4): e1006352.

Plonsky I, Kingsley DH, Rashtian A, Blank PS and Zimmerberg J (2008). "Initial size and dynamics of viral fusion pores are a function of the fusion protein mediating membrane fusion." *Biol Cell* **100**(6): 377-386.

Polcicova K, Goldsmith K, Rainish BL, Wisner TW and Johnson DC (2005). "The extracellular domain of herpes simplex virus gE is indispensable for efficient cell-to-cell spread: evidence for gE/gI receptors." *J Virol* **79**(18): 11990-12001.

Pomeranz LE, Reynolds AE and Hengartner CJ (2005). "Molecular biology of pseudorabies virus: impact on neurovirology and veterinary medicine." *Microbiol Mol Biol Rev* **69**(3): 462-500.

Rand RP and Parsegian VA (1984). "Physical force considerations in model and biological membranes." *Can J Biochem Cell Biol* **62**(8): 752-759.

Rasile L, Ghosh K, Raviprakash K and Ghosh HP (1993). "Effects of deletions in the carboxy-terminal hydrophobic region of herpes simplex virus glycoprotein gB on intracellular transport and membrane anchoring." *J Virol* **67**(8): 4856-4866.

Rauh I and Mettenleiter TC (1991). "Pseudorabies virus glycoproteins gII and gp50 are essential for virus penetration." *J Virol* **65**(10): 5348-5356.

Read GS, Person S and Keller PM (1980). "Genetic studies of cell fusion induced by herpes simplex virus type 1." *J Virol* **35**(1): 105-113.

Rey FA, Heinz FX, Mandl C, Kunz C and Harrison SC (1995). "The envelope glycoprotein from tick-borne encephalitis virus at 2 A resolution." *Nature* **375**(6529): 291-298.

Rey FA and Lok SM (2018). "Common Features of Enveloped Viruses and Implications for Immunogen Design for Next-Generation Vaccines." *Cell* **172**(6): 1319-1334.

Roche S, Bressanelli S, Rey FA and Gaudin Y (2006). "Crystal structure of the low-pH form of the vesicular stomatitis virus glycoprotein G." *Science* **313**(5784): 187-191.

Roche S, Rey FA, Gaudin Y and Bressanelli S (2007). "Structure of the prefusion form of the vesicular stomatitis virus glycoprotein G." *Science* **315**(5813): 843-848.

Rogalin HB and Heldwein EE (2015). "Interplay between the Herpes Simplex Virus 1 gB Cytodomain and the gH Cytotail during Cell-Cell Fusion." *J Virol* **89**(24): 12262-12272.

Roop C, Hutchinson L and Johnson DC (1993). "A mutant herpes simplex virus type 1 unable to express glycoprotein L cannot enter cells, and its particles lack glycoprotein H." *J Virol* **67**(4): 2285-2297.

Rowe CL, Connolly SA, Chen J, Jardetzky TS and Longnecker R (2013). "A soluble form of Epstein-Barr virus gH/gL inhibits EBV-induced membrane fusion and does not function in fusion." *Virology* **436**(1): 118-126.

Ruel N, Zago A and Spear PG (2006). "Alanine substitution of conserved residues in the cytoplasmic tail of herpes simplex virus gB can enhance or abolish cell fusion activity and viral entry." *Virology* **346**(1): 229-237.

Ruigrok RW, Martin SR, Wharton SA, Skehel JJ, Bayley PM and Wiley DC (1986). "Conformational changes in the hemagglutinin of influenza virus which accompany heat-induced fusion of virus with liposomes." *Virology* **155**(2): 484-497.

Sapir A, Avinoam O, Podbilewicz B and Chernomordik LV (2008). "Viral and developmental cell fusion mechanisms: conservation and divergence." *Dev Cell* **14**(1): 11-21.

Sathiyamoorthy K, Chen J, Longnecker R and Jardetzky TS (2017). "The COMPLEXity in herpesvirus entry." *Curr Opin Virol* **24**: 97-104.

Sattentau Q (2008). "Avoiding the void: cell-to-cell spread of human viruses." *Nat Rev Microbiol* **6**(11): 815-826.

Schibli DJ and Weissenhorn W (2004). "Class I and class II viral fusion protein structures reveal similar principles in membrane fusion." *Mol Membr Biol* **21**(6): 361-371.

Schmidt J, Gerdts V, Beyer J, Klupp BG and Mettenleiter TC (2001). "Glycoprotein D-independent infectivity of pseudorabies virus results in an alteration of in vivo host range and correlates with mutations in glycoproteins B and H." *J Virol* **75**(21): 10054-10064.

Schmidt J, Klupp BG, Karger A and Mettenleiter TC (1997). "Adaptability in herpesviruses: glycoprotein D-independent infectivity of pseudorabies virus." *J Virol* **71**(1): 17-24.

Schröder C, Linde G, Fehler F and Keil GM (1997). "From essential to beneficial: glycoprotein D loses importance for replication of bovine herpesvirus 1 in cell culture." *J Virol* **71**(1): 25-33.

Schröter C, Klupp BG, Fuchs W, Gerhard M, Backovic M, Rey FA and Mettenleiter TC (2014). "The highly conserved proline at position 438 in pseudorabies virus gH is important for regulation of membrane fusion." *J Virol* **88**(22): 13064-13072.

Shelly SS, Cairns TM, Whitbeck JC, Lou H, Krummenacher C, Cohen GH and Eisenberg RJ (2012). "The membrane-proximal region (MPR) of herpes simplex virus gB regulates association of the fusion loops with lipid membranes." *MBio* **3**(6).

Shemer G and Podbilewicz B (2003). "The story of cell fusion: big lessons from little worms." *Bioessays* **25**(7): 672-682.

Shieh MT, WuDunn D, Montgomery RI, Esko JD and Spear PG (1992). "Cell surface receptors for herpes simplex virus are heparan sulfate proteoglycans." *J Cell Biol* **116**(5): 1273-1281.

Shukla D, Liu J, Blaiklock P, Shworak NW, Bai X, Esko JD, Cohen GH, Eisenberg RJ, Rosenberg RD and Spear PG (1999). "A novel role for 3-O-sulfated heparan sulfate in herpes simplex virus 1 entry." *Cell* **99**(1): 13-22.

Silverman JL, Greene NG, King DS and Heldwein EE (2012). "Membrane requirement for folding of the herpes simplex virus 1 gB cytodomain suggests a unique mechanism of fusion regulation." *J Virol* **86**(15): 8171-8184.

Silverman JL, Sharma S, Cairns TM and Heldwein EE (2010). "Fusion-deficient insertion mutants of herpes simplex virus type 1 glycoprotein B adopt the trimeric postfusion conformation." *J Virol* **84**(4): 2001-2012.

Skehel JJ and Wiley DC (2000). "Receptor binding and membrane fusion in virus entry: the influenza hemagglutinin." *Annu Rev Biochem* **69**: 531-569.

Smith EC, Popa A, Chang A, Masante C and Dutch RE (2009). "Viral entry mechanisms: the increasing diversity of paramyxovirus entry." *FEBS J* **276**(24): 7217-7227.

Smith EC, Smith SE, Carter JR, Webb SR, Gibson KM, Hellman LM, Fried MG and Dutch RE (2013). "Trimeric transmembrane domain interactions in paramyxovirus fusion proteins: roles in protein folding, stability, and function." *J Biol Chem* **288**(50): 35726-35735.

Spear PG, Eisenberg RJ and Cohen GH (2000). "Three classes of cell surface receptors for alphaherpesvirus entry." *Virology* **275**(1): 1-8.

Spear PG, Manoj S, Yoon M, Jogger CR, Zago A and Myscofski D (2006). "Different receptors binding to distinct interfaces on herpes simplex virus gD can trigger events leading to cell fusion and viral entry." *Virology* **344**(1): 17-24.

Stampfer SD and Heldwein EE (2013). "Stuck in the middle: structural insights into the role of the gH/gL heterodimer in herpesvirus entry." *Curr Opin Virol* **3**(1): 13-19.

Stampfer SD, Lou H, Cohen GH, Eisenberg RJ and Heldwein EE (2010). "Structural basis of local, pH-dependent conformational changes in glycoprotein B from herpes simplex virus type 1." *J Virol* **84**(24): 12924-12933.

Stein KK, Primakoff P and Myles D (2004). "Sperm-egg fusion: events at the plasma membrane." *J Cell Sci* **117**(Pt 26): 6269-6274.

Steven AC and Spear PG (2006). "Biochemistry. Viral glycoproteins and an evolutionary conundrum." *Science* **313**(5784): 177-178.

Stiasny K, Allison SL, Mandl CW and Heinz FX (2001). "Role of metastability and acidic pH in membrane fusion by tick-borne encephalitis virus." *J Virol* **75**(16): 7392-7398.

Strive T, Borst E, Messerle M and Radsak K (2002). "Proteolytic processing of human cytomegalovirus glycoprotein B is dispensable for viral growth in culture." *J Virol* **76**(3): 1252-1264.

Suenaga T, Satoh T, Somboonthum P, Kawaguchi Y, Mori Y and Arase H (2010). "Myelin-associated glycoprotein mediates membrane fusion and entry of neurotropic herpesviruses." *Proc Natl Acad Sci U S A* **107**(2): 866-871.

Sun X, Belouzard S and Whittaker GR (2008). "Molecular architecture of the bipartite fusion loops of vesicular stomatitis virus glycoprotein G, a class III viral fusion protein." *J Biol Chem* **283**(10): 6418-6427.

Sun X and Whittaker GR (2003). "Role for influenza virus envelope cholesterol in virus entry and infection." *J Virol* **77**(23): 12543-12551.

Turner A, Bruun B, Minson T and Browne H (1998). "Glycoproteins gB, gD, and gHgL of herpes simplex virus type 1 are necessary and sufficient to mediate membrane fusion in a Cos cell transfection system." *J Virol* **72**(1): 873-875.

Uchida H, Chan J, Shrivastava I, Reinhart B, Grandi P, Glorioso JC and Cohen JB (2013). "Novel mutations in gB and gH circumvent the requirement for known gD Receptors in herpes simplex virus 1 entry and cell-to-cell spread." *J Virol* **87**(3): 1430-1442.

Vallbracht M, Brun D, Tassinari M, Vaney MC, Pehau-Arnaudet G, Guardado-Calvo P, Haouz A, Klupp BG, Mettenleiter TC, Rey FA and Backovic M (2017). "Structure-function dissection of the Pseudorabies virus glycoprotein B fusion loops." *J Virol*.

Vitu E, Sharma S, Stampfer SD and Heldwein EE (2013). "Extensive mutagenesis of the HSV-1 gB ectodomain reveals remarkable stability of its postfusion form." *J Mol Biol* **425**(11): 2056-2071.

Wanzeck K, Boyd KL and McCullers JA (2011). "Glycan shielding of the influenza virus hemagglutinin contributes to immunopathology in mice." *Am J Respir Crit Care Med* **183**(6): 767-773.

Warner MS, Geraghty RJ, Martinez WM, Montgomery RI, Whitbeck JC, Xu R, Eisenberg RJ, Cohen GH and Spear PG (1998). "A cell surface protein with herpesvirus entry activity (HveB) confers susceptibility to infection by mutants of herpes simplex virus type 1, herpes simplex virus type 2, and pseudorabies virus." *Virology* **246**(1): 179-189.

Webb SR, Smith SE, Fried MG and Dutch RE (2018). "Transmembrane Domains of Highly Pathogenic Viral Fusion Proteins Exhibit Trimeric Association In Vitro." *mSphere* **3**(2).

Wei X, Decker JM, Wang S, Hui H, Kappes JC, Wu X, Salazar-Gonzalez JF, Salazar MG, Kilby JM, Saag MS, Komarova NL, Nowak MA, Hahn BH, Kwong PD and Shaw GM (2003). "Antibody neutralization and escape by HIV-1." *Nature* **422**(6929): 307-312.

Weissenhorn W, Dessen A, Harrison SC, Skehel JJ and Wiley DC (1997). "Atomic structure of the ectodomain from HIV-1 gp41." *Nature* **387**(6631): 426-430.

Weissenhorn W, Hinz A and Gaudin Y (2007). "Virus membrane fusion." *FEBS Lett* **581**(11): 2150-2155.

Wessels L and Weninger K (2009). "Physical aspects of viral membrane fusion." *ScientificWorldJournal* **9**: 764-780.

White JM, Delos SE, Brecher M and Schornberg K (2008). "Structures and mechanisms of viral membrane fusion proteins: multiple variations on a common theme." *Crit Rev Biochem Mol Biol* **43**(3): 189-219.

White JM and Whittaker GR (2016). "Fusion of Enveloped Viruses in Endosomes." *Traffic* **17**(6): 593-614.

Wilen CB, Tilton JC and Doms RW (2012). "HIV: cell binding and entry." *Cold Spring Harb Perspect Med* **2**(8).

Wilson DW, Davis-Poynter N and Minson AC (1994). "Mutations in the cytoplasmic tail of herpes simplex virus glycoprotein H suppress cell fusion by a syncytial strain." *J Virol* **68**(11): 6985-6993.

Wilson IA, Skehel JJ and Wiley DC (1981). "Structure of the haemagglutinin membrane glycoprotein of influenza virus at 3 A resolution." *Nature* **289**(5796): 366-373.

Xing Y, Oliver SL, Nguyen T, Ciferri C, Nandi A, Hickman J, Giovani C, Yang E, Palladino G, Grose C, Uematsu Y, Lilja AE, Arvin AM and Carfi A (2015). "A site of varicella-zoster virus vulnerability identified by structural studies of neutralizing antibodies bound to the glycoprotein complex gHgL." *Proc Natl Acad Sci U S A* **112**(19): 6056-6061.

Yamauchi Y and Helenius A (2013). "Virus entry at a glance." *J Cell Sci* **126**(Pt 6): 1289-1295.

Yang E, Arvin AM and Oliver SL (2014). "The cytoplasmic domain of varicella-zoster virus glycoprotein H regulates syncytia formation and skin pathogenesis." *PLoS Pathog* **10**(5): e1004173.

Yang ST, Kiessling V and Tamm LK (2016). "Line tension at lipid phase boundaries as driving force for HIV fusion peptide-mediated fusion." *Nat Commun* **7**: 11401.

Yang ST, Kreutzberger AJB, Lee J, Kiessling V and Tamm LK (2016). "The role of cholesterol in membrane fusion." *Chem Phys Lipids* **199**: 136-143.

Yaswen LR, Stephens EB, Davenport LC and Hutt-Fletcher LM (1993). "Epstein-Barr virus glycoprotein gp85 associates with the BKRF2 gene product and is incompletely processed as a recombinant protein." *Virology* **195**(2): 387-396.

Zeev-Ben-Mordehai T, Vasishtan D, Hernandez Duran A, Vollmer B, White P, Prasad Pandurangan A, Siebert CA, Topf M and Grunewald K (2016). "Two distinct trimeric conformations of natively membrane-anchored full-length herpes simplex virus 1 glycoprotein B." *Proc Natl Acad Sci U S A* **113**(15): 4176-4181.

Zhang N, Yan J, Lu G, Guo Z, Fan Z, Wang J, Shi Y, Qi J and Gao GF (2011). "Binding of herpes simplex virus glycoprotein D to nectin-1 exploits host cell adhesion." *Nat Commun* **2**: 577.

Zhao WD, Hamid E, Shin W, Wen PJ, Krystofiak ES, Villarreal SA, Chiang HC, Kachar B and Wu LG (2016). "Hemi-fused structure mediates and controls fusion and fission in live cells." *Nature* **534**(7608): 548-552.

Zheng Z, Maidji E, Tugizov S and Pereira L (1996). "Mutations in the carboxyl-terminal hydrophobic sequence of human cytomegalovirus glycoprotein B alter transport and protein chaperone binding." *J Virol* **70**(11): 8029-8040.

Zhong P, Agosto LM, Munro JB and Mothes W (2013). "Cell-to-cell transmission of viruses." *Curr Opin Virol* **3**(1): 44-50.

Zhou ZH, Chen DH, Jakana J, Rixon FJ and Chiu W (1999). "Visualization of tegument-capsid interactions and DNA in intact herpes simplex virus type 1 virions." *J Virol* **73**(4): 3210-3218.

8 Appendix

8.1 Eigenständigkeitserklärung

Hiermit erkläre ich, dass diese Arbeit bisher von mir weder an der Mathematisch-Naturwissenschaftlichen Fakultät der Universität Greifswald noch einer anderen wissenschaftlichen Einrichtung zum Zwecke der Promotion eingereicht wurde.
Ferner erkläre ich, dass ich diese Arbeit selbstständig verfasst und keine anderen als die darin angegebenen Hilfsmittel und Hilfen benutzt und keine Textabschnitte eines Dritten ohne Kennzeichnung übernommen habe.

……
Melina Vallbracht

8.2 Publications

Schröter C, Vallbracht M, Altenschmidt J, Kargoll S, Fuchs W, Klupp BG, Mettenleiter TC. 2016. Mutations in Pseudorabies Virus Glycoproteins gB, gD, and gH Functionally Compensate for the Absence of gL. J Virol 90:2264-2272.

Vallbracht M, Schröter, C., Klupp, B. G. and Mettenleiter, T. C. 2017. Transient Transfection-based Fusion Assay for Viral Proteins. Bio-protocol 7.

Vallbracht M, Brun D, Tassinari M, Vaney MC, Pehau-Arnaudet G, Guardado-Calvo P, Haouz A, Klupp BG, Mettenleiter TC, Rey FA, Backovic M. 2017. Structure-Function Dissection of Pseudorabies Virus Glycoprotein B Fusion Loops. J Virol doi:10.1128/JVI.01203-17.

Vallbracht M, Rehwaldt S, Klupp BG, Mettenleiter TC, Fuchs W. 2017. Functional Relevance of the N-Terminal Domain of Pseudorabies Virus Envelope Glycoprotein H and Its Interaction with Glycoprotein L. J Virol 91.

Vallbracht M, Rehwaldt S, Klupp BG, Mettenleiter TC, Fuchs W. 2018. Functional Role of N-Linked Glycosylation in Pseudorabies Virus Glycoprotein gH. J Virol 92.

Vallbracht M, Fuchs W, Klupp BG, Mettenleiter TC. 2018. Functional Relevance of the Transmembrane Domain and Cytoplasmic Tail of the Pseudorabies Virus Glycoprotein H for Membrane Fusion. J Virol 92.

8.3 Oral and poster presentations

14.-17. Mar. 2018	28th Annual Meeting of the Society for Virology, Würzburg, Poster. Title: Role of N-linked glycosylation sites in PrV gH for its function during entry and spread. Melina Vallbracht, Barbara G. Klupp, Thomas C. Mettenleiter, and Walter Fuchs
8.–10. Nov. 2017	16th Workshop "Cell Biology of Viral Infections'' of the Society of Virology, Schöntal, Talk. Title: Analysis of minimal requirements for herpesvirus mediated membrane fusion. Melina Vallbracht, Barbara G. Klupp, Walter Fuchs, Thomas C. Mettenleiter
20.-22. Sep. 2017	Junior Scientist Symposium FLI, Braunschweig, Talk. Title: Membrane fusion in herpesviruses: role of the conserved glycoprotein gH/gL complex. Melina Vallbracht, Barbara G. Klupp, Thomas C. Mettenleiter
29.07–2 Aug. 2017	42nd International Herpesvirus Workshop, Ghent, Poster. Title: A single point mutation in the transmembrane domain of pseudorabies virus gH compensates for absence of gL in membrane fusion. Melina Vallbracht, Walter Fuchs, Barbara G. Klupp, Thomas C. Mettenleiter
29.07–2 Aug. 2017	42nd International Herpesvirus Workshop, Ghent, Poster. Title: Structural and functional studies of Pseudorabies glycoprotein B. Melina Vallbracht, Delphine Brun, Matteo Tassinari, Marie-Christine Vaney, Gérard Pehau-Arnaudet, Pablo Guardado-Calvo, Ahmed Haouz, Barbara G. Klupp, Thomas C. Mettenleiter, Felix A. Rey, Marija Backovic
22.–25. Mar. 2017	27th Annual Meeting of the Society for Virology, Marburg, Poster. Title: Functional relevance of the N-terminal domain of pseudorabies virus envelope glycoprotein H and its interactions with glycoprotein L. Melina Vallbracht, Sascha Rehwaldt, Barbara G. Klupp, Thomas C. Mettenleiter, Walter Fuchs
21.–23. Oct. 2016	Junior Scientist Symposium 2016 FLI, Jena, Talk. Title: Mutational analysis of the cytoplasmic domain of PrV glycoprotein – in search of the super-fuser. Melina Vallbracht, Christina Schröter, Barbara G. Klupp, Joachim Kühn, Thomas C. Mettenleiter

28.-30. Sep. 2016	1st Summer School "Infection Biology", Greifswald, Poster. Title: Hyperfusogenic mutations in the herpesvirus fusion protein – in search of a super-fuser. Melina Vallbracht, Christina Schröter, Joachim Kühn, Barbara G. Klupp, Thomas C. Mettenleiter
06.-09. Apr. 2016	26th Annual Meeting of the Society for Virology, Münster, Poster. Title: Functional relevance of the N-terminal domain of pseudorabies virus envelope glycoprotein H and its interactions with glycoprotein L. Walter Fuchs, Sascha Rehwaldt, Melina Vallbracht, Christina Schröter, Barbara G. Klupp, Thomas C. Mettenleiter, Thomas
06.-09. Apr. 2016	26th Annual Meeting of the Society for Virology, Münster, Poster. Title: Hyperfusogenic mutations in PrV glycoprotein gB - in search of the super-fuser. Melina Vallbracht, Christina Schröter, Joachim Kühn, Barbara G. Klupp, Thomas C. Mettenleiter
21.–23. Sep. 2015	Junior Scientist Symposium 2015 FLI, Greifswald, Talk. Title: Mutational analysis of the cytoplasmic domain of PrV glycoprotein – in search of the super-fuser. Melina Vallbracht, Christina Schröter, Barbara G. Klupp, Joachim Kühn, Thomas C. Mettenleiter
18. Sep. 2015	10th Mini-Herpesvirus workshop, Hamburg, Poster. Title: Mutational analysis of the cytoplasmic domain of PrV glycoprotein B – in search of the super-fuser. Melina Vallbracht, Christina Schröter, Barbara G. Klupp, Joachim Kühn, Thomas C. Mettenleiter

8.4 Acknowledgement

Mein besonderer Dank gilt dem Präsidenten des FLI und gleichzeitigem Institutsleiter des IMVZ Herrn **Prof. Dr. Dr. h.c. Thomas C. Mettenleiter** für die Möglichkeit, diese Arbeit an seinem Institut anfertigen zu dürfen. Ich danke Ihm für die hervorragende wissenschaftliche Betreuung während meiner Doktorarbeit, die stets offene Tür, die spannenden und lehrreichen Diskussionen und nicht zuletzt für die Möglichkeit an Konferenzen im In- und Ausland teilzunehmen. Seine Erfahrung im Feld der Wissenschaft, Begeisterung für die Virologie und immer positiv motivierende Art haben bedeutend zum Gelingen dieser Arbeit beigetragen. Es ist bemerkenswert und nicht selbstverständlich, dass Prof. Mettenleiter es trotz seiner vielen Tätigkeiten immer schafft direkt und kompetent zu helfen **–** vielen herzlichen Dank!

Frau Dr. Barbara G. Klupp möchte ich herzlich für die schöne und lehrreiche Zeit im Labor danken. Vielen Dank für die hervorragende wissenschaftliche Unterstützung während meiner gesamten Doktorarbeitszeit. Besonders möchte ich mich für die vielen spannenden, lehrreichen und motivierenden Diskussionen bedanken sowie für die Unterstützung bei den Publikationen. Es war und ist mir sehr viel wert die Begeisterung für ein Thema zu teilen **–** so hat mir die Forschung und die Arbeit im Labor immer Freude bereitet!

Bei Herrn **Dr. Walter Fuchs** möchte ich mich besonders für die schöne und erfolgreiche Zusammenarbeit bedanken. Vielen Dank für die Einarbeitung in die Methode der BAC-Mutagenese, für die Unterstützung bei den Publikationen und auch für den Spaß beim anschließenden „Paper-Sekt“.

I address special thanks to my cooperation partners **Dr. Marija Backovic** and **Prof. Dr. Felix A. Rey** from the Institut Pasteur in Paris. It was a great pleasure for me to work with you. Thank you for all the fruitful discussions and the insights into structural biology. Thank you very much for having me over at PI – I really enjoyed the research stay and learned a lot during that time. In this context, I want to thank all the **members of the Rey laboratory** for the great time!

I also want to acknowledge the **DFG** for funding during my PhD.

Herrn **PD Dr. Stefan Finke** und seiner Arbeitsgruppe möchte ich für die hervorragende Einarbeitung in die Methode der konfokalen Laser-Scanning-Mikroskopie danken.

Herrn **Prof. Dr. Joachim Kühn** danke ich dafür, dass er mich damals mit seiner Leidenschaft für dieses Forschungsfeld angesteckt und begeistert hat **–** Vielen Dank für die vielen tollen und motivierenden Diskussionen und die schöne und lehrreiche Zeit damals in Münster!

Herrn **PD Dr. Michael Knittler** und Frau **Dr. Birke A. Tews** danke ich für die ausgezeichnete und freundliche Hilfestellung in Bezug auf die FACS Analysen.

Ein ganz besonderer Dank gilt den Mitgliedern und Ehemaligen der **Arbeitsgruppe Klupp-Met**: **Annemarie Seyfarth, Dr. Christina Schröter, Cindy Krüper, Julia Hölper, Julia Sehl, Karla Günther, Dr. Teresa Hellberg** und **Sebastian Rönfeldt** sowie **Annika Kühn** und **Henning Peters** - vielen Dank für die schöne Arbeitsatmosphäre im Labor, Eure Hilfsbereitschaft und die lustige Zeit mit Euch!

Bei Frau **Katrin Giesow** und **Dr. Anja Bauer** möchte ich mich herzlich für die liebe Aufnahme in Ihr Labor bedanken (auch wenn es leider nur für sehr kurze Zeit war) und besonders für ihre Hilfsbereitschaft in jeglicher Hinsicht.

Dem gesamten **IMVZ** danke ich für die schöne gemeinsame Zeit **–** besonders **Stephanie Peitsch** und **Svenja Mamerow** für diverse Ohrwürmer!

Ein großer Dank geht auch an all die fleißigen **Institutshelfer**, die mir und uns die Arbeit wesentlich erleichtern.

Dem **Riemser Volleyballteam** danke ich für den nötigen sportlichen Ausgleich!

Meinen Freund(inn)en **Marie-Christine**, **Julia** und **Yannik**, **Jan**, **Helen**, **Krissi** und **Fiona**, sowie Familie **Appelbaum, Henning, Henser, Lipka** und **Timmermann** danke ich für Ihre seelische und moralische Unterstützung!

Mein größter Dank ist für meine **Familie**, insbesondere meine Eltern, **Jochem** und **Monika Vallbracht**, und **Mathis** reserviert, die mir stets ein zuverlässiger Rückhalt sind und mich bedingungslos mit viel Herz und Geduld unterstützt haben.